

Some pages of this thesis may have been removed for copyright restrictions.

If you have discovered material in Aston Research Explorer which is unlawful e.g. breaches copyright, (either yours or that of a third party) or any other law, including but not limited to those relating to patent, trademark, confidentiality, data protection, obscenity, defamation, libel, then please read our [Takedown policy](#) and contact the service immediately (openaccess@aston.ac.uk)

Porphyromonas gingivalis gingipains cause defective macrophage migration towards apoptotic cells and inhibit phagocytosis of primary apoptotic neutrophils

Sowmya Ajay Castro
Doctor of Philosophy

Aston University

June 2017

© Sowmya Ajay Castro, 2017. Sowmya Ajay Castro asserts her moral right to be identified as the author of this thesis. This copy of the thesis has been supplied on condition that anyone who consults it is understood to recognise that its copyright rests with its author and that no quotation from the thesis and no information derived from it may be published without appropriate permission or acknowledgement.

Aston University

Periodontitis – Understanding the relationship between pathogens, neutrophils, macrophages and chronic inflammation

Sowmya Ajay Castro
Doctor of Philosophy
2017

Thesis summary

Resolution of inflammation involves suppression of inflammatory cell infiltration, effective clearance of apoptotic cells and induction of an anti-inflammatory response thereby re-establishing tissue homeostasis. Defects in this process may lead to chronic inflammatory diseases and tissue destruction. Periodontitis is a chronic oral inflammatory disease characterised by an aberrant host response to a pathogenic plaque biofilm resulting in local tissue damage and frustrated healing that can result in tooth loss. Cysteine proteases (Gingipains) from the key periodontal pathogen *Porphyromonas gingivalis* have been implicated in periodontal disease pathogenesis by inhibiting inflammation resolution and are linked with systemic chronic inflammatory disease e.g. rheumatoid arthritis. Given the importance of successful clearance of AC by the innate immune system in the restoration of tissue homeostasis and maintenance of healthy tissues, this project sought to characterise the impact of proteolytic enzymes from *P.gingivalis* on the innate immune response. The impact on AC clearance and innate immune responses was assessed.

This project addressed the specific hypothesis that gingipains promote disease by acting to inhibit multiple stages of the AC clearance process. The effect of gingipains on the ability of macrophages to find AC, interact with and remove AC and respond appropriately were assessed. Gingipain treatment of macrophages was shown to reduce the ability of macrophages to migrate towards AC. In addition, expression of CD14, a key receptor known to tether AC, was also reduced. Together these gingipain-induced innate immune changes reduced effective clearance of AC at two separate points in the clearance process (migration and tethering) thus reducing the AC binding to phagocytes. Data presented here also suggest that gingipains reduced anti-inflammatory mediators (TGF- β and IL-10) in macrophages phagocytosing apoptotic neutrophils. Furthermore, whilst apoptotic neutrophils turn off the inflammation induced by lipopolysaccharide from *P.gingivalis*, they fail to turn off the novel gingipain induced inflammatory cytokine production. These data suggest that gingipains induce a strong and dominant pro-inflammatory response that may be resistant to inhibition by AC. Taken together, the work presented here reveals several key stages of the resolution phase of inflammation are inhibited. The failure of this process will result in immune cell necrosis and release of inflammatory mediators into the gingival crevicular fluid to cause catastrophic consequences of inflammation in the periodontal region. For the first time, this work suggests that gingipains may be potent contributors to chronic periodontal inflammation via their impact on multiple stages of the AC clearance process and thus represent a potential therapeutic target.

Acknowledgments

First all, I would like to express my sincere gratitude to my supervisor, Prof Andrew Devitt for his tremendous academic support, guidance, and motivation during my Ph.D. It was an amazing experience to work in Prof Devitt's lab, his enthusiasm for science instilled in me a passion for research.

My acknowledgment also goes to associate supervisors Prof Paul Cooper and Dr. Mike Milward, from University of Birmingham for their valuable scientific discussion over the last three years. Besides my advisors, I would also like to thank Aston University academics for their advice and support.

I would also like to acknowledge members of Prof Devitt group Khaled, Parbata, Ross, Allan, Roberta, Laura and Charlie for all the support, fun and importantly for their friendship for past three years. Similar mention goes to Dr. Ivana for proofreading my thesis, thank you for your time.

My appreciation also goes to Gill Pilfold and Caroline Brocklebank for helping me in settling down at Aston during my first year of Ph.D. Also, I am thankful for international scholarship scheme and technical support provided by Aston University. I would also like to extend my thanks to the donors for donating blood for science.

Lastly, I would like to thank my mom and Ajay for their love and encouragement.

Thank you very much.

Table of contents

Introduction	17
1.1 Acute inflammation	17
1.2 Chronic inflammation	18
1.3 Mechanisms of resolution of inflammation	19
1.4 Chronic inflammatory diseases	22
1.4.1 Periodontal disease (PD).....	23
1.4.2 Pathogenic mechanisms in PD.....	24
The table presents the pro-inflammatory and anti-inflammatory cytokines which if in excess could result in periodontal tissue damage.....	26
1.4.3 Oral Biology and Inflammation.....	26
1.4.4 Bacterial aetiology of periodontitis	27
1.4.5 <i>Porphyromonas gingivalis</i>	28
1.4.5.1 <i>P. gingivalis</i> LPS.....	28
1.4.5.1.1 Toll-like receptors (TLRs)	29
1.4.5.2 Gingipains.....	31
1.4.5.2.1 Structure and homologies of gingipains.....	31
1.4.5.2.2 Hemagglutinin adhesion domains (HA).....	32
1.4.5.3 Gingipain effects on host immune cells	33
1.4.5.4 Evasion of host immune system by gingipains	33
1.4.5.5 Inhibition of gingipains, a potential treatment for PD?	34
1.4.6 <i>P. gingivalis</i> virulence factors in host immune cells	34
1.4.7 Periodontitis and chronic diseases: A Global burden.....	35
1.4.7.1 Periodontitis and Diabetes: Interrelationship	35
1.4.7.2 Periodontitis and Atherosclerosis: A Complex relationship.....	36
1.4.7.3 Periodontitis and Rheumatoid arthritis: The mouth – joint connection	36
1.5 Apoptosis – An essential death in life.....	37
1.5.1 Apoptosis in the oral cavity.....	39
1.5.2 Apoptotic-cell associated molecular patterns (ACAMPs) – ‘eat-me’ signals.....	39
1.5.2.1 Phosphatidylserine (PS).....	40
1.5.2.2 ICAM-3	40
1.5.3 AC clearance receptors associated with phagocytes.....	41
1.5.3.1 Scavenger receptor – CD36.....	41
1.5.3.2 Low density lipoprotein receptor-related protein 1 (LRP1) CD91.....	42
1.5.3.3 CD14	43
1.5.3.3.1 Role of CD14 in AC clearance.....	44
1.5.4 Soluble mediators of AC clearance: ‘bridging’ molecules.....	44
1.5.5 Don’t ‘eat me’ signals	45

1.5.5.1 CD31	45
1.5.5.2 CD47	45
1.5.5.3 CD46	46
1.6 Phagocytosis	46
1.6.1 NØ.....	47
1.6.1.1 NØ in periodontal disease.....	47
1.6.1.2 NØ elastase in periodontitis	49
1.6.2 MØ	50
1.6.2.1 Chemotaxis of MØ in periodontal environment.....	54
1.7 Aims and objectives	55
Materials and Methods	57
2.1 Equipment and software	57
2.2 Antibodies.....	58
➤ Anti-Mouse IgG (whole molecule) – FITC antibody produced in goat	58
➤ Anti-human IgG (Fc specific)-FITC, mouse IgG1 (MOPC 21)	58
2.3 Cell culture.....	58
2.3.1 Materials and reagents for cell culture	58
2.3.2 Cell lines.....	59
2.3.3 Freezing and thawing of cell lines.....	59
2.3.4 Culturing of cells.....	60
2.3.5 THP-1 differentiation to MØ-like cells	60
2.3.6 Immunofluorescence	60
2.3.6.1 Indirect Immunofluorescence staining of cells	60
2.3.6.2 Direct Immunofluorescence staining of cells	60
2.4 Isolation of NØ from peripheral whole human blood using the Percoll gradient method	61
2.4.1 Materials for isolation of NØ	61
2.4.2 Blood collection	61
2.4.3 Preparation of Percoll gradient	62
2.4.4 Confirmation analysis of NØ purity	63
2.4.4.1 Direct Immunofluorescence	63
2.4.4.2 Indirect Immunofluorescence	63
2.4.4.3 4', 6-diamidino-2-phenylindole (DAPI) nuclear stain	63
2.5 Induction and characterization of apoptosis	64
2.5.1 Generation of AC (AC)	64
2.5.1.1 B cells	64
2.5.1.2 NØ	64
2.5.2 Generation of secretomes (AS) from AC	64
2.5.3 Identification and quantification of apoptosis	64

2.5.3.1 Annexin-V FITC/Propidium Iodide Staining	64
2.5.3.2 Nuclear stain	65
2.6 Assays of phagocyte interaction with AC	65
2.6.1 Phagocytosis of AC by MØ through interaction assay	65
2.6.2 <i>In vitro</i> cell migration assay	66
2.6.2.1 Horizontal migration	66
2.6.2.2 Vertical migration	66
2.7 Isolation and characterisation of gingipains from <i>P.gingivalis</i> HG66 and W83.....	67
2.7.1 Bacterial strains of <i>P.gingivalis</i>	67
2.7.1.1 W83	67
2.7.1.2 HG66	67
2.7.2 Materials and buffers for gingipain isolation	67
2.7.2.1 Materials for bacterial growth	67
2.7.2.2 Buffers for W83	67
2.7.2.3 Buffers for HG66	68
2.7.3 Bacterial strains and growth conditions	68
2.7.4 Gram stain of W83 and HG66	68
2.7.5 Growth curve of bacterial culture W83 and HG66	70
2.7.6 Isolation of membrane-bound proteins from <i>P.gingivalis</i> strain W83.....	70
2.7.7 Isolation and purification of soluble proteins from culture supernatant HG66:..	70
2.7.8 Confirmatory analysis of gingipain purity	71
2.7.8.1 Enzyme activity assay	71
2.7.8.2 Determination of molecular weight using SDS-PAGE electrophoresis.....	71
2.7.8.2.1 Protein determination using BCA assay	71
2.7.8.2.2 Trichloroacetic Acid (TCA) precipitation of eluted proteins derived from the W83 and HG66 strains	72
2.7.8.2.3 SDS-PAGE electrophoresis	72
2.7.9 Mass spectrometry	73
2.7.9.1 Sample preparation	73
2.7.9.2 LC-MS/MS	73
2.7.10 Limulus Amebocyte Lysate (LAL) assay for LPS detection	74
2.7.11 MØ or NØ treatment with gingipains	74
2.7.12 Inhibition of gingipains using N α -p-tosyl-L-lysine chloromethyl ketone	74
2.8 LPS from <i>P.gingivalis</i> induced TNF- α response in THP-1 derived MØs	75
2.8.1 Measurement of TNF- α levels in MØ co-cultured with AC	75
2.8.2 ELISA	75
2.9 Determination of anti-inflammatory cytokines (TGF- β and IL-10) mRNA levels using quantitative PCR	76
2.9.1 Materials	76

2.9.2 Preparation of cells.....	77
2.9.3 RNA isolation	77
2.9.4 Confirmatory analysis of RNA purity	77
2.9.4.1 Nanodrop.....	77
2.9.4.2 Agarose gel electrophoresis.....	78
2.9.5.1 Reverse transcribe RNA into cDNA.....	78
2.9.5.2 Extension step reaction mixture	78
2.9.6 Quantification of TGF- β and IL-10 gene expression	78
2.9.6.1 Housekeeping gene (Human β -actin).....	78
2.9.6.2 TGF- β and IL-10 gene expression	78
2.9.6.3 Quantification of mRNA.....	79
2.10 Statistical analysis.....	79
Chapter 3.....	80
Results	80
Results 1: Establishing a model assay system for M\emptyset interaction with primary apoptotic N\emptyset	80
3.1 Introduction.....	80
3.2 Phenotypic characterisation of primary N \emptyset isolated from peripheral blood.....	81
3.2.1 Characterisation of primary N \emptyset	81
3.3 Generation of AC.....	82
3.3.1 B cells	82
3.3.2 Primary N \emptyset	84
3.3.3 Temperature dependent apoptosis in N \emptyset	86
3.4 THP-1 differentiated M \emptyset model	88
3.4.1 THP-1- derived M \emptyset model system.....	88
3.4.2 Cell surface receptor expression	89
3.4.2.1 CD14	89
3.4.2.2 CD36	90
3.5 M \emptyset chemotaxis to AC	91
3.5.1 Dunn chamber model-horizontal chemotaxis.....	91
3.5.1.1 M \emptyset chemotaxis to AC B cells.....	93
3.5.1.2 Determination of efficiency of migration	94
3.5.1.2.1 Forward migration index (FMI).....	94
3.5.1.2.2 Measurement of distance, directness and velocity.....	95
3.5.1.2.3 Angle.....	96
3.5.1.3 M \emptyset chemotaxis to AC N \emptyset	99
3.5.2 Cell-IQ model – Vertical chemotaxis.....	102
3.6 Phagocyte interaction with AC	106
3.6.1 M \emptyset -AC Interaction assay	106

3.7 Discussion	107
3.7.1 Characterisation of human NØ	108
3.7.1.1 Induction of apoptosis in NØ by UV and spontaneous method.....	108
3.7.2 Phenotypic characterisation and function of THP-1-derived MØ	110
3.7.3 Modelling of AC clearance <i>in vitro</i>	112
3.7.3.1 Chemotaxis and interaction of MØ with AC	112
3.8 Conclusion.....	115
Result 2: Purification of gingipains from <i>P.gingivalis</i>	116
4.1 Introduction.....	116
4.2 Establishment of appropriate growth conditions for <i>P.gingivalis</i> strains W83 and HG66.....	116
4.3 Characterisation of cysteine proteases from <i>P.gingivalis</i> strains W83 and HG66.....	117
4.4 Purification of gingipains from <i>P.gingivalis</i> HG66.....	121
4.5 Characterisation of isolated proteins using mass spectrometric analysis	125
4.6 Discussion	127
4.6.1 Comparison of <i>P.gingivalis</i> W83 and HG66 derived cysteine proteases.....	127
4.6.2 Purified gingipain activity from the strain HG66	131
4.7 Conclusion.....	133
Result 3: Gingipain selectively cleaves CD14 leading to MØ hypo-responsiveness towards AC	135
5.1 Introduction.....	135
5.2 Gingipains fail to induce apoptosis in primary NØ and THP-1 MØ	136
5.3 Gingipain cleaves CD14, an AC clearance receptor.....	140
5.4 TLCK inhibits CD14 cleavage in THP-1 MØ.....	144
5.5 Expression of AC clearance receptors on gingipain-treated THP-1 MØ and primary NØ.....	144
5.6 Gingipains inhibit the directional migration of phagocytes to AC	151
5.7 Rgp and Kgp inhibits MØ migration towards AC NØ in a vertical cell migration assay	156
5.8 Gingipains inhibit interaction of MØ with AC	159
5.9 Discussion	162
5.9.1 Gingipain modulation of CD14 on MØ	164
5.9.2 CD14 on NØ.....	166
5.9.3 Possible receptor modulation in periodontal disease	167
5.9.4 Gingipain-mediated alterations in MØ response in the migration to AC	169
5.9.5 Gingipain-mediated alterations in MØ response in the clearance of AC.....	172
5.10 Conclusion.....	173
Result 4: Regulation of pro and anti-inflammatory cytokines in RgpB and Kgp induced THP-1 MØ	174
6.1 Introduction.....	174

6.2 LPS-induced TNF- α production.....	174
6.3 Gingipain induced TNF- α production.....	178
6.4 Inhibition of gene expression of TGF- β and IL-10 anti-inflammatory cytokines on gingipain-treated M \emptyset	181
6.4.1 Quality assessment of isolated RNA.....	182
6.4.2 Relative mRNA expression level of TGF- β and IL-10	183
6.5 Discussion	185
6.5.1 TNF- α production by LPS and gingipains from <i>P.gingivalis</i>	185
6.5.2 Role of anti-inflammatory cytokines in PD	189
6.5.3 Other cytokine levels in periodontal diseases	191
6.6 Conclusion	191
7 Discussion	193
7.1 M \emptyset phagocytosis mechanisms in human periodontal disease	194
7.2 Mechanistic differences in AC N \emptyset response to LPS and gingipains.....	198
7.3 Conclusion.....	200
7.4 Future work.....	200
References.....	203

List of figures

Figure 1: Illustration of acute inflammation pathways	18
Figure 2: Illustration of chronic inflammation pathways.....	19
Figure 3: Phases involved in acute inflammation and its resolution	22
Figure 4: Structure of the periodontium	23
Figure 5: CD14 signals LPS binding through TLR4-MD2 pathways.....	30
Figure 6: Structure and homologies of gingipains.....	32
Figure 7: Stages of apoptotic cell death.....	38
Figure 8: Illustration of activation of MØ challenged with LPS in PD.....	50
Figure 9: Possible scenarios involved in the AC clearance mechanism within PD.....	56
Figure 10: Isolation of NØ from whole blood.....	62
Figure 11: The Dunn chamber model.....	66
Figure 12: The Cell-IQ model	67
Figure 13: Culture and Gram staining of the <i>P.gingivalis</i> strains W83 and HG66	69
Figure 14: Phenotypic analysis of isolated NØ	82
Figure 15: Induction and analysis of apoptosis by UV in B cells	83
Figure 16: Induction and analysis of apoptosis by UV in primary NØ.....	85
Figure 17: Quantification of spontaneous NØ cell death incubated at 4°C and 37°C	87
Figure 18: Morphology of THP-1-derived MØ induced to differentiation with various stimulants.....	89
Figure 19: CD14 surface expression on THP-1-derived MØ.....	90
Figure 20: CD36 surface expression of THP-1-derived MØ.....	91
Figure 21: THP-1- derived MØ migration towards AC B cells and their derived AS	94
Figure 22: Schematic representation of forward migration index calculated from cell migration Dunn chamber assay using Chemotaxis and Migration Tool software	95
Figure 23: Schematic representation of the distance travelled by the phagocytes calculated using the Chemotaxis and Migration Tool software	96
Figure 24: Schematic representation of angle measurement of phagocyte migration calculated from Chemotaxis and Migration Tool software.....	97
Figure 25: Quantitative measurement of MØ migration towards AC B and AS B	98
Figure 26: Angle and directness of MØ migration towards AC B or AS B	99
Figure 27: THP-1-derived MØ migration towards AC NØ or AS NØ	100
Figure 28: Quantitative measurement of MØ migration towards AC NØ	101
Figure 29: Angle and directness of THP-1 differentiated MØ migration towards the AC NØ or AS NØ.....	102
Figure 30: Representative Cell-IQ image of THP-1-derived MØ migration to putative attractants using a vertical chemotaxis model	103
Figure 31: THP-1-derived MØ migration to AC B or AS B using Cell IQ tracking system	104
Figure 32: THP-1-derived MØ migration to AC NØ or AS NØ using Cell IQ tracking system	105
Figure 33: Interaction of apoptotic B cells and apoptotic NØ with THP-1-derived MØ....	106
Figure 34: Growth curves of W83 and HG66 strains of <i>P.gingivalis</i>	117
Figure 35: Determination of the amidolytic activity of <i>P.gingivalis</i> strains W83 and HG66 following culture fractionation.	118
Figure 36: Characterisation of molecular weights of proteases from <i>P.gingivalis</i> strains W83 and HG66 using SDS-PAGE.....	119
Figure 37: Determination of amidolytic activity in the presence or absence of cysteine derived from <i>P.gingivalis</i> strains W83 and HG66.....	120
Figure 38: Representative chromatogram of a gel chromatography column performed on Sephadex G-150 fractions followed by arginine sepharose affinity chromatography.....	122

Figure 39: Determination of the amidolytic activity of gingipains purified from <i>P.gingivalis</i> strain HG66.....	123
Figure 40: Determination of molecular weights using SDS-PAGE analysis for the final purified proteins from the HG66 strain of <i>P.gingivalis</i>	124
Figure 41: Inhibition of purified proteins from <i>P.gingivalis</i> HG66 using TLCK	124
Figure 42: Measurement of cell viability, size, and granularity of gingipain-treated THP-1 MØ	137
Figure 43: Confocal analysis of cell and nuclear morphology of gingipain-treated MØ ..	138
Figure 44: Measurement of cell viability, size, and granularity of gingipain-treated primary NØ	139
Figure 45: Fluorescent images of gingipain-treated primary NØ.....	140
Figure 46: Quantification of CD14 expression on <i>P.gingivalis</i> LPS treated THP-1 MØ ..	141
Figure 47: CD14 surface expression on THP-1 MØ treated with gingipains	142
Figure 48: CD14 surface expression on primary NØ treated with gingipains	143
Figure 49: TLCK inhibits CD14 reduction on Kgp gingipain-treated THP-1 MØ	144
Figure 50: Gingipain treatment of MØ does not alter the expression of CD36, ICAM-3 or CD91.....	145
Figure 51: Gingipain treatment of primary NØ does not alter the expression of CD36, ICAM-3 or CD91.....	146
Figure 52: CD31 expression on gingipain-treated THP-1 MØ at various time points.....	147
Figure 53: CD47 expression on gingipain-treated THP-1 MØ at various time points.....	148
Figure 54: CD31 expression on gingipain-treated primary viable and AC NØ treatment at different time points.....	149
Figure 55: CD47 expression on gingipain-treated primary viable and AC NØ treatment at different time points.....	150
Figure 56: Gingipains inhibit MØ migration towards AC B cells	152
Figure 57: Gingipain treatment of THP-1 MØ does not affect distance, velocity or angle of migration towards AC B cells.....	153
Figure 58: Gingipains inhibit MØ migration towards AC NØ	154
Figure 59: Gingipain treatment of THP-1 MØ does not affect distance, velocity or angle of migration towards AC NØ.....	155
Figure 60: Gingipains does not inhibits vertical migration of MØ migration towards AC B or AS B cells.....	157
Figure 61: Gingipain treatment of MØ inhibits MØ migration towards AC NØ using vertical assay.....	158
Figure 62: Gingipain does not inhibit vertical migration of MØ migration towards AS NØ	159
Figure 63: Gingipain treatment of MØ inhibits the interaction of MØ with AC B	160
Figure 64: Gingipain treatment of MØ inhibits interaction of MØ with AC NØ	162
Figure 65: AC B or AS B cells fail to inhibit <i>E.coli</i> LPS -induced TNF- α production by MØ	175
Figure 66: AC NØ or AS NØ cells fail to inhibit <i>E.coli</i> LPS -induced TNF- α production by MØ	176
Figure 67: TNF- α response in an LPS (<i>P.gingivalis</i>) induced THP-1 derived MØ model	177
Figure 68: AC inhibit <i>Pg</i> LPS-induced TNF- α production.....	178
Figure 69: TNF- α release from gingipain-treated MØ	179
Figure 70: AC B or AS B cells fails to inhibit gingipain-induced TNF- α production	180
Figure 71: AC NØ or AS NØ cells failed to inhibit gingipain-induced TNF- α production .	181
Figure 72: Quality assessment of isolated RNA using agarose gel electrophoresis	183
Figure 73: Relative gene expression of TGF- β in gingipain-treated MØ using PCR analysis	184
Figure 74: Relative gene expression of IL-10 in gingipain-treated MØ using PCR analysis	185

Figure 75: Structure of <i>Pg</i> LPS and <i>Ec</i> LPS	187
Figure 76: Possible defective AC clearance mechanism involved in PD	199

List of Tables

Table 1: List of inflammatory mediators reported to be in PD	26
Table 2: List of risk factors associated with PD.....	53
Table 3: Direct immunofluorescence staining using flow cytometry	61
Table 4: Percoll density composition for isolation of NØ	62
Table 5: Composition of reagents to prepare resolving and stacking gel	72
.....	86
Table 6: Induction and analysis of various forms of apoptosis on primary NØ analysed using flow cytometry.....	86
Table 7: Characterisation of purified proteins from P.gingivalis HG66 using mass spectrometric analysis.....	126
Table 8: List of receptors that participate in AC clearance	136
Table 9: Quantification of RNA for PCR analysis using the NanoDrop 2000c.....	182

Abbreviations

ABC	ATP-binding cassette transporters
AC	Apoptotic cells
AC B	Apoptotic B cells
AC NØ	Apoptotic neutrophils
ACAMPs	Apoptotic cell-associated molecular patterns
AS B	Apoptotic B cell-derived secretomes
AS NØ	Apoptotic neutrophils-derived secretomes
BAI1	Brain-specific angiogenesis inhibitor 1
BL	Burkitt's lymphoma
BSA	Bovine serum albumin
CHO	Chinese hamster ovary
cRPMI	Complete Roswell Park Memorial Institute medium
CXCL	Chemokine (C-X-C motif) ligand
DAMPs	Damage-associated molecular patterns
DISC	Death-inducing signalling complex
DMSO	Dimethyl sulphoxide
DS	Double stimulated (VD3/PMA)
EGF	Epidermal growth factor
FCS	Foetal calf serum
FITC	Fluorescein isothiocyanate
FMLP	N-Formylmethionine-leucyl-phenylalanine
GAS-6	Growth arrest-specific 6
GCF	Gingival crevicular fluid
GM-CSF	Granulocyte-MØ colony-stimulating factor
GTP	Guanosine triphosphate
HMDM	Human monocyte-derived macrophages
HRP	Horseradish peroxidase
HSP	Heat shock proteins
ICAM-3	Intercellular adhesion molecule 3
IFN	Interferon
IL-10	Interleukin 10
IRF3	Interferon-regulatory factor
Kgp	Lysine gingipain
LBP	Lipopolysaccharide binding protein
LDL	Low-density lipoproteins
LFA-1	Leukointegrin: leukocyte function associated antigen-1
LPC	Lysophosphatidylcholine
LPS	Lipopolysaccharide
LP <i>E. coli</i>	LPS <i>Escherichia coli</i>
LR1	Leukocyte response integrin
mAb	Monoclonal antibody
MAP	Mitogen-activated protein
MBL	Mannose-binding lectin

mCD14	Membrane CD14
MCP-1	Macrophage chemokine protein
M-CSF	Macrophage colony-stimulating factor
MFG-E8	Milk fat globule epidermal growth factor
MIF	MØ migration inhibitory factor
MIP-1 α	Macrophage inflammatory protein 1 alpha
MMPs	Metalloproteinases
MØ	Macrophages
MPO	Myeloperoxidase
MYD88	Myeloid differentiation primary response protein 88
NETs	Neutrophil extracellular traps
NF- κ B	Nuclear factor- κ B
NGS	Normal goat serum
NHS	Normal human serum
NØ	Neutrophils
OD	Optical density
OPD	O-Phenylenediamine dihydrochloride
<i>P. gingivalis</i>	<i>Porphyromonas gingivalis</i>
<i>P. gingivalis</i>	<i>Porphyromonas gingivalis</i>
LPS	<i>Pg</i> LPS
PAMP	Pathogen-associated molecular patterns
PARs	Protease activated receptors
PBS	Phosphate-buffered saline
PBS-T	PBS containing tween
PC	Phosphatidylcholine
PCR	Polymerase chain reaction
PD	Periodontal disease
PDL	Periodontal ligament
PE	Phycoerythrin
PECAM-1	Platelet endothelial cell adhesion molecule-1
PGD2	Prostaglandin D2
PI	Propidium Iodide
PI	Phosphoinositide
PI3K	Phosphatidylinositol 3-kinase
PKC	Protein kinase C
PMA	Phorbol 12-myristate 13-acetate
PRRs	Pattern recognition receptors
PS	Phosphatidylserine
PSR	Phosphatidylserine receptor
RgpB	Arginine gingipain
ROS	Reactive oxygen species
S1P	Sphingosine 1-phosphate
S1PRs	Sphingosine 1-phosphate receptors
sCD14	Soluble CD14
SDS	Sodium dodecyl sulphate
sfRPMI	Serum-free RPMI
SHP-1	Src homology region 2 domain-containing phosphatase-1

SIRP- α	Signal-regulatory protein alpha
SLE	Systemic lupus erythematosus
SP-A	Surfactant protein A
SP-D	Surfactant protein D
SR-A	Class A Scavenger receptor
TG	Transglutaminase
TGF- β	Transforming Growth Factor beta
TIRAP	TIR domain-containing adapter protein
TLRs	Toll-like receptors
TNF-R	Tumour necrosis factor receptor
TNF- α	Tumour-necrosis factor
TRIF	TIR-domain-containing adapter-inducing interferon- β
Tris	Tris(hydroxymethyl)methylamine
TSP-1	Thombospondin-1
TSP-1	Thrombospondin
TUNEL	Terminal TdT-mediated dUTP-biotin nick end labelling
Tween 20	Polysorbate 20
VD3	Dihydroxyvitamin D3
VEGF	Vascular endothelial growth factors
WASP	Wiskott-Aldrich syndrome protein
α 2MR	α -2 macroglobulin receptors

Chapter 1

Introduction

Inflammation is a form of self-protection that defends our body from infection stimulated by foreign invaders, trauma and immune reactions. To combat infection or repair tissue damage and restore tissue homeostasis, the inflammatory cascade begins with a rapid, and coordinated reaction generating the cardinal signs of redness, heat, pain and swelling which ultimately lead to resolution and healing. The generation of inflamed tissue is mediated by a broad range of molecular mediators, immune cells, biochemical pathways and blood vessels ¹. Notably, cells of the innate and adaptive immune system differ in their sensing of microbial infection and the innate immune system provides the first line of defence by triggering phagocytic cells such as neutrophils (NØ) and macrophages (MØ) to eliminate the microbial infection ². However the innate immune system does not 'remember' pathogens and consequently input from the adaptive immune system is required, which involves instructing lymphocytes to 'remember' the antigens of intruding pathogens ³. The mechanism of resolution of inflammation unfolds in several phases and each stage has been studied and its importance has been identified as any failures in repair result in tissue destruction and release of toxic mediators which lead to chronic inflammatory diseases ⁴. Traditionally, removal of pro-inflammatory mediators (e.g. invading bacteria) was understood to resolve inflammation in a passive manner. More recently, however, it has become accepted that the phases (explained in section 1.3) involved in resolving inflammation are active rather than passive which offers opportunities to design novel approaches to treat chronic inflammatory diseases. The restoration of tissue homeostasis occurs during acute inflammation and is normally self-limiting resulting in tissue healing. In addition, the basal level of the MØ and lymphocyte counts returns to normal when the infected tissue is healed ⁵.

1.1 Acute inflammation

At a site of injury, granulocytes such as NØ, eosinophils, and basophils are recruited rapidly to neutralise and remove harmful agents such as bacteria or other inflammatory stimuli derived from the host immune system. Resolving the inflammation is a tightly-regulated process which involves activation and production of proteins important for cell signalling to enable clearance of dead cell debris thereby resulting in tissue homeostasis. Restoration of tissue homeostasis via immune regulatory molecules such as anti-inflammatory cytokines is a finite process which is controlled by a range of cellular and biochemical mechanism designed to remove the inflammatory stimuli as soon as the immune system is activated ⁶ (figure 1).

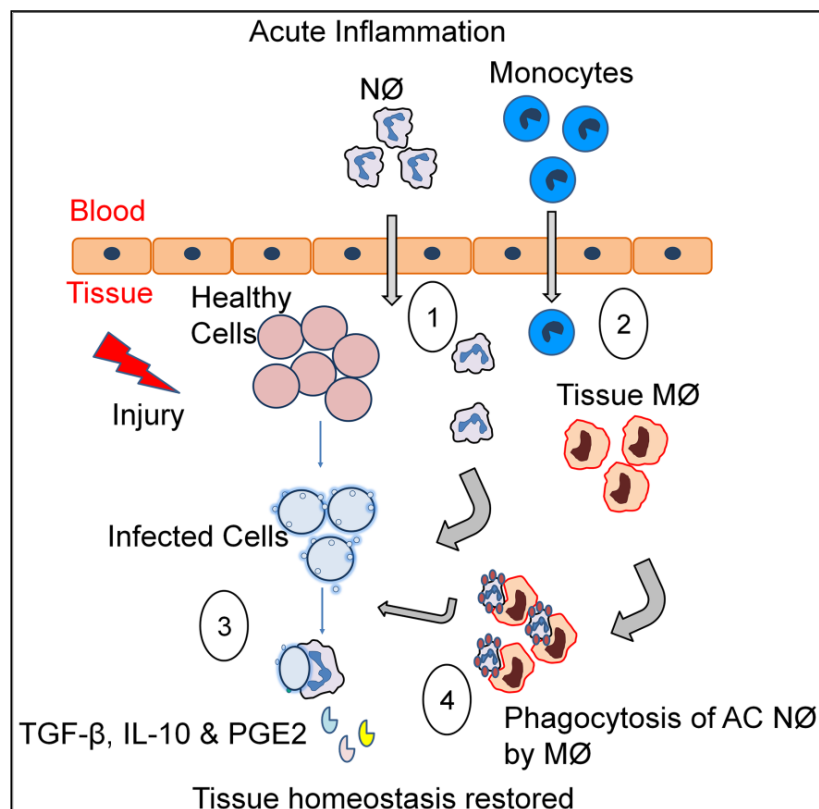


Figure 1: Illustration of acute inflammation pathways

Following an infection or injury, the inflammatory process is triggered in the host immune system with the aim to eliminate the pathogenic insult and the damaged tissues and/or cell debris. In acute inflammation, upon sensing the inflammatory stimuli : 1) NØ are recruited from the blood to the tissue to attack and clear the pathogens, 2) NØ subsequently recruit monocytes from the circulating blood which become differentiated into MØ, 3) At this stage, the pathogens and infected cells are phagocytosed by the NØ and become apoptotic (AC). 4) MØ present in the tissues uptake and engulf the apoptotic NØ and thereby suppress inflammation via their release of anti-inflammatory mediators such as Transforming Growth Factor beta (TGF-β1), Interleukin 10 (IL-10) and prostaglandin E2 (PGE2) which ultimately leads to healing of the damaged tissue.

1.2 Chronic inflammation

If acute inflammation fails to resolve effectively or if inflammatory stimuli persist the production of pro-inflammatory cytokines are chronically triggered leading to dysregulation of tissue homeostasis mechanisms resulting in chronic inflammatory diseases such as chronic periodontitis, rheumatoid arthritis, cardiovascular diseases, atherosclerosis, neurodegenerative diseases and other systemic diseases⁷⁻¹⁴. Failure of any of the phases (as described in figure 1), such as NØ undergoing apoptosis or alteration in apoptotic cell (AC) surface ligand expression required for phagocytosis or modification of chemical mediators misleading the recruitment of professional phagocytes, might inhibit the repair of inflamed tissue leading to the release of toxic cellular contents which cause further tissue destruction (figure 2)¹⁵⁻¹⁷. Therefore, understanding the mechanisms involved in

the resolution of inflammation will provide important insight into the role of associated cell and molecular mediators involved in achieving the restoration of tissue homeostasis and hence may identify novel therapeutic targets for use in the treatment of chronic inflammatory diseases.

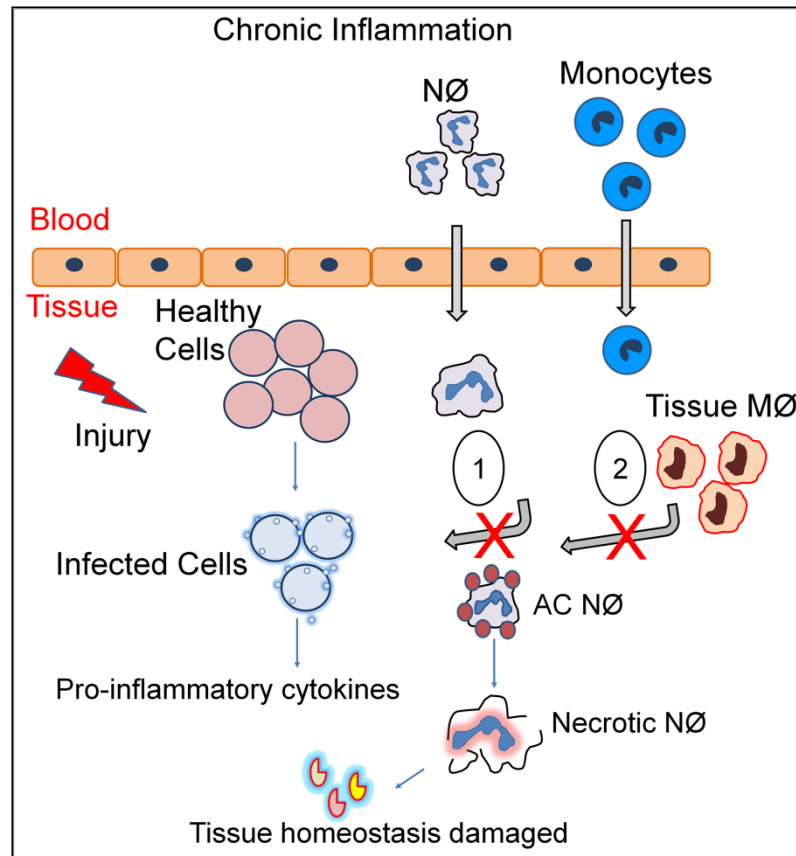


Figure 2: Illustration of chronic inflammation pathways

Following an infection or injury, inflammation is triggered in the host immune system which aims to eliminate the pathogenic insult and the damaged tissues or cell debris. Failure of any phases in acute inflammation might result in chronic inflammation. E.g. as shown in this diagram if: 1) NØ fail to sense the pathogens or infected cells or 2) MØ recognition of AC NØ were inhibited. Failure of either of these events might trigger the discharge of pro-inflammatory cytokines causing further inflammatory process activation and associated damage to the tissues.

1.3 Mechanisms of resolution of inflammation

Inflammation resolution is a tightly-regulated process involving apoptosis of recruited cells and rapid removal of AC and clearance of activated inflammatory cells. Recognition of pathogenic insults by tissue-resident immune cells such as mast cells and MØ along with the recruitment of NØ promotes anti-inflammatory mediator release thereby leading to tissue homeostasis. The following phases describe the process of inflammation regulation.

Phase I: Tissue MØ alert NØ following pathogenic insult

At a site of injury, e.g. in inflamed or infected skin, the invading foreign organisms or particles are sensed by specialised receptors present in the resident MØ and mast cells in the host. MØ are equipped with the pattern recognition receptors (PRRs) such as Toll-like receptors (TLRs), C-type lectin receptors and membrane-bound surface receptors which recognise the pathogen-associated molecular patterns (PAMPs) and damage-associated molecular patterns (DAMPs) ¹⁸. DAMPs result from the release of cytoplasmic and nuclear contents from the infected cells and these can initiate the inflammatory response by alarming resident phagocytes. Following this, the MØ produce TNF- α , interleukin-6 (IL-6), CXCL1 and CXCL2 to alert and recruit NØ present in the vasculature ¹⁹.

Phase II: NØ attract monocytes

NØ are the first cells recruited to the site of inflammation and they rapidly migrate from the blood stream to the site of infection via extravasation. NØ migration from the blood to the infected site is guided by various chemoattractants released by the invaded pathogens, e.g. N-Formylmethionine-leucyl-phenylalanine (FMLP) or by the activated resident MØ at the site of inflammation e.g. CXCL8 ^{20, 21}. To execute a timely recruitment of the NØ to the site of infection, increased blood flow and increased permeability occurs by dilation of the blood vessels and this promotes the release of plasma proteins together aiding the NØ rolling and adhesion cascade ²².

The initial key events involved in NØ migration are weak adhesion to the inner surface of the endothelium allowing slow rolling along the surface of the vessel wall and firm adhesion and spreading to initiate intravascular crawling and finally transmigration through the extravascular space. To accomplish these events mediators such as selectins, cytokines, and integrins play a major role ²³.

NØ use two types of defence against the invaded or infected agents. Oxygen-dependent mechanisms, the Fc receptors present on the NØ bind to the antibodies on the pathogen stimulating increased oxygen usage by a process called respiratory burst ²⁴. This influx of oxygen triggers the release of oxygen radicals referred to as reactive oxygen species (ROS) through the activation of NADPH oxidase which reduces the molecular oxygen (O₂) to superoxide radical (O₂⁻) thereby producing oxygen radicals which attack the bacterial organism. On the other hand, singlet oxygen radicals are produced by the fusion of myeloperoxidase (MPO) with a phagosome resulting in the secretion of MPO into the phagolysosome which produces hypochlorite, a toxic agent to assist in the killing of pathogens ²⁵. In the oxygen-independent mechanism, the NØ releases numerous

antimicrobial proteins such as cathepsin, lysozyme, lactoferrin and other hydrolytic enzymes required to break down the bacterial cell wall membrane and causing a deprivation of iron nutrients essential for the survival of the pathogens ²⁶. Other than the above two methods, NØ are also armed with the ability to generate a trap around the microorganisms by synthesising NØ extracellular traps (NETs). NETs have recently been widely studied for their role in the pathogenesis of infectious and inflammatory diseases ^{27, 28}. Using the mechanisms described above NØ are able to combat most microbial infections.

Also at this stage, NØ release LL-37, cathepsin G, azurocidin and α -defensins, molecules which are known to promote the inflammatory response in monocytes recruited from the circulating blood to the infected site ^{29, 30}. Circulating monocytes are recruited by a CCR2-dependent pathway which guides these cells to the site of infection and ultimately differentiate into MØ ³¹. MØ differentiation involves MØ colony-stimulating factor (M-CSF), granulocyte–MØ colony-stimulating factor (GM-CSF) and other cytokines which prepare the differentiated MØ with various receptors required for resolving the inflammation ³².

Phase III: Viable NØ to apoptotic NØ

The lifespan of an emigrated NØ is rather short and cells rapidly undergo apoptosis. At this stage, lipoxins are released by other resident cells such as platelets and endothelial cells to inhibit NØ influx and promote infiltration of monocytes ³³. Following the activation of NØ by resident MØ, the NØ releases annexin I from tertiary granules to promote their own death by apoptosis. The expression of annexin I is followed by other AC death markers such as phosphatidylserine (PS), a well-known marker which reveals AC death. At this phase, lipoxin A4 also contributes to the enhancement of apoptotic NØ uptake by MØ and inhibits CXCL8 release, a NØ chemoattractant ³⁴.

Phase IV: Restoration of tissue homeostasis

Clearance of AC is a vital phase in the inflammation resolution process necessary for regulating the restoration of the extracellular matrix. NØ undergoing apoptosis release 'find-me' signals and display 'eat-me' signals that enable MØ receptors to recognise the dying cells ³⁵. Various receptors such as phosphatidylserine receptors (PS-R), CD14, CD36, ICAM-3, tyrosine kinase receptor, integrins and complement receptors have been found to participate in recognising AC-associated molecules either directly or indirectly using soluble molecules ³⁶⁻⁴⁰. The uptake and phagocytosis of AC promotes the release of anti-inflammatory agents such as TGF β , IL-10, PGE₂, and vascular endothelial growth factors (VEGF). For the inflamed tissue to return to normal tissue homeostasis the mediators released by the phagocytosis process have been reported to have anti-inflammatory and pro- resolution properties which suppress further inflammation and clear

the inflammatory debris^{33, 41}. Notably the failure of the clearance phase has been linked with the pathogenesis of several autoimmune and chronic inflammatory diseases (figure 3)^{42, 43}.

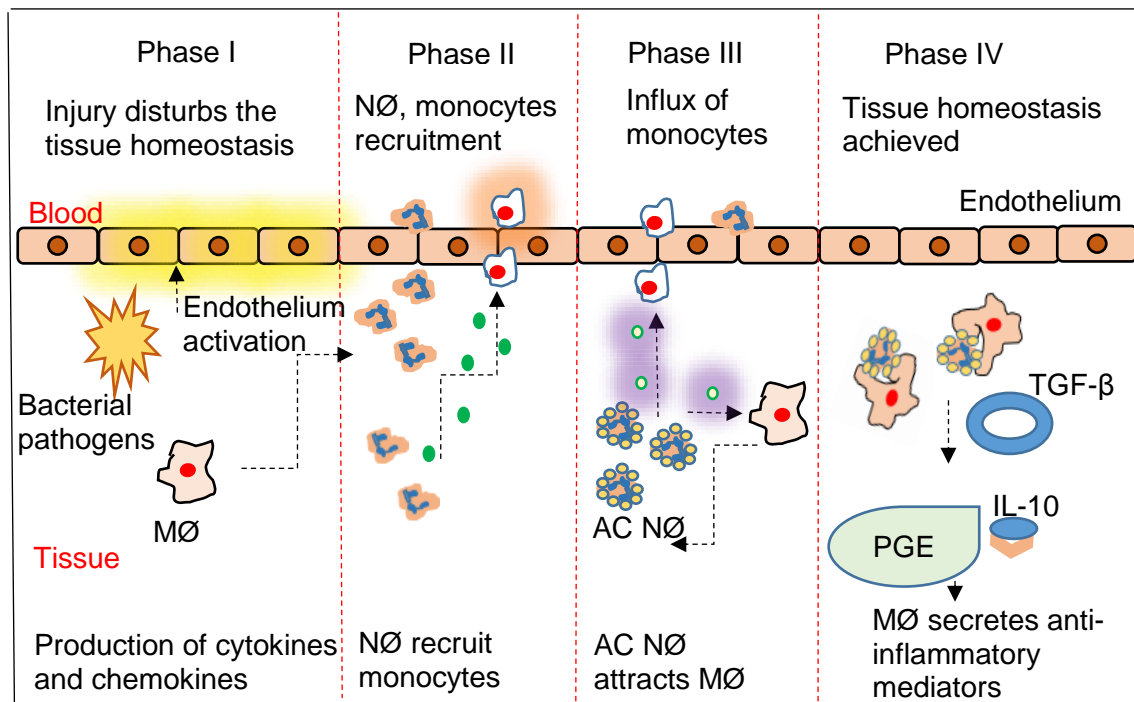


Figure 3: Phases involved in acute inflammation and its resolution

Phase I: upon tissue injury, the resident MØ are the first cells to sense the disturbance in tissue homeostasis. This is followed by the activation of endothelium by upregulation of adhesion molecules on their surface, sending signals to alert NØ by stimulating cytokines and chemokines. Phase II: Recruited NØ secrete granule contents such as LL-37 and azurocidin to promote inflammatory monocyte extravasation. Phase III: Further infiltrations of NØ cease however influx of monocytes continues. MØ at this point have a control over the life span of NØ by producing pro- or anti- apoptotic signals. Phase IV: Apoptotic NØ taken up by the MØ by phagocytosis and MØ release anti-inflammatory mediators leading to tissue healing. Adapted from⁴⁴.

1.4 Chronic inflammatory diseases

Considerable research has investigated the function of phagocytes in relation to their anti-microbial ability and promoted AC clearance, leading to the production of anti-inflammatory mediators essential to “turn off” the inflammation to enable tissue healing⁴⁵⁻⁴⁹. Understanding of the inflammatory mechanism provides potential therapeutic strategies to promote healing in chronic inflammatory diseases^{42, 50}. Due to the occurrence of numerous microorganisms in the oral cavity followed by the stimulation of inflammatory agents, periodontal disease (PD) serves as an excellent model to study host-pathogen interactions in relation to AC clearance mechanisms and inflammation.

1.4.1 Periodontal disease (PD)

PD is a multifactorial disease characterised by an aberrant inflammatory immune response to plaque bacteria. The periodontium is composed of dentine, cementum, gingiva, periodontal ligament and alveolar bone (figure 4). Disease progression in the periodontium results in loss of these key supporting tissue structures⁵¹. PD is highly prevalent affecting 90% of the worldwide population⁵². Furthermore, a recent large Adult Dental Health Survey conducted in the United Kingdom estimated that 45 percent of adults are prone to PD as characterised by periodontal pocket measurement using a periodontal probe, an instrument used to measure the depth of the pocket space between the tooth and gum to detect the severity of periodontitis^{53, 54}. Notably a periodontal pocket depth exceeding 6-7mm in addition to bone loss is considered as an advanced PD (figure 4)⁵³.

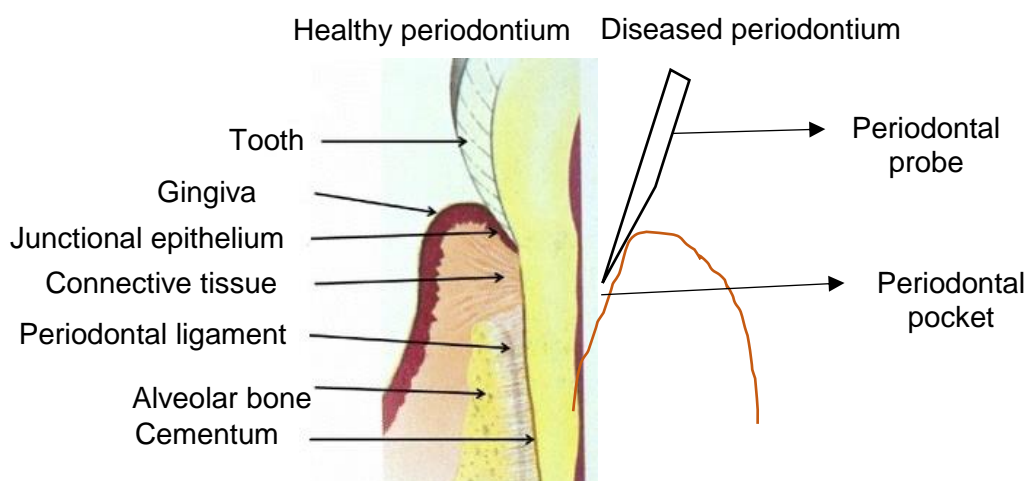


Figure 4: Structure of the periodontium

The main components include the gingiva which surrounds the tooth, cementum surrounding the root of the tooth, alveolar bone which provides the bony housing for the tooth and the periodontal ligament (PDL). The PDL enables anchoring of the tooth root to the alveolar bone. Adapted from⁵¹.

In the 1960's the understanding of the epidemiology of PD highlighted that: a) the development of gingivitis, frequently, but not always, progressed to periodontitis leading to periodontal pocket formation, bone loss and subsequent loss of teeth; b) the prevalence of periodontitis increased with age as tooth loss occurred predominantly after the age of 35; and c) that almost all adults were susceptible to severe periodontitis^{55, 56}. However, advances in periodontal research have now changed our understanding of the relationship between gingivitis and periodontitis in regard to the role of the immune system.

Goodson *et al.* (1982) developed the "burst" theory which concluded that not all gingivitis cases progressed to periodontitis. Underpinning this were two models: a) contained gingivitis- where few inflamed gingival sites "burst" to cause severe periodontitis followed

by tooth loss, and b) stable gingivitis – where many inflamed gingival sites continue to be free of any destruction of tooth or bone for their lifespan⁵⁷. Following Goodson (1982), Prayitno (1993) *et al.* in the early 1990s conducted research into the periodontal health of students and tea pickers evaluating whether gingivitis always progressed to severe PD⁵⁸. Data indicated that gingivitis was less prevalent in students whereas chronic periodontitis was common in both the groups suggesting that gingivitis was a poor predictor of progression to periodontitis⁵⁸. Later developments in dentistry have utilised advanced technology such as dental X-rays and intraoral X-rays to differentiate diseased gums from normal healthy gums⁵⁹.

Traditionally, the periodontal epithelium has been considered as a passive, physical barrier which protects underlying tissue from bacterial invasion. However, stimulating this tissue with bacterial components results in epithelial responses leading to rupture of the barrier⁶⁰. In response to inflammatory stimuli e.g. periodontal pathogens, the epithelial cells alter their proliferation and differentiation to facilitate restoration of tissue homeostasis. Research, however, indicates that while the epithelium has a barrier function it also plays an active role in innate host defence⁶¹. Subsequently, further study on the interaction of the periodontal epithelium with the immune system will aid our insights into mechanisms involved in regulating oral health and disease.

1.4.2 Pathogenic mechanisms in PD

To begin to understand the pathogenesis of periodontitis it is important to consider how inflammatory responses and immune mechanisms are regulated. Since complex mixes of pathogens are associated with the progressive forms of the disease, it is not clear which specific pathogen(s) is/are responsible for pathogenesis. Furthermore, the disease is also the result of the host response combined with the presence of bacteria. This is highlighted by the fact that there have been cases where individuals have the presence of certain microorganisms yet have no signs of disease, suggesting that immune- inflammatory responses drive the disease process⁸. Moreover, results from studies of twins have demonstrated that both environmental and genetic factors may also influence the clinical development of PD⁶². A study by Loe demonstrated that destruction of the periodontal tissue occurs in two ways, via a direct mechanism and an indirect mechanism⁶³. The production of histolytic enzymes, cytotoxic agents and lethal metabolites by plaque bacteria affects directly the metabolism of the normal tissue which in turn activates inflammatory responses. It has been proposed that subsequent immunopathological responses, followed by the direct mechanism in addition to the endogenous enzymes indirectly lead to initiation and progression of periodontitis⁶³.

Whilst there has been much research concentrating on the regulation of immune mechanisms and inflammatory responses in the pathogenesis of periodontitis, it is important to consider the inflammatory mediators involved in the development of the disease. Upon bacterial invasion of the gingival region, lipopolysaccharide (LPS), proteases and other toxic components from bacteria stimulate local mast cells to produce TNF- α and other potent pro-inflammatory mediators such as histamine, cytokines, chemokines, prostaglandins and matrix metalloproteinases (MMPs). Released mediators recruit inflammatory phagocytic cells (e.g. N \emptyset) and subsequently, these leukocytes release relatively high levels of MMPs which destroy the gingival tissues via their deleterious effects on connective tissue and bone metabolism⁶⁴. At this point, it is important for the host immune system to remove or reduce the microbes as, if this is unsuccessful, tissue redness, swelling and bleeding occur. Failure to resolve inflammation may be due to poor innate immune responses from the host or due to environmental modifying factors which prevent tissue repair and remodelling. This project aims to understand the poor inflammation resolution by scrutinising M \emptyset phagocytosis mechanisms in the presence of periodontal pathogens and their products.

M \emptyset , and antigen-presenting cells trigger CD4 T helper cells to either reduce or increase the inflammatory mediators by producing cytokines. Immune mediators release subsequently affects prostaglandins, particularly PGE2 which plays a prominent role in the pathogenic mechanism of PD^{65, 66}. The activation of prostaglandins along with leukotrienes and cytokines triggers the cardinal signs of inflammation. At a later stage of inflammation, PGE2 and prostaglandin D2 (PGD2) promote anti-inflammatory mediator release by inducing the production of key factors such as lipoxins, resolvins, and protectins which activate homeostatic mechanisms³³.

The nuclear factor- κ B (NF- κ B) ligand (RANKL), a member of TNF- α superfamily, is involved in activation of osteoclast differentiation and stimulation in periodontitis patients' leads to degradation of alveolar bone⁶⁷. Additionally, IL-8, GM-CSF, IFN- γ are reported to be hyperactive in peripheral N \emptyset of periodontitis patients indicating the type and level of cytokines present determine the nature of the periodontal inflammation⁶⁸. Interestingly Page differentiated periodontal health and disease by the production of pro- and anti-inflammatory cytokines⁶⁹. High levels of pro-inflammatory agents, PGE2 and MMPs and relatively low levels of anti-inflammatory cytokines and tissue inhibitor of metalloproteinases (TIMPs) are indicated as causative of periodontitis while the reverse characterises periodontal health. However, recent research reported other than pro-inflammatory, the anti-inflammatory cytokines were also present in higher levels in periodontitis patients contributing to the tissue destruction due to lack of balance between these mediators (Table 1).

Cytokines present in periodontal disease	References
IL-1 β	70, 71
TNF- α	72-74
INF- γ	75-77
PGE2	78-80
MMPs	81-83
IL-6	72, 84, 85
TGF- β	86-88
IL-8	72, 89, 90
IL-12	91, 92

Table 1: List of inflammatory mediators reported to be in PD

The table presents the pro-inflammatory and anti-inflammatory cytokines which if in excess could result in periodontal tissue damage.

1.4.3 Oral Biology and Inflammation

Gingivitis can be initiated by the formation of plaque (bacterial biofilm) at the gingival surface. Whilst bacteria appear to be a major aetiological factor in oral disease, significant literature suggests that it is the host inflammatory responses that drives the pathogenesis⁹³⁻⁹⁵. Subsequently, it has been proposed that the activation of the innate immune system due to bacteria-derived factors plays a major role in triggering inflammation in the PD patients⁹⁶. The significant tissue recruitment of N \emptyset due to the production of IL-8 from the periodontal epithelial cells paves the way for the trafficking of immune cells⁹⁷. Consequently, the presence of large numbers of N \emptyset is either primed by bacterial proteases or an inflammatory stimuli in the periodontal environment triggering the cells to produce pro-inflammatory mediators or undergo necrosis exacerbating the tissue damage. Furthermore, the oral microorganisms have been shown to evade M \emptyset by inducing activation of protein kinase A via cyclic AMP-dependent pathway⁹⁸. Protein kinase A activation inhibits the secretion of nitric oxide which is essential for M \emptyset killing of pathogens⁹⁹. Additionally, periodontal tissue resident cells such as gingival fibroblast, epithelial cells, and periodontal ligament fibroblasts have been shown to release pro-inflammatory mediators such as IL-1 β , IL-6, IL-8 and TNF- α on encountering bacteria agents¹⁰⁰.

Although, the above-mentioned studies suggest that aggressive inflammation is an important factor it is also vital to note that to initiate the inflammation the presence of microorganisms is essential. Hence, knowledge of the association between bacterial species and PD will advance our focus on virulent species that contribute to the oral infection.

1.4.4 Bacterial aetiology of periodontitis

Around 500 bacterial species have been reported as being present in plaque from beneath the gingival margin and this includes Gram-positive, Gram-negative, aerobic, anaerobic microbes along with traces of yeast ¹⁰¹. Certain bacteria including ones from the genera *Bacteroides*, *Actinobacillus*, *Eikenella*, *Fusobacterium*, *Capnocytophaga*, and *Eubacterium* are known to adhere to the tooth surface and their involvement is associated with deep periodontal pockets which eventually leads to the destruction of the tooth's supporting healthy tissues. Depending on the tooth position the level of bacterial accumulation and retention varies. The combination of various bacterial species reports that Gram-negative bacteria or the anaerobic organisms are not the only microbial species that contribute to periodontitis. Moreover, the mechanism by which gingivitis transits to aggressive periodontal disease is unclear. The accumulation of large numbers of bacterial species in the gingival region is now subsequently associated with gingivitis and gum inflammation ¹⁰². However, studies analysing dental plaque samples using molecular techniques such as 16S rRNA sequencing identified an even more diverse number of bacterial species in the subgingival region suggesting that a greater number of species in the microbial environment of the tooth are yet to be characterised ¹⁰³.

Bacterial virulence factor expression is dependent on the nature of the environment. Strains of pathogenic species can sense environmental cues and this, in turn, regulates the network of genes which modulates virulence factor production ¹⁰⁴⁻¹⁰⁶. Socransky *et al.* originally proposed that aggressive PD was strongly associated with two pathogens *Aggregatibacter actinomycetemcomitans* (in juvenile periodontitis) and *Porphyromonas gingivalis* (*P. gingivalis*) (adult periodontitis) ¹⁰⁷. Later, the same study grouped the oral microbiota into a complex and proposed that each complex is identified with a colour based on their level of virulence associated with periodontal disease. In this microbiota complex, *Porphyromonas gingivalis*, *Tannerella forsythia*, and *Treponema denticola* showed the strongest relationship with PD based on association studies, elimination of lesions, host response, virulence factors and animal studies ¹⁰⁷. Additionally, genome sequencing studies of oral bacteria were applied to understand the pathogenesis of the subgingival microbiota. In these genome sequencing studies, 15 environmentally important oral microorganisms were studied and among these *A.actinomycetemcomitans* and *P. gingivalis* were selected for determination of their complete DNA sequence. Data

generated provided new insight into metabolic pathways and their potential virulence mechanisms¹⁰⁸. For this reason and their ability to manipulate genetically quickly, *P. gingivalis* was used to study its impact on host immune cells within PD¹⁰⁹⁻¹¹¹.

1.4.5 *Porphyromonas gingivalis*

P. gingivalis, a Gram-negative anaerobic rod-shaped bacterium, is a virulent pathogen involved in inflammatory oral infections in humans¹⁰⁷. Recent studies have shown that *P. gingivalis* can reside inside epithelial, endothelial and smooth muscle cells without inducing apoptosis for a maximum period of 48 hours however infected host cells do become activated^{112, 113}. The ability to invade host cells intracellularly demonstrates one of the approaches *P. gingivalis* uses to escape the host immunity. So far invasion of *P. gingivalis* has been demonstrated in human gingival epithelial cells, periodontal ligament, fibroblasts and aortic endothelial cells^{60, 114-117}.

P. gingivalis components such as fimbriae, LPS, proteases, haemagglutinin adhesion domains, outer membrane proteins and exopolysaccharides have been reported to participate in disrupting the regulation of host immune responses¹¹⁸⁻¹³⁰. The proteases of *P. gingivalis* include enzymes such as collagenase, trypsin-like cysteine protease and gelatinase which are responsible for the destruction of periodontal tissues^{95, 131}. Among all the proteases, gingipains composed of cysteine proteases, account for 85% of the extracellular proteolytic activity from *P. gingivalis* and they significantly contribute to the damage of the tooth's supporting tissues by the colonisation in the periodontal pockets¹³². Moreover, the most commonly studied *P. gingivalis* components are LPS and gingipains due to their activity contributing to the pathogenesis of PD by eliciting inflammatory mediator production from immune cells and causing destruction of the inflamed periodontal tissue¹³³⁻¹³⁵.

1.4.5.1 *P. gingivalis* LPS

Lipopolysaccharide (LPS), present in the outer membrane of Gram-negative bacteria, contributes to the stimulation of the host innate immune response by binding to the resident cells present in the periodontal tissues resulting in the synthesis of pro-inflammatory mediators¹³⁶⁻¹³⁸. *P. gingivalis* LPS has been implicated in activating human monocytes via CD14-dependent pathways¹³⁸. However, in non-myeloid cells such as human endothelial cells *P. gingivalis* LPS stimulates weaker expression of E-selectin and interleukin-8 (IL-8) secretion due to the expression of low copy numbers of membrane CD14 (mCD14) compared with monocytes. Furthermore, the endothelial cells on treatment with *Ec* LPS and higher dose of *P. gingivalis* LPS resulting in inhibition of E-selectin expression suggesting that *P. gingivalis* LPS might be an antagonist for human endothelial cells¹³⁹. Moreover, the addition of MY4 (anti-CD14 antibody) in human

endothelial cell cultures resulted in inhibition of the E-selectin response indicating the requirement of CD14 in eliciting E-selectin expression ¹⁴⁰. However, soluble CD14 (sCD14) has been demonstrated to promote LPS-induced responses in human epithelial and endothelial cells through LPS being transferred to soluble CD14 from the LPS-lipopolysaccharide binding protein (LBP) complex ¹⁴¹. Collectively, these data suggest that CD14 either in the membrane or soluble form is able to stimulate cytokine levels in myeloid and non-myeloid cells.

Early work has suggested that the main function of CD14 is to serve as pattern recognition receptor (PRR) for LPS and in association with LBP it elicits a strong inflammatory responses as revealed by studies in heparinized human blood exposed to LPS ¹⁴². Furthermore, treating human blood with monoclonal antibodies (mAb) blocking CD14 inhibited the release and synthesis of TNF- α demonstrating that CD14 regulates LPS-mediated inflammation in the innate immune response to bacterial components ¹⁴². Upon invading the host, bacteria are sensed by the immune cells via LBP which transfers the LPS to CD14. The CD14 present in both forms, mCD14 anchored to the plasma membrane by a phosphatidylinositol linkage and the soluble form sCD14 participate in endotoxin recognition ¹⁴³. At this stage, the CD14 divides the LPS to monomers and transfers the complex to Toll-like receptors, an important receptor for sensing foreign agents to elicit an immune response.

1.4.5.1.1 Toll-like receptors (TLRs)

TLRs are best characterised for recognising PAMPs along with CD14 and are located on the cell surface or in intracellular compartments of the cell. Based on the reported human and mouse TLR studies, the TLR4 intracellular signalling cascades were established: TLR4 signals via MD-2 (Lymphocyte antigen 96) protein through two pathways: i) the TIR domain-containing adapter protein (TIRAP) and myeloid differentiation primary response protein 88 (MyD88) pathway accelerates translocation of NF- κ B inducing expression of pro-inflammatory cytokine genes, and ii) the TIR-domain-containing adapter-inducing interferon- β (TRIF) – and their adaptor molecules (TRAM) pathway regulates interferon regulatory factor-3 (IRF-3) or NF- κ B translocation in an MYD88 independent pathway that effectuates the upregulation of pro-inflammatory cytokines (figure 5) ^{144, 145}.

Interestingly TLR4 deficient mice fail to respond to LPS from *E.coli* via peritoneal M ϕ and B cells indicating that TLR4 regulates endotoxin responses on phagocytic cells ¹⁴⁶. However, depending on the endotoxin present on the bacteria TLR recognition might differ, indeed *P. gingivalis* LPS has been shown previously to be detected by both TLR2 and TLR4 ¹⁴⁷.

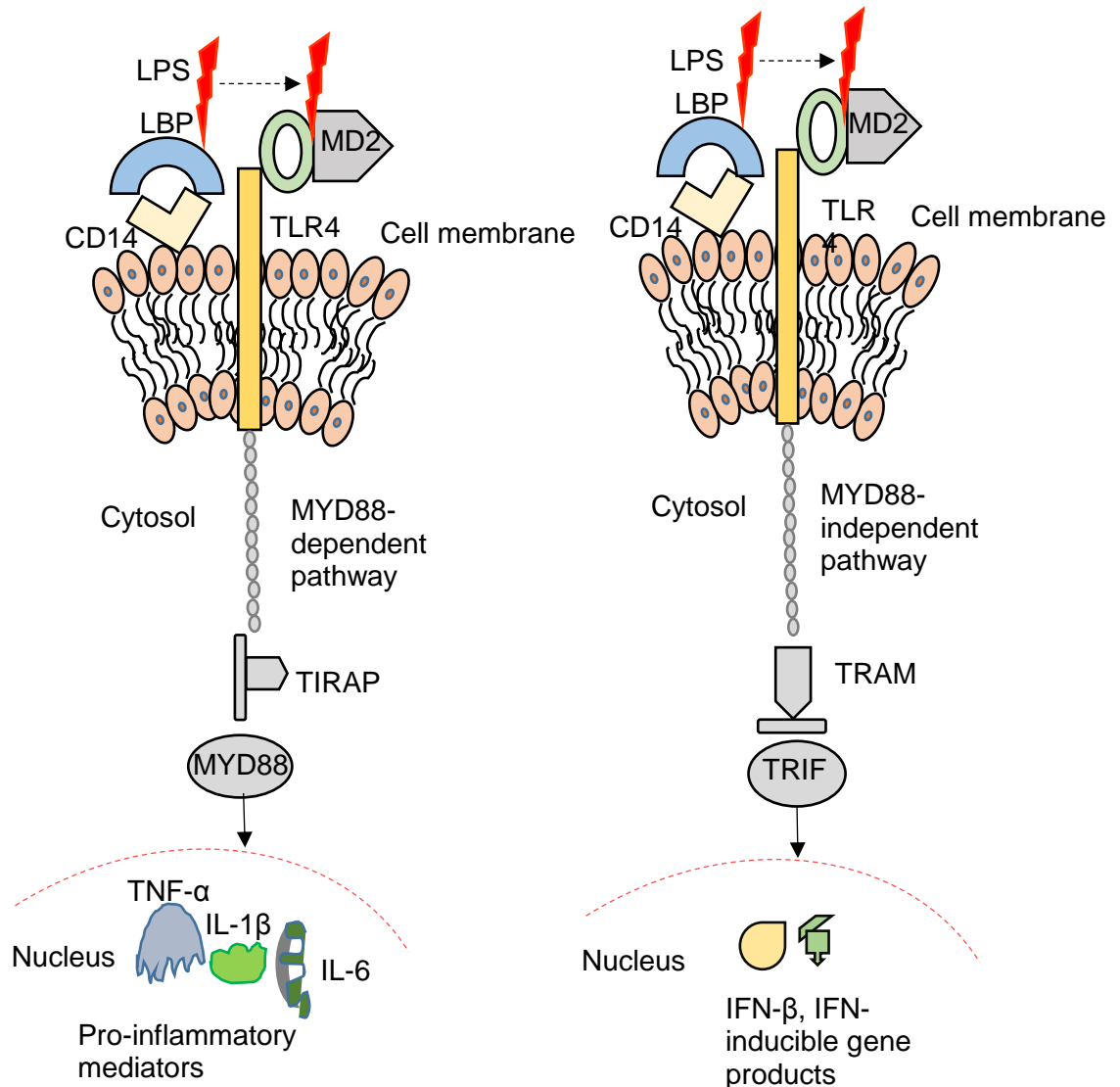


Figure 5: CD14 signals LPS binding through TLR4-MD2 pathways

Invading bacterial toxins such as LPS are sensed by the lipopolysaccharide-binding protein (LBP) mediated by CD14. Binding of lipid A to TLR4 associated MD2 complex signals through MYD88 and (TIRAP) to stimulate the release of cytokines and chemokines. The MYD88 –independent pathway engages the TRIF and their adaptor molecules TRAM to stimulates the activation of interferon (IFN)-regulatory factor (IRF3) resulting in the production of IFN-beta and the expression of IFN-inducible genes.

Initial reports characterised the role of TLR2 as a LPS signalling molecule for *P. gingivalis*. By treating murine M ϕ with *P. gingivalis* LPS there was an upregulation of TLR2 along with higher levels of TNF- α secretions¹⁴⁸. In addition, *P. gingivalis* LPS activates p38 mitogen-activated protein (MAP) kinase, a key component in intracellular signalling pathways in human monocytes but not in human endothelial cells or Chinese hamster ovary (CHO) cells transfected with TLR4¹⁴⁹. These findings suggest that though *P. gingivalis* LPS alerts the host immunity selective modification of the immune response was observed on the cellular level. On the other hand, extensive TLR4 research demonstrates the *P. gingivalis* LPS activates mouse Ba/F3 cells via the TLR4/MD2-

MyD88-dependent pathway and it was proposed that contamination from the proteases present in *P. gingivalis* LPS might have induced cell activation mediated by TLR2¹⁵⁰. Moreover, mCD14 participates with TLR4 in activating gingival fibroblast, though both TLR2 and TLR4 were expressed by the fibroblasts in the gingiva^{134, 151}. Additionally, *P. gingivalis* LPS has been shown to be activated weakly on monocytes/MØ compared with *E.coli* LPS due to the difference in the lipid A structure of *P. gingivalis* LPS which is composed of branched fatty acids and absence of phosphate groups compared with *E.coli* LPS^{121, 139, 148, 149, 152, 153}. However, both molecules have been shown to induce a similar level of inflammatory mediators¹⁵⁴.

1.4.5.2 Gingipains

Gingipains belong to the C25 peptidase family and are classified into two types based on their ability to cleave proteins at particular amino acid sequences¹⁵⁵. Arginine gingipains (Rgp) cleave after the ARG-amino acid with a capacity to degrade immunoglobulin and complement components, integrin-fibronectin-binding and cytokines. Arginine gingipains, based on their structure and molecular weight, are divided into two types RgpA and RgpB. RgpA, sometimes referred as HrgpA is ~95kda in size and is non-covalently complexed by catalytic and hemagglutinin/adhesion domains (figure 6). While RgpB is ~50kda and lacks hemagglutinin/adhesion domains, however, it does have a catalytic domain similar to RgpA (figure 6). There is also a lysine gingipain (Kgp) of molecular mass ~60kDa, which cleaves after LYS-amino acids and contains a catalytic and hemagglutinin/adhesion domains similar to RgpA (figure 6). Kgp has been reported to be the most potent of all the gingipains due to its ability to aid invasion of the host immune cells^{95, 122, 156, 157}.

1.4.5.2.1 Structure and homologies of gingipains

P. gingivalis genomic studies have revealed that RgpA, RgpB, and Kgp are encoded by separate gene loci and this is consistent in all *P. gingivalis* strains¹⁵⁸⁻¹⁶². RgpA and Kgp are composed of an Arg-specific or Lys-specific catalytic domain followed by a large C-terminal hemagglutinin/adhesion (HA) region (figure 6)^{158, 160}. On the other hand, RgpB consists of an Arg-specific catalytic domain followed by a small C-terminal fragment (figure 6)¹⁶³. All three gingipains carry a signal peptide and an N-terminal 'pro'-fragment at the beginning of their specific catalytic domains. The C-terminal HA region present in the RgpA and Kgp is responsible for the additional virulence factor by carrying biological specificities such as adhesion properties in the HA domain (figure 6)¹⁶⁴. RgpA and RgpB are 98% identical in their amino acid sequence in almost all *P. gingivalis* strains^{165, 166}. RgpA catalytic domains (RgpA_{cat}) and RgpB catalytic domains (RgpB_{cat}) share ~90% of amino acid sequence identity and ~75% of protein identity in the propeptide regions¹⁶⁴.

However, Kgp catalytic domains (Kgp_{cat}) share only ~30% of amino acid sequence identity with RgpA_{cat} and RgpB_{cat}.

Since, Kgp and RgpA contain the HA domain (figure 6) responsible for adhesion binding properties they have been studied for their ability to interact with host immune cells and cause disruption of the periodontal tissues compared with RgpB protease, which lacks the HA domain (figure 6) ^{162, 163, 167}.

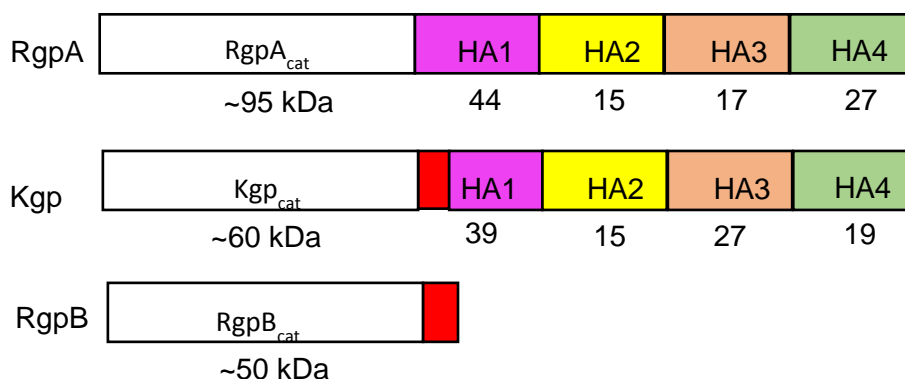


Figure 6: Structure and homologies of gingipains

Three forms of gingipain are depicted with catalytic domains (cat) (open boxes) with a molecular weight in kilodaltons (kDa) followed by four regions of hemagglutinin adhesion domains (HA) denoted in coloured boxes. The numbers found below the HA1 to HA4 domain marks the specific peptide regions for the gingipains. The homologies shared between the gingipains are identified using the same colours. Adapted from ^{168, 169}

1.4.5.2.2 Hemagglutinin adhesion domains (HA)

HA domains have been shown to be responsible for the adhesion and lysis of erythrocytes demonstrating the ability of HA domains to bind haemoglobin to acquire iron and protoporphyrin IX (PPIX) for their own survival ^{170, 171}. Other than HA domains, fimbriae and outer membrane vesicles have been observed to participate in the adherence to erythrocytes and epithelial cells ¹⁷²⁻¹⁷⁴. The hemagglutinin proteins (HagA) are the primary reason for the black pigmentation of the colonies grown on blood agar plates ¹⁷⁵. HagA proteins produced from *P. gingivalis* invasion on the host immune cells helps in survival of the bacteria by binding to erythrocytes thereby providing haem for the bacterial survival and resulting on haemolysis. Data also indicates that HagA proteins are involved in mediating the binding and arrest of immune cell functions in the initial phases of *P. gingivalis* invasion ^{164, 176}. Both RgpA and Kgp have been described for their ability to bind to haemin, using purified proteins such as monomeric and heterodimeric forms ¹²⁹. In addition, both RgpA and Kgp lose their ability to bind to haemin on denaturation through boiling indicating the vital role of the HA region binding affinity for destruction of tissues ¹⁷⁷. For both RgpA and Kgp, the specific region of haemoglobin-binding to gingipains was identified as the HA2 domain, more precisely the Kgp15/Rgp15 region (figure 6). Kgp has

been suggested as the major active haemoglobinase in *P. gingivalis* due to its ability to cleave haemoglobin with the highest efficiency, data obtained using the *kgp*⁺ *rgpA*⁻ mutant strain in comparison to the *kgp*⁻ *rgpA*⁺ mutant strain ¹⁷⁸.

1.4.5.3 Gingipain effects on host immune cells

Extensive research on gingipain biology has shown that these proteases enable bacterial evasion of the host immune system either by degrading the chemokine IL-8 and impairing NØ recruitment or by activating the kallikrein/kinin pathway ¹⁷⁹⁻¹⁸¹. The kallikrein/kinin pathway, a metabolic cascade releasing bradykinin, kallidin and vasodilator related peptides has been proposed to be involved in the pathophysiology of PD ¹⁸². Gingipains activate kallikrein/kinin pathways by enhancing vascular permeability and triggering blood coagulation at gingival sites ¹⁸³. Furthermore, modulation of IL-8 on human NØ via slow degradation, by soluble form of gingipains, and quicker degradation by membrane-associated gingipains, demonstrates that gingipains also target inflammatory mediators by regulating the cytokine networks in the host ¹⁸⁴.

Gingipains have also been implicated in inducing AC death in cells e.g. bovine coronary artery and human microvascular endothelial cells, human gingival fibroblasts and human gingival epithelial cells ¹⁸⁵⁻¹⁸⁷. In contrast, gingipains have been shown not to induce apoptosis in human NØ and THP-1 MØ ^{188, 189}. Subsequently it has been suggested that the reason for the delayed or hyperactive or inhibited NØ apoptosis found frequently in the chronic periodontitis patients is due to gingipains attacking the immune system ¹⁹⁰⁻¹⁹².

1.4.5.4 Evasion of host immune system by gingipains

Gingipains have been shown to cleave IL-8 precisely at the N-terminal portion of 5- and 11-amino acid peptides by Rgp and 8-amino acid peptide at the N-terminal by Kgp resulting in low chemotactic activity ¹⁹³. This suggests that cleavage of IL-8, a chemoattractant for NØ might indirectly modulate NØ chemotaxis, resulting in a poor immune response. Additionally, cleavage of C5a complement receptor, another potent chemoattractant for NØ was also reported to be cleaved by gingipains on NØ ¹⁹⁴. In rheumatoid arthritis, C5a has been demonstrated to activate mast cells which in turn recruit NØ to the joints indicating a possible mechanistic association between periodontitis and rheumatoid arthritis ^{195, 196}. CD4 T cells participate in recognising MHC-II peptide complexes on MØ or dendritic cells and activate antigen presentation during an infection to play an important role in promoting an immune response. Gingipains are also known to suppress this immune response promoted by T cells by cleaving CD4 and CD8 and weakening the immune cells in response to the bacterial invasion ¹⁹⁷. A previous study also reports degradation of protease-activated receptors (PARs) by gingipains on oral epithelial cell lines ¹⁹⁸. PARs have been shown to participate in keratinocyte uptake and

engulfment of *E. coli*¹⁹⁹. Taken together, it is clear that the gingipains evade the host immune system by either modulating or cleaving the receptors essential to mediate the AC clearance mechanism of the immune cells. The project here focus on gingipains ability to effect MØ migration and phagocytosis activity which may explain the prevalence of poor inflammation resolution in periodontitis patients.

Subsequently studies on gingipains inhibitors might provide an insight into the role of gingipains contribution in the suppression of inflammation in periodontal disease.

1.4.5.5 Inhibition of gingipains, a potential treatment for PD?

As *P. gingivalis* is a major bacterium contributing to the pathogenesis of chronic periodontal diseases in adults, *P. gingivalis* surface components have been studied for their mechanisms in evading host immune responses which include involvement of gingipains and LPS^{179, 180, 188, 200, 201}. Subsequently several studies have proposed the possible use of gingipain inhibitors to prevent the virulence factor activity in host cells.

In the late 1990's, Potempa *et al.* observed that all chloromethane compounds inhibited all forms of gingipains (RgpA, RgpB, and Kgp)²⁰². P1 residues in the chloromethane compounds inactivated the gingipains however chloromethane-P2 residues exhibited some specificity in blocking gingipain protease activity. This suggests that depending on the peptidyl component of chloromethane compounds the degree of inhibition varied²⁰². Gingipains, named after clostripain, due to the structural similarities, were also inhibited by Aza-Lys and Aza-Orn derivatives of Aza-peptide Michael acceptors. Aza-peptide Michael acceptors were irreversible inhibitors specific for the cysteine protease family which inhibited Kgp gingipain and clostripain precisely²⁰³. The commonly used cysteine protease inhibitor in gingipain studies is N α -p-tosyl-L-lysine chloromethyl ketone (TLCK), which has been reported to inhibit caspase 3 activated apoptosis of gingipain-treated bovine coronary artery endothelial cells and prevents a CD31 reduction in gingipain-treated endothelial cells^{185, 204}. Proteinase inhibitors such as antithrombin III and human alpha-2-macroglobulin (α 2M) also block the activity of RgpA and RgpB while macroglobulin alpha-1-inhibitor 3 from rat plasma inhibited all three forms of gingipain proteases^{205, 206}. Moreover, antibacterial activities against gingipains are also observed with cystatin and cystatin-derivatives, cysteine protease inhibitors^{207, 208}.

1.4.6 *P. gingivalis* virulence factors in host immune cells

Though gingipains are essential for the colonisation of the host tissue, it is reported that other components of *P.gingivalis* such as lipoteichoic acids, haemagglutinins, fimbriae, capsules, LPS, outer membrane proteins, and their vesicles participate in driving the chronic inflammation observed in PD⁹⁵. *P. gingivalis* fimbriae have been reported to

modulate CD11b/CD18 on monocytes via TLR2 signalling²⁰⁹. In addition, the same work demonstrated that *P. gingivalis* fimbriae activates the CD14-TLR2 complex on CHO cells suggesting that fimbriae regulates the production of pro-inflammatory cytokines via TLR2 mediated activation of NF-κB. The lipid-A-associated protein from the haemagglutinin domain of the gingipains has been shown to be responsible for inducing increased levels of IL-6 in human gingival fibroblast and human peripheral blood mononuclear cells²¹⁰. IL-6 has been previously reported to be linked with tissue destruction in the gingival region of the periodontium⁷². Before colonisation, the bacteria adhere to the oral cavity firmly to avoid any resistance from the flow of saliva. The *P. gingivalis* capsules have been shown to participate in the adherence which is mediated by adhesins within the haemagglutinins. Based on the level of sugar the capsule components differ in the *P. gingivalis* strains²¹¹. A previous report suggested that capsules participate in the evasion of the host immune system through inhibiting phagocytosis of *P. gingivalis* by MØ treated with encapsulated components²¹². Elicited IgG antibody levels were found in mice injected with the vesicles from the outer membrane proteins of *P. gingivalis* through transcutaneous immunisation²¹³. Additionally, reduced alveolar bone loss was observed in IgG elicited mice suggesting a possible therapy for periodontal disease-associated bone degradation. While other *P. gingivalis* components, such as lipoteichoic acid, induce interleukin-1β and cyclooxygenase-2 in human gingival fibroblasts through activation of p38, peptidoglycan from *P. gingivalis* has been shown to induce increased IL-6 in mouse peritoneal MØ^{84, 85}. Therefore, the above studies suggest that invasion of *P. gingivalis* on the immune cells results in aberrant or exacerbated inflammation leading to bone loss in the alveolar region²¹⁴. If not resolved, this inflammation will drive chronic disease³⁵.

1.4.7 Periodontitis and chronic diseases: A Global burden

The World Health Organisation (WHO) predicts that by 2020 the major chronic disease such as cardiovascular disorders, diabetes, rheumatoid arthritis, cancer and chronic obstructive pulmonary disease will rise in incidence from 40% to 60%²¹⁵. Chronic inflammation plays a central role in the association of periodontitis with other chronic inflammatory diseases. Notably, bacterial toxins from periodontitis indicate that periodontal inflammation enhances metabolic dysregulation in other chronic inflammatory disease²¹⁶.

1.4.7.1 Periodontitis and Diabetes: Interrelationship

Chronic inflammation of the periodontium leads to progressive destruction of tissues in specific organs leading to life-threatening conditions. One such association is demonstrated by the poor glycaemic control in the periodontitis patients showing an increased risk for non-insulin-dependent diabetics²¹⁷. In addition, previous work has

stated that inoculating type II diabetic rats with periodontal bacteria results in bone degradation through increased expression of caspase-3 compared with diabetic rats without inoculation ²¹⁸. These data suggest that both diseases, i.e. periodontitis and diabetes, influence each other and this has been described previously by Preshaw *et al.* as a two-way "relationship" ²¹⁹.

1.4.7.2 Periodontitis and Atherosclerosis: A Complex relationship

Prevalence of cardiovascular problems in individuals with periodontitis is 25-50% higher compared with orally healthy individuals. Poor oral hygiene is a possible risk factor for periodontitis and the development of periodontitis is highly connected with atherosclerosis ²²⁰. Mounting evidence indicates that periodontitis influences the process of vascular inflammation ¹⁸¹. Notably, *P. gingivalis* can stimulate the host to produce proteases such as MMPs which deactivate cytokines. MMPs activated by *P. gingivalis* gingipains have been shown to stimulate IL-1 and TNF- α at the transcriptional level ²²¹. The initiation of the inflammatory response by MMP-1 (collagenase) in endothelial cells and other components of the artery wall is regarded as the first sign of atherosclerosis ²²². Furthermore, epidemiological studies indicate that bacterial components such as LPS and heat shock proteins (HSP) in serum lead to atherosclerosis development ²²³. As described earlier with regards to the pathogenesis of periodontitis LPS stimulates monocytes or M ϕ by binding to the CD14 receptor. CD14 in myocardial infarction patients exhibits an elevated frequency of allele T (-260) compared with controls ²²⁴. Secondly, cross-reactivity between *P. gingivalis* and HSPs produced by the endothelium demonstrates an additional role in inflammation of vascular tissue and hence in causing atherosclerosis ^{181, 225}. Finally, the involvement of reactive oxygen species in the periodontal lesions has been reported to influence tissue damage in the aorta of rats exhibiting higher levels of hexanoyl-lysine expression, a marker for lipid peroxidation on initiating atherosclerosis, including cardiovascular diseases ^{226, 227}.

1.4.7.3 Periodontitis and Rheumatoid arthritis: The mouth – joint connection

Increasing evidence suggests that periodontitis and rheumatoid arthritis share a common pathology as a result of cytokines and MMPs. Interestingly these effector molecules and inflammatory cytokine profiles appear to be raised in both diseases ²²⁸. *P. gingivalis* peptidyl-arginine deiminase (PPAD), a bacterial enzyme which has the ability to transform arginine residues in proteins to citrulline, generates citrullinated proteins directly contributing to bone loss in the development of rheumatoid arthritis ^{229, 230}. The human protein-arginine deiminase (PAD), an enzyme necessary for NET formation, together with PPAD are present in the periodontium region and mucosal oral epithelium ²³¹. Though the

mechanism requires further elucidation, *P. gingivalis* seems to be an important factor likely to be associated with citrullination of autoantigens in *in vivo* conditions ²³².

1.5 Apoptosis – An essential death in life

Apoptosis is a form of cell suicide and tightly-regulated programmed cell death occurs in the human body throughout life to support tissue development, growth and differentiation and pathogenic processes ²³³. The apoptotic machinery is proposed to remove 10^9 cells per day which comprise defective, aged or inflammatory cells in multicellular organisms ²³⁴. A cell undergoing apoptosis goes through physical, molecular and biochemical transformations to help the tissue-resident professional phagocytes such as MØ, NØ, dendritic cells and the non-professional phagocytes such as epithelial and endothelial cells recognise and phagocytose ^{235, 236}.

Apart from developmental and aging processes, cell death also occurs during a pathogenic insult or during traumatic tissue damage. Not all cells undergo death on receiving stimuli. Indeed, corticosteroids, steroid hormones which cause thymocyte cell death leave other cells unaffected ^{233, 237}. In *Caenorhabditis elegans*, damage in DNA fails to signal the P53 pathway to induce apoptosis in somatic cells due to the inactivation of caspase-dependent apoptosis pathways ²³⁸. This study shows that DNA damage does not always lead to AC death ²³⁸⁻²⁴¹.

When a cell undergoes death, its morphology changes. To begin with cell shrinkage occurs and studies using light and electron microscopy identified that pyknosis, condensation of chromatin and cell shrinkage, is the first noticeable characteristic feature of apoptosis ^{242, 243}. Initial stages of cell death also include the appearance of blebs on the plasma membrane. Upon apoptosis induction, the cell gets smaller in size with the nucleus condensing gradually until it segregates into smaller fragments, these are termed apoptotic bodies (figure 7). Aggregation of ribosomes, dilation of endoplasmic reticulum and vacuoles in the cytoplasm are also observed. The discharged apoptotic bodies are later ingested by professional phagocytes and digested by lysosomal pathways. If AC remain uningested necrosis can occur and this is a major causative factor for chronic inflammatory diseases ^{233, 242, 243}. Notably, for the above morphological changes to occur activation of caspases is necessary ²⁴⁴⁻²⁴⁷.

Caspases are one of the important enzymes involved in regulation of apoptosis. Caspase activation occurs either by intrinsic or extrinsic pathways. The intrinsic pathway is mediated by mitochondria hence they are also termed mitochondrial pathways. Intracellular stress, such as oxidative stress, activates caspase enzymes by the formation of the 'apoptosome' protein complex. The apoptosome is formed by the efflux of cytochrome C from the permeabilized outer mitochondrial membrane which binds to an

adaptor molecule known as apoptotic protease activating factor 1 (APAF-1) and pro-caspase-9^{248, 249}. On the other hand, extrinsic pathways are mediated by the death receptor pathways forming a death-inducing signalling complex (DISC). The extrinsic pathway is activated by death ligands such as TNF- α , FAS-L and TRAIL. The death ligands binds to the surface of the target cell through transmembrane death receptors (e.g TNF-R, Fas, Death receptors) resulting in the formation of DISC, composed of pro-caspase 8. Upon activation of the DISC or apoptosome, the accumulation of relatively inactive pro-caspases results in the release of active caspase into the cytoplasm to trigger the caspase cascades^{249, 250}. Caspases play an important role in apoptosis and it is also argued that they play an important role in causing changes in AC morphology^{243, 251-253}. Caspase-1 has been linked with pyroptosis, a highly inflammatory form of AC death which occurs following infection with bacterial compounds which causes DNA damage. This process has been demonstrated in J774A M \emptyset under *in vivo* condition²⁵⁴.

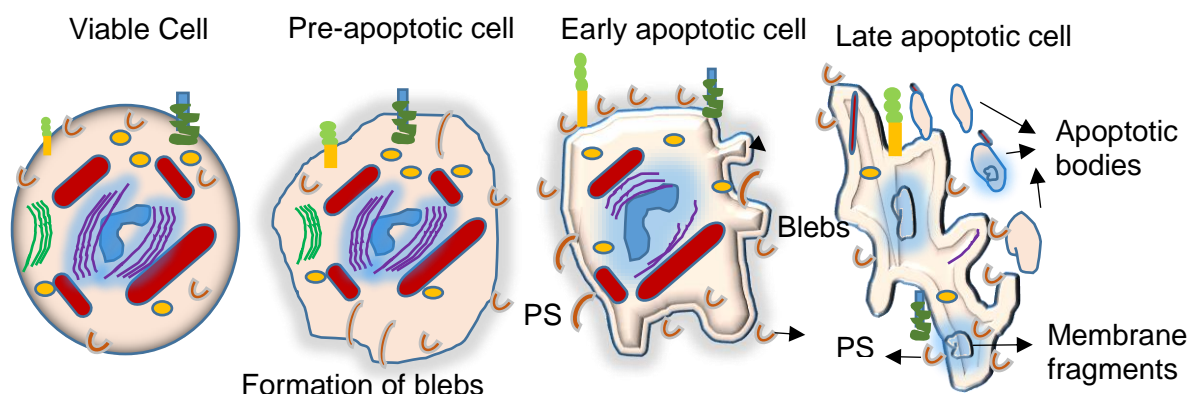


Figure 7: Stages of apoptotic cell death

Healthy viable cells undergo programmed cell death (apoptosis). Morphological and biochemical changes are two characteristic features which determine the process of cell death. During the early stages, the first observable morphological changes are shrinkage of the cell membrane, resulting in dense cytoplasm due to smaller cell size appearance. The important characteristic features of apoptosis are condensation of chromatin followed by the formation of blebs. In the later stages, extensive plasma membrane blebbing occurs and the cell fragments in preparation to separate and form apoptotic bodies, which contain cytoplasm with or without the nuclear membrane fragments. The apoptotic bodies will later be engulfed by M \emptyset . Phosphatidylserine, a traditional "Gold standard" biochemical marker is also observed on the external leaflet of the plasma membrane, flipped from the internal leaflet.

Of all caspases, caspase-3 (CASP3) was found to be the critical mediator of programmed cell death processes. Caspase-6 and -2 facilitate DNA fragmentation by triggering activation of DNase enzymes followed by degradation of nuclear lamina which results in cell shrinkage²⁵⁵⁻²⁵⁷. Importantly, caspase-3 mediates the uptake of MCF7 AC by monocytic THP-1 and human monocyte-derived M \emptyset (HMDM) cells by stimulating the release of lysophosphatidylcholine (LPC) mediated through the activation of the calcium-independent phospholipase²⁵⁸.

1.5.1 Apoptosis in the oral cavity

In the oral cavity host-bacterial interactions occur at the mucosal surface and studies of this have facilitated our understanding of the composition of the biological fluids and immune cell responses involved in this process. Notably, mucosal tissues including the gingival tissues of the oral cavity are exposed to a wide range of microorganisms. Recent evidence now indicates that local tissue apoptosis drives the regulation of immune-inflammatory responses in response to microbes, inhibiting the anti-inflammatory signals affecting the phagocytes at the site of infection ²⁵⁹.

Caspases, Bcl-2 family proteins, tumour necrosis factor receptor (TNF-R) superfamily, and adaptor proteins aid in regulating the apoptotic process ²⁶⁰. Gamonal *et al.* demonstrated that apoptotic MØ stained with the terminal TdT-mediated dUTP-biotin nick end labelling TUNEL technique remained positive for active caspase-3, Fas, FasL, p53, and chromatin condensation in the inflammatory infiltrate from periodontitis samples and negative in normal healthy controls suggesting that apoptotic mechanisms play a vital role in the inflammatory process associated with gingival tissue destruction detected in periodontitis patients ²⁶¹. Notably however, Bcl-2 presence was unaltered in both groups ²⁶¹.

Other than the regulation of apoptosis-associated enzymes, a dying cell exhibits AC associated molecular patterns (ACAMPs) which enable recognition and uptake by the phagocytic receptor cells for appropriate disposal.

1.5.2 Apoptotic-cell associated molecular patterns (ACAMPs) – ‘eat-me’ signals

Over the past few decades, it has become evident that the clearance of AC by phagocytes is a non-inflammatory process even though innate immune receptors are involved. ACAMPs are specifically a subtype of ligand that binds to PRR and hence are similar to PAMPs ³⁵. Additionally, Tennant *et al.* showed that anti-LPS Abs bind AC and so hypothesised that both PAMPs and ACAMPs share common epitopes ²⁶².

In the 1990s, the MØ vitronectin receptor (VnR), $\alpha_v\beta_3$ integrin was identified, through the use of antibody and peptide-mediated blockade. Data subsequently indicated that the MØ VnR played a significant role in recognition of AC ²⁶³. Various ‘eat-me’ markers on dying cells, soluble bridging molecules and their specific phagocytic receptors identified in recent years, highlight the remarkable complexity in efficient cell clearance. Discrimination of a dying/dead cell from a healthy cell requires specific markers generating a recognition ‘synapse’ between phagocytes and their target cells ²⁶⁴. It is not however clear whether a MØ modifies their receptor levels depending on the ligands that are expressed on the surface of AC. Understanding the role of AC-associated ligands as ‘eat me’ signals to

phagocytes will provide insights into the defective AC clearance potentially linked with periodontitis and other persistent inflammatory disease.

1.5.2.1 Phosphatidylserine (PS)

The major component of the cell membrane are phospholipids. PS is located at the cytoplasmic side of the plasma membrane and though quantitatively relatively low in cellular organelles it plays a vital role within the structures of biological membranes ²⁶⁵. Most immune cells, including monocytes, mature MØ, dendritic cells and activated B cells, express the PS receptor (PS-R) on their surface ²⁶⁶⁻²⁶⁹. Activation of protein kinase C in the cell modifies the PS by phosphorylation via caspase enzymes and triggers PS movement from the inner leaflet to the outer surface membrane. This phenomenon is one of the major biochemical reactions which occurs during programmed cell death ^{270, 271}. The translocation of PS from the inner to the outer leaflet of the plasma membrane is due to loss of aminophospholipid translocase activity in the inner leaflet and increased trans-bilayer movement of phospholipids requiring calcium as a mediator ^{272, 273}. Nevertheless, Bratton *et al.* reported that inhibition of extracellular calcium on NØ prevented the expression of PS on the outer surface suggesting that extracellular calcium along with the loss of inner leaflet of aminophospholipid translocase activity increase the expression of PS on the outer leaflet ²⁷⁴. Other than PS-R, brain angiogenesis inhibitor 1(BAI1), LDL-receptor-related protein 1 (LRP1) and calreticulin have all been proposed to bind directly to PS on AC ²⁷⁵⁻²⁷⁸.

PS-mediated ingestion of AC by PS-R MØ deactivates the pro-inflammatory mediators and thereby enhances expression of anti-inflammatory cytokines such as TGF-β1 in an autocrine/paracrine fashion promoting inflammation resolution ²⁷⁹. Notably engulfment of avidin-biotinylated coated erythrocytes were prevented in PS-blocked particles in MØ ²⁸⁰. Furthermore, the same study investigated that ligation of CD14, CD68, CD36, and α_vβ₃ integrin resulted in adhesion of particles however the particles were substantially engulfed only in the presence of PS along with the non-ligated receptors. The above studies indicate that several receptors are involved in recognising PS on the AC to promote binding and engulfment by phagocytes.

1.5.2.2 ICAM-3

The CD50 gene encodes the intercellular adhesion molecule 3 (ICAM-3), an immunoglobulin superfamily member gene present in humans. The first report of AC-associated ICAM-3 acting as an important ligand mediating recognition by MØ revealed that as leukocytes undergo apoptosis, surface expression of ICAM-3 reduces as it becomes active as an 'eat me' signal ²⁸¹. Moreover, membrane-distal Ig-like domains are the key region on apoptotic ICAM-3 for recognition by phagocytes. The distal Ig-like

domain of leukocyte ICAM-3 interacts with MØ leukointegrin LFA-1 to bind to viable cells but not for phagocytosis however adhesion/phagocytosis of AC were LFA-1 independent and also were not dependent on the ICAM-3 receptor $\alpha_d\beta_2$ on MØ²⁸¹. Recent research has shown that apoptosis stimulates release from dying leukocytes of ICAM-3 on extracellular vesicles in order to encourage MØ recruitment and phagocytosis of AC in addition to promoting a domain 1–2-dependent binding communication with phagocytes³⁷. This work revealed that using anti-ICAM-3 monoclonal antibodies or the absence of ICAM-3 results in defective MØ chemotaxis towards apoptotic leukocytes³⁷. Therefore, next to PS, ICAM-3 is the second AC associated molecule involved in the process of MØ recognition and clearance of dying leukocytes.

1.5.3 AC clearance receptors associated with phagocytes

Phagocyte recruitment towards AC involves various receptors expressed on the surface of MØ, soluble mediators and the 'find' and 'eat-me' signals associated with AC. In addition, healthy viable cells including phagocytes can also express 'don't eat-me' signals which can bind phagocytic receptors on MØ in order to suppress phagocytic uptake by other phagocytes. One of the key molecular features of the AC clearance is the expression of cell surface receptors expressed on the phagocytes that mediate AC binding and uptake. A defect in any of the receptors could lead to reduced AC clearance and hence resulting in disease. However, a few studies have investigated the phenotype of mice lacking AC clearance receptors^{282, 283}. Whilst some show no phenotype (e.g. scavenger receptor–A (SRA1^{-/-}) mice) perhaps as a result of other receptors taking over the role of SRA1, others (e.g. CD14^{-/-}; milk-fat-globule-EGF-factor 8, MFG-E8^{-/-}) show defective uptake of AC by phagocytes but not autoimmunity^{43, 284}. However defective clearance of AC and an autoimmune phenotype has been revealed clearly in the case of the C1q^{-/-} mouse and the TG-2^{-/-} mouse^{285, 286}. The glomerulonephritis mouse gene targeted to result in C1q^{-/-} and TG-2^{-/-} showed elevated number of glomerular apoptotic bodies compared to wild type. Also, lack of TG2 not only prevented the clearance of dying cells but also deficient in TGF- β , associated with the development of autoantibodies.

1.5.3.1 Scavenger receptor – CD36

CD36 is a scavenger receptor that also acts as a receptor for wide range of ligands such as long chain fatty acids and thrombospondin²⁸⁷. Previous research indicates that MØ utilise CD36 to recognise apoptotic NØ irrespective of whether their primary clearance mechanism utilises the PS-R or $\alpha_v\beta_3$ receptor²⁸⁸. Though PS is a potential candidate in facilitating AC uptake by MØ, CD36 on MØ participates in ingestion by interacting with membrane-associated oxidised PS (OX-PS) on AC. The Mass spectrometry analysis of apoptotic membranes showed that OX-PS is the ligand for CD36 suggesting that CD36

might be another possible MØ receptor involved in engulfment of AC ²⁸⁹. Thrombospondin (TSP), a multi-functional adhesive molecule helps in mediating adhesive interactions by acting as a “molecular bridge” between erythrocytes and monocytes/MØ ²⁹⁰⁻²⁹². TSP not only regulates platelet-platelet interactions but it also promotes HMDM recognition of aged NØ by binding to Glycoprotein VI (platelet) (GPVI) associated with platelet glycoprotein 4 and CD36 forming a trimeric complex ^{293, 294}. CD36’s function in AC clearance was also demonstrated by transfecting CD36 into human Bowes melanoma cells where it improved the ability to ingest apoptotic NØ, lymphocytes, and fibroblasts ²⁹⁵. Moreover, upon transfecting CD36 into the monkey COS-7 cells, which naturally have a limited capacity for phagocytosis, these cells now showed enhanced phagocytosis of AC underscoring the role of CD36 in the uptake of dying cells ²⁹⁵. As a potential oxidized low-density lipoprotein (oxLDL) receptor, CD36 binds to LDL, regulated by the myeloperoxidase–hydrogen peroxide–nitrite system of phagocytic cells (MPO-oxLDL), enabling the synthesis of foam cells and regulation of plaque build-up in atherosclerosis patients ²⁹⁶. Following application of anti-CD36 mAbs, foam cell generation was downregulated by ~80% and monocytes/MØ deficient in CD36 exhibited reduced binding of oxLDL by 40-60% compared with CD36 expressing MØ. These data implicated CD36’s significance in uptake of oxLDL and foam cell formation ²⁹⁷⁻²⁹⁹.

1.5.3.2 Low density lipoprotein receptor-related protein 1 (LRP1) CD91

CD91 acts as a signalling partner for calreticulin which itself cannot transduce intracellular signals as it is a non-transmembrane protein however combined they signal the uptake and removal of dying/dead cells ³⁰⁰. The CD91-calreticulin complex regulates the collectin family of innate immune proteins including C1q, surfactant protein A (SP-A) and surfactant protein D (SP-D) to enhance the function of pulmonary murine and human alveolar MØ in the clearance of AC *in vitro* ³⁰¹. SP-A and SP-D maintain tissue homeostasis in the lungs by binding to signal inhibitory regulatory protein α (SIRP α) through their globular head domains thereby downregulating Src-family kinases and p38 map kinase, suppressing pro-inflammatory mediator activity. On the other hand, when the globular head domains of SP-A and SP-D bind to pathogen-associated molecular patterns (PAMPs) or CD91-calreticulin complex on alveolar cells, this initiates the ingestion of AC causing pro-inflammatory and pro-immunogenic responses, indicating that CD91 participates in triggering the pro-inflammatory mediators through binding to the collagenous tails of SP-A and SP-D in the lung environment resulting in inflammation ³⁰². Deficiency in C1q, a complement component, prevents the binding of C1q to apoptotic NØ in systemic lupus erythematosus (SLE) with patients failing to initiate the calreticulin-CD91 complex for the uptake and clearance of apoptotic NØ resulting in necrosis and tissue damage due to the release of noxious contents from the necrotic NØ ³⁰³. The same study also identified that

other than monocytes and MØ, CD91 is also expressed on NØ confirming that all professional phagocytes utilise the CD91-calreticulin apoptotic recognition pathway for engulfment processes³⁰³. Notably as one of the α -2 macroglobulin receptors (α 2MR), CD91 modulation affects HMDM uptake of α 2-macroglobulin coated erythrocytes acting as an alternative ligand for CD91³⁰¹.

1.5.3.3 CD14

The cluster of differentiation antigen 14 (CD14), is a 55 kilodalton (kDa) glycoprotein expressed abundantly on monocytes and MØ but its expression is ten-fold weaker on NØ^{304, 305}. Other than LPS, CD14 binds to various bacteria components such as lipoteichoic acid, peptidoglycan, muramyl dipeptide, *Mycobacterium tuberculosis*, and lipoarabinomannan as well as other molecules such as uronic acid polymers, and rhamnose-glucose polymers derived from streptococcal cell wall polysaccharides. Consequently CD14 is regarded as a "pattern recognition receptor" (PRR) as it serves as a receptor within immune cells to detect foreign molecules to enable them to orchestrate the host's immune response³⁰⁶⁻³¹⁰. Extensive studies on LPS induced TNF- α production on monocytes or MØ at the protein and mRNA level show that CD14 recognises a substantial array of ligands present on the pathogens³¹¹⁻³¹⁴.

Non-myeloid cells or cells devoid of membrane bound CD14 expression utilise sCD14–LPS complexes to interact with TLR4 to induce TNF- α expression³¹⁵. The sCD14–LPS complex has also been reported to activate epithelial, endothelial, vascular smooth muscle cells, monocytes and polymorphonuclear leukocytes^{141, 316-319}. Interestingly, a significant increase in sCD14 was observed in the saliva of periodontitis patients compared with healthy controls indicating that sCD14 provides a biomarker for PD³²⁰. However, no difference in sCD14 levels were observed between the chronic and aggressive periodontitis groups³²⁰.

Polymorphism of CD14 has been linked with several systemic diseases. The C (-260) -->T nucleotide polymorphism in the promoter of the CD14 gene has been shown to affect myocardial infarction survival²²⁴. In Alzheimer disease patients, CD14 expression on microglial cells stimulates toxic agent in the brain by binding with fibrils of Alzheimer's amyloid peptide causing the induction of neuroinflammatory mediators³²¹. Anti-CD14 monoclonal antibodies have also been shown to inhibit bone resorption in mouse embryonic calvarial cells exposed to LPS indicating that CD14 might have a role to play in anti-resorptive therapy for bone loss³²². Since the first description of the prototypic monocyte/MØ immunophenotypic marker CD14 in the human immune system, research has come a long way³²³. However it is notable that the earlier studies emphasised the

role of CD14 as a receptor on MØ cells vital as an essential mediator for recognition and phagocytosis of AC ³²⁴.

1.5.3.3.1 Role of CD14 in AC clearance

MØ use many receptors to recognise dying or dead cells and at least five receptors (PS-R, vitronectin integrin with CD36- class B scavenger receptor (SR), the class A SR-A, ATP-binding cassette transporters (ABC1) and CD14) which are regarded as major molecules for the recognition and engulfment process. CD14 has been proposed as an important receptor in the removal of AC for cell binding and uptake by MØ highlighting their contribution to immunomodulatory effects of the phagocytic process ^{288, 325}. Devitt *et al.* proposed that CD14 stimulates a distinct response in MØ upon interaction with LPS or AC, as LPS is pro-inflammatory and AC are regarded as being anti-inflammatory ³²⁴. This previous study used the anti-CD14 monoclonal antibodies 61D3 and MEM-18 to reduce uptake of apoptotic lymphocytes by MØ.

Subsequently, Moffatt *et al.* proposed that CD14 could also bind ICAM-3; an apoptotic ligand which binds with MØ phagocytic receptors to enable the uptake of apoptotic Burkitt lymphomas (BL) cells. However to date, there has been no direct evidence that these molecules interact ²⁸¹. CD14-dependent clearance of AC was also reported for apoptotic lymphocytes and apoptotic NØ demonstrating that CD14 may utilise multiple apoptosis-associated plasma membrane structures to promote the clearance of dying cells as their ability is not limited to the uptake of apoptotic leukocytes. ^{288, 326}. Also, thus far there is no evidence demonstrating that PS represents a ligand for CD14.

CD14 is a molecule of significant interest as it mediates a pro-inflammatory response in MØ challenged with endotoxins and other bacterial components ^{327, 328}. Notably MØ CD14, following binding of AC, mediates an anti-inflammatory response ³²⁹. Though microorganisms such as *P. gingivalis* are regarded as being essential to initiate periodontal disease, it is the host's aggressive inflammatory response that is understood to exacerbate the disease. Notably *P. gingivalis* LPS or gingipains or poor uptake of AC clearance could be essential in this process and the involvement of CD14 will be discussed in further detail in this thesis.

1.5.4 Soluble mediators of AC clearance: 'bridging' molecules

To facilitate phagocyte binding to AC, numerous bridging molecules have been identified, serving as extracellular mediators which 'decorate' AC to enable engulfment by MØ. Expression of PS on the AC surface binds to milk-fat-globule-EGF-factor 8 (MFG-E8), growth arrest-specific 6 (Gas6), β 2-glycoprotein I (β 2-GPI) and protein S, all of which aid in additional recognition by the phagocyte for AC uptake ^{43, 330-332}. The Arg-Gly-Asp (RGD)

motif present in the second epidermal growth factor (EGF) domain of MFG-E8 binds to $\alpha_v\beta_3$ and $\alpha_v\beta_5$ integrins and interacts with oxidised PS to a high degree and to a lesser degree with non-oxidized PS and phosphatidylcholine (PC) serving as an opsonin for AC^{43, 333}. $\alpha_v\beta_3$ and $\alpha_v\beta_5$ integrins promote complement-dependent clearance of AC by associating with complement receptor 3 and 4 on MØ stimulating the attachment to C3b/bi activation sites on the AC⁴⁰. Gas6 mediates uptake of PS liposomes and AC by acting as a ligand for the tyrosine kinase family receptor Axl/Mer/Sky to facilitate the clearance of PS-expressing AC³³⁰. Additionally, PS liposome clearance by MØ in *in vitro* phagocytosis was also shown to be mediated by β_2 GPI³³¹. Other than this collagenous tails from collectin family members and binding to calreticulin triggers LRP-1/CD91 signalling for their uptake by phagocytes³⁰². Also, TSP-1 binds to TSP-1 binding sites on the surface of AC triggering the MØ-associated with integrin $\alpha_v\beta_3$ /CD36 for the engulfment procedure²⁹⁴. Moreover, the modified sugars and/or lipids on the AC surface also play a role in assisting in tissue homeostasis by clearing dying/dead cells^{334, 335}.

1.5.5 Don't 'eat me' signals

To discriminate a viable cell from a dying/dead cell, 'eat me' signal inhibitors might be present on viable cells in order to avoid accidental phagocytotic ingestion. A healthy viable cell declares "don't-eat me" by expressing ligands that cause repulsion/detachment of the phagocytes. This signal will be dominant even if the viable cell also presents 'eat-me' ligands. However during AC death, only 'eat me' signals are expressed so the cells are cleared by phagocytes³³⁶.

1.5.5.1 CD31

Initial studies on CD31, also known as platelet endothelial cell adhesion molecule-1 (PECAM-1), established that it was required for transmigration of leukocytes across vascular endothelial cell membranes through intracellular junctions³³⁷. Brown *et al.* demonstrated that CD31 on a viable cell interacts with the phagocyte CD31 homotypically to promote a repulsion mode after initial tethering ultimately resulting in prevention of engulfment. However, CD31 on a AC on interaction with the phagocytes CD31 switch from a repulsive to an adhesion mode preparing the cells to tether prior to being engulfed by the phagocytes³³⁸.

1.5.5.2 CD47

CD47 is expressed by many cell types and is an integrin-associated membrane protein which binds to signal-regulatory protein alpha (SIRP- α) and upregulates Src homology region 2 domain-containing phosphatase-1 (SHP-1) to prevent the uptake of AC³³⁹⁻³⁴¹. Reduced or altered CD47 expression occurs on cells undergoing apoptosis and is used as

a marker for 'find and eat me' due to the inactivation of SIRP- α signals²⁷⁵. Other than CD31, transendothelial migration of N \emptyset requires CD47 molecules on their surface in order to reach inflammatory sites across the endothelium³⁴². Increased CD47 expression on the surface of N \emptyset correlates with increased efficiency of N \emptyset transmigration³⁴³. CD47-deficient mice infected with *E.coli* to induce peritonitis show a delay in accumulation of N \emptyset at the infected sites indicating CD47 is necessary to mediate N \emptyset inflammatory responses³⁴⁴. Moreover, CD47-dependent N \emptyset chemotaxis is observed in N \emptyset stimulated with the RGD motif of entactin, a component of basement membranes and leukocyte response integrin (LRI), suggesting the interactions between N \emptyset and entactin occur through CD47 molecules³⁴⁵. Therefore, CD47 not only aids in differentiating viable and AC but is also involved in N \emptyset adhesion and migration.

1.5.5.3 CD46

Other than the above described receptors, CD46, a complement protection factor, is also involved in signalling as "don't – eat me". Modification or losses of CD46 are observed in caspase-dependent apoptotic Jurkat cells resulting in their clearance while viable cells expressed uniform CD46. Additionally, cleavage of caspase 3 in senescent keratinocytes and ionophore-treated sperm cells showed CD46 on apoptotic blebs or microparticles confirming the redistribution of CD46 into patches from the viable cell surface to apoptotic membrane bodies³⁴⁶. Collectively, this shows that viable cells are tested constantly to prove they are alive to avoid their ingestion by phagocytes by potentially masking the 'eat-me' signals.

1.6 Phagocytosis

Phagocytosis plays a key host defensive role against foreign species' invasion by ingesting the microorganism and generating protective responses e.g. antibodies and T cells³⁴⁷. AC clearance is essential for the maintenance of normal tissue structure and function and phagocytosis plays a key role in this process. The dying cell and the released apoptotic bodies are engulfed by the cell membrane of phagocytic cells forming a large fluid vesicle termed a phagosome. During this process the phagocyte e.g. a M \emptyset , becomes activated and induces healing of the damaged tissues by modulating inflammation³⁴⁸. This clearance phase is regarded as the most important process in the apoptosis programme as it removes dead cells associated with inflammation, infection and tissue homeostatic process³⁴⁹. The presence of pattern recognition receptors such as Toll-like receptors in M \emptyset and N \emptyset , two major professional phagocytes, facilitates the differentiation between cells of the host and the pathogen. Acute inflammation, which represents the initial response, attracts phagocytes by generating cytokines and chemokines in addition to the complement peptides C3a, C4a, C5a which have the ability to kill bacteria directly⁸.

The engulfment of AC is essential to avoid further tissue inflammation as every dead cell carries intracellular components that are potentially toxic and can stimulate the immune system³⁵⁰. Invading microbes are disarmed by NØ, the first recruited line of defence in the innate immune system, by producing antimicrobial species to avoid spreading the infection in the host. Professional phagocytes have a higher degree and ability for phagocytosis compared with non-professional phagocytes. While there are differences in clearance kinetics the mechanisms involved in clearing up dead cells are similar²³⁶.

1.6.1 NØ

Polymorphonuclear NØ are the predominant white blood cell and research has shown that NØ 'decide' the fate of the inflammation either by resolving it or by exacerbating it. Packed with an armoury of anti-microbial granules, NØ differentiate from bone marrow transcriptionally and translationally and they undergo a second round of transcription regulation referred to as the "immune response programme" on entering inflamed tissue to promote wound healing and achieve tissue homeostasis^{351, 352}. Antigen peptides produced from digested pathogens, phagocytosed by MØ and dendritic cells, are presented by MHC class II molecules, presenting these cells to CD4 T-cells. Indeed cytokine activated NØ display an up-regulation of MHC molecules whereas resting NØ lack these professional antigen presenting molecules³⁵³. The concept of NØ function as antigen presenters has been rejected by many researchers because of the short lifespan of NØ. However NØ interactions with the adaptive immune system work through NØ soluble mediators and cytokine production contributing to their influence on the immune response.

1.6.1.1 NØ in periodontal disease

Leukocytes from periodontitis patients triggered lymphocyte transformation, from small resting lymphocytes to large cells on exposure to oral bacteria resulting in cell-mediated immune response and this marked a significant breakthrough in the pathogenic understanding of PD³⁵⁴. This was followed by a demonstration that NØ from localized juvenile periodontitis (LJP) are impaired in their chemoattractant ability and this was the first systemic abnormality demonstrated in patients with severe PD³⁵⁵. NØ are found in large numbers in the gingival crevice, periodontal pockets and saliva derived from the oral cavity^{351, 356}. Granulocyte monocyte-colony stimulating factor (GM-CSF) reduces NØ apoptosis in gingival crevicular fluid (GCF) by regulating Bax expression exerting control over the lifespan of NØ in the oral cavity¹⁹⁰. Moreover, smoking influences the inhibition of NØ apoptosis in the gingival connective tissue of chronic periodontitis patients³⁵⁷. These studies indicate that delayed apoptosis may contribute to tissue destruction in the infected PD patients. On the other hand, necrotic NØ (30%) are found in higher numbers

compared with apoptotic NØ (1%) in the gingival crevice, periodontal pockets and in the saliva from the oral cavity ³⁵⁶. These necrotic NØ might be present due to the failed clearance of AC and thus have been allowed to proceed to secondary necrosis though the nature of the defect is unknown.

CXCL12, also known as stromal cell-derived factor-1, is increased in GCF from periodontitis patients along with other chemoattractants produced by immune cells, (e.g. IL-8, IL-1 β , C5a) and exogenous chemotactic signals, (e.g. LPS, FMLP) ³⁵⁸. These attractants may be responsible for NØ trafficking at the crevicular site and if AC clearance is not sufficient they may become necrotic. Over recent years, peripheral NØ hyper-responsiveness and impaired NØ function have been proposed as a major cause of tissue destruction in periodontitis ³⁵⁹⁻³⁶¹. The Fc- γ receptor in NØ reportedly mediates hyper-reactivity and oxygen radical release resulting in tissue damage in patients with oral inflammation ³⁶². Indeed higher levels of reactive oxygen species have been shown to be generated by chronic periodontitis patients ^{363, 364}. Studies on the recruitment of NØ to the subgingival area support either a reduction or increase in phagocytosis by NØ, subsequent release of NØ elastase and reactive oxygen species purportedly contributes to the destruction of the periodontal tissue ^{97, 365-369}. Notably elastase from NØ has been reported to cleave CD14, an established AC clearance receptor on MØ resulting in impairment of apoptotic lymphocyte clearance ³⁷⁰.

During gingivitis, the microenvironment around the tooth surface is activated by inflammatory infiltrates enhancing the serum level of TNF-alpha and IL-1 which affects NØ function ³⁷¹. Decreased priming activity and chemotaxis of NØ were found towards gingipain-treated IL-8 from immune 72-amino-acid variants on subsequent exposure to FMLP. However exposure to gingipain-treated IL-8 from non-immune 77-amino-acid variants and exposure to FMLP resulted in enhanced oxidative burst activation and chemotactic activity of NØ suggesting that, depending on the cellular source of the chemokine, gingipains regulate their effects differentially by modulating NØ activation and chemotaxis ¹⁹³.

NØ in their activated form also utilise a defence mechanism, NETs that ensnare and kill pathogens in the human body. These NETs are composed of DNA, histones and anti-microbial granules which entrap microbes and degrade their virulence factors ³⁷². The formation of NETs was initially observed in humans by Brinkmann ²⁷. NETs can be generated within 10 minutes, depending on the dose and nature of stimuli. Virulence factors and exposure to LPS, IL-8 or phorbol myristate acetate (PMA) showed flat membrane protrusions with smooth fibres and globular domains together with granule proteins and chromatin forming an anti-microbial extracellular structure ²⁷. The mechanisms by which NØ produce NETs remains to be fully understood. Recently NETs

have been found to be abundant on the gingival surface during periodontitis progression in the GCF and are flushed out of the gingival pocket by the crevicular exudate ³⁷³. Inflammatory exudate samples from periodontitis patients, analysed using scanning electron microscopy and immuno-staining for confocal laser scanning microscopy, demonstrated the abundance of NETs in GCF and periodontal pockets ^{28, 373, 374}. Atherothrombosis patient samples have also been shown to contain *P. gingivalis* DNA in increased levels along with the presence of NETs suggesting that periodontal bacteria may impact via NET stimulation on other systemic diseases ³⁷⁵. The influence of NETs in modulating the host-pathogen interaction through immune cells and protection against the inflammatory environment in PD are yet to be fully elucidated.

1.6.1.2 NØ elastase in periodontitis

The activation of NØ results in NØ elastase release, which is a serine protease that is secreted in azurophilic granules to destroy bacteria. Notably NØ elastase-deficient mice have shown susceptibility to Gram-positive and Gram-negative bacteria ³⁷⁶. However, increased NØ elastase activity along with MMP-9 has been found in chronic periodontitis patients compared with healthy controls ³⁷⁷. Moreover, NØ elastase has been reported to cause tissue destruction in the periodontium region by digesting the non-collagenous proteins which protect the collagen fibrils involved in the maintenance of supporting vasculature of the gums ³⁷⁸. The previous report also stated that NØ were hyperactive in chronic and aggressive periodontitis patients in terms of NØ elastase levels found in the gingival crevicular fluid ³⁶⁸. Also, phagocytosis of *P. gingivalis* by NØ has been shown to lead to increased levels of NØ elastase and reactive oxygen species release which attack not only the pathogens but also the host cells indicating the ability of periodontal bacteria to modulate the host response ³⁶⁸.

NØ elastase has also been shown to play a role in migrational activities. NØ elastase-deficient mice exhibit reduced adhesion and transmigration towards zymosan particles indicating a non-redundant role of NØ elastase in this process ³⁷⁹. In contrast, another recent study showed that the CD14 receptor was cleaved by NØ elastase on MØ resulting in prevention of phagocytosis of apoptotic lymphocytes ³⁷⁰. These findings are also further supported by work from Nemoto *et al.* who demonstrated the cleavage of platelet-derived growth factor receptor (PDGF) by NØ elastase on periodontal ligament cells ³⁸⁰. Taken together, data indicates that increased levels of NØ elastase such as in periodontitis patients might result in cleavage of receptors essential for cell clearance and growth factor induction and thereby resulting in compromised bacterial invasion at the periodontal sites.

1.6.2 MØ

MØ are a phagocytic cell activated in response to an infection and they differentiate from circulating blood monocytes as they enter tissues ³⁸¹. Notably an inflammatory stimulus (e.g. microbial components) can trigger infiltration of immune cells comprising NØ, MØ, and lymphocytes. LPS is an important outer membrane component of Gram-negative bacteria, which activates MØ at the site of infection to elaborate pro-inflammatory cytokines such as IL-1 and TNF- α ^{36, 382}. These molecules, in association with PGE2 and hydrolytic enzymes, generate strong pro-inflammatory gradients leading to the destruction of the primary human periodontal epithelium and bone resorption ³⁸³ (figure 8).

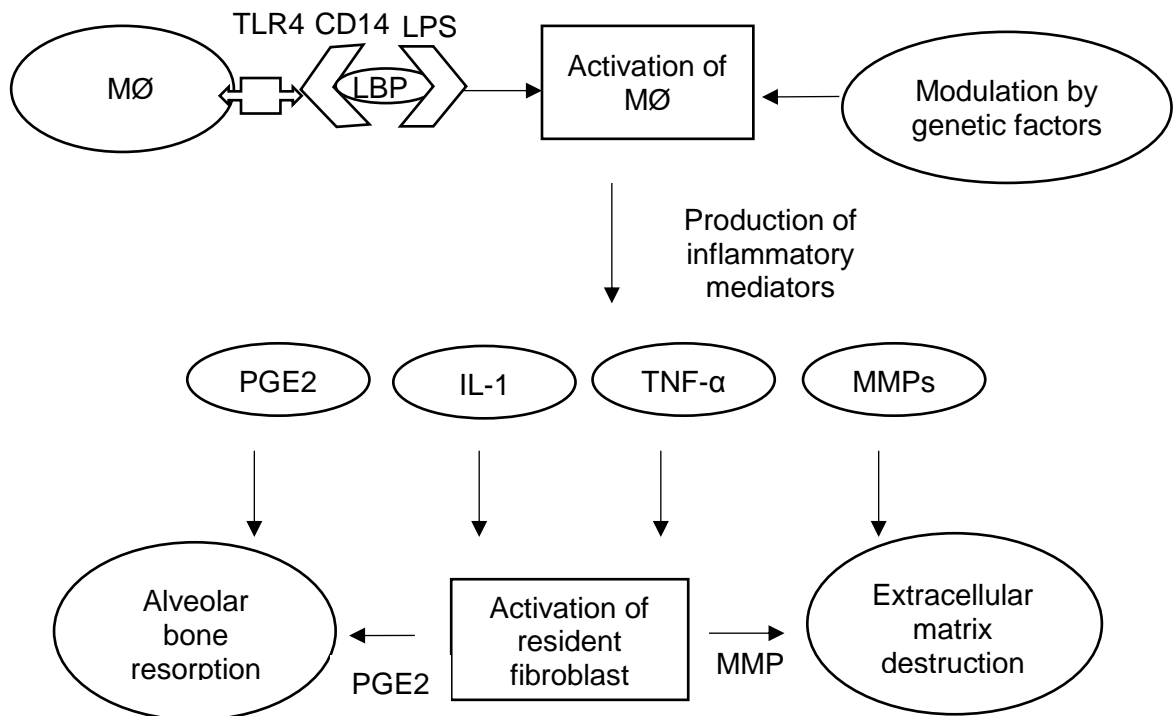


Figure 8: Illustration of activation of MØ challenged with LPS in PD

LPS in association with lipopolysaccharide-binding protein (LBP) associates with MØ and mediates production of pro-inflammatory mediators resulting in activation of fibroblasts. This activation leads to the production of PGE2 and MMPs which resorb alveolar bone and damage the connective tissue in periodontal disease. Adapted from ⁶⁹.

Clearance of dead cells and activation of anti-inflammatory responses is a major role performed by MØ phagocytosis ^{324, 384}. Earlier studies have reported that MØ attraction towards AC followed by cell corpse clearance is an essential phase in the phagocytosis process necessary to achieve tissue homeostasis ³⁷. Failure of AC clearance has been demonstrated in both the C1q^{-/-} and the transglutaminase TG-2^{-/-} knock out mice and underlines their association with an autoimmune mechanism ^{285, 286}.

Notably monocytes and MØ are activated by oral pathogens, such as *A. actinomycetemcomitans* and *P. gingivalis* leading to secretion of pro-inflammatory and

tissue-destructive mediators³⁸⁵. Reports demonstrate that, compared with minimally-inflamed tissues, chronic periodontitis comprises no increase in MØ recruitment however failure of the activation process may underlie the pathological process of PD³⁸⁶. Moreover, this premise has been supported by a recent report indicating that periodontal pathogens can modify MØ migration and activation by preventing the production of monocyte chemoattractant protein-1 (MCP-1), a key chemokine which regulates infiltration and migration of MØ³⁸⁷. The project presented here also focused on the migratory role of MØ towards apoptotic NØ and determined whether *P. gingivalis* components effect the MØ phagocytosis function. Findings might shed further light on the inflammatory mediators involved with the periodontal environment.

MØ play an indispensable role in the initiation, maintenance, and resolution of inflammation by controlling the release of pro- and anti-inflammatory mediators in responses to different immune challenges. MØ can be classified into two polar types, by their specific function in inflammation, as M1 or M2. M1 have been identified as having a pro-inflammatory role contributing to driving disease whilst M2 aid in resolving inflammation via production of anti-inflammatory cytokines. MØ that clear AC are skewed towards an M2 phenotype by producing anti-inflammatory cytokines aiding AC clearance and restoring tissue homeostasis³⁸⁸. A strong M1 host response potentially plays an important role in chronic adult periodontitis progression along with the causative bacteria. Indeed, the host response is considered to be protective however tissue destruction is known to take place when there is a hypo-responsiveness or hyper-responsiveness by the host immune system³⁸⁹. Furthermore, increased severity of periodontitis can be associated with diseases caused by impairment of the immune system e.g agranulocytosis, leucocyte adhesion deficiency, leukaemia, cyclic neutropenia and thrombocytopenia⁵². Indeed, chronic periodontitis serves as an experimental model for the understanding of systemic diseases that are triggered by inflammatory pathways³⁹⁰.

Although the host immune response impacts on periodontal inflammatory disease it is also the environmental factors that regulate immune-inflammatory mechanisms contributing to the manifestations of the disease (Table 2).

Introduction

Risk Factors	Association with periodontitis	Cell defect	Reference
Smoking	Upregulation of TLR4 mRNA expression was found in periodontitis patients who smoked compared with non-smoking periodontitis patients.	Reduced NØ count and NØ elastase activity have been reported. Additionally, increased Th2 response was found in smoking periodontitis patients which have been linked with autoimmune disease.	391-393
Psychological factors	Activation of hypothalamus secretes mediators due to chronic stress stimulating the release of glucocorticoid hormones which in turn activates interleukins. Increased production of IL-6 in response to psychological stress has been associated with depression and negative thoughts thereby having an impact on oral hygiene.	The release of glucocorticoid from the adrenal cortex reduced the recruitment of immune cells and inhibited the immune response by inhibiting MØ antigen presentation.	394-396
Genetic factors	Studies of identical twins indicate that genetic predisposition plays a role in causing periodontitis.	A study in the Turkish population indicated gene variation in myeloperoxidase (MPO) and nitric oxide synthase contributes towards aggressive periodontitis.	397-399
Ageing	Butyric acid, a secondary metabolite released by the periodontopathogenic bacteria, has been reported to associate with oxidative stress induction. Subsequently, studies show that oxidative stress has a potential impact on age-related disease.	NØ function declines with age notably affecting phagocytosis process and higher gene expression of pro-inflammatory cytokines in NØ has also been reported.	400, 401

Introduction

Pre term delivery	Research indicates that premature labour and low-birth-weight (PLBW) babies may be affected by the inflammation triggered by bacteria which can travel to the blood stream and affect the foetus. It is also indicated that pre-term delivery may be an independent risk factor associated with periodontitis but not directly causative.	Unknown	402, 403
Other systemic disease	Agranulocytosis and leukocyte adhesion deficiency were related to impairment in NØ function though they are not proven to have a definitive association with periodontitis.	NØ dysfunction diseases	404, 405

Table 2: List of risk factors associated with PD

The table shows the environmental risk factors associated with PD and their involvement in modulation of specific cell types via their receptors. The table also presents information as to how the modulation of cytokine production might provide a further factor that contributes to periodontitis.

1.6.2.1 Chemotaxis of MØ in periodontal environment

Recruitment of monocytes and MØ to the gingival sites in response to bacterial infection is a key factor involved in inflammation of periodontal sites ⁴⁰⁶. The continuous influx of phagocytes indicates the challenge to stabilise wound healing by resolution pathways. Initiation of systemic diseases linked with oral disease underlines the potential importance of immune cell migration to carry bacterial toxins or impaired immune cell responses in causing tissue destruction at sites other than the primary site of infection. Both MØ and endothelial cells recruit inflammatory monocytes via CCR2 to the inflamed tissue ^{31, 407}. However, increased amounts of chemokines can result in the tissue damage observed in periodontal tissue. MØ chemokine protein (MCP-1), another chemokine involved in the recruitment of monocytes/MØ has been reported to be expressed in greater amounts in periodontal gingival tissues resulting in increased infiltration of monocytes and increased severity of disease ⁴⁰⁸. In addition, MØ inflammatory protein 1 alpha (MIP-1 α), IFN-gamma-inducible protein-10, CCR3, and CCR5 have been reported to be elevated in inflamed human gingival tissue compared with healthy controls. These data suggest that these active chemokines might be responsible for the accumulation of immune cells at the infected sites in the periodontitis patients ^{409, 410}. Moreover, MØ migration inhibitory factor (MIF) deficient mice exhibited reduced bone resorption by inhibiting differentiation and activity of osteoclasts and also decreased infiltration of NØ along with increased production of IL-10 ⁴¹¹.

During inflammation the immigrated monocytes from the blood differentiate into classical MØ which are equipped with TLRs and receptors to enable cell clearance. Impairment of MØ phagocytosis by *A. actinomycetemcomitans*, a periodontal pathogenic bacterium, has been reported causing significantly less phagocytosis activity compared with wild-type MØ and the underlying reason for this has been associated with higher TNF- α in periodontitis patients ⁴¹¹. Also, the type and the level of cytokines in GCF indicates the coordination of MØ in achieving tissue homeostasis ⁴¹²⁻⁴¹⁴. Overall, these data indicate that the regulation of immune-inflammatory mechanisms in PD is largely governed by the aggressive inflammatory mediators initiated by the oral microorganisms ²¹⁴.

Once the MØ have cleared the pathogens and AC, it is important for the MØ to emigrate the inflamed tissue and enter the lymph nodes. At the lymph nodes, the MØ stimulate T cells in order to activate the adaptive immune system ⁴¹⁵. This process has been shown to be inhibited in PD due to the infiltration of CD4+ and CD25+ T cells in the periodontal lesions suggesting that regulatory T cells might play an important role in regulating PD ⁴¹⁶. However, the reason for this T cell infiltration is yet to be determined.

While the above studies indicate that the infiltration of phagocytes or other immune cells are an underlying problem in the periodontal environment, in this thesis the reasons for the persistence of the AC were examined by studying the role of MØ migration on exposure to bacteria or their components. Given the previous lack of knowledge, this study examined the efficiency of MØ migration following exposure to gingipains from *P. gingivalis* using quantitative and qualitative measurements in various chemotaxis models.

1.7 Aims and objectives

Gingipains, proteolytic enzymes from a major aetiologic agent *P. gingivalis*, are associated with PD and reportedly are a major cause of evasion of the host immune system and tissue destruction in the inflamed oral region. A growing body of research suggests failure to restore homeostasis may be a major factor involved in the pathogenesis of chronic inflammatory periodontal diseases and the main toxic agent is gingipains which act by “confusing” phagocytic cells’ recognition and phagocytosing ability of AC. While previous studies have established AC clearance mechanisms underlying the non-inflammatory physiological clearance of dying cells, there is minimal work that has studied how these mechanisms are affected by pathogens in disease. This project seeks to address why there appears to be poor inflammation resolution in PD and whether this results from defective AC clearance. Though inflammatory NØ have been identified widely as a major cause for aberrant inflammation in periodontitis patients, to date there has been no study aimed at the ability of MØ phagocytosis in the gingipain-exposed environment. Therefore this project aims to analyse for the first time the AC clearance mechanisms involved in PD by scrutinising MØ receptors associated with clearance and MØ migratory and phagocytosing ability in addition to the inflammatory mediators associated with apoptotic human NØ (figure 9). This research may open up new strategies for intervention in the disease process.

The hypothesis underlying this project is that MØ lose their ability to find, recognise and phagocytose AC due to their cleavage of AC clearance receptors by factors released from *P. gingivalis* prompting a dominant inflammatory response causing the tissue destruction observed in periodontal disease.

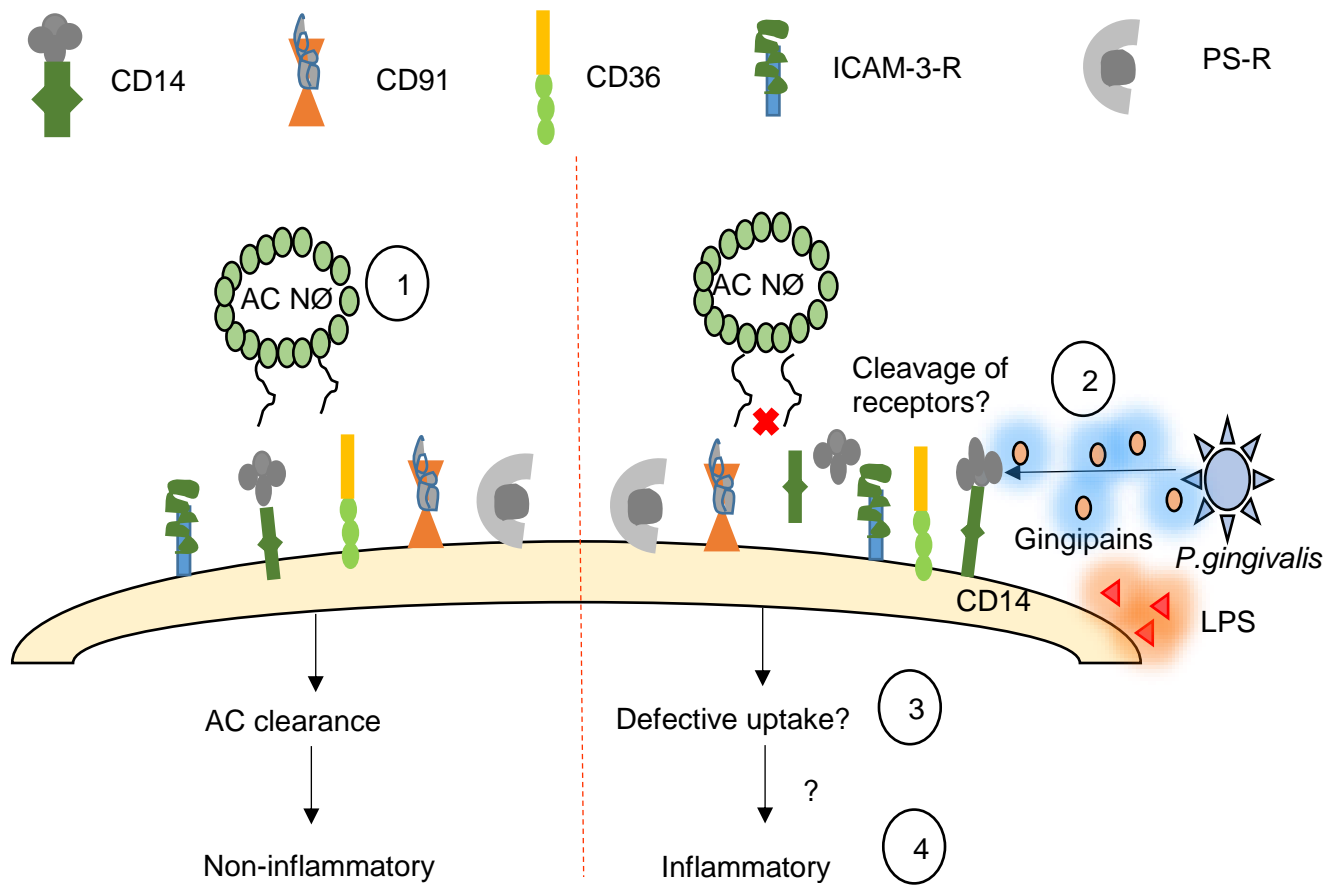


Figure 9: Possible scenarios involved in the AC clearance mechanism within PD

1) MØ receptors essential for AC clearance bind to 'eat-me' ligands expressed on the surface of an AC for the uptake and phagocytosis resulting in an anti-inflammatory response. 2) The ability of MØ receptor on exposure to bacterial virulence such as LPS or gingipains from *P. gingivalis*, might be dysregulated by cleaving essential AC clearance receptors. 3) Failure of uptake of AC due to the cleaved receptors on the phagocytes results in inflammation. 4) If the AC were taken up by the non-cleaved MØ receptors this might produce a dominant inflammatory response by suppressing anti-inflammatory mediators in the host immune system.

In order to address this hypothesis, the specific aims and objectives of this project are

- 1) To establish an *in vitro* model for AC clearance using THP-1 MØ and primary apoptotic NØ.
- 2) To purify and characterise the ~50 kDa and ~60kDa RgpB and Kgp respectively from *P. gingivalis*.
- 3) To determine MØ migrational and phagocytosis ability towards AC human NØ in the gingipain environment.
- 4) To quantify the capacity of AC NØ in inhibiting the inflammation induced by gingipains and LPS by measuring the pro- and anti-inflammatory mediators at protein and gene expression levels.

Chapter 2

Materials and Methods

2.1 Equipment and software

- Anaerobic chamber (Don Whitley Scientific, UK)
- Avanti J-E centrifuge (Beckman Coulter, UK)
- Benchtop centrifuge (Sigma, Germany)
- Biosafety cabinet (Thermo Fisher Scientific, UK)
- Cell-IQ Analyser™ software (CM Technologies, UK)
- Cell-IQ tracking system device (CM Technologies, UK)
- Chemotaxis Dunn CTG chamber, DCC100 (Hawksley and Sons Ltd, UK)
- Chromata-Vue C71 light box and UVX radiometer (UV-P Inc, USA)
- Cryo-freezing container NALGENE (Fisher, UK)
- Eppendorf Centrifuge 5810R (DJB Lab care Ltd, UK)
- Flow cytometer cytomics FC 500 (Beckmann Coulter, UK)
- FlowJO Version 10 software (FlowJo INK, USA)
- Gel imaging for fluorescence and chemiluminescence G: BOX Chemi XRQ (Syngene, UK)
- Gyro-rocker (SSL3, UK)
- Haemocytometer double cell standard (Camlab Ltd, UK)
- Ibidi web tool for Chemotaxis and Migration (<http://ibidi.com/xtproducts/en/Software-and-Image-Analysis/Manual-Image-Analysis/Chemotaxis-and-Migration-Tool>)
- Image J web tool (<https://imagej.nih.gov/ij/>)
- Incubator (Sanyo Biomedical, Europe)
- Inverted fluorescence microscope Zeiss Axiovert 200M (Zeiss, UK)
- Inverted microscope (Nikon Eclipse, Europe)
- Minigel Vertical Electrophoresis Apparatus and Western Blot wet transfer system (Bio-Rad, UK)
- Nanodrop 1000 spectrophotometer (Thermo Scientific, UK)
- Optima L-look Ultracentrifuge (Beckman Coulter, UK)
- Orbital shaker (Thermo Fisher Scientific, UK)
- Plate reader EL800 (BioTek Potton, UK)
- Plate spinner, Perfect spin (Peqlab, Germany)
- qPCR software MxPro-Mx3000P SYBR Green software (Thermo Fisher Scientific, UK)
- Spectrophotometer Model DU-7 (Beckman Instrument (UK) Ltd, UK)

- Stratagene Mx3000P (Thermo Fisher Scientific, UK)
- 70Ti rotor (Beckman Coulter, UK)

2.2 Antibodies

Mouse (Affymetrix eBioscience, UK)

- Mouse IgG1 K Isotype control PE (clone P3.6.2.8.1)
- Mouse IgG1 K Isotype control FITC (clone: P3.6.2.8.1)
- Mouse IgM Isotype Control FITC (clone: 11E10)

Anti-mouse (Sigma-Aldrich, UK)

- Anti-Mouse IgG (whole molecule) – FITC antibody produced in goat
- Anti-human IgG (Fc specific)-FITC, mouse IgG1 (MOPC 21)

Anti-Human (Affymetrix eBioscience, UK)

- Anti-Human CD47-FITC (clone: B6H12)
- Anti-Human CD31, PE (clone WM-59)
- Anti-Human CD36, FITC (clone: eBioNL07)
- Anti-Human CD91, PE (clone A2MR-92)

Biotin binding protein (Life technologies, UK)

- Streptavidin HRP

2.3 Cell culture

2.3.1 Materials and reagents for cell culture

All reagents for this study were supplied by Sigma - Aldrich, UK unless otherwise stated.

Complete Roswell Park Memorial Institute medium (cRPMI): cRPMI was used as a suspension growth medium for the human-derived cells in this study. RPMI 1640 was supplemented with penicillin (100U/ml) (PAA Laboratories, UK), streptomycin (100µg/ml) (PAA Laboratories, UK), 2 mM L-glutamine (PAA Laboratories, UK) and 10% (v/v) foetal calf serum (FCS) (PAA Laboratories, UK).

Serum-free medium (sfRPMI): RPMI was supplemented with penicillin (100U/ml) and 2 mM L-glutamine.

Phagocyte interaction with AC assay medium: Serum-free medium (sfRPMI) supplemented with 0.2% w/v BSA.

Cell freezing medium: 5% (v/v) Dimethyl sulphoxide (DMSO) in FCS. The cell lines were frozen using the Cryo-freezing container (Fisher, UK) prior to storing in liquid nitrogen.

MØ medium (Sigma Aldrich, UK): To study MØ migration using DUNN chamber the MØ medium was used as a negative control.

Flow wash buffer: PBS containing 1% (w/v) BSA.

Cell fixative: 1% (w/v) formaldehyde in PBS.

PMA: 250µM stock made up in absolute ethanol (CEAC, UK).

Dihydroxyvitamin D3 (VD3) (Enzo Life Sciences, UK): 100µM stock diluted using RPMI+10% FCS following solubilization in DMSO.

2.3.2 Cell lines

THP-1: A human monocytic leukaemia cell line. THP-1 cells can be differentiated into MØ-like cells using a range of stimulants ³⁶.

Mutu: This EBV-positive Burkitt lymphoma cell line (B - cell line) were kindly provided by Professor Christopher D Gregory (University of Edinburgh, UK) ⁴¹⁷

All cell lines were routinely cultured by passaging them every 48-72h and maintained at 37°C, 5% CO₂ humidified incubator. Depending on the size of the Cell Culture EasYFlasks™ (Thermo scientific, UK), the required number of cells were left in the flask and resuspended in pre-warmed cRPMI.

2.3.3 Freezing and thawing of cell lines

Liquid nitrogen was used for storage of cells in cryovials. Before freezing, the cells were checked for viability. 5 X 10⁶ cells were centrifuged (300xg for 5 min) from the suspension culture and the pellet resuspended in 1 ml of cell freezing medium (as described in section 2.3). Before transferring the culture aliquots to cryovials, the cryovial was labelled with the cell line details, followed by the passage number and the date of freezing the cells. The cryovial was then placed in a cryo-freezing container (Fisher, UK) at -80°C for 24h and then transferred to liquid nitrogen vapour for long-term storage.

Cell thawing was performed by placing the frozen cryovial of cells in a water bath at 37°C. In a biosafety cabinet, the defrosted cells were transferred into a centrifuge tube containing cRPMI medium and cells were then centrifuged at 300xg for 5 min and the pellet resuspended in cRPMI media (as described above) prior to culturing. Cells were seeded in Cell Culture treated EasYFlasks™ and cultured at 37°C, 5% CO₂ in an incubator.

2.3.4 Culturing of cells

THP-1 and B cell lines were cultured in cRPMI and maintained at 37°C in 5% CO₂ humidified incubator. Cells were passaged at an interval of 48-72h to avoid high levels of confluence and appropriate cells were counted using a graduated haemocytometer and maintained at a density of 2×10^5 - 1×10^6 cells/ml by feeding the cells with the fresh pre-warmed (37°C) culture medium.

2.3.5 THP-1 differentiation to MØ-like cells

THP-1 cells were differentiated into MØ-like cells by treating cultures in fresh medium with either 100nM dihydroxy vitamin D3 (VD3) or 250 nM PMA or double-stimulated (DS) with both VD3 and PMA for 48-72h at 37°C in 5% CO₂ incubator³⁶.

2.3.6 Immunofluorescence

2.3.6.1 Indirect Immunofluorescence staining of cells

VD3 or DS stimulated THP-1 differentiated MØ (1×10^6 cells/ml) or NØ (1×10^6 cells/ml) were washed in the flow wash buffer (as described in section 2.3) by centrifugation for 300xg for 5 min and incubated with 100µl of primary antibodies anti-CD14 clones 61D3/63D3 (1:100 made in house) or IgG1_k isotype- control MOPC 21 (20 µg/ml) for 20 min on ice in the dark. Cell surface expression of ICAM-3 was detected with 100µl of anti-ICAM-3 clone MA4 (1:100 made in house) or the isotype control MOPC 21 (20 µg/ml) for 20 min on ice in the dark. Following incubation, the cells were washed three times with flow wash buffer. 100µl of goat anti-mouse FITC was used as a secondary antibody at a dilution of 1: 100 for cells stained with the primary antibody and incubated again for 20 min on ice in the dark and the cells were washed again three times with flow wash buffer. Cells were then fixed with 500µl of 1% w/v formaldehyde and analysed immediately using flow cytometry (as described in 2.1) or stored at 4°C until further analysis.

2.3.6.2 Direct Immunofluorescence staining of cells

Cell surface expression of the molecules CD31, CD91, CD47 and CD36 was determined using direct immunofluorescence assay as described in Table 3. To the VD3 or DS differentiated THP-1 MØ (as described in section 2.3.5) 5µl of appropriate primary antibody conjugated with the fluorochrome or 5µl of appropriate isotype control conjugated with fluorochrome was added and then incubated for 20 min on ice in the dark. Following incubation, the cells were washed three times with the flow buffer and fixed with 500µl of 1% w/v formaldehyde and analysed immediately using flow cytometry or stored at 4°C until further analysis.

Receptor	Antibodies conjugated with fluorochrome	Isotype control conjugated with fluorochrome
CD36	anti- human CD36 conjugated with FITC (0.125 µg/ml)	mouse IgM isotype control FITC (0.15 mg/ml),
CD91	anti- human CD91 conjugated with PE (0.06 µg/ml)	mouse IgG ₁ κ isotype control PE (0.5 µg/ml)
CD31	anti- human CD31 conjugated with PE (0.125 µg/ml)	mouse IgG ₁ κ isotype control PE (0.5 µg/ml)
CD47	anti- human CD47 conjugated with FITC (1 µg/ml)	mouse IgG κ isotype control FITC (1 µg/ml)

Table 3: Direct immunofluorescence staining using flow cytometry

List of primary antibodies conjugated with fluorochromes and their appropriate isotype control studied for direct immunofluorescent staining of cell surface receptor expression on MØ-like cells analysed using flow cytometry.

2.4 Isolation of NØ from peripheral whole human blood using the Percoll gradient method

2.4.1 Materials for isolation of NØ

- Winged infusion set needle 21G X 0.75" X 12", tourniquet, Vacurette holdex, BD Vacutainer EDTA, cotton balls, plasters were all purchased from Nu-Care Products, UK.
- Percoll (GE Healthcare, UK)
- **RBC lysis Buffer:** 8.3 g/L NH₄Cl, 1 g/L KHCO₃, 0.04 g/L Na₂EDTA-2H₂O and 2.5g/L BSA to sterile water and stored at 4°C
- **NØ medium:** Freshly isolated NØ were seeded in 1 x 10⁶ cells/ml in sfRPMI with 0.15%BSA
- **GPBS:** Glucose (1.5% v/v) supplemented with PBS, 1mM MgCl₂ and 1.5mM CaCl₂
- Anti-Human CD66b, PE clone G10F5 (Affymetrix eBioscience, UK)

2.4.2 Blood collection

Healthy blood donors were selected and the nature of the study was explained prior to blood collection and written and signed consent was obtained. A winged infusion set (21G X 0.75" X 12") was used to collect 10ml of venous blood from healthy volunteers using 10ml EDTA BD Vacutainers and the collected fresh venous blood was used

immediately for NØ isolation. Blood handling was undertaken in accordance with ethical guidelines (Aston University Ethics Committee).

2.4.3 Preparation of Percoll gradient

Percoll was used to prepare two density media of 1.098g/ml and 1.079g/ml in 150mM NaCl solution. Percoll solutions were prepared according to the following Table 4.

Density (g/ml)	1.079 (g/ml)	1.098 (g/ml)
Percoll (ml)	19.7	24.8
Distilled water (ml)	11.7	6.6
1.5 M NaCl (ml)	3.5	3.5

Table 4: Percoll density composition for isolation of NØ

Preparation of Percoll gradients with compositions for two different densities used for NØ isolation.

The entire NØ isolation procedure (section 2.4) was performed at room temperature immediately after blood collection. 8ml of 1.098g/ml Percoll was layered carefully beneath 8ml of 1.079g/ml Percoll using a 10ml pipette in a 50ml universal tube (Sarstedt, UK). To the layered gradient, 10ml of whole blood was layered carefully using a sterile Pasteur pipette. The blood was centrifuged using a benchtop centrifuge at 150xg for 8min at 20°C and then immediately centrifuged again at 1200xg for 10 min at 20°C with the brake off. After centrifugation, the visible layers from top to bottom were plasma, lymphocytes, clear liquid or Percoll, NØ and red blood cells (RBC) (figure 10).

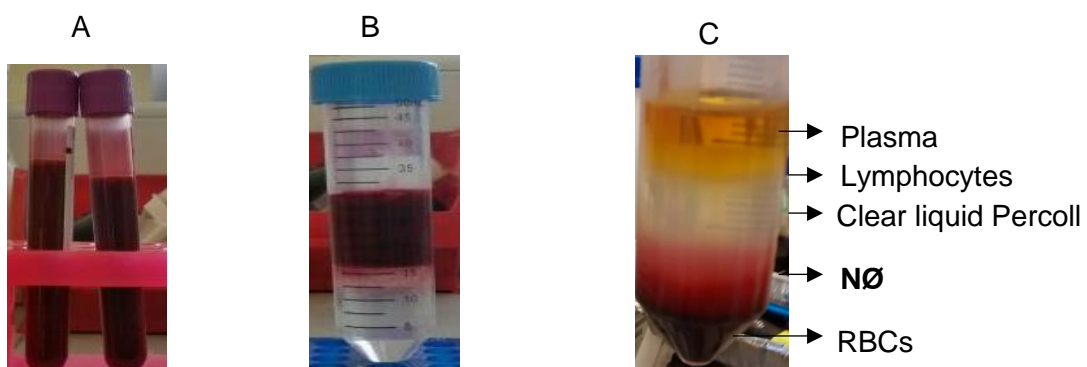


Figure 10: Isolation of NØ from whole blood

Image showing various stages in the NØ isolation procedure. The whole blood was collected at room temperature (A) and layered on the Percoll gradient (B) and centrifuged to obtain the resultant layers of cells (C).

Using a plastic Pasteur pipette plasma, lymphocytes and most of the clear liquid Percoll were removed by aspiration and discarded. NØ and the majority of the red blood cells were subsequently extracted using a Pasteur pipette and transferred to a sterile centrifuge

tube (Sterilin Ltd, Newport, UK) containing 30ml of lysis buffer and incubated at room temperature for 20 min with gentle mixing until the solution became transparent, an indication of haemolysis. After centrifugation at 500xg for 10 min, the cell pellet was resuspended in 3ml of lysis buffer and incubated at room temperature for 5 min to lyse any remaining red blood cells. This mixture was then centrifuged at 500xg for 10 min and to the resultant pellet 3 ml of PBS was used for resuspension and to remove remaining cell debris. This mixture was further centrifuged (500xg for 10 minutes), and the supernatant removed and the pellet was resuspended in GPBS prior to assessment of NØ purity or in RPMI medium containing 0.15% (w/v) BSA (NØ medium) for generation of AC (AC) ⁴¹⁸.

Isolated cells were counted using a haemocytometer. The NØ count typically ranged from 2×10^7 to 1×10^6 cells/ml and varied between each isolation and for each donor. Cell viability was analysed by trypan blue exclusion method (Sigma-Aldrich, UK) using 10µl of isolated NØ added to 10µl of 0.4% trypan Blue solution and incubated at room temperature for 1-2 min. This suspension was carefully loaded to a graduated haemocytometer chamber and the unstained viable cells and stained non-viable cells were counted using light microscopy and the percentage of viable cells was calculated.

2.4.4 Confirmation analysis of NØ purity

2.4.4.1 Direct Immunofluorescence

1×10^6 /ml NØ were washed with flow wash buffer by centrifuging for 300xg for 5 min and to the pellet 5µl of anti-human CD66b conjugated with PE (0.06 µg/ml) or Mouse IgM Isotype Control - PE (0.125 µg/test) was added and incubated on ice in the dark for 20 min and analysed using flow cytometry to detect the percentage of NØ purity. Cell surface expression of CD31, CD91, CD47 and CD36 were determined using direct immunofluorescence assay as described in section 2.3.6.2

2.4.4.2 Indirect Immunofluorescence

The cell surface expression of CD14 and ICAM-3 on NØ (1×10^6 /ml) was determined using indirect immunofluorescence assay as described in section 2.3.6.1

2.4.4.3 4', 6-diamidino-2-phenylindole (DAPI) nuclear stain

Prior to seeding on a multiwell glass slide, NØ (1×10^5 cells/ml) were fixed using 1% (v/v) formaldehyde in PBS for 15 min. Glass slides containing cells were mounted with a hard fix using 100µl of DAPI stain (100ng/ml) (Vector Labs, UK) and incubated on ice for 5 min. The stained cells were analysed using fluorescence microscopy to image the nuclear morphology of viable and apoptotic NØ.

2.5 Induction and characterization of apoptosis

2.5.1 Generation of AC (AC)

2.5.1.1 B cells

1 X 10⁶ cells/ml of B cells were resuspended in cRPMI medium and apoptosis was induced using a Chromata-Vue C71 light box and UVX radiometer (UV-P Inc., Upland, CA, USA). The radiometer was used precisely to provide the UV dose which ranged from 25-100mJ/cm². Apoptosis was allowed to proceed overnight for 16h at 37°C in 5% (v/v) CO₂ in a humidified incubator⁴¹⁸.

2.5.1.2 NØ

Isolated NØ were either induced to apoptosis using Chromata-Vue C71 light box and UVX radiometer and incubated overnight for 16h at 37°C in 5% (v/v) CO₂ in a humidified incubator or incubated at 37°C for 16 h in sfRMI with 0.15% BSA without induction.

2.5.2 Generation of secretomes (AS) from AC

AS from B cells and NØ were generated using whole AC culture (as described in section 2.5.1) by centrifuging at 2000xg for 5 min. Supernatants containing the secreted factors and extracellular vesicles were considered as AS and were used in future studies.

2.5.3 Identification and quantification of apoptosis

2.5.3.1 Annexin-V FITC/Propidium Iodide Staining

Reagents:

- 1) Binding buffer: 150mM NaCl, 10mM HEPES pH 7.4, 2.5mM CaCl₂ in dH₂O.
- 2) Annexin V-FITC (AxV) and propidium iodide (PI) kit (Bender MedSystems, Vienna, Austria).

Procedure

PS, a well characterised marker for apoptosis “flips” from the inner leaflet of a membrane to the external leaflet which forms the basis of the AxV/PI assay analysed using flow cytometry. AxV binds to PS on exposure in the outer leaflet of the plasma membrane whilst PI specifically binds to DNA as cells lose their membrane integrity. Staining with AxV but not PI indicates apoptosis whilst double staining indicates necrosis and negative staining indicates viability²⁸⁰.

Briefly, 100µl of 1 X 10⁶ cells/ml of AC (B cells or NØ) were resuspended in 900µl of binding buffer containing 2µl of AxV-FITC and incubated in the dark on ice for 15 min. Prior to analysis of samples by Beckman Coulter flow cytometry, 5µl of PI was added to a

final concentration of 20µg/ml and samples were analysed immediately to detect viable, apoptotic and necrotic cells.

2.5.3.2 Nuclear stain

Nuclear changes in AC were observed using DAPI staining as described in section 2.4.4.3 or by acridine orange (Sigma, UK) added at a concentration of 10µg/ml to the cells and incubated for 10 minutes at 4°C on dark and washed the cells with PBS to remove unbound stain. The Percentages of AC was scored.

2.6 Assays of phagocyte interaction with AC

2.6.1 Phagocytosis of AC by MØ through interaction assay

To assess the interaction (i.e. tethering and phagocytosis) with AC (B cells or NØ) THP-1/DS derived MØ were cultured in multi well glass slides (Hendley Essex PH-005, Loughton, England) for 48-72h according to the procedure described in section 2.3.5 Untreated or gingipain (5µg/ml) -treated MØ (as described in section (2.7.11) (5×10^5) were co-cultured with AC (B cells or NØ) 1×10^6 / well in multiwell glass slides for 1h at 37°C in the cRPMI medium. Care was taken not to mix the supernatant from different wells. After co-culture, the multiwell glass slides were washed with ice-cold PBS three times to remove unbound cells and the bound cells were fixed with methanol for 10 minutes prior to standing with Jenner-Giemsa stain ³⁶.

Staining method for Jenner - Giemsa

- Jenner and Giemsa stain (Oxoid, Basingstoke, UK).
- Jenner Giemsa buffer (JG) (50X stock): Two solutions were prepared. Solution A 200mM NaH₂ PO₄ and solution B: 200mM Na₂ HPO₄. To make a 1X working solution, 20ml of solution B was added to 190ml of solution A until the pH reached 5.6 and then the volume was increased to 1 litre with distilled H₂O.
- Preparation of Jenner buffer (1:3): To avoid precipitates, the buffer was made fresh 1 part of Jenner stain was mixed with 3 parts of JG buffer.
- Preparation of Giemsa buffer (1:10): 1 part of Giemsa stain was mixed with 10 parts of JG buffer and used immediately for staining of cells.

The co-cultured air-dried methanol fixed slides were stained by immersing the slides with Jenner buffer for 6 min. The unbound stains were removed by extensive washing with JG buffer and following this the slides were immersed in Giemsa buffer for 11 min and again washed with JG buffer three times with the final wash in distilled water. Slides were mounted with DePeX mounting medium and cells scored following visualisation under light microscopy for at least 200 MØ in each of the quadruplicate wells.

2.6.2 *In vitro* cell migration assay

2.6.2.1 Horizontal migration

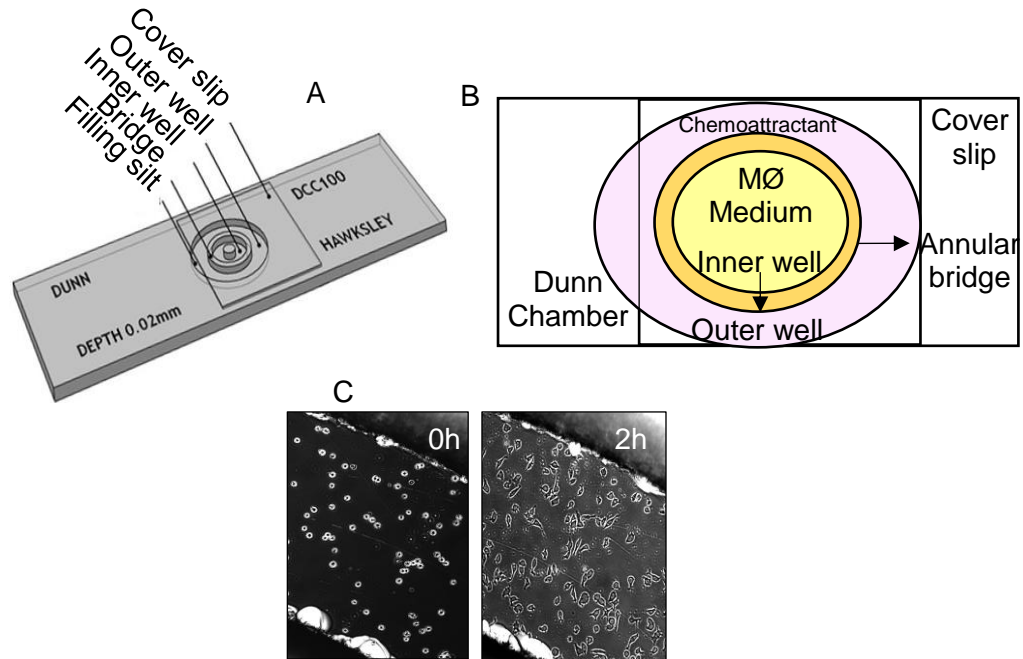


Figure 11: The Dunn chamber model

Diagram showing the Dunn chamber used for MØ migration towards a putative chemoattractant. A) The Dunn chamber used to study MØ chemotaxis. B) The design of the interior of the chamber. The chamber consists of two wells the inner well containing MØ medium and an outer well containing the putative attractant. The outer well and the inner well were separated by an annular bridge which is covered by a cover slip carrying MØ placed on the top of the chamber. C) MØ migration viewed from the top of the annular bridge at 0h where the MØ showed no or minimal movement and at 2h showing random or defined migration.

2.6.2.2 Vertical migration

MØ migration towards a chemoattractant was also studied using the vertical Cell-IQ live cell imaging and analysis platform system. To set up the experiment, 700µl per well of AC (1×10^6) (B cells or NØ) or AS were added to the lower chamber of a 24 well plate and a transwell with 8.0 µm pore polycarbonate membranes (Corning, Life Science, NY, USA) was subsequently placed in each well. To each transwell 300µl of THP-1/VD3 stimulated MØ (5×10^5) was added and the 24- well plate was covered by a Cell-IQ lid and sealed using adhesive paper tape (figure 12). The output connector from the Cell-IQ lid was connected to the Cell-IQ analyser with the gas (5% CO₂) enabled on the system. Vertical migration of MØ towards AC or AS was recorded for up to 12h with an image captured every 20 minutes using the Cell-IQ tracking system and software. The migrated MØ found in the lower chamber of a 24 well plate were calculated and analysed using the Cell-IQ software.

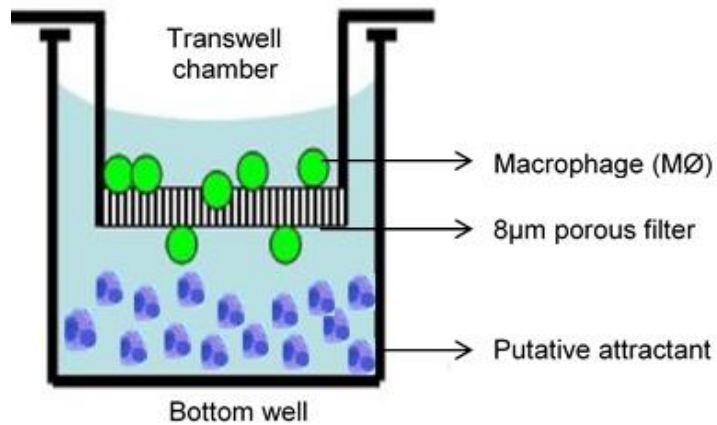


Figure 12: The Cell-IQ model

Diagram showing the Cell-IQ model set up to study MØ migration. The bottom chamber of a 24-well plate was loaded with a putative attractant (blue) and the transwell containing 8µm porous filter membrane were placed on the top of each well in a 24-well plate. The MØ (green) were loaded on the transwell and analysed for their migration using the Cell-IQ equipment. Adapted from ⁴¹⁹.

2.7 Isolation and characterisation of gingipains from *P.gingivalis* HG66 and W83

2.7.1 Bacterial strains of *P.gingivalis*

2.7.1.1 W83: *P. gingivalis* W83 was originally isolated from an undocumented human oral infection in Bonn, Germany in the 1950s ⁴²⁰⁻⁴²²

2.7.1.2 HG66: *P. gingivalis* HG66 DSM-No: 28984, was isolated from the oral cavity and proven to produce gingipains in a soluble form unlike strain W83 which retained the enzymes on the cell surface ⁴²³

Both the strains W83 and HG66 of *P.gingivalis* were provided by the Periodontal Research Group, School of Dentistry, University of Birmingham, United Kingdom.

2.7.2 Materials and buffers for gingipain isolation

2.7.2.1 Materials for bacterial growth

Fastidious agar plate (Oxoid, Thermo Fisher Scientific, UK)

Fastidious anaerobe broth (FAB) (LAB M, UK)

2.7.2.2 Buffers for W83

TLCK buffer: To 100ml of PBS, 100µl of Na-p-tosyl-L-lysine chloromethyl ketone (TLCK) 0.1mM, 1 ml of leupeptin (0.1mM) and 100µl of 0.5mM EDTA were added.

Triton and MgCl₂ buffer: To 100 ml of PBS, 1ml of Triton X-100, 20 mM of MgCl₂ were added.

Dialysis buffer: 150 mM NaCl, 20 mM Bis-tris (Bisiminotris-methane), 5 mM CaCl₂ were added to a litre of sterile distilled water.

2.7.2.3 Buffers for HG66

Buffer A: 20 mM Bis-Tris-HCl, 150 mM NaCl, 5 mM CaCl₂, 0.02% (w/v) NaN₃, pH 6.8

Buffer A for dialysis: 20 mM Bis-Tris-HCl, 150 mM NaCl, 5 mM CaCl₂, 0.02% (w/v) NaN₃, pH 6.8 with 1.5 M 4, 4'-dithiodipyridine disulphide (Aldrithiol)

Buffer B: 50 mM Tris-HCl, 1 mM CaCl₂, 0.02% NaN₃, pH 7.4

Buffer B with NaCl gradient: A step gradient of 500 mM NaCl was applied in buffer B

Buffer B with arginine gradient: A gradient of 100 mM L-arginine was applied in buffer B

Buffer B with lysine gradient: A gradient of 0-750 mM L-lysine was applied in buffer B

Buffer C: 20 mM Bis-Tris- HCl, 1 mM CaCl₂, 0.02% (w/v) NaN₃, pH 6.4

Enzyme activity buffer (pH 7.6): 0.2 M Tris-HCl, 0.1M NaCl, 5 mM CaCl₂, 0.02% (w/v) NaN₃, 10 mM L-cysteine were added to sterile distilled water.

Sodium Dodecyl Sulphate Polyacrylamide Gel Electrophoresis (SDS-PAGE) running buffer: 3.03 g/L of Tris, 14.4 g/L of glycine (Alfa Aesar, UK) and 1 g/L of SDS (Fisher Scientific, UK) pH 8.3

TBS (10x): 24.23 g/L Trizma HCl, 80.06 g/L NaCl, pH 7.6

Destaining buffer: To 800 ml of distilled water 100 ml of methanol, 100 ml of acetic acid (17.5M) were added

Pierce BCA Protein Assay Kit (Thermo Scientific, UK)

LAL chromogenic endotoxin quantitation kit, Thermo Scientific Pierce, UK

2.7.3 Bacterial strains and growth conditions: Bacteria (W83 and HG66) were grown on fastidious agar plates containing 7% (v/v) sterile horse blood and incubated for 24- 48h at 37°C in an anaerobic chamber of 10% H₂, 10% CO₂, and 80% N₂. The bacterial colonies were transferred to the sterile fastidious anaerobe broth containing 10.0g yeast extract, 5 mg haemin, 0.5 mg vitamin K1, 500 mg L-cysteine and subsequently incubated at 37°C in an anaerobic chamber with gentle agitation overnight.

2.7.4 Gram stain of W83 and HG66

P. gingivalis strains W83 and HG66 were grown on horse blood agar fastidious plates to form distinctive black pigmented colonies. After 48h, these colonies were prepared for Gram staining by creating a slide smear of the bacterial culture ⁴²⁴. Based on the

composition of the cell wall of bacteria, the Gram stain procedure aids differentiation of Gram-positive from Gram-negative bacteria. In brief, on a clean microscope glass slide, a loopful of water was placed prior to addition of bacterial culture from the petri dish. Care was taken to add a small amount of bacteria culture. The culture mixed with water was spread on the glass slide surface creating a thin film on its centre. This smear was allowed to air dry for a few seconds and fixed over a gentle flame using a circular motion. To the fixed culture, crystal violet stain was added for 1 minute prior to rinsing with water. The crystal violet stains penetrates the cell wall of both Gram-positive and Gram-negative bacteria. Following this, a mordant dye-iodine solution was added to the smear to enhance the interaction between the culture and the dye and was incubated for 1 minute prior to rinsing with water. Gram-positive bacteria resists the decolourisation because of their thick peptidoglycan layer while Gram-negative bacteria, due to their thin layer of peptidoglycan, the crystal violet-iodine complex was decolourised while washing with acetone for a minute. Following this step, safranin, the positively charged counterstain dye was added and incubated for 1 minute and washed with running tap water. Since Gram-negative cells lose the purple colouration unlike Gram-positive bacteria they take up the safranin and they appear red or pink in colour upon visualisation under light microscopy (figure 13).

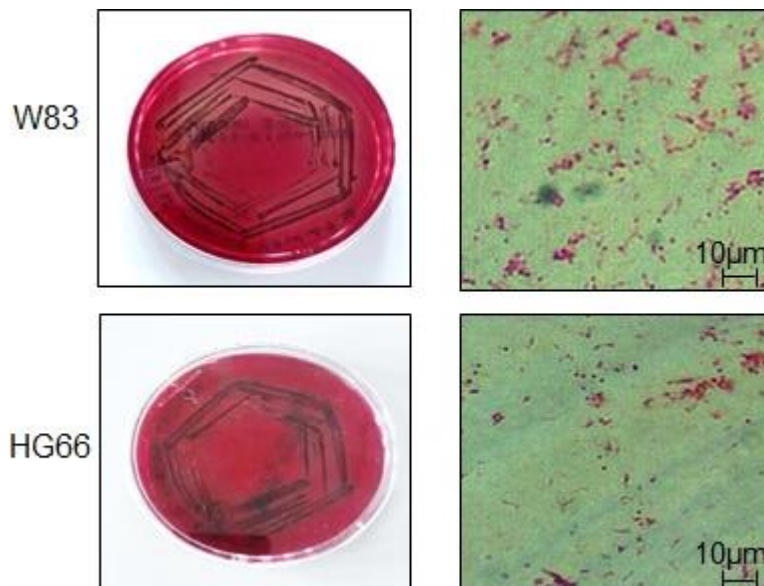


Figure 13: Culture and Gram staining of the *P.gingivalis* strains W83 and HG66

Images show bacterial solid state culture of *P.gingivalis* strains and their corresponding Gram stains. On the top panel W83 is shown and the HG66 strain is shown on the bottom panel. The bacterial strains were grown on fastidious agar plates incubated for 24-48h in an anaerobic chamber at 37°C (as described in section 2.7.3). The black pigmented colonies were analysed for purity by Gram stain procedure. The right-hand panels show pink rod-shaped bacilli confirming the purity of Gram-negative bacteria of both W83 and HG66.

2.7.5 Growth curve of bacterial culture W83 and HG66

To study bacterial growth, the healthy viable bacterial culture were inoculated into FAB broth and incubated in an anaerobic chamber with gentle agitation for 72h. At a range of time points during the growth period, a sample of broth containing multiplying bacteria was removed for spectrophotometric analysis at 600nm. Gram staining (as described in section 2.7.4) was also undertaken to ensure purity. The degree of turbidity at 600nm relates to the absorbance value in a spectrophotometer and bacterial cell number. The growth curve plots determine the dynamics of the bacterial growth in four phases lag, exponential or logarithmic (log) phase, stationary phase, decline or death phase.

2.7.6 Isolation of membrane-bound proteins from *P.gingivalis* strain W83:

Bacterial cultures were centrifuged at 10,000xg for 30 min at 4° C to produce a pellet and cell-free culture supernatant. The cell pellet was used for isolating cytosol-derived fractions of gingipains as described ⁴²⁵. Briefly, the pelleted bacterial cells were resuspended in TLCK buffer (as described in section 2.7.2.2) and disrupted using sonication (Bandelin Sonopuls). The cells were disrupted at 65 MPa on 6 occasions with a time gap of 30 seconds to avoid the disruption of the proteins in the samples. The sonicated bacterial cells were centrifuged at 2,400Xg for 10 min in order to release the proteins into the supernatant. The resulting supernatant was subjected to ultracentrifugation (Beckman 70Ti rotor) at 100,000xg for 60 min at 4°C. The pellet, consisting of the outer membrane fragments, was resuspended in Triton and MgCl₂ buffer (as described in 2.7.2.2) and mixed gently for 30 min at 20 °C. These fragments were then ultracentrifuged at 100,000Xg for 60 min at 4°C and the pellet resuspended in dialysis buffer (as described in section 2.7.2.2) to recover the outer membrane proteins as a precipitate.

2.7.7 Isolation and purification of soluble proteins from culture supernatant HG66:

Gingipains were isolated according to the method described ⁴²⁶. Briefly, 24h bacterial cultures (1 litre) (optical density – 1.763 at 600nm) were centrifuged at 12,000xg for 45 min at 4°C and to the cell-free-culture supernatant chilled acetone was added at a ratio 40:60 (culture supernatant:acetone) slowly with gentle agitation and incubated for 2h at -20°C. The resultant protein precipitate was centrifuged at 12,000xg for 30 min at 4°C and the pelleted precipitate was resuspended in 290ml of buffer A with aldrithiol (as described in section 2.7.2.3) for 4h and dialysed against buffer A without aldrithiol overnight. In order to concentrate the dialysed fractions, Amicon PM-10 membranes (Merck Millipore, UK) were used prior to application of the fractions to Sephadex G-150 columns (5 x 115 cm) equilibrated with buffer A at a flow rate of 0.5ml/min. Fractions were tested for activity against Bz-L-Arg-pNA (BAPNA) (Sigma-Aldrich, UK) and Z-L-Lys-pNA (Sigma-Aldrich,

UK) (as described in section 2.7.8.1) and were pooled and dialysed overnight against buffer B with 2 changes. Dialysed fractions were applied to a 10ml arginine-Sepharose column (GE healthcare, UK) (1.5 x 30 cm) equilibrated with buffer B (as described in section 2.7.2.3). Following the washes, buffer B with 500mM NaCl gradient was applied and the A_{280nm} baseline decreased to zero. RgpB was eluted by equilibrating the column with buffer B containing an 100 mM arginine gradient (as described in section 2.7.2.3).and the Kgp eluted with Buffer B containing a 750 mM lysine gradient at a flow rate of $0.5ml/min^{-1}$ (as described in section 2.7.2.3). The eluted fractions were concentrated again using Amicon PM-10 membrane at a speed 4000xg for 20 min at 4°C. The concentrated samples were resuspended in buffer C (as described in section 2.7.2.3) and centrifuged again at 4000xg for 20 min at 4°C to obtain a pure RgpB or Kgp protease. Eluted gingipains were stored at -80°C.

2.7.8 Confirmatory analysis of gingipain purity

2.7.8.1 Enzyme activity assay

To measure the purified RgpB and Kgp activities, 100µl of enzyme buffer containing 1mM Bz-Arg-pNA for RgpB or 0.5 mM Z-L-Lys-pNA for Kgp were added to 100µl of eluted RgpB or Kgp fractions from W83 and HG66 and incubated for 1h at 37 °C. The reaction was stopped by adding 50µl of glacial acetic acid (Sigma-Aldrich, UK) and p-nitroaniline (pNA) released from the substrate was read at 405nm on a spectrophotometer. One unit of enzyme activity corresponds to 1 µmol of pNA released during 1h of incubation at 37°C.

2.7.8.2 Determination of molecular weight using SDS-PAGE electrophoresis

2.7.8.2.1 Protein determination using BCA assay

The concentration of eluted protein fractions from the W83 and HG66 strains was determined using a protein assay kit (as described in section 2.7.2.3). In brief, the Bicinchoninic acid assay is based on the principle involving a temperature-dependent reaction, where Cu^{2+} ions are reduced from copper (II) to copper (I) sulphate by the peptide bonds present in the protein thereby resulting in purple colouration as BCA chelates Cu (I) ion. The colour correlates with the amount of protein present in the sample. The BSA standards were prepared in the same buffer as samples to avoid interference. Standards or samples were incubated with the BCA reagent for 30 minutes at 37°C prior to reading the absorbance at 562nm using a spectrophotometer. The samples were cooled for several minutes at room temperature to enable increased sensitivity.

2.7.8.2.2 Trichloroacetic Acid (TCA) precipitation of eluted proteins derived from the W83 and HG66 strains

Once the known amount of protein was calculated in the eluted fractions from the W83 and HG66 strains the protein samples were concentrated using the TCA method. The eluted protein fractions were treated with 0.15 % (w/v) sodium deoxycholate (DOC) at a 1: 10 ratio and 72 % (v/v) TCA (1: 10 ratio) and centrifuged at 16,000xg for 10 minutes to precipitate the proteins. The resulting pellet was either used directly for SDS-PAGE (as described in section 2.7.8.2.3) or stored at –80°C until analysis.

2.7.8.2.3 SDS-PAGE electrophoresis

Separation of proteins based on the electric charge or mass is a common method of gel electrophoresis ⁴²⁷. Here, SDS was used to denature the proteins and to provide a net negative charge to all the proteins that have been denatured such that mass to charge ratio is equalised and proteins are separated simply based on their molecular mass. SDS-PAGE was performed on a 10% resolving gel with a 4% stacking gel in Tris-glycine running buffer as detailed in Table 5 according to the manufacturer instructions (Mini-protean II apparatus from Bio-Rad).

Gel reagents

Reagents	10% resolving gel	4% stacking gel
Acrylamide solution (30%) (37.5:1)	3.33 ml	666 µl
1.5 M Tris- HCl	2.5 ml	1.25 ml
dH ₂ O	4.015 ml	3 ml
10% SDS	100 µl	50 µl
10% APS	100 µl	50 µl
TEMED	10 µl	5 µl

Table 5: Composition of reagents to prepare resolving and stacking gel

The percentage of resolving and stacking recipes for preparation of one gel used for SDS-PAGE electrophoresis for molecular weight determination of extracted proteins from the W83 and HG66 strains.

The gel was prepared according to the details provided in Table 5 and depending on the number of gels needed the volume of individual recipes were calculated accordingly. Briefly, the 10% resolving gel was prepared (as detailed in Table 5) and added to cleaned gel plates and the gel was allowed to polymerise. The 4% stacking gel was prepared (as detailed in Table 5) and added to the top of the polymerised resolving gel. Gel set ups

were then placed in the buffer chamber containing the SDS-PAGE running buffer. To prepare the samples, 40µg of TCA-precipitated protein (as described in section 2.7.8.2.2) were mixed with 2 X Laemmli buffer and denatured at 95°C for 5 min and incubated on ice for 1 minute prior to loading on the SDS- PAGE gel and electrophoresed using a Hoefer buffer chamber at 200V for 40 min. Electrophoresis was performed at 60V through the stacking gel and at 120V through the resolving gel until the marker standard reached the bottom of the resolving gel. The pre-stained protein ladder (Life Technologies, UK) was used alongside the samples to estimate the approximate size of separated proteins. The protein bands were visualized by staining with coomassie blue (GE Healthcare Life Sciences, UK) and destaining buffer (as described in section 2.7.2.3) and homogeneity was determined using laser densitometry by scanning the gel under gel imager (as described in 2.1).

2.7.9 Mass spectrometry

2.7.9.1 Sample preparation

Purified samples of gingipains (x µg) were separated by SDS-PAGE, and was subjected to mass spectrometry analysis after in-gel digestion of the gel band of the appropriate molecular size ⁴²⁸. Briefly, the Coomassie blue-stained gel was layered over a clean glass plate, and the protein band of interest (40-50 kDa) was excised using a clean scalpel blade. The excised gel was transferred into a 0.5 ml polypropylene Eppendorf tube and diced. Gel pieces were destained using 200 µl of 50 % aqueous ammonium bicarbonate in acetonitrile (50 mM) for 90 min on the orbital thermoshaker (550 rpm) at 37°C. After destaining was completed the supernatant was removed and gel pieces were repeatedly dehydrated with 100 µl of acetonitrile until the gel shrunk and turned white. Excess of acetonitrile was removed in the vacuum concentrator for 10 min and sample was stored at -20 °C prior to sending for further analysis at the University of Birmingham where trypsin in-digestion and nLC-MS/MS were carried out.

2.7.9.2 LC-MS/MS

The samples were trypsin digested using 40µl of 100mM ammonium bicarbonate (pH 8) added to 10µl of the protein samples (~1-100µg of protein). Following this, 50 µL 10 mM dithiothreitol (DTT) was added to the protein samples and incubated at 56°C for 30 mins. To the cooled protein samples, 50µl 50mM iodoacetamide, were gently mixed incubated for 30 mins at dark. In the final step, samples were incubated overnight at 37°C with 25 µl of trypsin gold (Promega, Southampton, Hampshire, UK, 6 ng/µl).

Digested samples were analysed using-nLC-MS/MS (QExactive™ Thermo Fisher, UK). The peptide concentration was carried out using UltiMate® 3000 HPLC series (Dionex,

Sunnyvale, CA USA). The gradients were performed for 30 mins using 3.2% to 44% formic acid (0.1%) in acetonitrile. LTQ Orbitrap Elite ETD mass spectrometer (ThermoFisher Scientific, Germany) was used to elute the peptides.

Acquired data were searched against SwissProt database for *Porphyromonas gingivalis* taxonomy using Sequest search engine allowing for a maximum two trypsin mis-cleavages and with the *m/z* confidence of 5 ppm.

2.7.10 Limulus Amebocyte Lysate (LAL) assay for LPS detection

To detect and quantify Gram-negative bacterial LPS in the eluted proteinase from W83 and HG66 of the *P.gingivalis* strains, a LAL assay (as described in section 2.7.2.3) was performed. LAL, sourced from horseshoe crab's blood cells reacts with bacterial endotoxins in the eluted samples by activating the proteolytic enzymes and catalyses pNA upon adding the chromogenic substrate resulting in a yellow colouration which is quantified by measuring the absorbance at 405nm (A_{405}). Briefly, the microplate was equilibrated in a heating block for 10 minutes at 37°C prior to addition of 50µl of standard (BSA) or samples (10µg) and incubated for 5 minutes at 37°C. Following the addition of samples, 50µl of LAL reagent was added and incubated for 10 minutes at 37°C and subsequently 100µl of chromogenic substrate was added and incubated for 6 minutes at 37°C prior to gently mixing the contents using a plate mixer. The reaction was stopped by adding 50µl of acetic acid (25%) and the plate was gently homogenised using a plate mixer for 10 seconds and measured for absorbance at 405nm. All reagents were prepared using the endotoxin-free water provided with the kit. A standard curve was established using LPS from 0.1 -1.0 EU/ml (endotoxin/mL) and 1EU/ml is equivalent to 0.1 to 0.2 ng endotoxin/ml of solution.

2.7.11 MØ or NØ treatment with gingipains

VD3 or DS THP-1 differentiated for 48h MØ (990µl) (1×10^6 cells/ml) or freshly isolated viable NØ (990µl) (1×10^6 cells/ml) were treated with 10µl of the eluted gingipains fractions of either RgpB or Kgp (5µg/ml) derived from HG66 *P.gingivalis* in sfRPMI medium for 1h at 37°C. Treated cells were used for further analysis to study MØ behaviour in response to AC.

2.7.12 Inhibition of gingipains using Na-p-tosyl-L-lysine chloromethyl ketone

THP-1 VD3 or DS MØ (1×10^6 cells/ml) were treated with the cysteine protease inhibitor, TLCK (0.1mM) for 10 minutes at 37°C prior to treatment with gingipains (5µg/ml) as described in section 2.7.11.

2.8 LPS from *P.gingivalis* induced TNF- α response in THP-1 derived M \emptyset s

VD3 or PMA stimulated THP-1 differentiated M \emptyset were washed and seeded in 850 μ l of fresh cRPMI at 6×10^5 cells/well in a 24 well plate. The cells were challenged with a range of doses of 50 μ l of lipopolysaccharide (LPS 0-500ng/ml/assay) from *Escherichia coli* (*Ec* LPS) (positive control) or LPS (0-100 μ g/ml) from *P.gingivalis* (*Pg* LPS) (Invivo Gen, UK) in the presence of 100 μ l of 10% (v/v) normal human serum (NHS) to act as a source of LPS-binding protein and incubated for 4h at 37°C. The reaction was stopped by freezing at -20°C until the TNF- α ELISA was performed. The supernatant was harvested and used for analysis of TNF- α release in the M \emptyset using the anti-human TNF- α capture ELISA (R & D systems, Minneapolis, USA).

Gingipains from *P.gingivalis* induced TNF- α response in THP-1 derived M \emptyset s

Gingipains (5 μ g/ml) 10 μ l were used to induce TNF- α response in THP-1 derived M \emptyset (both VD3 and DS) (990 μ l) (1×10^6 cells/ml) (as detailed in section 2.7.11) and incubated for 1h at 37°C and either analysed immediately for TNF- α response or left at -20°C until indirect ELISA was performed. The supernatant was harvested and used for analysis of TNF- α release in the M \emptyset using the anti-human TNF- α capture ELISA (R & D systems, Minneapolis, USA).

2.8.1 Measurement of TNF- α levels in M \emptyset co-cultured with AC

The effect of AC or their derived AS (from either B cells or N \emptyset) on TNF- α production in LPS or gingipain-stimulated M \emptyset were studied using ELISA. Briefly, 750 μ l of VD3 or DS THP-1 differentiated M \emptyset (as described in section 2.3.5) were seeded (6×10^5 cells/well) in wells of a 24 well plate. As appropriate to each well, 100 μ l of AC (1×10^6) or AS (1×10^6) or N \emptyset medium alone (control) (as described in section 2.4.1) were added to the M \emptyset and incubated for 18-24h at 37°C. After the incubation period, 50 μ l of *Ec* LPS (20ng/ml) or 50 μ l of *Pg* LPS (1 μ g/ml) were added in the presence 100 μ l of NHS (10% v/v) and incubated for 4h at 37°C or 10 μ l of gingipains (RgpB or Kgp) were added and incubated for 1h at 37°C. The supernatants were harvested and stored at -20°C until further analysis.

2.8.2 ELISA

Materials

- Anti-human TNF- α capture ELISA from R & D systems, Minneapolis, USA
- Recombinant TNF- α from R & D systems, Minneapolis, USA
- TNF- α detection antibody from R & D systems, Minneapolis, USA
- ELISA Diluent (PBS-T): 0.05% (v/v) Tween 20 in PBS (Fisher, UK).
- ELISA wash buffer: 0.9% (w/v) NaCl, 0.05% (v/v) Tween 20 in PBS

- ELISA block buffer: 1% (w/v) BSA, 5% (w/v) sucrose and 0.05% (w/v) sodium azide in PBS

ELISA plates were coated with 100µl of 2µg/ml of the TNF-α capture antibody diluted in PBS and incubated overnight at 4°C. Prior to experimentation, the antibody coated ELISA plate was washed with ELISA wash buffer three times and TNF-α ELISA block buffer (100µl/well) was added to the 96 well plate and incubated for 1h at 37°C. The plates were washed for three times with ELISA wash buffer and 100µl of known concentrations of recombinant TNF-α (standard) or supernatant of the samples were added to the designated wells and incubated at 37°C for 2h. The plate was washed again three times using ELISA wash buffer to remove unbound samples and 100µl of TNF-α detection antibody (200ng/ml) diluted in ELISA diluent was added to each well and incubated for 2h at 37°C. Prior to the addition of 100µl of streptavidin-Horseradish peroxidase (HRP) at 1:2000 concentration in ELISA diluent, the plate was washed three times with ELISA wash buffer and incubated with HRP for 1h at 37°C. Bound HRP was detected by addition of 100µl of Ortho-Phenylenediamine (OPD) to each well and incubated at room temperature in the dark until the colour developed. The reaction was stopped by the addition of 50µl of 1M HCl and the plate was read at a 490nm absorbance.

2.9 Determination of anti-inflammatory cytokines (TGF-β and IL-10) mRNA levels using quantitative PCR

2.9.1 Materials

- RNA isolation kit includes TRK lysis buffer, RNA wash buffer I, RNA wash buffer II, DEPC treated water, HiBind RNA column (E.Z.N.A total RNA kit I, Omega bio-tek, VWR, UK)
- RNase free TBE buffer (Geneflow, UK)
- 1kb RNA Ladder (Geneflow, UK)
- Ethidium bromide (Fisher Scientific, UK)
- Norgen 2x loading sample buffer (Geneflow, UK)
- Reverse transcription (RT)-nanoScript2 (Primer design, UK)
- Reverse transcription polymerase chain reaction (RT-PCR) primer kit TGF-β (Primer design, UK) (forward primer: 5' CAC TCC CAC TCC CTC TCT C 3' and reverse primer: 3' GTC CCC TGT GCC TTG ATG 5')
- RT-PCR primer kit IL-10 (Primer design, UK) (forward primer: 5' GCT GGA GGA CTT TAA GGG TTA C 3' and reverse primer: 3' TGA TGT CTG GGT CTT GGT TCT 5')
- Human β-actin forward primer (h ACT F) – 5' CTG GAA CGG TGA AGG TGA CA 3' (ThermoFisher Scientific, UK)

- Human β -actin reverse primer (h ACT R) – 3' AAG GGA CTT CCT GTA ACA ATG CA 5' (ThermoFisher Scientific, UK)
- SYBR (Syber green) (Primer design, UK)
- RNase/DNase free water (Primer design, UK)

2.9.2 Preparation of cells

VD3 stimulated THP-1 MØ (1×10^6 /ml) (as described in section 2.3.5) were cultured with or without AC NØ (3×10^6) for 6h and treated with gingipains for 1h at 37°C or left untreated. Following the treatment, the cells were centrifuged at 2000xg for 10 min. The supernatant discarded and the pelleted cells were stored -80°C until RNA isolation was performed ⁴²⁹.

2.9.3 RNA isolation

RNA was isolated at room temperature from the VD3 MØ co-cultured with AC NØ, and treated with or without gingipains, according to the manufacturer's instructions as described in section 2.9.1. In brief, 350 μ l of TRK lysis buffer was added to the thawed pellet followed by 350 μ l of ethanol (70%). This sample mixture was then vortexed and transferred to the HiBind RNA column (as described in 2.9.1). The column is inserted into a 2ml collection tube prior to addition of the sample mixture. The column was centrifuged at 10,000xg for 1 minute and the flow through was discarded. To the column 500 μ l of RNA wash buffer I was added and centrifuged at 10,000xg for 30 seconds. The resultant filtrate was discarded and 500 μ l of RNA wash buffer II was added and centrifuged at 10,000xg for 30 seconds and the washing step was repeated again with the centrifugation speed at 16,000 x g for 2 minutes. The column was transferred to a 1.5ml microcentrifuge tube (Fisher Scientific, UK) and 50 μ l of DEPC-treated water was added and centrifuged again at 16, 000xg for 2 minutes. The resulting flow through was stored at -20°C until further analysis.

2.9.4 Confirmatory analysis of RNA purity

2.9.4.1 Nanodrop

Isolated RNA was quantified by Nanodrop to determine the purity of the RNA samples. To the cleaned Nanodrop sample contact 1 μ l of the RNA sample was added to assess the purity of the RNA. The value above 2.0 within the 260/280 ratio indicates the purity of the RNA samples and analysed further using PCR. 100ng of isolated RNA was used for each PCR.

2.9.4.2 Agarose gel electrophoresis

To test the integrity of the isolated RNA 1% (w/v) agarose was dissolved in RNase-free TBE buffer (as described in section 2.9.1) and microwaved until the agarose melted completely and, prior to addition of ethidium bromide (to give a final concentration of 0.5µg/ml), the agarose gel was cooled and stained for RNA visualisation. 100ng of RNA samples (as described in section 2.9.3) were mixed with 2X sample buffer (as described in 2.9.1) and incubated for 5 minutes at 95°C. Samples were left on ice for one minute and then loaded on the agarose gels. Gels were electrophoresed at 60 Volts, 120 Watts 250 mA for up to 1h and RNA profiles viewed using a UVP transilluminator.

2.9.5 RNA reverse transcription

2.9.5.1 Reverse transcribe RNA into cDNA

Once the quality of RNA was determined the RNA was reverse transcribed to cDNA using the Primer design RT-nanoscript kit (as described in section 2.9.1). To 100ng of each RNA sample, 1µl of reverse transcription primer was added and made up to 10 µl using RNase/ DNase free water. Samples were incubated at 65°C for 5 mins in a heat block and were frozen immediately on ice.

2.9.5.2 Extension step reaction mixture

To the above mixture generated as described in section 2.9.5.1, 2µl of Nanoscript 2 4X buffer, 1µl of dNTP mix (10mM), 4µl of RNase/DNase free water and 1µl of Nanoscript 2 enzyme were added to each sample or a master mix was prepared depending on the sample count and 10 µl of the master mix was added to each sample. The RNA samples were amplified using a thermocycler programmed for 42°C for 20 min followed by 75°C for 10 min. The resultant cDNA samples were diluted 1:10 using RNase/DNase free water and stored at -20°C until further PCR analysis was performed.

2.9.6 Quantification of TGF-β and IL-10 gene expression

2.9.6.1 Housekeeping gene (Human β-actin)

To 5µl of each cDNA samples (1:10) generated from RNA using RT-PCR, 3µl of RNase/DNase free water, 1µl of human actin forward primer (as described in section 2.9.1), 1µl of human actin reverse primer (as described in section 2.9.1) and 10µl of Syber green were added to a PCR 96 well plate (Primer design, UK) or a master mix of the reagents were prepared and 15µl of the master mix were added to 5µl of cDNA sample.

2.9.6.2 TGF-β and IL-10 gene expression

To 5µl of each cDNA samples (1:10) generated from RNA using RT-PCR, 4µl of RNase/DNase free water, 1µl of human primers IL-10 or TGF-β (as described in section

2.9.1) and 10µl of SYBR were added to a PCR 96 well plate (Primer design, UK) or a master mix of the reagents were prepared and 15µl from the master mix were added to 5µl of the cDNA sample. The plate was covered using PCR seal adhesive plates and gently mixed by spinning the plate for 10 seconds using a plate spinner (as described in section 2.9.1). The plate was amplified using a Stratagene Mx3000P thermocycler (as described in section 2.1) using the PCR program comprising 10 minutes at 95°C, 15 seconds at 95°C and 1 minute at 60°C for 40 cycles, 30 seconds at 95°C, 30 seconds at 55°C and 30 seconds at 95°C and results were analysed using qPCR software (as described in section 2.1).

2.9.6.3 Quantification of mRNA

The comparative method was used to interpret the cycle threshold (Ct) value of the target gene. First, Ct values of the gene of interest was subtracted from the house keeping gene to calculate the delta Ct (Δ Ct). Δ Ct refers to the amount of target nucleic acid present in the given sample. Second, to the obtained Δ Ct value for each sample were compared with the Δ Ct of the control (untreated MØ) to acquire $\Delta\Delta$ Ct. The resulting $\Delta\Delta$ Ct were powered by $2^{\Delta\Delta$ Ct} to determine the fold-difference between the untreated and the treated samples.

2.10 Statistical analysis

Data were analysed using InStat (GraphPad prism v7, La Jolla, CA, USA) and general statistical analysis using mean \pm Standard error of the mean (S.E.M) for independent replicates (n \geq 3) and different test are used as appropriate.

Chapter 3

Results

Results 1: Establishing a model assay system for MØ interaction with primary apoptotic NØ

3.1 Introduction

Polymorphonuclear cells (PMNs), the most abundant leukocytes which are mostly involved in the innate immune response, are the main players to participate in the body's fight against host-derived danger signals or pathogenic insult⁴³⁰. Circulating NØ migrate towards encountered pathogens by using their specialised adhesion and migration qualities, and eradicate the culprit microorganism by producing primary antibacterial effectors such as azurophilic granules containing NØ elastase, serine protease and alpha-defensins and secondary granules such as lysozyme, lactoferrin, NADPH oxidase and histaminase to combat infection⁴³¹. To facilitate NØ recruitment and migration, MØ upon receiving an inflammatory stimulus produce IL-8, a chemoattractant cytokine that elicits activation of NØ to participate in chemotaxis towards and phagocytosis of the pathogens. Thus NØ are important for the resolution of inflammation⁴³²⁻⁴³⁴. Other chemoattractants, such as FMLP, leukotriene B4 and complement peptides (e.g. C3a, C5a), also recruit NØ to migrate towards the site of inflammation and stimulate clearance of the pathogens using anti-microbial molecules or by generating NETs, to trap and kill the invading pathogens. In order to prevent exacerbating inflammation timely removal and disposal of recruited NØ, which die by apoptosis at injury sites, is essential. Dysregulation of NØ has been linked with major chronic inflammatory diseases, causing significant disruption of normal physiology and influencing the behaviour of other cell types by inhibiting tissue homeostasis restoration^{372, 435, 436}.

NØ influx, an important process in response to bacterial infection, results in phagocytosis and digestion of the pathogen via NØ toxic contents within their NØ phagosome²¹. Phagocytosis-induced cell death is an important process. NØ is primed to undergo apoptosis so that they are cleared rapidly by resident tissue MØ and this critical step aids prevention of NØ necrosis, a potential inducer of tissue damage^{437, 438}. NØ apoptosis, is a tightly-regulated event that enables recognition of the dying cell by professional phagocytes such as MØ and thus prevents the release of toxic contents such as elastases to the surrounding tissues⁴³⁹. Apoptotic NØ undergo cell surface modulation to enable their recognition. For example, flipping of phosphatidylserine from the inner to outer leaflet of the plasma membrane in order to expose 'eat me' signals to local phagocytes allowing

phagocytosis of apoptotic NØ whilst also triggering anti-inflammatory responses^{266, 324, 329, 440}.

To fully understand inflammatory diseases such as periodontitis, it is important to understand the process of cell death to produce apoptotic NØ, the mechanism by which they are removed by MØ and how they stimulate anti-inflammatory cytokines that promote resolution of inflammation. **The aim of this chapter, therefore was to establish an *in vitro* model of primary apoptotic NØ and study how well they interact with and are recognised by THP-1 MØ.**

3.2 Phenotypic characterisation of primary NØ isolated from peripheral blood

Human NØ apoptosis has been widely studied to understand the critical molecular mechanisms behind inflammation resolution²⁴. NØ accumulated at a site of bacterial infection have the potential to damage the surrounding tissue if the timely elimination of activated NØ fails, leading to NØ necrosis and thus exacerbating inflammation. Here, NØ were isolated by a Percoll gradient method and purity of the isolated cells was confirmed by analysis of specific surface receptor expression and nuclear staining for NØ. Following successful isolation, NØ were induced to apoptosis by various methods to identify the optimal AC death induction method. The subsequent interaction and phagocytosis by MØ was then assessed.

3.2.1 Characterisation of primary NØ

In order to separate NØ from other white and red blood cells present within donor blood, fresh human venous blood was collected from healthy volunteers and layered onto a Percoll density column which was centrifuged to separate different cell populations, including NØ (figure 10, Materials & Methods). Following NØ harvesting from columns and red blood cell lysis, the purity of NØ was estimated. The presence of CD66b expression, a surface marker of NØ, was determined both in whole blood and isolated NØ by immunofluorescence and flow cytometry (figure 14). The results demonstrate high CD66b expression as shown by the mean fluorescence intensity (MFI) (figure 14A) of isolated NØ as MFI=703 compared to isotype control MFI = 51. Coupled with the percentage of cells positive by flow cytometry (figure 14B) confirming the purity of NØ as 96%±2 (figure 14B). Additionally, nuclear (DNA) staining reveals characteristic polymorphic nuclei with two-lobed or three-lobed segmented nuclei connected by a strand or filament (figure 14C) as assessed by DAPI staining, again confirming the purity of isolated NØ. Depending on the nature of the NØ the shape of the nucleus changes⁴⁴¹. Normal healthy NØ nuclei have a 3-5 lobed shape, however, NØ are very sensitive and tend to become activated quickly. Activated NØ appear more amorphous and lose their natural shape and adapt to an

amoeba-like structure inducing NØ chemotaxis⁴⁴². These data support the successful approach adopted for NØ isolation from whole blood.

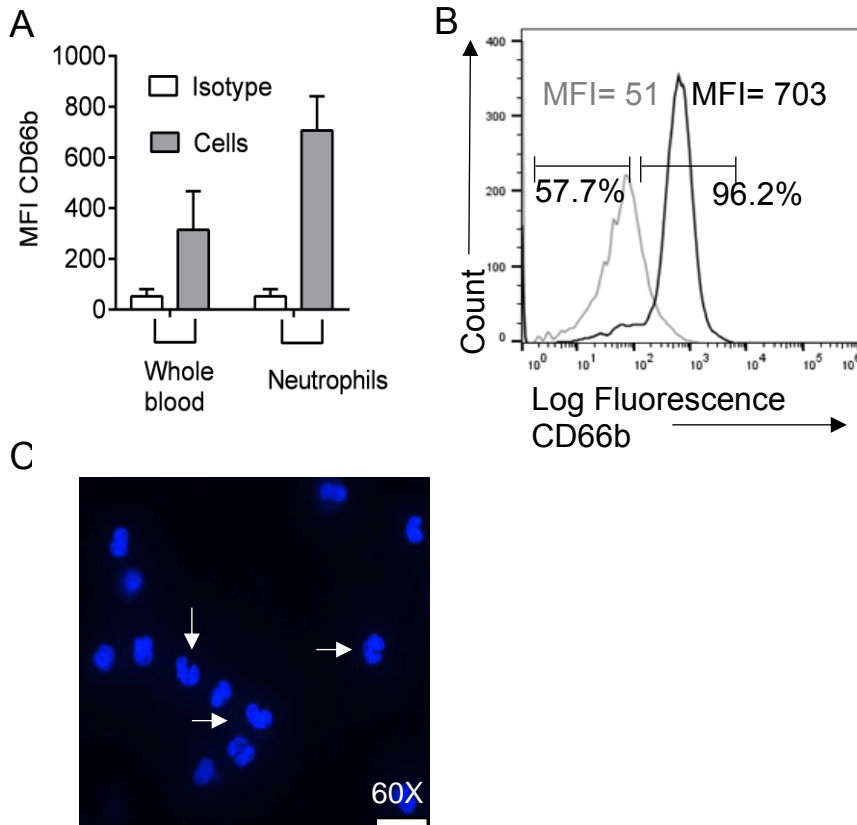


Figure 14: Phenotypic analysis of isolated NØ

NØ were isolated from healthy donor blood using Percoll-mediated fractionation. Isolated cells were assessed for activation marker CD66b (highly expressed on the surface of NØ cells) using flow cytometry and nuclear morphology by DAPI staining. A) Histogram showing MFI of CD66b incubated with whole blood or isolated NØ. B) Flow cytometric frequency histograms of cells stained with isotype control antibody (solid grey line) or anti-CD66b (solid black line) confirming that 96.2% of isolated cells are NØ. The MFI of both isotype and NØ are shown. C) Representative fluorescent image displaying (60X) DAPI stained isolated viable NØ cells (arrows) showing mature segmented nuclei with 3 -5 lobes connected by a filament. Data shown are representative of three independent experiments.

3.3 Generation of AC

3.3.1 B cells

The Mutu Burkitt's lymphoma (B) cell line, is an important AC model used for much of the current study as this cell line has been highly characterised within the Devitt research lab over many years and will play an important role as a control for many assays in this study^{37, 282, 324, 384, 418}. Various doses (25, 50, 75, 100 mJ/cm²) of UV were used to induce apoptosis in B cells. Following overnight incubation at 37°C, which allowed apoptosis to proceed, the cells were washed with binding buffer and stained with annexin V- FITC and propidium iodide (PI) to assess exposure of PS and membrane integrity (i.e. apoptotic and

necrotic cell presence) and accordingly the cells are sorted on the flow cytometric quadrant plot (figure 15A).

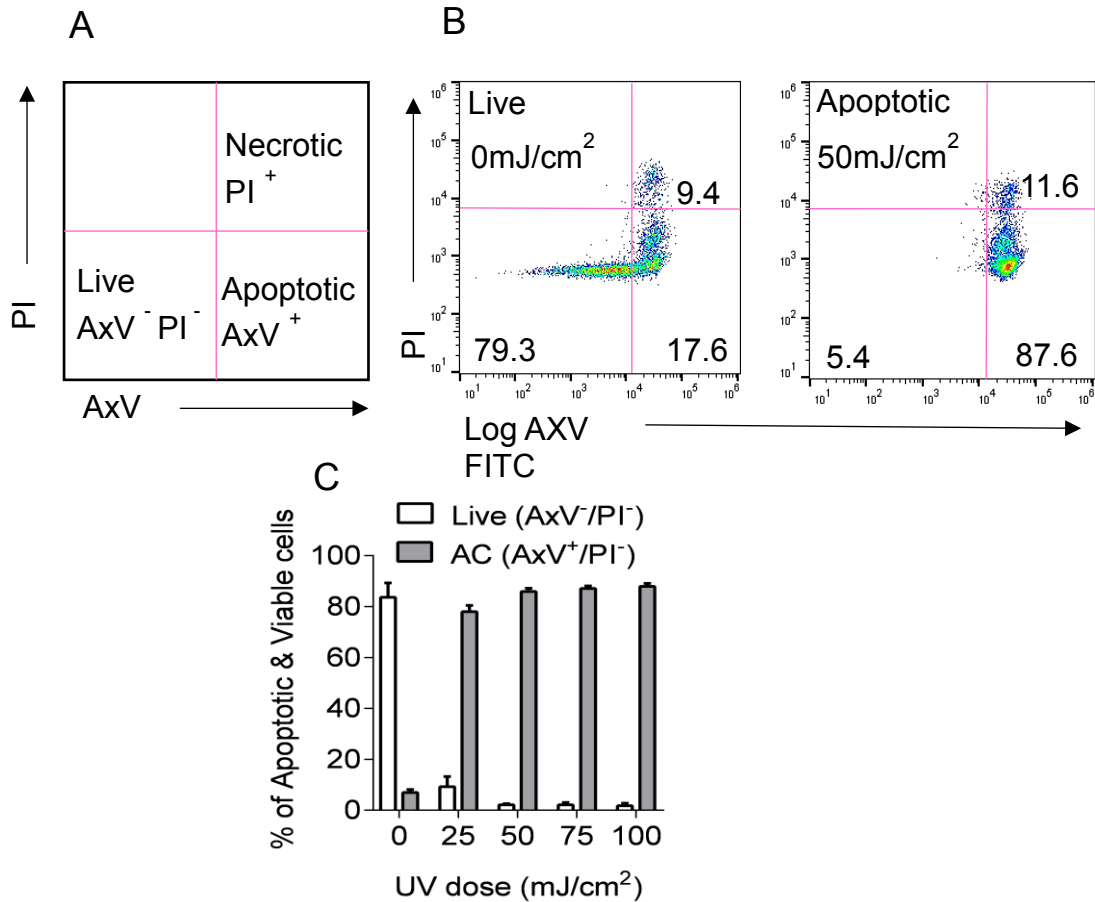


Figure 15: Induction and analysis of apoptosis by UV in B cells

B cells were induced to undergo apoptosis by exposing to the indicated doses of UV ranging from 0 to 100 mJ/cm². Following 16h incubation at 37°C, cells were stained with annexin-V FITC and PI to reveal the levels of cell death in B cells via flow cytometry. A) An example of flow cytometric AxV/PI quadrant plot showing gated regions of stained cells. B) Representative flow cytometric analysis of AxV and PI showing untreated B cells (left) and UV (50mJ/cm²) induced cells (right). C) The percentage of viable and AC of UV-induced B cells was quantified. The data shown are representative from three independent experiments for (B) and the mean ± S.E.M of three independent experiments for (C).

The data in figure 15 suggest that exposure to 50mJ/cm² UV and 16h incubation allows death to proceed which is confirmed by 87.6% of cells stained positive for AxV when plotted against PI (figure 15B) while untreated cells remained mostly negative for AxV/PI stain (figure 15B). Analysis of cell death at various UV doses indicate that 50mJ/cm² at 16h incubation provides maximum apoptosis in B cells (figure 15C) in agreement with the published kinetics of cell death in B cells⁴¹⁸. These data confirm UV as a useful method for the rapid induction of apoptosis in B cells and for future studies 50mJ/cm² UV was used to induce apoptosis in B cells.

3.3.2 Primary NØ

Being the primary responder to bacterial infection, NØ help to resolve an infection by phagocytosis and inflammation, and then by silently triggering the 'self-destruct switch' called apoptosis to remove inflammatory cells that are no longer required. It was important to undertake the present study to determine the methods required to trigger the execution phase of apoptosis in isolated NØ so that apoptotic NØ could be used in future experiments. Here various methods of inducing apoptosis were developed and tested to allow further studies to employ the method that produced a high level of apoptosis with minimal necrosis or lysis (autolysis) of NØ.

Isolated NØ were resuspended in RPMI/ BSA medium (section 2.4.1) and used immediately as healthy viable control cells. Similar to B cells, the isolated NØ were induced to undergo apoptosis by exposing cells to UV at a range of doses prior to allowing apoptosis to proceed before staining with AxV-FITC and PI. The results are shown in figure 16A.

The data indicate that freshly isolated NØ show little staining with AxV (figure 16A & B) and that UV at 50mJ/cm² induces an increase in PS exposure at 16h incubation marking approximately 82% of cells as apoptotic with further higher doses of UV failing to increase the apoptosis level in NØ (figure 16B). DAPI nuclear dye was used to detect characteristic nuclear changes in NØ undergoing apoptosis by fluorescence microscopy. Figure 16C displays representative fluorescence images at time point's 0h post-UV showing viable NØ (V) and 16h post-UV showing condensed chromatin as a sign of AC death for a UV dose of 50 mJ/cm². Higher doses of UV induced necrosis and loss of cells as shown by AxV/PI stain (figure 16D).

NØ exposed to various doses of UV showed wide-ranging levels of apoptosis, however, it was noted that there was a low cell count following higher doses of UV analysed by flow cytometry. On further study, it was observed that cells were lost, presumably through lysis, as the number of events (i.e. number of cells) was reduced. Where possible, 10,000 events were analysed per condition but in some cases this was not possible due to cell loss. Table 6 shows the level of apoptosis and the number of cells analysed per second by spontaneous ageing at 4°C or 37°C at various time points. While the spontaneous ageing at 37°C showed an increased number of cells analysed per second with higher percentage for apoptosis, the UV-induced NØ revealed a higher NØ apoptosis however lower cell count per second. This can be seen with 50 mJ/cm² induced increased level of apoptosis in NØ at 16h however the cell count was lower indicating loss of cells (Table 6).

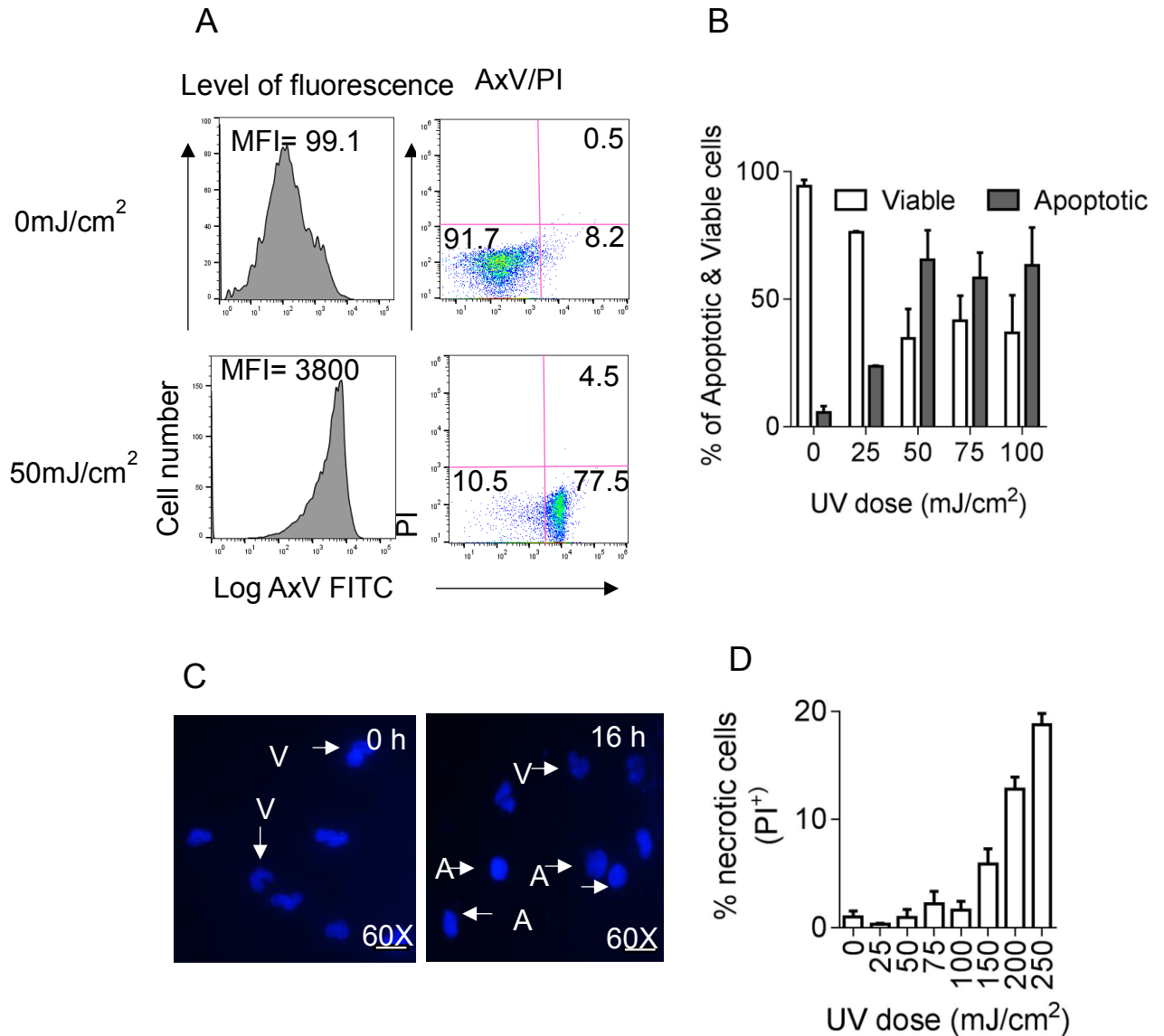


Figure 16: Induction and analysis of apoptosis by UV in primary NØ

Freshly isolated NØ were irradiated with UV at the indicated doses of UV (mJ/cm²) followed by incubation for 16h before quantification of cell death via staining cells with AxV/PI and analysis by flow cytometry. A) Histogram showing level of fluorescence for NØ stained of AxV-FITC plotted against PI. B) Histogram showing the percentage of apoptotic and viable cells in NØ cultures exposed to different doses of UV. C) Nuclear morphology was studied using DAPI stained NØ at 0h showing viable (V) cells and 16h showing condensed nuclei or bleb nuclei, a marker for apoptosis (A). Magnification 60X. D) Histogram shows the percentage of necrotic cells (i.e. cells stained positive for PI). The data shown are mean and ± SEM from three independent experiments (B and D) and flow cytometric and microscopic image (A and D) are representative of three independent experiments.

Time points	NØ cultured at 4°C		NØ cultured at 37°C		UV induced NØ at 37°C (16h)		
	% of AC	No. of cells (Events) analysed/ sec	% of AC	No. of cells (Events) analysed / sec	mJ/cm ²	% of AC	No. of cells (Events) analysed / sec
0h	2.64	142	2.84	127.2	0	2.12	31.1
4h	6.54	127.7	8.45	74.4	25	23.16	20.1
16h	13.42	94.3	82.39	59.9	50	76.52	15.7
20h	13.67	59.95	82.89	30.3	75	73.56	15.4
24h	25.43	43.5	87.65	20.9	100	72.16	10.3
40h	35.86	24.4	80.27	7.6	150	67.12	5.1

Table 6: Induction and analysis of various forms of apoptosis on primary NØ analysed using flow cytometry

Freshly isolated NØ were induced to apoptosis either by UV followed by culturing at 37°C for 16h (as described in section 2.5.1.1 and 2.5.1.2) or by the spontaneous ageing in culture at 4°C or 37°C at various time points (as described in section 2.5.1.2). Cells were analysed for apoptosis by AxV/PI staining (as described in section 2.5.3.1) at the indicated time by flow cytometry. The table on the left shows the percentage of apoptosis induced by spontaneous ageing at 4°C, 37°C and the table on the right shows percentage of apoptosis by UV-induced NØ at indicated doses cultured for 16h at 37°C. Time (seconds) taken to analyse the indicated number of cells (events) (maximum 10000) using flow cytometry were also shown. The data shown are mean ± SEM from three independent experiments.

3.3.3 Temperature dependent apoptosis in NØ

Since the UV method of apoptosis induction failed to give a large yield of AC, temperature dependent apoptosis was analysed by culturing isolated NØ at 37°C or 4°C in NØ medium (as described in 2.5.1.2) and monitored for AC death over 40h using flow cytometry. To assess cell death, NØ at various time points post-isolation were stained with AxV and PI to detect apoptosis and necrosis. Time points observed were 0h, 4h, 16h, 20h, 24h and 40h post-isolation with incubation at 4°C or 37°C (figure 17A). NØ incubated at 37°C showed increased apoptosis at 8h of culture and beyond while NØ incubated at 4°C demonstrated much lower levels of apoptosis that even after 40h of culture did not reach

the levels seen with 37°C (figure 17A). Overall, the levels of necrosis remained low (<0.5%) in cells cultured at either 4°C or 37°C (figure 17B). The results were consistent with analysis of nuclear morphology shown by DAPI staining (figure 17C) where classical apoptosis was only noted at 16h following incubation at 37°C.

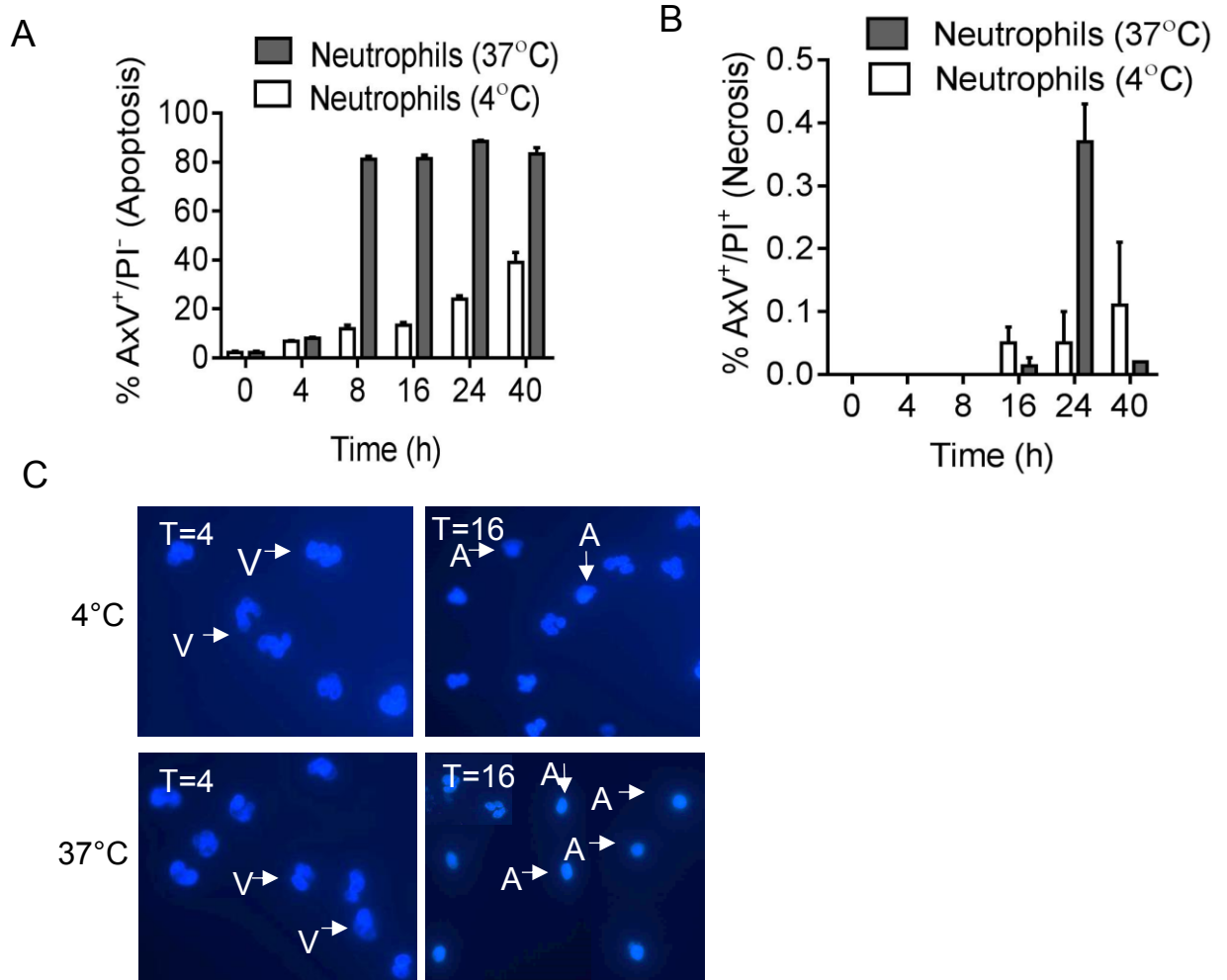


Figure 17: Quantification of spontaneous NØ cell death incubated at 4°C and 37°C

NØ were isolated from healthy donor blood using Percoll-mediated fractionation. Freshly isolated NØ were incubated at 4°C or 37°C in sfRPMI with 0.2% BSA and analysed for AC death by staining the cells with AxV/PI using flow cytometry (as described in section 2.5.3.1) at the indicated time points. A) The percentage of AC (AxV⁺/PI⁻) in NØ cultured at 4°C or 37°C at various time points. B) The percentage of total necrotic cells (PI⁺) in NØ cultured at 4°C or 37°C at various time points. C) Representative fluorescent image of DAPI stained NØ cultured at 4°C or 37°C showing viable (V) and AC (A) at time points 4h and 16h. Magnification 60X. Data shown is mean ± SEM from three independent experiments (A and B) and the images are representative of three independent experiments (C).

The results in figure 17 suggest that 37°C culturing of NØ induces robust spontaneous apoptosis at maximal levels with minimal necrosis compared to the UV-induction method. Additionally, the number of cells analysed per second were comparatively higher to the UV-induced method (Table 6). For future studies, to induce apoptosis in NØ, cells were

cultured at 37°C for 16h to allow spontaneous apoptosis to proceed and then were used to study the interaction assays with THP-1 MØ.

3.4 THP-1 differentiated MØ model

Tissue MØ are multifunctional cells that are widely distributed in connective tissue and organs e.g. bone marrow, lungs, liver, nervous system ⁴⁴³. To understand the MØ host defences it is important to study the interaction between MØ and immune challenges (invading pathogens and AC) because MØ are considered as a professional scavenger of AC and their function has a vital role in tissue homeostasis ³⁵. In order to allow these studies, a MØ model system was developed from THP-1 cells, a human monocytic leukaemia cell line which was used to study the ability of THP-1 differentiated MØ to migrate towards dying cells, to tether and remove AC and to mediate pro-/anti-inflammatory cytokine responses. Similar models have been used previously ^{36, 444}.

3.4.1 THP-1- derived MØ model system

The THP-1 cell line derived from peripheral blood of a 1-year-old human male with acute monocytic leukaemia was stimulated with VD3 or PMA or DS for 48h at 37°C to produce MØ-like cells (as described in section 2.3.5). MØ produced from THP-1 cells treated with different stimulants (VD3 or PMA or DS) have been assessed for their role in AC clearance and these models will be used for further assay in characterising the role of MØ in interaction with apoptotic NØ ³⁶

Depending on the environmental stimuli (e.g. bacterial signals, PAMPs) the functional phenotype varies from monocyte to MØ. This includes the development of characteristics such as specialised functions (e.g. cell adhesion), or cell features (e.g. nuclear-cytoplasmic ratio, increased cell size, granularity, surface receptor expression, mitochondrial organelle number and secretory vesicles) as differentiated tissue MØ prepare to live longer to maintain tissue homeostasis ⁴⁴⁵. To assess THP-1 changes in response to differentiation with VD3, PMA or DS cells were treated for 48h and their morphological appearance recorded (figure 18).

The results in figure 18 show clear morphological changes analysed using microscopic analysis of monocytes differentiating to MØ. MØ differentiated from THP-1 /VD3 and untreated THP-1 cells were semi-adherent and no consistent difference was observed in the cell morphology whereas THP-1 cells induced with PMA or DS appeared to be strongly adherent and elongated unlike VD3 stimulated THP-1 cells which appeared relatively small and spherical in morphology.

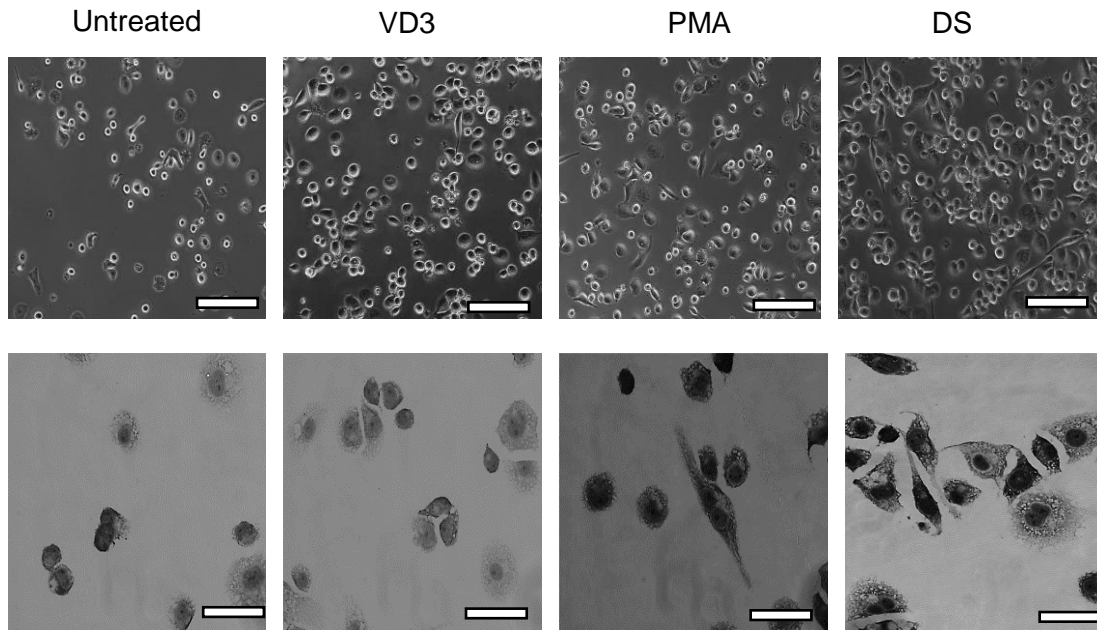


Figure 18: Morphology of THP-1-derived MØ induced to differentiation with various stimulants

THP-1 (1×10^5) cells were seeded in a 24 well plate with various stimulants VD3 (100 nM), PMA (250nM) or DS or left untreated. Monolayer formation of THP-1 cells was analysed for phenotypic variation after 48h microscopically. The microscopic images in the top row are 10X magnification and the bottom row images are 60X. The images are representative of three independent experiments.

3.4.2 Cell surface receptor expression

3.4.2.1 CD14

The glycosylphosphatidylinositol-linked plasma membrane glycoprotein CD14, is an innate immune PRR and a feature of differentiated MØ. It has been established as a receptor for multiple ligands including PAMPs (e.g. LPS) and AC³²⁴. To study the CD14 receptor expression as a measure of MØ differentiation, cell surface CD14 levels were assessed using indirect immunofluorescence staining on THP-1 monocytes and differentiated MØ using the established anti-CD14 mAb (63D3) by flow cytometric analysis (figure 19). Analysis of the function of CD14 in mediating inflammatory responses and taking up and phagocytosing apoptotic NØ, an anti-inflammatory event, is key to the current study. This will allow analysis of pathogen factors and AC present in chronic inflammatory diseases such as PD to understand the impact on CD14 and MØ function.

Flow cytometric results in figure 19 suggest that nearly 100% of VD3-stimulated MØ express CD14 compared to THP-1 monocytes and that these cells are highly positive for CD14, as assessed by the MFI. This indicates a clear differentiation from monocytes to MØ. The MFI value is higher on all the stimulated THP-1 cells except the PMA stimulated compared to unstimulated cells indicating CD14 levels are increased as a marker for

differentiation into MØ in agreement with previous studies ⁴⁴⁶. However of all the stimulants, VD3 showed the highest positive fluorescence for CD14, across all cells compared to PMA or DS which showed lower levels of CD14 in a sub-population of cells, with 40-60% of cell being positive for CD14. For PMA stimulated cells, they showed a detectable level of CD14 compared to DS culture suggesting VD3 presence is essential to enhance the CD14 surface receptor ⁴⁴⁷. These findings are supported by previous work demonstrating a similar difference on CD14 expression level on myeloid cells i.e. monocytes and MØ ³⁶.

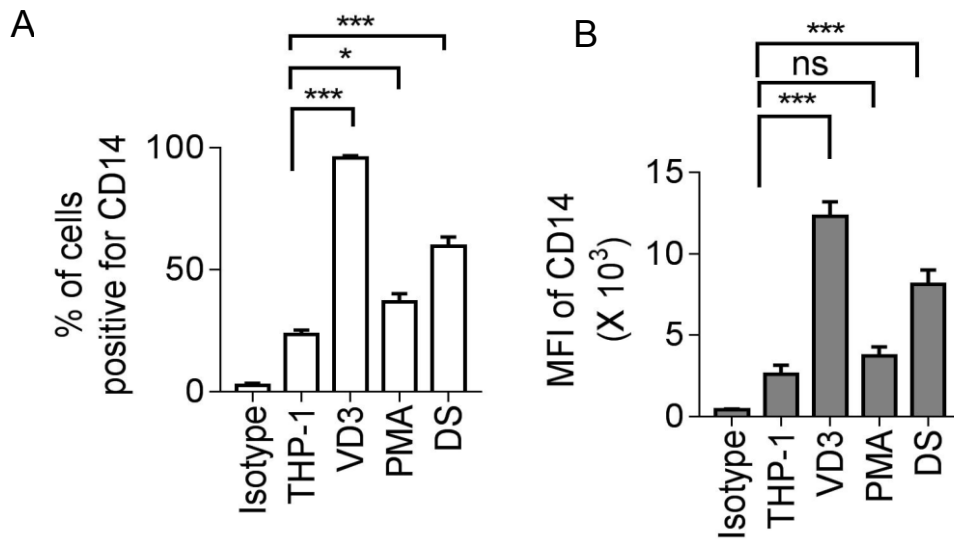


Figure 19: CD14 surface expression on THP-1-derived MØ

THP-1 cells were stimulated to differentiate with VD3, PMA or DS for 48h and the cells were stained with anti-CD14 (63D3) to assess the CD14 levels using immunofluorescence and flow cytometry. A) Histogram showing percentage of cells positive for CD14 staining B) The MFI of the stained population is shown. The data shown are of mean \pm S.E.M of three independent experiments. Statistical analysis was conducted using AVOVA with Dunnetts post-test (* P <0.05, *** P <0.001) compared to THP-1. ns- Non significant.

3.4.2.2 CD36

CD36, a class B scavenger receptor expressed on human monocytes, is found to be increased on the plasma membrane of HMDM cells upon differentiating from monocytes at mRNA levels ⁴⁴⁸. Additionally, CD36 is proven to be involved in PS recognition and AC clearance. It acts as a scavenger receptor for uptake of oxidised low-density lipoprotein (Ox-LDL) and is essential for MØ activation to initiate inflammatory signalling associated with the gingival epithelial cell inflammation ^{329, 449-451}. Here, CD36 surface receptor was assessed on THP-1 stimulated MØ using anti-CD36 or isotype control. The MFI and cells positive for fluorescence were measured using flow cytometry analysis. The results are shown in figure 20.

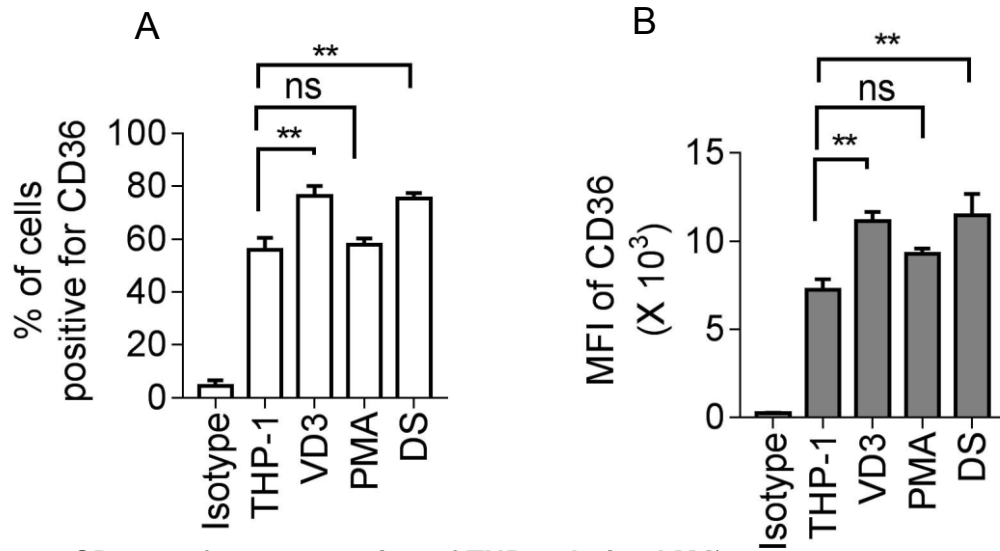


Figure 20: CD36 surface expression of THP-1-derived MØ

THP-1 cells were stimulated to differentiate with VD3, PMA or DS for 48h and the cells were stained with anti-CD36 to assess the CD36 levels using immunofluorescence and flow cytometry. A) Histogram showing percentage of cells positive for CD36 staining B) The MFI of the stained population is shown. The data shown are mean and \pm S.E.M of three independent experiments. Statistical analysis was conducted using AVOVA with Dunnett's post-test. (** $P < 0.01$) compared to THP-1. ns- Non significant.

Flow cytometric results in figure 20 suggest that each cell type irrespective of stimulant (VD3, PMA and DS) expressed CD36 on its surface with between 55% and 80% of cells positive for CD36. However, VD3 and DS stimulated THP-1 MØ expressed significantly higher CD36 compared to THP-1 monocytes and PMA differentiated THP-1 MØ as assessed by the MFI (level of CD36 per cell). While 55% of THP-1 monocytes and PMA MØ were positive for CD36, PMA showed a trend towards more CD36 per cells (MFI increased). For both VD3 and DS, the percentage of positive cells increased (to nearly 80%), as did the MFI suggesting more cells are positive for CD36.

3.5 MØ chemotaxis to AC

3.5.1 Dunn chamber model-horizontal chemotaxis

Introduction

Chemotaxis, is the active locomotion of cells guided by various signals in the form of extracellular chemical gradients. These signals may be released either by a pathogen (e.g. FMLP) or by immune cells on detecting microbes (e.g. IL-8), thus aiding cells to reach pathogen-infected tissue⁴⁵². Chemotaxis has been widely studied in physiological processes such as in embryogenesis for normal development of organs, in repairing infected tissue and healing wounds, and more recently reprogramming chemotaxis

pathways has been suggested as a model to study the dissemination of tumour cells and also proposed as therapy for cancer treatment ⁴⁵³⁻⁴⁵⁶.

Upon injury or bacterial invasion, circulating monocytes are recruited from the blood and differentiate into MØ as they migrate towards toxic components released by pathogenic bacteria ⁴⁴. Classic examples are the potent chemotactic microbial peptide FMLP or the chemokine IL-8 (CXCL8) that recruit NØ to the injured sites via chemotaxis ^{457, 458}. Upon infection, tissue resident leukocytes migrate to the endothelium of the infected tissue via histamine mediated recruitment. Once the NØ reach the endothelium, the NØ initiate adhesion through adhesion proteins such as β 2-integrins to prevent cell detachment by the flow of blood. Following adhesion, NØ will roll along the endothelium using low-affinity binding selectins (i.e. L-selectins) towards the chemotactic gradient. Binding of chemokines to specific NØ receptors strengthens the interaction between lymphocyte function associated antigen-1 (LFA-1) on the NØ and ICAM-1 expressed by the endothelium, which arrests NØ rolling. This immobilisation allows NØ to extravasate through the endothelium and migrate towards sites of inflammation ⁴⁵⁹. Defective activation or migration of phagocytes may contribute to poor AC clearance and a consequent failure to resolve inflammation. This has been suggested as a target for translational therapy in chronic inflammatory disorders such as PD ⁴⁶⁰.

Chemotactic factors create a chemical concentration gradient along which cells might migrate. Factors such as ICAM-3 shed from apoptotic B cells, and CX3CL1 released from apoptotic lymphocytes promote attraction of monocytes, MØ and dendritic cells leading to efficient clearance of dying cells ^{37, 461, 462}.

Based on the gradient of chemotactic factors released during apoptosis MØ migration towards dying cells may differ. Numerous assay systems have been developed to study chemotaxis including capillary movement ⁴⁶³, Boyden chambers ⁴⁶⁴, collagen or fibrin gels ⁴⁶⁵ and recently microfabrication ⁴⁶⁶. Due to the long term stability of the established gradient, Dunn chemotaxis chambers are used which operate on a 'true' linear concentration gradient making them an excellent model system to track cell movement by velocity, distance and the degree of angle traveled towards the chemoattractant ^{467, 468}. This section aims to study the recruitment of phagocytes by dissecting THP1-derived MØ migration towards apoptotic B cells and primary NØ.

The chemoattractive abilities of AC (B or NØ) were assessed using the low throughput Dunn chamber model. The Dunn chamber was set up according to methods described in section 2.6.2.1. Preliminary work suggests that VD3 stimulated MØ showed suitable adhesion capacity using PDL coated coverslips and efficient migration towards the chemoattractant compared to PMA or DS-derived MØ showing adhesion was too strong

to allow migration due to the firm anchoring phenotype. Consequently, VD3 stimulated THP-1 cells were used as the preferred model for the MØ migration assays. Additionally, various cell concentrations ranging from 4×10^5 to 6×10^5 cells/well in a six-well plate containing the cover slip were assessed to standardise the most appropriate concentration of MØ for migration assay. A density of 4×10^5 cells/well was too low to locate 40 cells for scoring (as recommended by the Ibidi chemotaxis tool) on the Dunn chamber viewing bridge to track migration; while 6×10^5 cells/well caused either crowded or clumped cells that were also difficult to track. Therefore, a density of 5×10^5 cells/well was used as standard, demonstrating a simple and clear migration phenotype of individual cells.

3.5.1.1 MØ chemotaxis to AC B cells

MØ migration towards serum-free medium serves as an essential negative control compared to migration towards apoptotic B cells (figure 21). This control reflects the medium in which the B cells were induced to apoptosis. The control checks were analysed to assess the level of MØ migration in the absence of AC and to confirm that there were no putative attractants contaminating the reusable Dunn chamber to stimulate MØ migration. THP-1/VD3 MØ were also assessed for their migration towards either AC B cells or their derived AS (figure 21). The data were analysed using 13 images taken every 6 minutes for 2h at 37°C using Zeiss automated microscope. To obtain the normalised plots shown in figure 21, 40 cells were tracked using the manual tracking plugin from Image J and the generated data were uploaded to the Chemotaxis and Migration Tool V2.0. This generated the plots shown in figure 21 where all cells are mapped at the start to the cross hairs, with the relative position of the putative attractant at the top of the plot (black diamond). Each plot is 400X400µm (figure 21).

Figure 21 shows MØ migration towards sfRPMI showed less migration or chemokinesis of THP-1 MØ confirming no chemotactic factors present in the gradient to trigger the migration. However directional migration of MØ was observed in MØ moving to apoptotic B whole culture or their derived AS indicating that B cells serves as an chemoattractant for MØ (figure 21B & 21C), this is in agreement with previous studies using vertical chambers ^{37, 469}.

To describe fully the migration of MØ, other measures were taken from the plots (e.g. accumulated distance travelled, Euclidean distance (direct distance between start and end points), velocity, directness, and angle of multiple chemotaxis assays using the Chemotaxis and Migration Tool as described below.

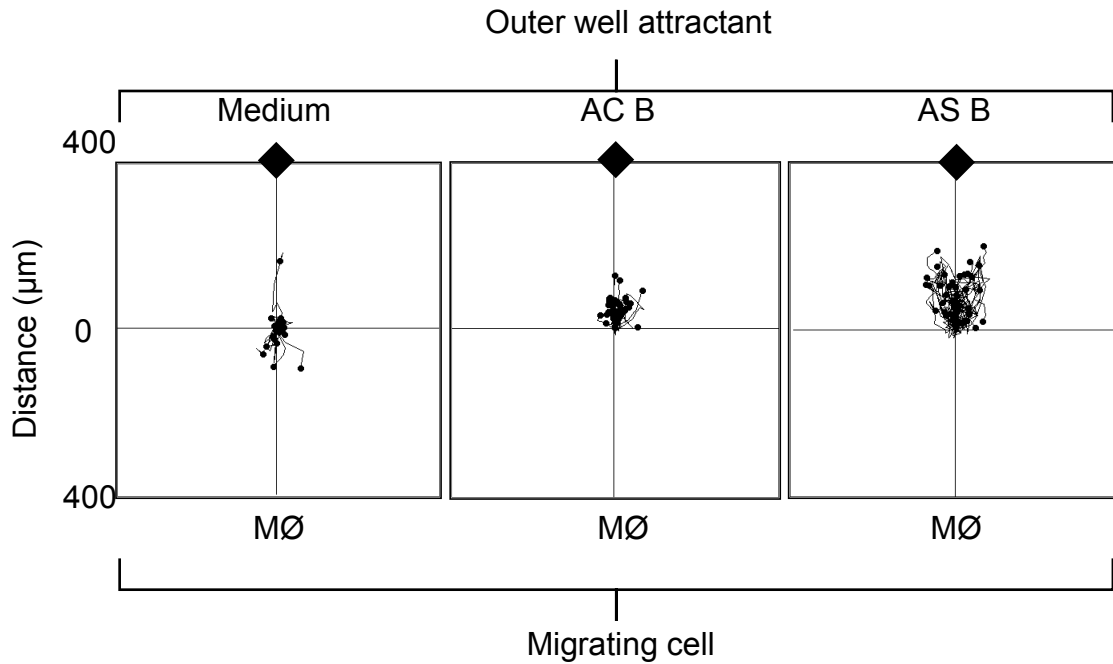


Figure 21: THP-1- derived MØ migration towards AC B cells and their derived AS

THP-1 cells were stimulated with VD3 in cRPMI and cultured on a coverslip for 48h at 37°C. B cells were induced to apoptosis with UV (50mJ/cm²) and cultured for 16h at 37°C for apoptosis to proceed and used either directly as an apoptotic whole culture or centrifuged (2000xg for 20 minutes) and the resultant supernatant (AS) used as an attractant. MØ migration from their starting point at the cross hairs towards the putative attractants on the top of plot (black diamond) were recorded. The putative attractant was sfRPMI- medium (control) (left panel) or AC B cells whole culture (middle panel) or AS B (right panel). Migration was monitored using time-lapse video microscopy (images were taken every 6 min for 2h) and analysed using image J to obtain the normalised plots. The plots are standardised such that all 40 MØ (as recommended by chemotaxis and migration tool) start at the centre of the cross showing their migration towards or away from the attractants. The plots shown are representative of three replicates.

3.5.1.2 Determination of efficiency of migration

To analyse cell migration, chemotactic effects were extracted from Ibidi Chemotaxis and Migration Tool software, examined and analysed using appropriate statistical tests. The migrated MØ were assessed for forward migration index, velocity, distance travelled (Euclidean and accumulated), and angle of cell movement towards the attractive gradient.

3.5.1.2.1 Forward migration index (FMI)

To quantify the movement of a cell in a direction parallel to the attractive gradient, yFMI data was extracted from the software (figure 22A). Similarly, movement in a direction perpendicular to the attractant gradient, xFMI data was extracted. The FMI data indicate the distance travelled by a single cell, here a MØ, from the starting point to the endpoint (after 2h) along both the axes (figure 22). An effective chemotactic migration is a high positive yFMI value which corresponds to parallel movement of cells towards the gradient (figure 22A) while low xFMI value corresponds to perpendicular movement of cells (figure

22B) towards the chemoattractant. The values that are closer to 1 are directional and the values that are closer to -1 corresponds to indirect migration.

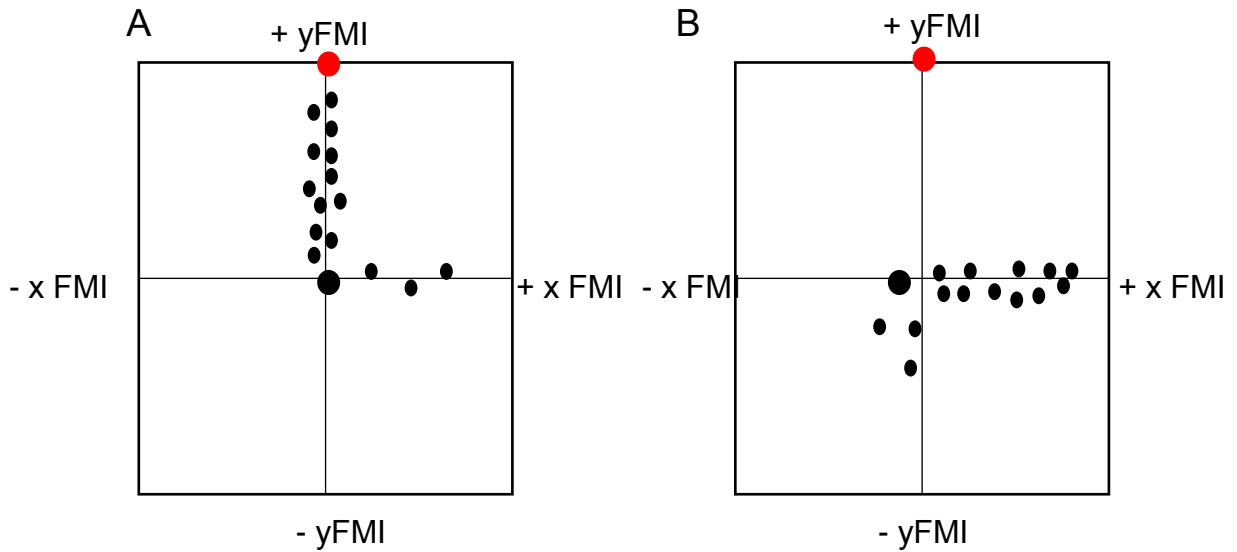


Figure 22: Schematic representation of forward migration index calculated from cell migration Dunn chamber assay using Chemotaxis and Migration Tool software

The picture shows FMI of MØ migration, starting at the centre of the plot (cross hairs) towards the attractive gradient at the top of the plot (red spot), calculated using parallel (yFMI) and perpendicular (xFMI) measures representing the directionality of cell migration. A) The plot shows strong chemotaxis effect with a high yFMI value and a low xFMI value. B) The plot shows poor chemotaxis effect with a high xFMI value and a low yFMI value, indicating the cells are moving either in a random direction or with limited directionality towards the attractant gradient. Adapted from ⁴⁷⁰.

3.5.1.2.2 Measurement of distance, directness and velocity

Two types of distance were measured (figure 23), Euclidean distance which measures the direct distance between the start and end points of a migrated cell, and the accumulated distance which measures the total distance travelled by the cell (i.e. the sum measurement of all incremental movements).

Directness demonstrates the straightness of migration or a cell's affinity to travel straight in a given direction however, directness fails to show the true MØ chemotaxis response as it does not take direction into account, only the distance. Directness is calculated by dividing the Euclidean distance by the accumulated distance for each cell. However, plotted separately, the accumulated and Euclidean distances of 40 cells describe the trajectories used to measure the distance and velocity of movement the cell undertakes in the 2h.

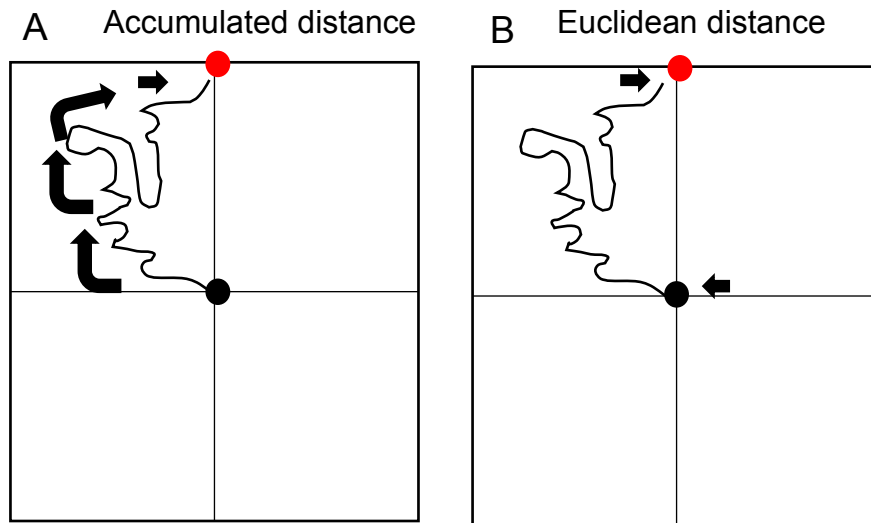


Figure 23: Schematic representation of the distance travelled by the phagocytes calculated using the Chemotaxis and Migration Tool software

The picture depicts the measurement of accumulated (A) and Euclidean distance (B) of cell migration from starting to end point of in a 2h assay performed in Dunn chamber model. A) The plot shows the measurement of accumulated distance by calculating the total distance travelled by a MØ from the centre of the plot (cross hairs) considering all the routes taken to reach the chemoattractants on the top of the plot (red spot) in a 2h time period. The arrow indicates all the incremental movements taken by the cell to reach the endpoint. B) The plot shows the measurement of the Euclidean distance by calculating the start (arrow) and the end point (arrow) location of a migrated cell. The arrow indicates the start of the MØ at the centre of the plot (cross hairs) and the endpoint. Adapted from ⁴⁷⁰.

3.5.1.2.3 Angle

In addition to the yFMI index, the uniformity of cell movement was determined using angle measurements extracted using the Chemotaxis and Migration Tool. Based on the location of the end points, the uniformity of each cell was tracked upon their migration to the attractants without taking into account the distance or direction of the migrated cells. The angle was calculated for 40 cells in each assay by normalising all cells to the starting point in the centre of the circle in a migration plot. The uniformity of phagocytes' migration was measured towards the attractant. Higher angle values indicate higher variability on the end points of the cell indicating deviation from the other endpoints of the cell (figure 24A). A lower angle displays low variability on the end points of the cell indicating most of the MØ were travelling closer towards the chemoattractant (figure 24B). While the angle measurement demonstrates the uniformity of all 40 cells' end points, the yFMI index shows the uniformity only in the cells that were moving towards the attractants.

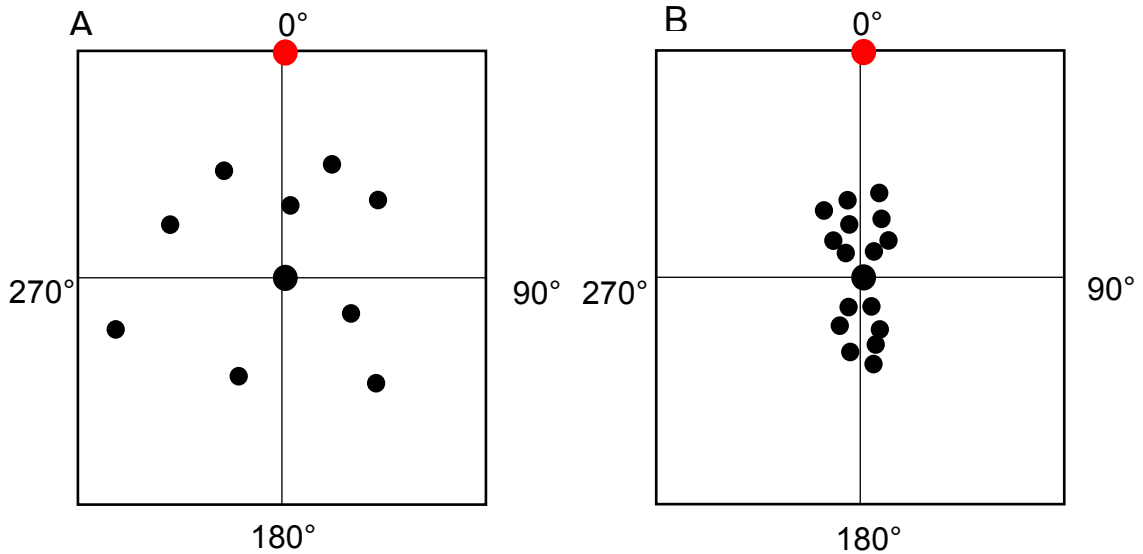


Figure 24: Schematic representation of angle measurement of phagocyte migration calculated from Chemotaxis and Migration Tool software

The diagram depicts the uniformity of cell migration towards the attractants using angle measurement of individual cell endpoints of all 40 cells migrated in a specified time period performed in a Dunn chamber model. A) The plot shows schematic representation of the endpoints of the MØ (black dots) migrated to the chemoattractant at the top of the plot (red spot) with a higher angle measurement indicating higher variability of cell endpoints. B) The plot shows schematic representation of the endpoints of the MØ (black dots) migrated to the chemoattractant present at the top of the plot (red spot) with a lower angle measurement indicating lower variability of cell endpoints. The angle measurement ensures only the variability of the movement of phagocytes but it does not grade whether the migration is strong or poor towards the chemoattractant. Adapted from ⁴⁷⁰.

These different measures of migration were extracted from the assays of MØ migration towards AC B or AS B (e.g. figure 21) and are presented in figure 25. The data in figure 25 show no significant differences in accumulated distance migrated towards control medium and AC B or AS B (figure 25A); Euclidean distance (figure 25B) or velocity (figure 25C) though a trend was observed in each case for increased migration towards AC B and again to AS B. However, AC B showed a significant difference ($P < 0.05$) in yFMI of MØ migration (figure 25D) compared to control indicating AC B as a stronger attractant compared to AS B cells (figure 25D).

To quantify the uniformity and direction of MØ migration, angle and directness were assessed using the Chemotaxis and Migration Tool. The data in figure 26A show significant difference ($P < 0.05$) between migration towards the attractants (AC B or AS B) and control indicating that MØ migration towards the attractants was in a uniform manner compared to the control, as a lower angle represents lower variability in cell movement. To characterise the migration directness (D) Euclidean distance was divided by the accumulated distance. If the D value is equal to 1, then cells migrate from their starting to

their end point in a perfect straight line. The data in figure 26B show no significant difference between the directness of migration to putative attractants and control, however directness values are always positive and do not take into account the direction (towards or away from the gradient) indicating that the directness is not a definite measure of chemotaxis.

Though VD3 stimulated THP-1 MØ were treated with two different components of apoptotic B cell culture (AC or AS) the migration of MØ was found to be stronger towards AC B (figure 25D) compared to AS B. Yet AS B showed a greater trend in distance and velocity travelled (figure 25A, B & C).

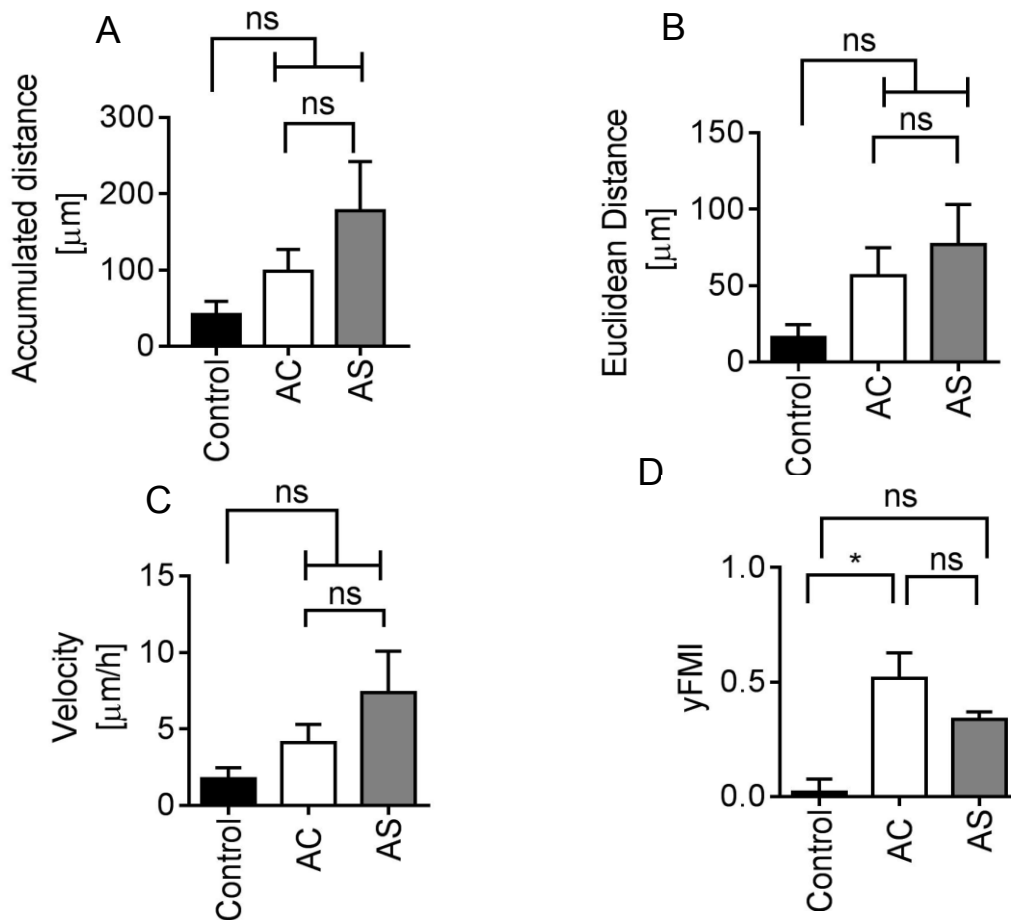


Figure 25: Quantitative measurement of MØ migration towards AC B and AS B

VD3 stimulated THP-1 MØ were allowed to migrate to either sfRPMI (control) or AC B cells whole culture (AC) or their derived secretomes, using a DUNN chemotaxis chamber for 2h at 37°C. Migration was monitored using time-lapse video microscopy. The data were extracted using image J by tracking 40 MØ per assay and standardised in a normalised plot. The plot obtained in figure 21 was used to extrapolate the measurements using Ibidi Chemotaxis and Migration Tool (V2.0). The figure shows A) accumulated distance B) Euclidean distance C) velocity and D) yFMI of MØ movement towards AC B cells or their derived AS or sfRPMI on its own. Data show the mean \pm SEM of three independent experiments. Statistical test conducted using AVOVA with Bonferroni post-test (* $P < 0.05$).

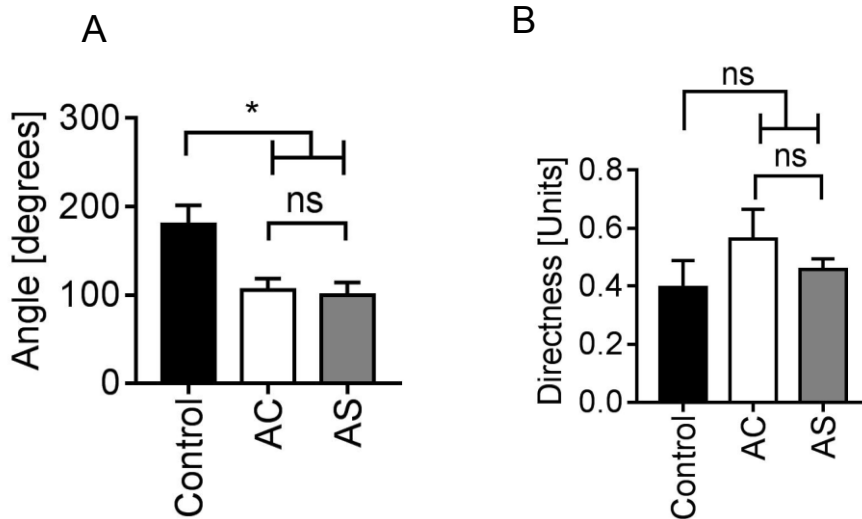


Figure 26: Angle and directness of MØ migration towards AC B or AS B

VD3 stimulated THP-1 MØ were allowed to migrate to either sfRPMI (control) or AC B or AS B using a Dunn chemotaxis chamber for 2h at 37°C and monitored using time-lapse video microscopy. The data were extracted using image J by tracking 40 MØ per assay and standardised in a normalised plot. The plot obtained in figure 21 were used to extrapolate the measurements using Ibidi Chemotaxis and Migration Tool (V2.0). The figure shows A) Angle in degrees B) Directness in units of MØ migration towards AC B AS B or sfRPMI on its own. Data show the mean \pm SEM of three independent experiments. Statistical test conducted using AVOVA with Bonferroni post-test. (* $P < 0.05$).

3.5.1.3 MØ chemotaxis to AC NØ

Similar to B cells, VD3 stimulated THP-1 MØ migration towards apoptotic NØ or their derived AS was assessed using the Dunn chamber model. The data in figure 27, obtained by tracking 40 cells using imageJ, shows non-directional movement of MØ to serum-free medium (control) indicating some limited chemokinesis of phagocytes (figure 27). However, MØ movement towards AC NØ or AS NØ was higher suggesting directional migration of MØ (figure 27).

Different measures of migration were extracted from the assays of MØ migration towards AC NØ or their AS (e.g. figure 27) and are presented in figure 28. The data in figure 28 show no significant difference between the MØ accumulated distance, Euclidean distance and velocity of MØ migration to putative attractants (AC NØ or AS NØ) (figure 28A, B & C). However, significant differences were observed in yFMI of MØ migrating to both AC NØ ($P < 0.001$) and AS NØ ($P < 0.05$) compared to the control (figure 28D), moreover, stronger attraction was seen towards AC NØ compared to AS NØ (figure 28D).

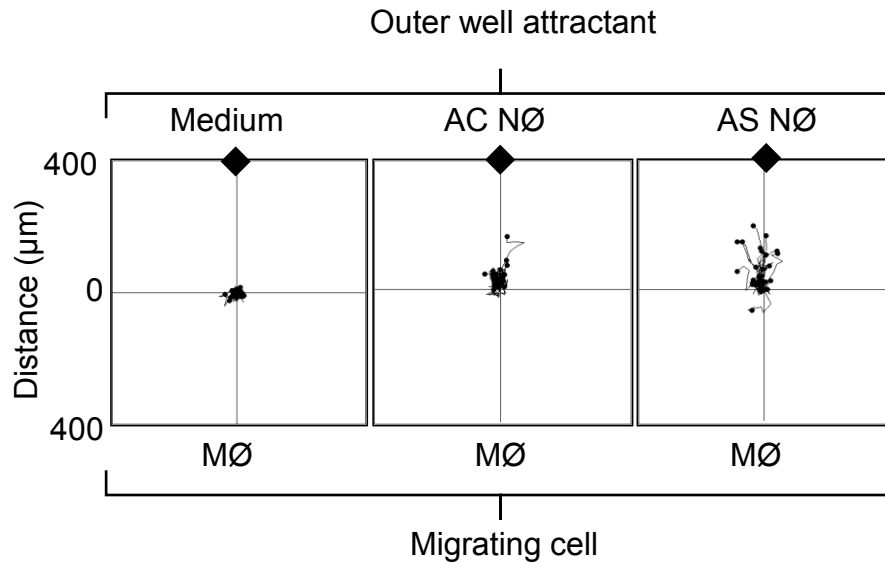


Figure 27: THP-1-derived MØ migration towards AC NØ or AS NØ

THP-1 cells were stimulated with VD3 in cRPMI and cultured on a coverslip for 48h at 37°C. Primary NØ were induced to apoptosis by culturing the cells for 16h at 37°C and used either directly as an apoptotic whole culture or centrifuged (2000xg for 20 mins) and the resultant supernatant (AS) was used as an attractant. MØ migration towards the putative attractants on the top of the plot (black diamond) showing sfRPMI +0.2% BSA-medium (control) (left panel) , AC NØ whole culture (middle panel), AS NØ (right panel) was monitored using time-lapse video microscopy (images were taken every 6 min for 2h) and analysed using image J to obtain the normalised plots. The plots are standardised such that all 40 MØ (as recommended by chemotaxis and migration tool) start at the centre of the cross showing their migration towards or away from the attractants. The plots shown are representative of four experiments.

Similar to AC B cells and their derived AS, the angle of MØ migration towards the AC NØ and their derived AS shows a significant difference compared to control (figure 29A), where the control indicates higher deviation suggesting less uniform movement by MØ towards the sfRPMI. However, the measure of directness fails to show any significant difference in migration towards either attractant or control (figure 29B), similar to AC B cells.

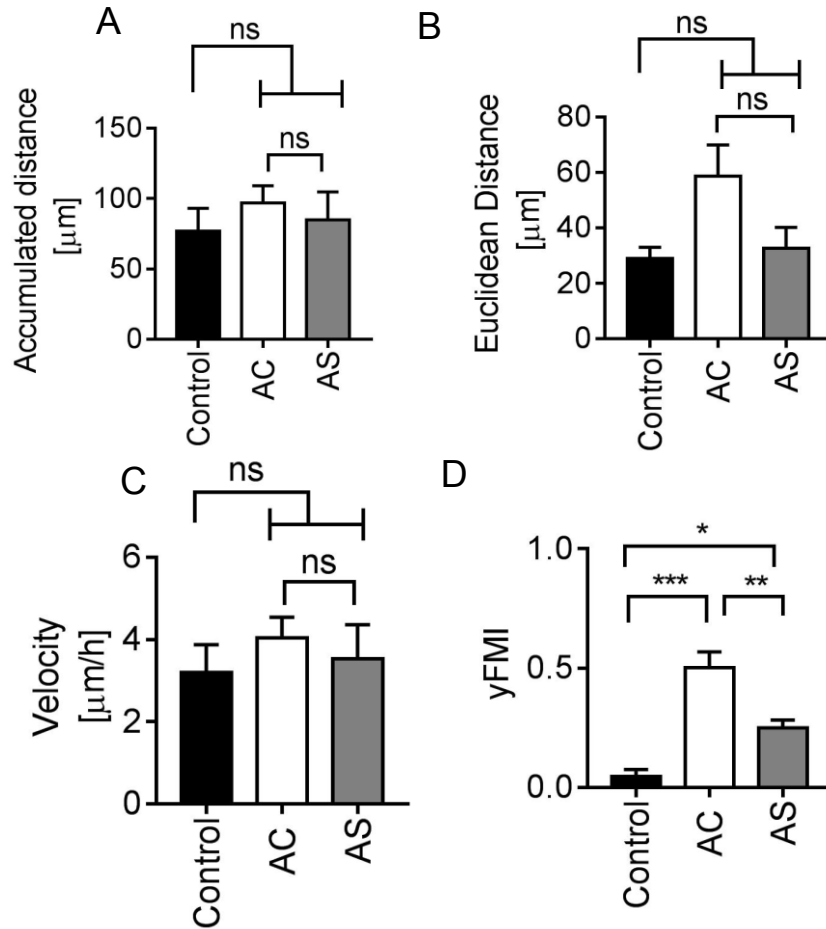


Figure 28: Quantitative measurement of MØ migration towards AC NØ

VD3 stimulated THP-1 MØ were allowed to migrate to either sfRPMI (control) or AC NØ or their derived AS using a Dunn chemotaxis chamber for 2h at 37°C and monitored using time-lapse video microscopy. The data were extracted using image J by tracking 40 MØ per assay and standardised in a normalised plot. The plot obtained in figure 27 were used to extrapolate the measurements using Ibidi Chemotaxis and Migration Tool (V2.0). The figure shows A) accumulated distance B) Euclidean distance C) velocity and D) yFMI of MØ movement towards the putative attractants or control medium. Data show the mean ± SEM of four independent experiments. Statistical test conducted using AVOVA with Bonferroni post-test (* $P < 0.05$, *** $P < 0.001$).

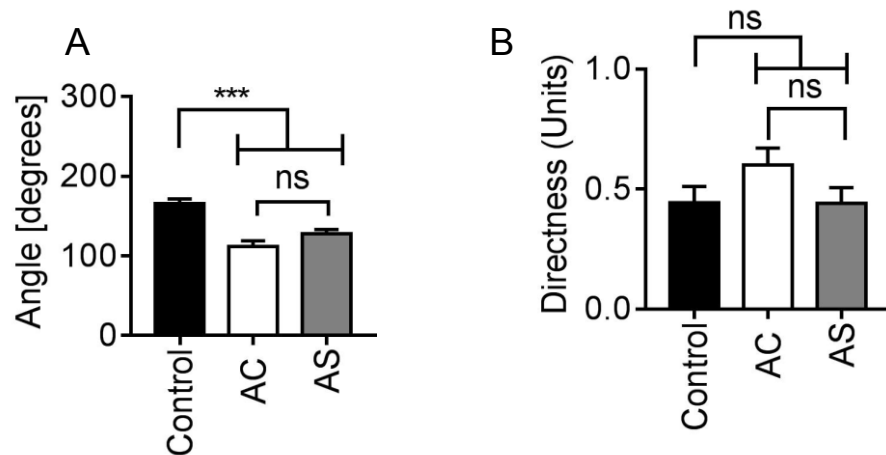


Figure 29: Angle and directness of THP-1 differentiated MØ migration towards the AC NØ or AS NØ

VD3 stimulated THP-1 MØ were allowed to migrate to either sfRPMI with 0.2% BSA or AC NØ or their derived AS using a Dunn chemotaxis chamber for 2h at 37°C and monitored using time-lapse video microscopy. The data were extracted using image J by tracking 40 MØ per assay and standardised in a normalised plot. The plot obtained in figure 27 was used to extrapolate the measurements using Ibidi Chemotaxis and Migration Tool (V2.0). The figure shows A) Angle in degrees B) Directness in units of MØ migration towards AC NØ or their derived AS or control medium. Data show the mean \pm SEM of four independent experiments with two internal replicates. Statistical test conducted using AVOVA with Bonferroni post-test (***) $P < 0.001$.

While both AC NØ whole culture and their derived AS recruited MØ (yFMI) (figure 28D) the AC NØ whole culture appears to have stronger attractive abilities compared to AS NØ (figure 28D).

3.5.2 Cell-IQ model – Vertical chemotaxis

Next, to complement the horizontal migration assays, the impact of THP-1 differentiated MØ migration using a vertical chemotaxis model was studied. The migration of MØ differs depending upon the gradient or linearity of the chamber used during the establishment of any migration assay⁴¹⁹. Gradients of biomolecules (e.g. cytokines) play an essential role in the migration of phagocytic immune cells *in vivo* but also provides directional cues involved in guiding immune cells towards chemical gradients released from the wounded tissue environment⁴¹⁹. To understand MØ migration *in vivo*, various *in vitro* gradient methods have been established for a better understanding of MØ transendothelial migration in pathogen-exposed environment.

From the Dunn chamber studies presented here, it is clear that the horizontal migration assay method reveals migration of MØ to AC chemoattractants, based on the linear concentration gradient. Here, the transwell-based Cell-IQ assay, a vertical migration assay of phagocytes to potential attractants as a step-gradient was studied. Unlike the

Dunn chamber model, this method allows a multitude of kinetic assays to be carried out simultaneously in a single experiment and thus provides a significant advantage to allow more replicates to be carried out. The experiment was established using a transwell-based system and a Cell-IQ tracking system to observe and capture data (detailed in section 2.6.2.2). Briefly, VD3 stimulated THP-1 MØ were placed inside the transwell, which serves as an upper compartment per well of a 24 well plate, and the transwell is directly placed into the bottom well containing AC cultures. The plate is sealed and loaded into the Cell-IQ instrument for cell imaging. Images were routinely collected every 20 minutes over a 12h period. Representative results are shown in figure 30.

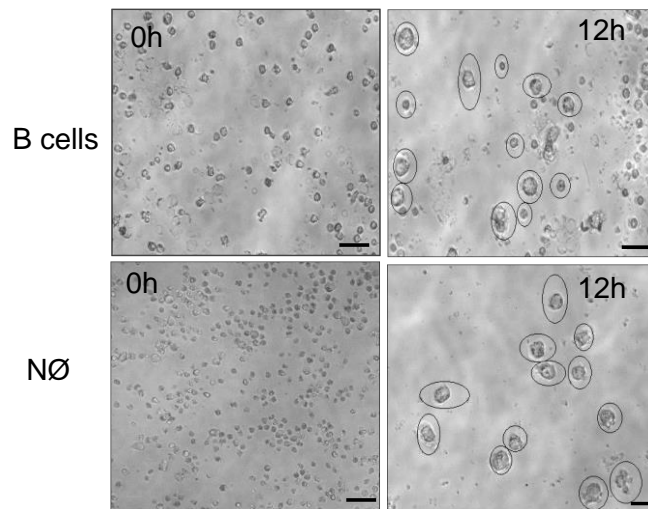


Figure 30: Representative Cell-IQ image of THP-1-derived MØ migration to putative attractants using a vertical chemotaxis model

VD3 stimulated THP-1 MØ migration towards the AC B cells or AC NØ was analysed using the Cell-IQ tracking system (as described in section 2.6.2.2). The transwell (8.0µm pore polycarbonate membrane) containing THP-1-derived MØ (8×10^5 /well) were placed over a bottom well of a 24 well plate containing putative attractants (1×10^6 /well) (either AC B cell whole culture or AC NØ whole culture) and imaged for every 20 minutes for 12h using cell IQ imaging system. The picture shows the Cell-IQ images (magnification 20X) of the bottom well of a 24-well plate containing AC B or AC NØ at 0h and migrated MØ (circled) at 12h from the top transwell. The images shown are representative of three independent experiments.

The data in figure 30 shows the microscopic images of the bottom well of a 24-well plate containing attractants (AC B or AC NØ) imaged at 0h and 12h. A clear difference in number of MØ is observed at 0h displaying no MØ however many MØ (highlighted as circle) can be viewed at 12h indicating that MØ have migrated from the transwell to the bottom well of a 24-well plate in response to the attractants present in the AC cells (AC B or AC NØ).

Results from microscopic image (figure 30) were extracted using the cell-IQ software and analysed by Graph Pad Prism. The results are shown in figure 31.

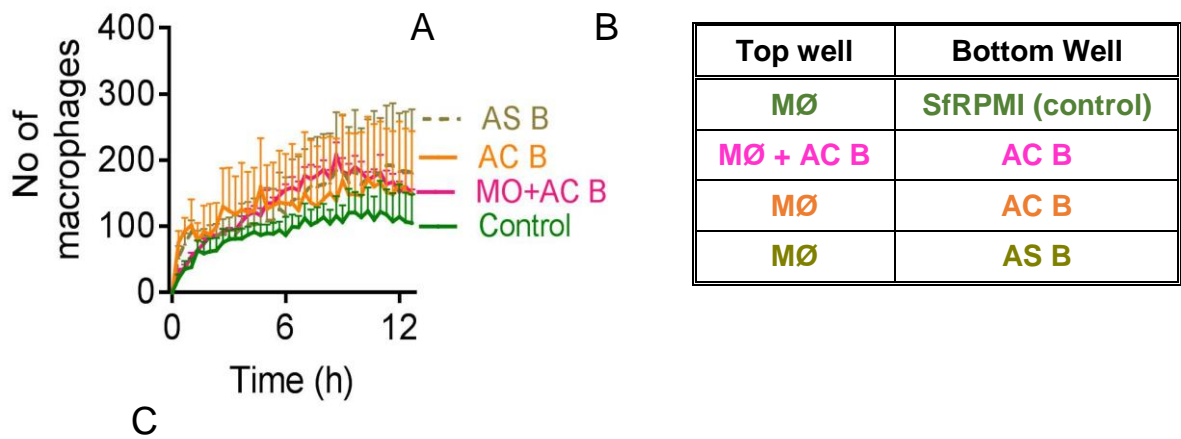


Figure 31: THP-1-derived MØ migration to AC B or AS B using Cell IQ tracking system

VD3 stimulated THP-1 MØ migration towards the AC or AS B cells was analysed using the Cell-IQ tracking system (as described in section 2.6.2.2). THP-1 MØ were placed in the upper transwell (8.0µm pore polycarbonate membrane; 8×10^5 /well) and AC or AS B (1×10^6 /well) in the bottom well of a 24 well plate. Where indicated AC B cells were also included in the upper well to destroy the gradient. Wells were imaged for every 20 minutes for 12h using cell IQ imaging system. A) The graph shows numbers of migrated MØ in the lower well over time for 12h. B) The table shows cells present in the top and bottom well. C) The tables shows the statistical test conducted between the groups. The results shown are the mean \pm SEM of three independent experiments with 2 replicates in each experiment. Statistical test conducted using AVOVA with Bonferroni post-test (** $P < 0.01$).

The data in figure 31 show a significant difference ($P < 0.01$) in MØ migration towards AC B or AS B compared to control. However, to check whether the MØ count was true chemotaxis and not simply the result of cell movement influenced by gravity, the experiment was repeated to add the putative attractant (AC B) to both the top and bottom wells to destroy the gradient. However, no significant difference was seen in MØ migration between lower well containing AC or AS B cells compared to the upper well containing attractant (AC B). Since the AC B cells appear similar in size to MØ the experiment was

repeated using the AC NØ, which appear smaller in size compared to MØ (figure 30). The results are shown in figure 32.

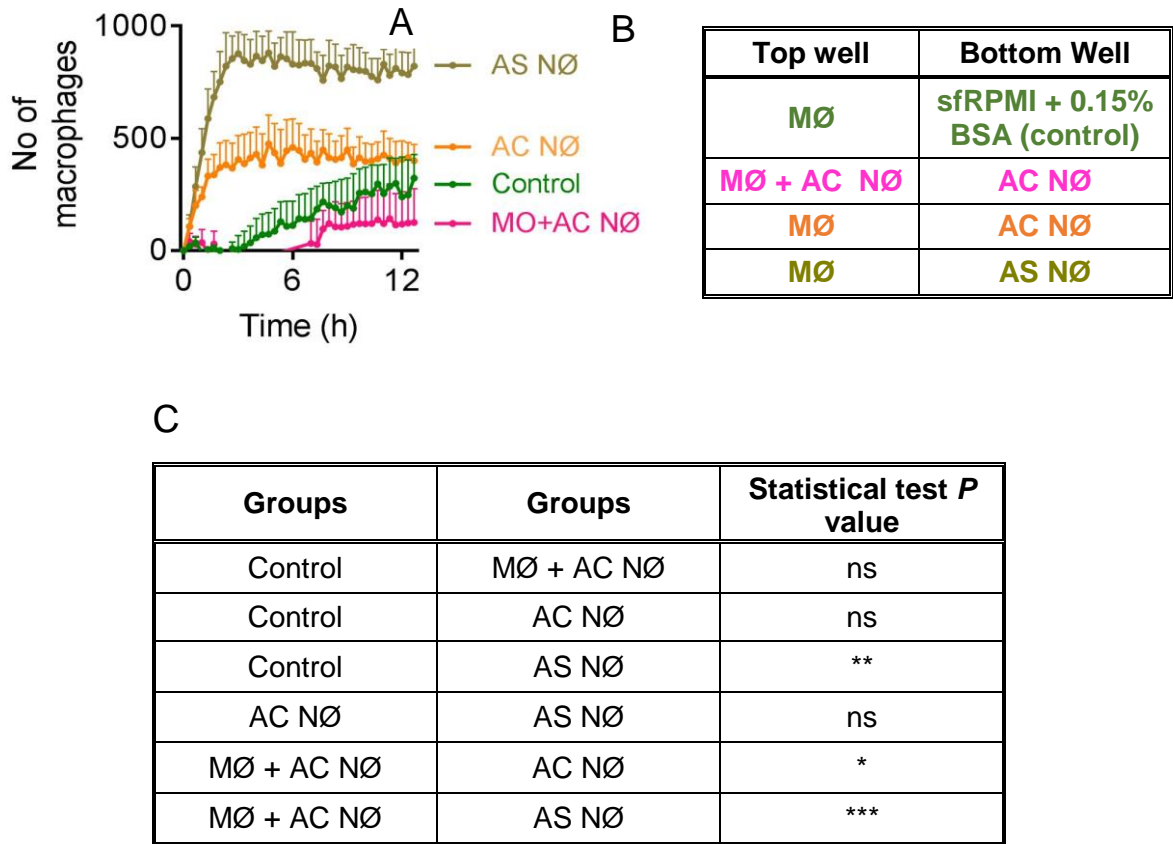


Figure 32: THP-1-derived MØ migration to AC NØ or AS NØ using Cell IQ tracking system

VD3 stimulated THP-1 MØ migration towards the AC or AS NØ was analysed using the Cell-IQ tracking system (as described in section 2.6.2.2). THP-1 MØ were placed in the upper transwell (8.0µm pore polycarbonate membrane; 8×10^5 /well) and AC NØ or AS NØ cells (1×10^6 /well) in the bottom well of a 24 well plate. Where AC NØ indicated were also included in the upper well to destroy the gradient. Wells were imaged for every 20 minutes for 12h using cell IQ imaging system. A) The graph shows numbers of migrated MØ in the lower well over time for 12h. B) The table shows cells present in the top and bottom well. C) The tables shows the statistical test conducted between the groups. The results shown are the mean \pm SEM of three independent experiments with 2 replicates in each experiment. Statistical test conducted using AVOVA with Bonferroni post-test (* $P < 0.05$, ** $P < 0.01$, *** $P < 0.001$).

A significant difference ($P < 0.001$) was observed in the MØ migration to AS NØ compared to control (sfRPMI +0.15% BSA). However, no difference was observed in migrated MØ towards AC NØ compared to control indicating AS NØ as a stronger attractant. Additionally, significant difference was observed in the migrated MØ towards AC NØ ($P < 0.05$) or AS NØ ($P < 0.001$) compared to MØ with putative attractant (AC NØ) indicating the true directional migration was occurring. Moreover, unlike the Dunn chemotaxis assays (figure 28D), AS NØ were highly attractive compared to whole AC NØ culture (figure 32).

3.6 Phagocyte interaction with AC

3.6.1 MØ-AC Interaction assay

The ability of MØ to recognise and remove AC is a crucial step in promoting the resolution of inflammation⁴. It is also a step that may be disrupted in inflammatory disease and the effect of periodontal pathogens on this step will be assessed later. From the migrational assay, it is understood that AC (B or NØ) may act as a chemoattractant for THP-1 MØ. Therefore the next logical step was to assess the interaction abilities i.e. tethering and phagocytosing of AC by THP-1 MØ by establishing an *in vitro* interaction assay model. Similar to the chemotaxis assays, B cells were used as a positive control in this experiment as it is a well-established model system to study MØ interaction with AC^{37, 282, 418, 469}. Savill *et al.* found that MØ use CD36 and $\alpha_v\beta_3$ as bridging molecules to interact with aged apoptotic NØ. As this assay requires extensive washing of unbound AC from MØ on glass slides, the ability of THP-1/DS differentiated MØ to interact with NØ was assessed as they showed a strong adherent phenotype to the glass slides (figure 18). The AC bound or eaten by MØ were assessed following Jenner-Giemsa staining to study the level of MØ interaction with AC NØ by scoring the percentage of MØ interacting with AC. Here, a MØ interacting with an AC(s) is defined as a MØ that is binding and/or phagocytosing at least one AC. The results are shown in figure 33.

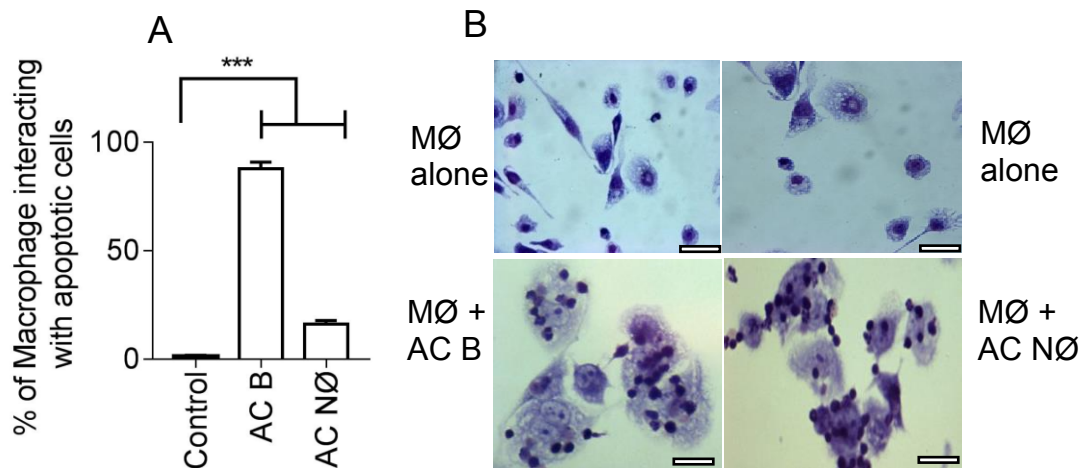


Figure 33: Interaction of apoptotic B cells and apoptotic NØ with THP-1-derived MØ
 THP-1 DS differentiated MØ were cultured in the absence (control) or presence of AC B or AC NØ at 37°C for 1h at a ratio of 20 AC per MØ. Cells were fixed with methanol after washing with cold PBS to remove unbound AC and stained for Jenna-Giemsa. Slides were mounted and assessed by light microscopy and values scored as the percentage of phagocytes interacting with AC (at least 200 MØ per well were counted). A) Graph shows the percentage of MØ that have interacted with AC B or AC NØ. B) Representative photomicrograph of THP-1-derived MØ (light blue) and their interaction with AC B and AC NØ (intense blue). Magnification 40X. The results shown are the mean \pm SEM of three independent experiments. Statistical analysis was conducted using AVOVA with Dunnett's post-test. (***) $P < 0.001$ compared to control.

The result in figure 33A indicates a significant difference was observed between MØ interaction with AC B cells and AC NØ. However, the interaction of MØ with apoptotic NØ shows a lesser percentage (20%) of interaction compared with apoptotic B cells (80%). Moreover, the percentage of cell death in all the groups (figure 33A) is not 100% indicating there are viable cells present which will not be engulfed by MØ. This is in agreement with previous work suggesting that viable cells do not bind to MØ^{281, 324}. Microscopy images show elongated MØ (light blue) and engulfment of apoptotic B cells (intense blue) (figure 33B bottom left image) and NØ (intense blue) (figure 33B bottom right image) scored using a light microscope.

3.7 Discussion

The aim of this chapter was to establish an *in vitro* working model of THP-1 differentiated MØ interaction with AC NØ. AC B were used as a positive control in this study as they have been well established in earlier studies^{36, 37, 324}. In this section, the role of primary AC NØ recognition and phagocytosis by THP-1 differentiated MØ was studied. MØ differentiated from the THP-1 monocyte cell line were used as an important immune cell to understand the mechanism by which phagocytes trigger efficient clearance of AC and subsequently secrete anti-inflammatory cytokines to achieve tissue homeostasis, which has been hypothesised in this study to be inhibited in PD patients.

One of the main *in vivo* events involved in AC clearance is how well MØ recognise signals from dying cells⁴⁷¹. This *in vivo* event has been modelled *in vitro* by isolating peripheral NØ from venous blood and inducing them to apoptosis. These apoptotic NØ have then been studied for their interaction with the THP-1 MØ cells. NØ help decide the result of an injury, either by helping heal the tissue by undergoing apoptosis to enable their phagocytosis by MØ and release of anti-inflammatory mediators, or by, turning necrotic and worsening the inflammation by secreting their toxic contents. One of the major challenges involved in PD is to understand the role of NØ in the inflamed tissue. Many studies have assessed the function and characterisation of NØ in juvenile to generalised periodontal patients and proposed that hyperactive NØ worsen the gingival bleeding by accumulating in the biofilm region and producing increased reactive oxygen intermediates and enzymes causing tissue damage and bone loss^{133, 472}. However, only a few studies have addressed the role of phagocytes in chronic inflammatory disease through a bacterially-mediated environment. Hence the *in vitro* model proposed in this study is a THP-1-derived MØ interaction with apoptotic human NØ, to study the mechanisms involved in recognition and interaction of MØ with apoptotic NØ and the release of cytokines in the presence of factors from *P.gingivalis*.

3.7.1 Characterisation of human NØ

NØ isolated from peripheral blood were confirmed for their purity using CD66b surface receptor expression and the nuclear stain DAPI (figure 14). CD66b, is a glycosylated GPI-anchored protein expressed on both human NØ and eosinophils^{473, 474}. Lakschevitz *et al.* also reported that CD66b was expressed at higher levels on healthy segmented NØ suggesting CD66b as a marker for mature NØ⁴⁷⁴. Moreover, CD66b on NØ regulates CD11/CD18 signals to mediate NØ interaction with endothelial surfaces thereby contributing to leukocyte migration⁴⁷⁵.

Nuclei of NØ vary depending on their lifespan⁴⁴¹. Generated from hematopoietic cells, immature NØ are seen with two lobe-shaped nuclei compared to matured nuclei displaying three lobed to six lobed nuclei⁴⁴². It is unclear whether, depending on the nature of NØ nuclei, the function of their immunity varies in relation to tissue homeostasis. However, activated NØ vary in nuclear lobe shape and each lobe has a diameter of around 2µm connected by a thin segment of nuclear material ranging from 0.2-0.5 µm^{476, 477}. Indeed NØ were considered to be active even if their nucleoli size is reduced. NØ undergo structural differentiation from a round nucleus to segmented lobe-shaped nucleus which is considered to be healthy in conducting chemotaxis and phagocytosis of the pathogens and to stimulate the cytokines essential to repair the wounded tissue⁴⁷⁸. The data presented in figure 14 confirms the purity of the NØ by phenotype CD66b expression as 96.2% and mature segmented nuclei of NØ by nuclear DAPI stain.

3.7.1.1 Induction of apoptosis in NØ by UV and spontaneous method

The characteristic structural and functional changes seen in viable cells on initiating apoptosis include alterations in the cell surface, cell shrinkage, nuclear fragmentation, plasma membrane blebbing and finally release of apoptotic bodies. The molecular and biochemical variations at the cell surface include modifications of lipid, carbohydrate and protein levels and most important PS exposure⁴⁷. PS, a traditional marker for apoptosis has been widely studied for its necessity for effective cell clearance by MØ⁴⁷⁹. Studies have however shown that exposure of this anionic phospholipid alone is not sufficient for recognition by phagocytes and innate immune receptors and ligands such as CD14, CD36, CD91 and ICAM-3 are required along with the presence of PS³²⁹. Furthermore annexin proteins secreted following caspase activation are released from intercellular domains of AC. The secreted annexins such as annexin A5 (annexin V) bind to PS, identifying the translocation of PS from the inner leaflet to the outer leaflet of the plasma membrane²⁶⁶. This knowledge has been used here to detect cell death of NØ or B cells, induced either by UV or spontaneously, using AxV-FITC and PI. The data in figure 15B

show an example of non-induced cells that stained mostly negative for both AxV and PI, revealing the presence of viable cells. After UV induction of apoptosis, a defined population of AC stained positive for AxV and negative for PI and a lesser number of necrotic cells stained positive for AxV and positive for PI.

Apoptosis-associated genes play an important role in regulating and controlling apoptosis in multicellular organisms²³³. Caspase-3, a frequently activated protease has been linked with DNA fragmentation in cell death by apoptosis⁴⁸⁰. Also characterised as an executioner caspase of apoptosis, caspase-3 degrades the nuclear lamina through DNase enzymes resulting in condensed shrinkage of the cell, another characteristic feature of apoptosis²⁵⁵. This correlates with the data presented here in figure 16C and 17C showing condensed chromatin in NØ following either UV or spontaneous apoptosis at 37°C. A study showed that procaspase-3, the inactive form of caspase-3 turned active only after 22h at 37°C in freshly isolated PMN while another study explained that low-temperature arrests apoptosis in NØ, however, warming the NØ to 37°C triggers a synchronous burst of apoptosis^{481, 482}. Taken together, the data presented here in figure 17 suggest that spontaneous aging culture at 4°C might have inhibited the proteolytic cleavage of pro-caspase-3 while higher temperature i.e. at 37°C the active form of caspase 3 might have developed. An earlier report states that cold shock treatment of Burkitt lymphoma cells protected the cell viability for a prolonged period compared to cells at 37°C which enter apoptosis within a few hours⁴⁸³. Weinmann *et al.* also observed that on inhibiting caspase-3 in PMN cells a down-regulation is seen in the expression of Bcl-X_L, a Bcl-2 family member that inhibits apoptosis suggesting that caspase-3 regulates Bcl protein expression. Similarly, another study explained that cleavage of Bcl-2 protein contributes to amplification of caspase cascades⁴⁸⁴. These studies highlight the close link between the activation of caspases to induce death and the expression of Bcl-2 family members to inhibit death.

Dunkern *et al.* have shown that UV-irradiation triggers apoptosis through degradation of Bcl-2 via caspase and proteasome enzyme activation⁴⁸⁵. The data in figure 15 suggests that B cells underwent effective apoptosis, possibly through Bcl-2 degradation and execution of caspases cascades. Additionally, P53, a major regulator of apoptosis has been shown to be activated by UV-irradiation via mitochondria-dependent apoptosis through interaction with apoptosis-regulating proteins⁴⁸⁶. Though, UV-induced NØ developed apoptosis at 16h a lower cell count (number of cells analysed per second) was noticed from 50mJ/cm² UV dose compared to spontaneous ageing at 37°C (Table 6). This might be because UV-induced NØ have been shown to express increased level of p38 MAP kinase in an activated form, which has been linked with TNF-α induced NØ apoptosis stimulating the release of soluble cytoplasmic proteins and triggering apoptosis-

induced autolysis^{487, 488}. In contrast, freshly isolated NØ or spontaneous aged NØ in culture at 37°C displayed a reduced level of p38 MAP kinase⁴⁸⁷. This correlates with the data presented in figure 16 and 17 showing UV-induced apoptosis resulted in a lower cell count presumably as cells underwent frequent autolysis compared to spontaneous aged NØ culture at 4°C or 37°C (Table 6).

Other than caspases, TLRs have been shown to have a modest effect during NØ apoptosis⁴⁸⁹. TLR4 signals stimulate endogenous or exogenous mediators in order to maintain the survival of NØ. Indeed TLR2 has been proven to mediate the pro- and anti-apoptotic signals in NØ and both TLR2 and TLR4 are effective mediators in the presence of monocytes/MØ⁴⁹⁰. On the other hand, LPS delays apoptosis in NØ *in vivo* in septic peritonitis patients revealing inflammatory cells' involvement in the host immune system⁴⁹¹. GM-CSF has been stated to reduce the apoptosis on NØ in chronic periodontitis patients by an unknown mechanism¹⁹⁰. This suggests that delayed apoptosis in NØ might also prevent the recruitment of MØ to phagocytose the AC, which in turn inhibit the release of anti-inflammatory mediators.

The lifespan of circulating NØ *in vivo* has been extensively studied in recent years. A recent study measured the life span of NØ *in vivo* and revealed an average life span of NØ in the peripheral blood as 5.4 days under normal conditions⁴⁹². However, a recent study demonstrated that based on the turnover rate the life span of circulatory and tissue-resident NØ were estimated as 8–12h in the blood and 1–2 days in tissues⁴⁹³. The data in figure 17 showed the apoptotic death of NØ isolated from peripheral blood from 8-40h at 37°C and around 40h at 4°C suggesting the viability of NØ might be upto 4h regardless of the temperature *in vitro*. Nevertheless, for the effective regulation of inflammation resolution timely clearance of apoptotic NØ is essential to prevent the secretion of toxic intracellular contents from necrotic NØ¹⁵.

3.7.2 Phenotypic characterisation and function of THP-1-derived MØ

Monocytes and MØ are a key cell type in the immune system and enable the host defense against pathogenic insults as well as contributing to the prevention of chronic inflammation through phagocytosis of AC and control of pro-inflammatory mediators⁴⁹⁴. Generation and activation of HMDM has been widely studied for their *in vivo* role in regulating inflammation resolution. Their differentiation from human monocytes takes several days and therefore it is a challenge to maintain the viability of these cells following stimulation. THP-1-derived MØ was produced using different stimulants (VD3 or PMA or DS) in this current study as the cell density were easy to maintain and importantly the role of THP-1 MØ like cells in AC clearance is well established^{418, 445, 495, 496}. Hence, THP-1 differentiated

MØ were used in characterising the resolution of inflammatory mechanisms which may be involved in periodontal disease.

Morphological changes were analysed using microscopic analysis through monocyte differentiation to MØ. Untreated THP-1 cells and VD3 stimulated MØ were similar in appearance (round shaped, semi-adherent) with no consistent differences in cell morphology (figure 18). However, THP-1 cells induced with PMA or double stimulated (VD3 and PMA) were strongly adherent, with a more flattened morphology and elongated (figure 18). These findings are in agreement with previous work ⁴⁴⁵. However, depending on the experimental need, different stimulants were selected to differentiate the THP-1 cells to MØ. Notably, the profound effect on cell density of the THP-1 cells depending on the stimulants was also increased using light microscopy. In VD3 stimulated THP-1 cells the density of cells was observed upto 72h. However, in THP-1 cells stimulated with THP-1/PMA or THP-1/DS the cell number remained relatively constant, likely due to their strong adherent capacity. Previous work has reported cell fusion in PMA treated BeWo cells resulting in larger multinucleated cells ⁴⁹⁷. Additionally, MØ have been reported to fuse with neighbouring MØ to form a giant multi-nucleated MØ during chronic inflammation, but their role in inflammatory mechanism is yet to be elucidated ⁴⁹⁸. However, PMA-induced THP-1 MØ have been widely studied due to their similarities with HMDM cells. Indeed they have been shown to share similar upregulated lysosomal and mitochondrial staining which is broadly distributed in the cytoplasm of PMA stimulated THP-1 cells ⁴⁴⁵.

CD14, an AC clearance and LPS receptor, has been widely used as a marker for differentiated MØ both in *in vivo* and *in vitro* conditions ^{142, 288, 326, 418, 447, 499-501}. THP-1 monocytes express a measurable level of CD14 before differentiation into MØ and upon incubation, the stimulants resulted in increased CD14 expression, except for PMA (figure 19). Of all the stimulants used, VD3 stimulated THP-1 MØ expressed the highest level of CD14; THP-1/DS MØ expressed considerable levels and PMA stimulated MØ expressed noticeable levels of CD14 (Figure 19) in agreement with a previous study ⁴⁴⁵. Nevertheless, all stimulants, except for PMA were capable of inducing MØ-like cells as analysed via CD14 surface receptor expression.

CD36, another expression marker for MØ differentiation was observed in THP-1 monocytes following exposure to any of the three stimulation methods ⁵⁰². Unlike CD14, CD36 was expressed to a high level on the THP-1 monocytes. Upon stimulation, with VD3 or with DS the percentage of cells expressing CD36 elevated to 80%. On the other hand, CD36 levels on PMA differentiated MØ remained similar to undifferentiated THP-1 monocytes (Figure 20). These data suggest that the three methods of stimulation create MØ-like cells that have different adhesion properties. So these may be of different value in

subsequent assays presented here. For e.g., in those experiments where strongly adherent MØ are to be used PMA or DS MØ may be most appropriate.

3.7.3 Modelling of AC clearance *in vitro*

3.7.3.1 Chemotaxis and interaction of MØ with AC

Recruitment of MØ in response to highly expressed chemokines in an inflamed tissue is vital for normal host defence to fight against the initiator of inflammation and to resolve the inflammation³³. Healthy tissue is susceptible to damage if inappropriate recruitment of phagocytes occurs⁵⁰³. To guide phagocytes to a site of infection or inflammation, directional cues are sent in the form of chemoattractants from the inflamed site. These signals can be detected by phagocytes which migrate up the chemoattractant gradient. A lack of directional migration will impair clearance of AC as phagocytes will not be in a position to clear the dying cells. A MØ exhibits a spindle-body shape followed by protruded edges to lead the migration directionally in addition to increased attachment and spreading towards the chemical gradients^{504, 505}. Loss of directional cues or modulation in the phagocytes results in an oscillating swing causing random movement in the cell body⁵⁰⁶.

In this study, directional MØ migration towards dying cells was assessed using horizontal (Dunn chamber) and vertical (Cell-IQ) chemotaxis assays. The Dunn chamber method measures not only the chemotactic cell behaviour but also adds precise information on the proportion of analysed cells moving towards or away from the attractants under controlled gradient conditions (yFMI) thereby aiding calculation of the true chemotaxis movement. Other measurements such as Euclidean distance, accumulated distance, velocity, and angle contributes knowledge to the speed, directness and uniformity of the phagocytes' migration towards putative attractants. yFMI is a measure of the parallel movement of MØ for each experiment and indicates the defined and consistent direction of MØ permitting analysis of the strength and level of chemotaxis in a stable chemoattractant environment. The data presented here in figure 25D and 28D suggests that AC B or AC NØ had a stronger MØ chemotaxis effect compared to their derived AS based on the yFMI. These data suggest that perhaps a combination of cells and secreted factors may be important in maximising MØ migration. It is established that AC B cells release AS (containing vesicles) which can be attractive to MØ³⁷. However, also could be that MØ release cytokines in response to the AC aiding in chemotaxis of other MØ cells⁵⁰⁷.

Both forms of AC (AC B or AC NØ or AS B or AS NØ) were inducers of chemotaxis for MØ compared to control (figure 25D and 28D). Moreover, lower variability in the movement of the migrated phagocytes' end points (angle measurement) suggests that MØ travelled in a uniform manner to the chemoattractant AC and AS (B cells and NØ)

compared to their own control showing higher variability in migration (figure 26A and 29A). However, the angle of measurement fails to show the true chemotaxis effect as all MØ were taken into account irrespective of the direction taken. The uniformity of the cell movement is essential to grade the strength of chemoattractant guiding MØ through directional cues.

While the Dunn chamber migration system is based on a true linear concentration gradient, the transwell migration assay using the Cell-IQ is based on a vertical step-gradient and as such is influenced by gravity due to the nature of the experimental setup. This means that once cells have left a transwell they can't change direction (unlike in the Dunn system). The MØ contained in the transwell were tracked for migration by counting the number of MØ reaching the bottom well containing putative attractants in a 24-well plate over a 12h period (figure 30). Similar to the Dunn chamber assay (figure 25D), the transwell system showed AC B cells as a strong attractant whilst AS B also showed chemoattractive abilities using the Cell-IQ (Figure 31). In contrast to the Dunn chamber system (figure 28D), the Cell-IQ model shows that MØ responses to AS NØ was stronger than to whole AC NØ culture (figure 32). These difference may be due to the gradients, the level of response of MØ towards the attractants might vary and in the Cell-IQ an excess of MØ is used leading to higher cell counts using the Cell-IQ software.

However, to confirm the true migration of phagocytes in a vertical assay, the experiment assay included two controls 1) No gradient: i.e. MØ migration towards a bottom well containing serum free medium alone; 2) Destroyed gradient: MØ co-cultured with the attractant i.e. AC in the transwell and the bottom well. Based on the above controls the migration of MØ towards the putative attractants was standardised and determined. In each case, where the gradient was absent, the migration of MØ was reduced (figure 31 and 32). In the case, where the attractant was added both on the top and bottom well to destroy the gradient the MØ migration was reduced towards AC or AS NØ (figure 32) but not in AC or AS B cells (figure 31), as they appeared similar in appearance to MØ under microscope (figure 30). All this ruled out the possibility that chemokinesis may be responsible for the MØ appearing in the lower well. Overall, these experimental results show that it is possible to measure MØ migration to AC and this allows analysis of how periodontal relevant factors may influence this process.

During inflammatory responses, MØ produce IL-8 and other chemokines to recruit NØ to the site of inflammation. However, upon turning apoptotic, NØ secrete a wide variety of intermediate factors to opsonise themselves with attractive components recognised by phagocytes. While factors such as ICAM-3 have been found to be key mediators involved as chemoattractants for MØ, the mediators that are released by AC NØ in recruiting MØ are unknown³⁷. However, annexin-1 and it's peptide fragments are proposed to act as a

pro-phagocytic signals in recruiting THP-1 differentiated MØ⁵⁰⁸. Also other known factors that promote the migration of phagocytes are stated to be CXCL1, CXCL2, CXCL5, CX₃CL₁, ATP, UTP and LPC^{258, 461, 509}

While molecular mediators regulate the bridge between the phagocytes and AC, innate immune surface receptors are reported to facilitate the clearance mechanisms through tethering and tickling to uptake the AC^{280, 479}. Many receptors have been reported to be involved in the recognition and tethering of AC such as PS-R⁵¹⁰, integrins⁵¹¹ and lectins^{512, 513}, scavenger receptors⁵¹⁴ and receptors like CD14³²⁴, CD36^{294, 295}, CD91⁵¹⁵ and ICAM-3²⁸¹. Once bound, the tethered AC are later ingested by MØ to suppress pro-inflammatory mediators through the release of anti-inflammatory cytokines to resolve the inflammation.

The ability of THP-1 DS-derived MØ to interact with AC was studied here using Jenner-Giemsa staining (figure 33). The data in figure 33 suggests that MØ successfully interact (i.e. tether and/or phagocytose) with AC B or AC NØ. Moreover, the data (figure 33B) indicates that MØ do not ingest viable cells. Brown *et al.* reported that viable cells tether to MØ initially due to the presence of unmodified CD31 and detach later. However on AC the CD31 undergoes an undefined variation at the cell surface which helps them to be tethered to phagocytes for a longer time and later to be engulfed³³⁸. However, the data (figure 33B) also indicates that THP-1-derived MØ show more efficient interaction with AC B cells compared to AC NØ. Though the induction of apoptosis in both of these cells varied, the percentage of cell death remained similar in both B and NØ at around 80% apoptotic (figure 15C and 17A). This suggests that *in vitro*, primary NØ may be less likely to be taken up by the THP-1 differentiated MØ. Devitt *et al.* also showed, using HMDM and primary AC NØ, lower interaction levels of ~20% ruling out the possibility that the effect is limited to the THP-1 MØ⁴¹⁸. A further study also demonstrated that primary NØ isolated from venous blood showed limited capacity to be ingested by primary AC NØ⁵¹⁶. Alternatively, participation of IgG autoantibodies present in the human serum have been stated in opsonising AC for the clearance⁵¹⁷. Subsequently, human neutrophils exhibited adhesion and phagocytosis of IgG opsonised zymosan in the presence of serum proposing that IgG mediated-cell target interaction recruits immune cells⁵¹⁸. Together, serum with other bridging molecules might be the missing factors in the attractants released by the apoptotic NØ that might make ingestion by MØ.

Alternatively, viable NØ might be present in the culture and being a phagocytic cell viable NØ might have phagocytosed AC NØ leading to a lower percentage of interaction with MØ. This is in line with previous work that has shown that viable NØ can phagocytose AC NØ in chlamydia cultures⁵¹⁶.

3.8 Conclusion

Results from this chapter confirm the purity of isolated NØ isolated from peripheral human blood as in excess of 96%. Additionally, THP-1 cells differentiated using various stimulants (VD3, PMA or DS) confirmed the expression of important receptors for AC clearance e.g. increased level of CD14 expression on the surface of the differentiated MØ. The apoptotic NØ and their derived AS recruited MØ as confirmed by the chemotaxis assay (both vertical and horizontal) and the recruited MØ efficiently interacted with apoptotic NØ through tethering and phagocytosing the AC. Additionally, AC B or AS B cells function as an effective attractant by recruiting and interacting with THP-1 MØ, acting as a positive control for the study. These established in *vitro* models will be further used to study the AC clearance mechanism in PD by analysing THP-1 differentiated MØ behaviour following exposure to periodontal pathogens and their ability to phagocytose the AC NØ will be elucidated in the following chapters.

Chapter 4

Result 2: Purification of gingipains from *P.gingivalis*

4.1 Introduction

Gingipains are cysteine proteases expressed by the key periodontal pathogen *P. gingivalis* and have been implicated in PD pathogenesis due to their ability to degrade cytokines, and complement components and anti-bacterial peptides, thereby facilitating *P. gingivalis* survival in the host by modulating the innate immune response^{180, 519}. *P. gingivalis* is a major causative agent for adult periodontitis, and gingipains predominantly exhibit 85% general proteolytic activity and 100% trypsin-like cysteine protease activity²⁰². From the onset of inflammation, *P. gingivalis* gingipain activity is documented as being able to attack and disarm professional phagocytes either by cleaving C1q and C3. These complement components are key to the amplification of the complement cascade and their digestion subsequently results in non-functional fragments, or inactivation of the production of cytokines such as membrane bound TNF- α ⁵²⁰⁻⁵²². The multiple pathogenic effects of gingipains also include downregulation of CD31 expression on endothelial cells. CD31 downregulation disrupts vascular barrier function causing intercellular gaps resulting in increased permeability for entry of pathogens^{204, 523}. Another possible mechanism by which gingipains might contribute to the pathogenesis of PD is via their production of inflammatory mediators such as kinins. These molecules are high-molecular-mass kininogens similar to bradykinin and other related peptides, which can interfere with homeostasis mechanisms within the infected tissue⁵²⁴.

In the work reported here, two major clinical strains (W83 and HG66) of *P.gingivalis* were studied. Strain W83 expresses membrane-bound gingipain activity, while, HG66 synthesises soluble forms^{525, 526}. Several studies indicate that of all virulence factors produced by *P.gingivalis*, such as LPS, fimbriae, hemagglutinins and other metabolites, it is the cysteine proteases that are recognised as the major virulence factors necessary for disrupting the host innate immune response^{157, 202}. **The aim of this chapter, therefore, was to purify and characterise the cysteine proteases from the HG66 strain of *P.gingivalis*. In this chapter, the isolation of arginine (ARG or RgpB) and lysine (LYS or Kgp) specific proteases is reported.**

4.2 Establishment of appropriate growth conditions for *P.gingivalis* strains W83 and HG66

Evidence indicates that *P.gingivalis* secretes major trypsin-like enzymes classified as cysteine proteases⁴²⁹. Isolation of these cysteine proteases from the strains W83 and HG66 was attempted as these strains play a predominant role in periodontal tissue

destruction^{420, 423}. In order to establish laboratory cultures of these anaerobes *P.gingivalis* strains W83 (ATCC 33277) and HG66 (DSM 28984) were grown and cultured as described in sections 2.7.3 and 2.7.5. Briefly, fastidious agar plates containing 7% sterile horse blood were used to culture the bacterial strains with incubation for 24-48h at 37°C in an anaerobic chamber. They were checked for purity by Gram staining as is shown in figure 13 in the Materials and Methods.

To enrich for gingipain activity, it is necessary to culture the *P.gingivalis* strains (W83 or HG66) to a high density. In order to do this, the black pigmented colonies obtained from anaerobic growth on agar plates for 48h were further cultured in fastidious anaerobe broth (FAB) containing vitamin K, haemin, and L-cysteine and monitored for bacterial growth by measurement of absorbance over a 72h period. Growth curve profiles are presented in figure 34.

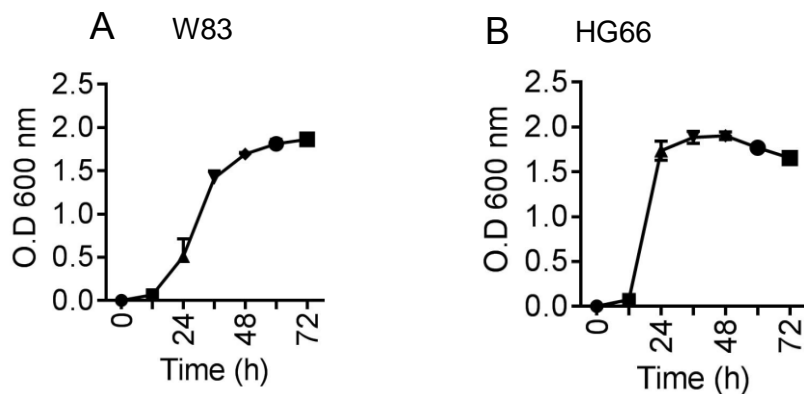


Figure 34: Growth curves of W83 and HG66 strains of *P.gingivalis*

W83 and HG66 bacterial strains were grown anaerobically in 7% horse blood agar containing haemin and vitamin K1 at 37°C in 10% H₂, 10% CO₂, and 80% N₂. The resultant black pigmented colonies of *P. gingivalis* were checked for purity by Gram staining. The bacterial colonies were inoculated into FAB broth in the anaerobic chamber with gentle agitation and were monitored for growth spectrophotometrically at O.D 600nm. The graph showing the growth curves for *P.gingivalis* strains A) W83 and B) HG66 for 72h are shown. Data are mean \pm SEM from three independent experiments.

The data in figure 34A show that W83 exhibits a log phase of growth up to 32h and slowly progressed towards the stationary phase by 72h. Additionally, HG66 exhibits rapid multiplication of bacteria between 8 and 24h followed by a stationary bacterial growth phase at 48h and a subsequent decrease in the number of bacteria by 72h (figure 34B). These data indicate successful growth of both strains of *P.gingivalis*.

4.3 Characterisation of cysteine proteases from *P.gingivalis* strains W83 and HG66

Bacterial cultures grown from W83 and HG66 were fractionated to determine the presence of enzyme activity for gingipains, either the RgpB or Kgp types, according to methods described in section 2.7.8.1. Initially, the bacterial cultures of W83 and HG66

were centrifuged to separate the cell-bound bacterial proteins in the pellet and soluble proteins in the culture supernatants (as described in sections 2.7.6 and 2.7.7). The cell-bound and soluble fractions were then analysed for the presence of RgpB and Kgp protein activity using their specific substrates Bz-L-Arg-pNA and Z-L-Lys-pNA, respectively. The activity for the gingipains (RgpB or Kgp) were measured as p-nitroanilide (pNA) released from the Bz-L-Arg-pNA and Z-L-Lys-pNA substrates and assayed by reading absorbance at 405nm and expressed as a percentage of total enzyme activity. The data from this analysis are presented in figure 35.

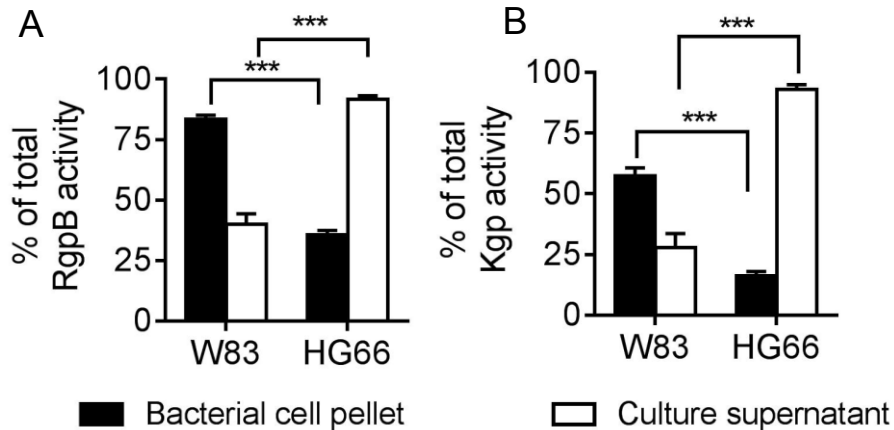


Figure 35: Determination of the amidolytic activity of *P.gingivalis* strains W83 and HG66 following culture fractionation.

Strains W83 or HG66 were cultured according to the methods described in sections 2.7.3 and 2.7.5. The log-phase bacterial cultures, grown for 32h for W83 and 24h for HG66 (O.D 600nm), were centrifuged to separate the bacterial pellet and supernatant and analysed for amidolytic activity. The histogram shows total amidolytic activity (%) assessed for A) RgpB activity against Bz-L-Arg-pNA and, B) for Kgp activity, against Z-L-Lys-pNA for cell-bound cell extract (black bars), cell-free culture supernatant (white bars) for both W83 and HG66 strains. Statistical analyses were conducted using ANOVA followed by a Bonferroni post-test, *** $P < 0.001$. Statistical tests compared differences between strains. Data shown are means \pm SEM of three independent experiments.

The data in figure 35 show the amidolytic activities tested for the presence of RgpB and Kgp in the bacterial pellet (black bars) and culture supernatant (white bars) of W83 and HG66. The RgpB enzyme activity was found to be significantly greater in the bacterial pellet of W83 compared with the HG66 pellet while the culture supernatant of HG66 exhibited significantly increased activity for RgpB compared with the W83 supernatant (figure 35A). Additionally, Kgp activity was significantly increased in the HG66 culture supernatant compared with both the W83 bacterial pellet and the culture supernatant indicating that HG66 secretes the soluble form of proteins specific for Kgp (figure 35B). Overall, HG66 demonstrates higher activity for both RgpB (figure 35A) and Kgp (figure 35B) over strain W83 which showed higher activity for RgpB (figure 35A) but weaker activity for Kgp (figure 35B) in the bacterial pellet. This indicates that RgpB and Kgp were

abundant in the cell-bound form in W83 while HG66 secretes soluble forms. These data are consistent with previous studies⁵²⁶⁻⁵²⁹.

In order to determine the molecular weights specific for RgpB (~50kDa) and Kgp (~60-70kDa) present in the bacterial pellet and culture supernatant of W83 and HG66, SDS-PAGE analysis was performed according to the method described in section 2.7.8.2.3. The separated protein bands were stained with Coomassie blue and the results are shown in figure 36.

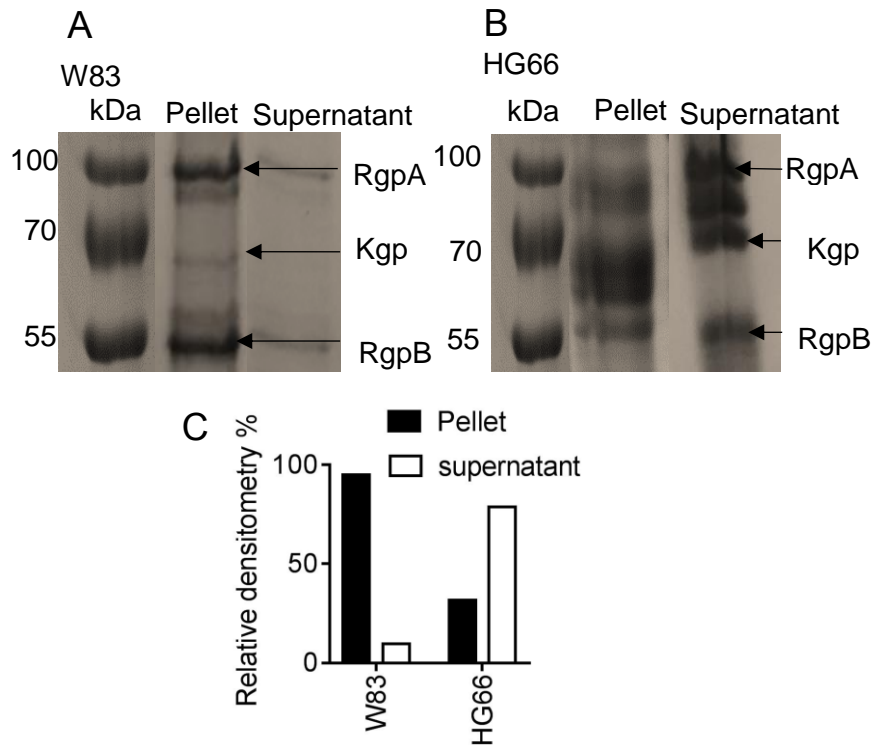


Figure 36: Characterisation of molecular weights of proteases from *P.gingivalis* strains W83 and HG66 using SDS-PAGE

Strains W83 or HG66 were cultured according to the methods described in sections 2.7.3 and 2.7.5. The log-phase bacterial cultures were grown for 32h (W83) or 24h (HG66), centrifuged to separate the bacterial pellet and supernatant. The SDS-PAGE analysis of proteins present in the cell pellets and the culture supernatants of *P.gingivalis* strains show the presence of RgpB (~50kDa) and Kgp (~60kDa) in strains W83 (A) and HG66 (B). The histograms (C) show the densitometry analysis of the gel images for the W83 and HG66 proteins obtained from A and B performed using ImageJ software. Densitometry values were expressed as % of relative density. SDS-PAGE gel profiles shown in A and B are representative of three different independent experiments.

In agreement with the patterns of proteolytic activity shown in figure 35, the SDS-PAGE analysis in figure 36 shows the presence of clear protein bands in the bacterial pellet of W83 compared with the supernatant which has relatively weak bands at ~50kDa and ~100kDa (figure 35A). In contrast, HG66 expressed cysteine protease activity both on the cell pellet and in the culture supernatant with protein bands between ~50kDa to ~100kDa, however, intense molecular weight bands were present only in the supernatant derived from the HG66 strain (figure 36B). Total protein levels were measured from the

representative image of SDS-PAGE gel (figure 36A&B) and relative densitometry was expressed as a percentage of the total activity (figure 36C). The relative densitometry analysis obtained from the *P.gingivalis* strains W83 and HG66 show the intensity of the proteins present in the pellet of W83 and supernatant of HG66 (figure 36C). Data indicating that most of the activity in W83 was cell-bound whilst in the HG66 strain activity was present in the soluble form.

The amidolytic enzyme activity (figure 35) and the SDS-PAGE analysis (figure 36) showed that W83 and HG66 released proteases in the form of cell-bound and soluble forms, respectively. In order to determine whether the proteins present in the bacterial pellet of W83 and culture supernatant of HG66 belong to the group of cysteine proteases, cysteine (50mM) was added to the substrates Bz-L-Arg-pNA and Z-L-Lys-pNA as a stimulating agent to fully activate the proteolytic activities of RgpB or Kgp, respectively. The results of this analysis are shown in figure 37.

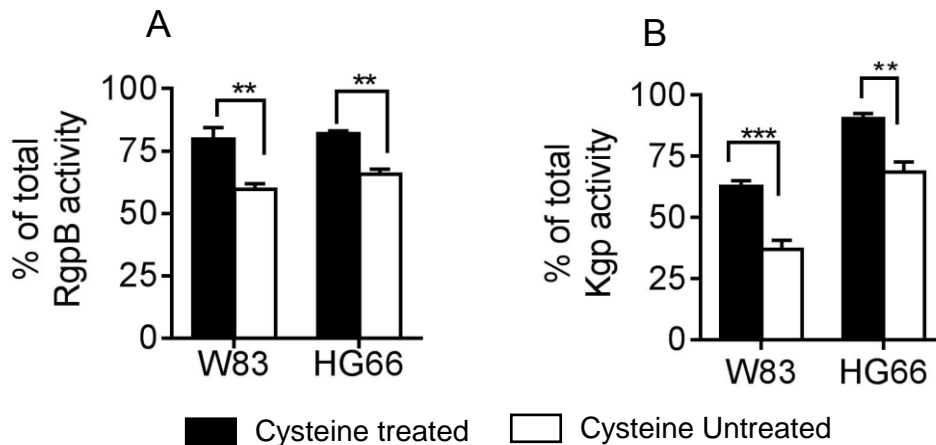


Figure 37: Determination of amidolytic activity in the presence or absence of cysteine derived from *P.gingivalis* strains W83 and HG66

Strains W83 or HG66 were grown according to the methods described in sections 2.7.3 and 2.7.5. Log-phase bacterial cultures were grown for 32h (W83) or 24h (HG66), centrifuged to separate the bacterial pellet and supernatant and analysed for amidolytic activity. The bacterial pellet of W83 and culture supernatant of HG66 were used to test for amidolytic activity in the presence or absence of cysteine. The histograms show the percentage of total enzyme activity against Bz-L-Arg-pNA assessed for RgpB (A) and Z-L-Lys-pNA assessed for Kgp (B) with and without cysteine. Statistical analyses were conducted using ANOVA followed by a Bonferroni post-test, ** $P < 0.01$, *** $P < 0.001$. Statistical tests compared differences between cysteine-treated and untreated samples. Data shown are means \pm SEM of three independent experiments.

The data in figure 37 show that a significant difference in amidolytic activity was detected between the cysteine-treated W83 cell-bound proteins or HG66 culture supernatants compared with untreated W83 or HG66 proteins assayed for RgpB (figure 37A) and Kgp (figure 37B) enzyme activities. These data indicate that cysteine was necessary to activate the total amidolytic activity in both the protease samples and this is consistent with previous studies to indicate the activity rises from cysteine proteases ⁴²⁶.

4.4 Purification of gingipains from *P.gingivalis* HG66

In line with previous work, the amidolytic activity (figure 35) and SDS-PAGE analysis (figure 36) confirmed the presence of enzymatically active proteins present in the bacterial pellet of the W83 strain and the culture supernatant of the HG66 strain. However, the W83 sample showed reduced Kgp activity (figure 35B) and a weaker protein band at the Kgp molecular weight (~60kDa) compared with the HG66 Kgp presence. Additionally, W83 activity was mostly cell-bound (figure 35 and 36) and this might result in the presence of LPS contaminants and other proteins. For this reason, the bacterial culture supernatant from HG66 was further fractionated as this strain appeared the more promising source of gingipains for use in further study. The presence of gingipains was tested according to the methods described in section 2.7.7. Briefly, acetone precipitated proteins from the culture fluid of HG66 were fractionated by gel filtration chromatography. One of the challenges involved in the isolation of purified gingipains by gel filtration was to remove haemin, added as a source of iron nutrient for the survival of bacteria from the bacterial culture medium. In order to avoid the interference of haemin in the gingipain isolation, gel filtration chromatography was coupled with Sephadex G-150 on an arginine-Sepharose column (figure 38). This process was performed as recommended by a previous successful gingipain purification method ⁴²⁶.

The acetone-precipitated proteins from the HG66 culture supernatant were applied to a Sephadex G-150 column equilibrated in and eluted with buffer containing NaCl, Bis-Tris, and CaCl₂ (pH 6.8) (as described in section 2.7.7). Fractions containing 280nm-absorbing material in the 50-100 kDa range were collected and applied to an arginine-Sepharose column which was previously equilibrated with loading buffer containing CaCl₂ and Tris-HCl (pH 7.4) (as described in section 2.7.7). Unbound proteins were removed from the column by washing with loading buffer until the absorbance at 280 nm reached a baseline value of 0. Once the baseline was achieved, the column was eluted sequentially with loading buffer containing NaCl (500 mM), followed by lysine (750 mM in loading buffer), loading buffer alone and finally arginine (100 mM in loading buffer). Material eluted from the affinity column was monitored at 280 nm for protein content and by conductivity. The results of this analyses are presented in figure 38.

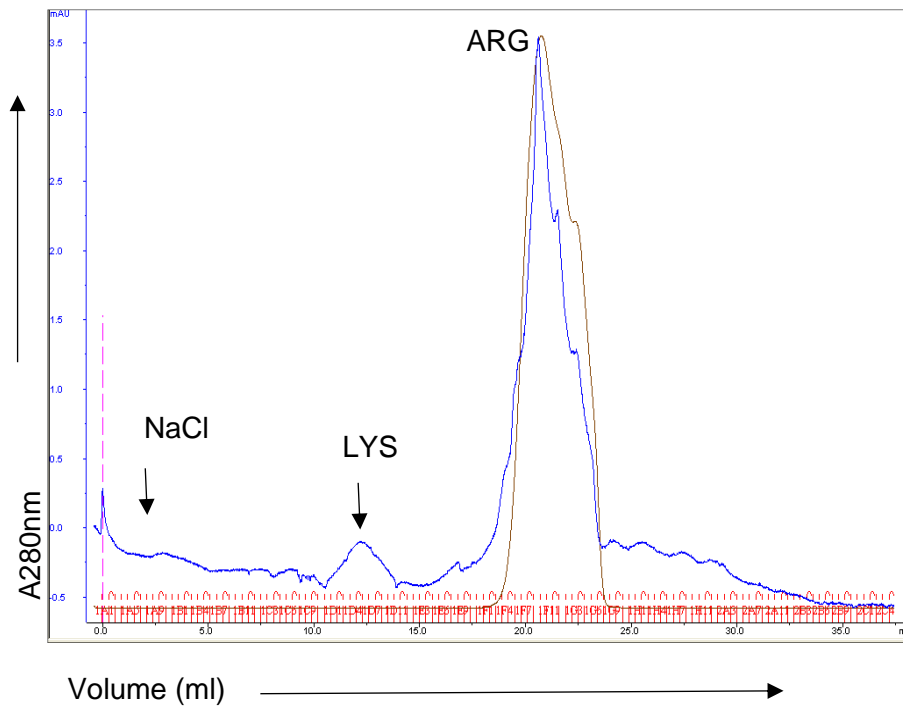


Figure 38: Representative chromatogram of a gel chromatography column performed on Sephadex G-150 fractions followed by arginine sepharose affinity chromatography

Strains W83 or HG66 were grown according to the methods described in sections 2.7.3 and section 2.7.5. Log-phase bacteria cultures grown for 24h for HG66 were used to isolate proteins according to methods described in section 2.7.7. The gel chromatography column analysis performed shows the 50-100 kDa material collected from a Sephadex G-150 column which was applied to an arginine sepharose column by washing the column with 500 mM NaCl prior to elution of fractions exhibiting proteinase activity against Z-L-Lys-pNA (LYS) and Bz-L-Arg-pNA (ARG) sequential elution with lysine (750 mM) and arginine (100 mM). The peaks in the chromatogram show (from left to right) gradient equilibrated with NaCl, 750 mM lysine gradient to elute Kgp and 100 mM arginine gradient to elute RgpB from *P.gingivalis* strain HG66. The blue line indicates absorbance at 280 nm. The brown line indicates conductivity. A representative chromatogram from three different runs by gel filtration chromatography is shown.

The data in figure 38 shows a representative image of Sephadex G-150 column applied on arginine sepharose chromatography to elute the proteins specific for RgpB and Kgp derived from *P.gingivalis* HG66. The chromatogram shows the NaCl elution profile used to wash the column and remove unwanted proteins at the beginning of the flow. Followed by the buffer wash and sequential elution with lysine, showing a peak for the eluted proteins specific for lysine (Kgp) and RgpB was eluted exhibiting a larger peak for proteins specific for arginine. The chromatogram was plotted for volume (ml) against absorbance 280nm.

The fractions collected for arginine and lysine eluted proteins (figure 38) were pooled and concentrated using an Amicon PM-10 filtration column as described in section 2.7.7. Amidolytic activity was determined using the specific substrates Bz-L-Arg-pNA for RgpB and Z-L-Lys-pNA for Kgp. The results of this analysis are shown in figure 39.

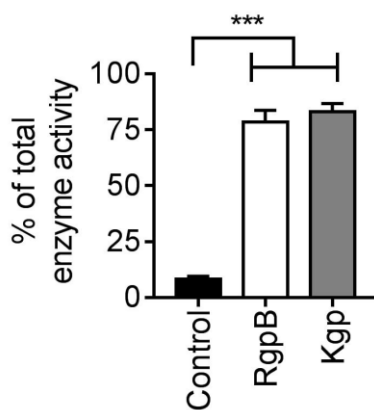


Figure 39: Determination of the amidolytic activity of gingipains purified from *P.gingivalis* strain HG66

Strain HG66 was grown according to the methods described in sections 2.7.3 and cultured in FAB broth as described in section 2.7.5. Log-phase cultures grown for 24h for HG66 were used to isolate proteins according to methods described in section 2.7.7. The isolated fractions ARG and LYS eluted from arginine-Sepharose using 100 mM arginine and 750 mM lysine (figure 38) were analysed for amidolytic activity. The histogram shows total enzyme amidolytic activity in percentage assessed for RgpB activity against Bz-L-Arg-pNA and Kgp activity against Z-L-Lys-pNA for the isolated fractions of HG66. Statistical analyses were conducted using ANOVA followed by a Dunnett's post-test, *** $P < 0.001$ compared to control (enzyme buffer on their own). Data shown are mean \pm SEM from three independent experiments.

The data in figure 39 show RgpB activity against Bz-L-Arg-pNA and Kgp activity against Z-L-LYS-pNA from HG66 and this exhibited 75% of recovered enzyme activity.

The ARG and LYS fractions collected using Sephadex G-150 fractions on arginine-Sepharose chromatography for HG66 of gingipains were assessed for molecular weight using SDS-PAGE according to the method described in section 2.7.8.2.3. The results of this analysis are shown in figure 40.

The data presented in figure 40A shows distinct intense double bands with the upper band presumed to represent mature RgpB at ~50kDa and the lower band revealing weaker expression for the presumed RgpB catalytic domain (~48kDa). The presumed Kgp protein appeared as a single major band (~60kDa) suggesting the presence of some additional gingipain activity in the final eluted proteins using gel filtration chromatography in agreement with previous studies⁵³⁰⁻⁵³². The absence of other bands compared with the supernatant of HG66 (figure 36B) indicates the successful isolation of purified gingipains without the contamination of other proteins or proteolytic enzymes. Additionally, data (figure 40B) shows the percentage of protein expression of RgpB as 89% and Kgp as 72.3% compared with the total dialysed proteins before separating them into RgpB and Kgp. The densitometric values shown demonstrate the intensity of RgpB and Kgp bands distinctly.

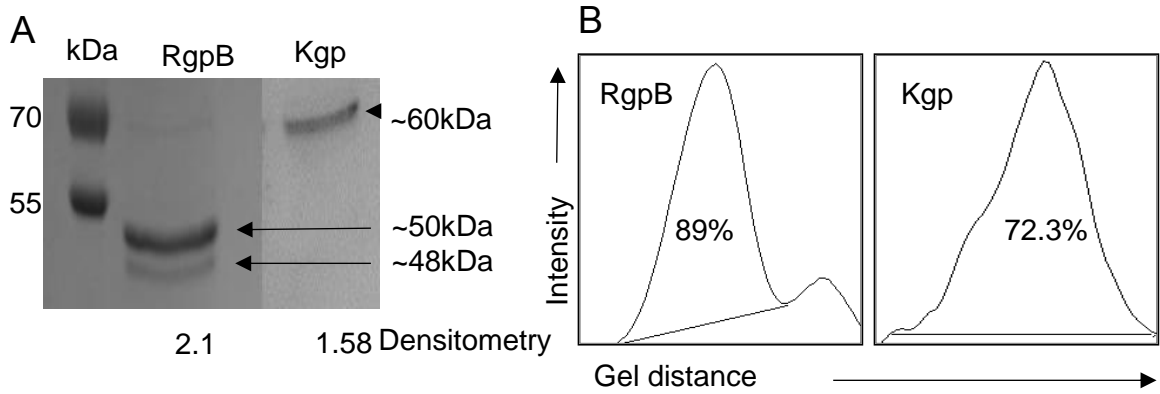


Figure 40: Determination of molecular weights using SDS-PAGE analysis for the final purified proteins from the HG66 strain of *P.gingivalis*

Strain HG66 was grown according to the methods described in sections 2.7.3 and 2.7.5. Log-phase cultures grown for 24h were used to isolate proteins according to methods described in section 2.7.7. The ARG and LYS fractions eluted from arginine-Sepharose using 100 mM arginine and 750 mM lysine (figure 38) were analysed by SDS-PAGE. A) SDS-PAGE gel showing the molecular weight for RgpB revealed double bands at ~50kDa and ~48kDa while Kgp showed a single band at ~60 - 70kDa. Densitometry values were obtained by using ImageJ and compared the purified protein bands with the dialysed culture fluid before separating them as RgpB and Kgp. B) The graph shows the area of surface positive for a protein expressed as a percentage using ImageJ analysis compared with the total dialysed and concentrated protein, which was used as a control. Data shown are representative of three independent experiments.

To check whether the isolated fractions from HG66, as shown in figure 38, were gingipains, assays were performed in the presence of the cysteine protease inhibitor, TLCK. The results of this analysis are presented in figure 41.

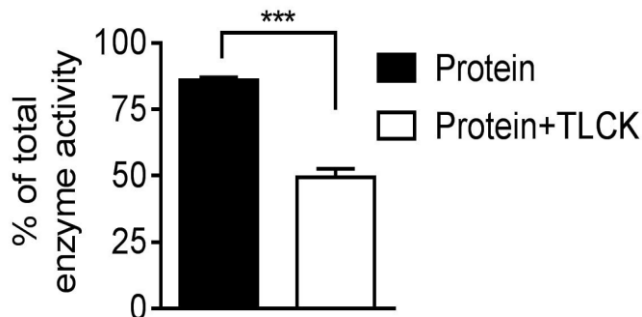


Figure 41: Inhibition of purified proteins from *P.gingivalis* HG66 using TLCK

Strain HG66 was grown according to the methods described in sections 2.7.3 2.7.5. Log-phase cultures grown for 24h were used to isolate proteins according to methods described in section 2.7.7. The isolated fractions specific for RgpB and Kgp from HG66 acquired using Sephadex G-150 and arginine-Sepharose chromatography (figure 38) were analysed for amidolytic activity in the presence of TLCK (100 μ M), as a measure of cysteine protease activity in the purified proteins (as described in section 2.7.12). The histogram shows the total enzyme activity (%) of the isolated fractions against L-BAPNA in the presence or absence of TLCK inhibitor. Statistical analyses were conducted using ANOVA followed by Bonferroni post-test, *** P <0.001. Data shown are mean \pm SEM of three independent experiments.

The data in figure 41 show a significant difference between TLCK treated protein fractions compared with untreated samples and indicating that TLCK inhibits the gingipain activity within the isolated fractions, findings which are consistent with a previous study⁴²⁶.

A major contaminant in the purification products of Gram-negative bacteria is LPS and this may have significant effects in downstream inflammation assays. Therefore, to assess the level of LPS contamination in the purified HG66 supernatant isolated gingipains, Limulus Amoebocyte Lysate tests were undertaken according to the methods described in section 2.7.10. These studies revealed that the LPS contamination levels were 2.9U/ml (RgpB) and 1.9U/ml (Kgp) from isolated gingipains of HG66.

The yield of the enzyme in the final eluted protein measured as described in section 2.7.8.2.1 and was estimated at approximately 0.5 mg/ml of protein starting from 1-litre of culture fluid.

4.5 Characterisation of isolated proteins using mass spectrometric analysis

The data presented in the previous section indicate that the proteins isolated using a strategy to purify gingipains exhibit appropriate molecular weights (figure 40) and carry appropriate cysteine protease activity (figure 41). However, to more robustly identify the presence of gingipains within the isolated fractions mass spectrometry analyses were undertaken. Subsequently isolated SDS-PAGE gel bands of ≈ 50 kDa and ≈ 60 kDa which correspond to the molecular weights for RgpB and Kgp, respectively, were subject to further analysis. Isolated bands were extracted cleaved via in-gel digestion according to the method described in section 2.7.9, and the released peptides were analysed by mass spectrometry. The data obtained were subjected to proteomic analysis using Swiss-Prot, a protein sequence database, followed by Sequest search engine analysis, a data tool used for protein identification. The likely identity of the proteins excised from the gel is shown in Table 7.

The results (Table 7) show analysis for the excised bands from the gel. More than 30 proteins with at least two unique peptide sequences were identified, thereby assuring at least 28% of total protein coverage and providing the highest identification scores (XCorr>1000) for RgpB and Kgp. Based on the XCorr values the top 6 likely identified abundant proteins were gingipains and this confirms the formal presence of arginine and lysine gingipains within the sample preparations. The presence of other contaminating proteins such as major fimbrium subunit and peptidyl arginine deiminase enzyme show significantly lower scores than gingipains. Given this characterisation of the gingipains within the isolated fractions and the clear cysteine protease activity along with the appropriate molecular weight banding, data indicates the successful isolation of RgpB and Kgp from *P.gingivalis* HG66.

Results

Accession	Description	Score	Coverage	# Proteins	# Unique Peptides	# Peptides	MW [kDa]
B2RM93	Gingipain R1 OS=Porphyromonas gingivalis (strain ATCC 33277 / DSM 20709 / CIP 103683 / JCM 12257 / NCTC 11834 / 2561) GN=RgpB A PE=3 SV=1 - [CPG1_PORG3]	1833.17	37.29	2	3	52	185.2
B2RKU0	Gingipain R2 OS=Porphyromonas gingivalis (strain ATCC 33277 / DSM 20709 / CIP 103683 / JCM 12257 / NCTC 11834 / 2561) GN=RgpB B PE=3 SV=1 - [CPG2_PORG3]	1522.05	52.58	1	1	30	80.9
P28784	Gingipain R1 OS=Porphyromonas gingivalis GN=RgpB A PE=1 SV=2 - [CPG1_PORGN]	1448.00	45.21	1	1	38	108.7
P95493	Gingipain R2 OS=Porphyromonas gingivalis (strain ATCC BAA-308 / W83) GN=RgpB B PE=1 SV=2 - [CPG2_PORGI]	1206.98	34.92	1	1	23	80.9
B2RLK2	Lys-gingipain OS=Porphyromonas gingivalis (strain ATCC 33277 / DSM 20709 / CIP 103683 / JCM 12257 / NCTC 11834 / 2561) GN=kgp PE=1 SV=1 - [KGP_PORG3]	1082.04	28.50	1	2	33	187.1
P72197	Lys-gingipain HG66 OS=Porphyromonas gingivalis GN=kgp PE=1 SV=1 - [KGP66_PORGN]	1076.46	30.88	2	2	35	186.7
Q9RQJ2	Peptidylarginine deiminase OS=Porphyromonas gingivalis (strain ATCC BAA-308 / W83) GN=PG_1424 PE=1 SV=1 - [PAD_PORGI]	344.40	68.35	1	29	29	61.7
Q51845	Hemagglutinin A OS=Porphyromonas gingivalis GN=hagA PE=3 SV=1 - [HAGA2_PORGN]	146.89	14.80	1	6	10	283.1
B2RH57	Major fimbrium subunit FimC OS=Porphyromonas gingivalis (strain ATCC 33277 / DSM 20709 / CIP 103683 / JCM 12257 / NCTC 11834 / 2561) GN=fimC PE=1 SV=2 - [FIMC_PORG3]	132.26	34.22	1	13	13	50.1
B2RH59	Major fimbrium tip subunit FimE OS=Porphyromonas gingivalis (strain ATCC 33277 / DSM 20709 / CIP 103683 / JCM 12257 / NCTC 11834 / 2561) GN=fimE PE=1 SV=1 - [FIME_PORG3]	103.50	49.27	1	20	20	60.6
B2RH54	Major fimbrium subunit FimA type-1 OS=Porphyromonas gingivalis (strain ATCC 33277 / DSM 20709 / CIP 103683 / JCM 12257 / NCTC 11834 / 2561) GN=fimA PE=1 SV=3 - [FIMA1_PORG3]	81.91	34.46	3	8	8	41.3
P0C934	NAD-specific glutamate dehydrogenase OS=Porphyromonas gingivalis (strain ATCC BAA-308 / W83) GN=gdh PE=1 SV=1 - [DHE2_PORGI]	63.10	37.98	1	14	14	49.2
B2RHG1	Minor fimbrium subunit Mfa1 OS=Porphyromonas gingivalis (strain ATCC 33277 / DSM 20709 / CIP 103683 / JCM 12257 / NCTC 11834 / 2561) GN=mfa1 PE=1 SV=1 - [MFA1_PORG3]	21.66	11.19	1	5	5	60.7
Q9S3R8	Outer membrane protein 40 OS=Porphyromonas gingivalis (strain ATCC BAA-308 / W83) GN=PG_0694 PE=1 SV=1 - [OMP40_PORGI]	19.83	18.95	1	5	5	42.4
B2RLL7	Enolase OS=Porphyromonas gingivalis (strain ATCC 33277 / DSM 20709 / CIP 103683 / JCM 12257 / NCTC 11834 / 2561) GN=eno PE=3 SV=1 - [ENO_PORG3]	19.01	16.24	2	5	5	45.8
B2RHG3	Minor fimbrium tip subunit Mfa3 OS=Porphyromonas gingivalis (strain ATCC 33277 / DSM 20709 / CIP 103683 / JCM 12257 / NCTC 11834 / 2561) GN=mfa3 PE=1 SV=1 - [MFA3_PORG3]	18.10	20.40	1	5	5	50.0
Q9S3R9	Outer membrane protein 41 OS=Porphyromonas gingivalis (strain ATCC BAA-308 / W83) GN=PG_0695 PE=1 SV=2 - [OMP41_PORGI]	13.12	14.58	1	5	5	43.4
B2RHV8	Phosphoenolpyruvate carboxykinase [ATP] OS=Porphyromonas gingivalis (strain ATCC 33277 / DSM 20709 / CIP 103683 / JCM 12257 / NCTC 11834 / 2561) GN=pckA PE=3 SV=1 - [PCKA_PORG3]	12.82	10.65	2	4	4	59.4
B2RJM1	Hydroxylamine reductase OS=Porphyromonas gingivalis (strain ATCC 33277 / DSM 20709 / CIP 103683 / JCM 12257 / NCTC 11834 / 2561) GN=hcp PE=3 SV=1 - [HCP_PORG3]	12.39	8.00	2	4	4	60.4
B2RH58	Major fimbrium tip subunit FimD OS=Porphyromonas gingivalis (strain ATCC 33277 / DSM 20709 / CIP 103683 / JCM 12257 / NCTC 11834 / 2561) GN=fimD PE=1 SV=1 - [FIMD_PORG3]	10.40	5.97	1	4	4	75.8
B2RGR2	Serine hydroxymethyltransferase OS=Porphyromonas gingivalis (strain ATCC 33277 / DSM 20709 / CIP 103683 / JCM 12257 / NCTC 11834 / 2561) GN=glyA PE=3 SV=1 - [GLYA_PORG3]	6.29	7.75	1	3	3	46.6

Table 7: Characterisation of purified proteins from *P.gingivalis* HG66 using mass spectrometric analysis: The table shows the numbers of proteins identified as a result of the Sequest search against the SwissProt database, using *P. gingivalis* taxonomy, trypsin as a proteolytic enzyme and allowing up to two miss-cleavages. Oxidation of the methionine residue, carbamidomethylation on the cysteine thiol, and deamidation of asparagine and glutamine were used as variable post-translational modifications. Only the high confidence, rank 1 and unique peptides were used for the identification, with at least two different sequences identified per protein.

4.6 Discussion

The aim of the studies presented here were to purify and characterise the cysteine proteases from *P.gingivalis*. These enzymes, gingipains, are considered to be a major virulence factor in advanced PD ¹⁵⁷. Indeed several virulence agents such as collagenases, serine proteinase, trypsin-like enzymes and other forms of proteases from *P.gingivalis* are also involved in the hydrolysis of tissue factors, e.g. fibrin, fibrinogen, fibronectin, collagen, lysozyme, as well as complement factors such as C3, C5 and plasma coagulation factors ⁵³³⁻⁵⁴¹. However, gingipains are proposed to be the major virulence factors due to their ability to invade the host system by contributing at least 85% of proteolytic activity compared to other components in *P.gingivalis* ¹⁵⁶. Therefore, *P.gingivalis* cleave key molecules and interfere with the host immune system which can cause severe destruction of the gingival and periodontal tissues ⁹⁴.

Previous studies report that many forms of proteolytic enzymes exist in *P.gingivalis*. These are in the range of 29-110kDa molecular masses, of which two are serine proteases and the rest are classified as cysteine proteases with a specificity for ARG and LYS residues. These enzymes are known as arginine gingipains (RgpB) or lysine gingipains (Kgp) and are capable of cleaving the synthetic substrates Bz-L-Arg-pNA and Z-L-Lys-pNA respectively as was utilised in this study ⁵⁴². Chen *et al.* described the first enzymes classified as cysteine proteases from *P.gingivalis*. These were 50kDa in size and were termed gingipains which show specific cleavage at arginine residues ⁵²⁵. Subsequently, Pike *et al.* demonstrated an enzyme associated with the ability to cleave Bz-L-Arg-pNA using SDS-PAGE. This enzyme gave a single SDS-PAGE band of high molecular mass at 95kDa in size in the absence of sample boiling. However, upon denaturation by heat, protein bands were seen at 50, 44, 27 and 17kDa, with 50kDa being accepted as the source of the arginine-specific activity ⁴²⁶. Another form of gingipain has been identified which cleaves following lysine residues. This enzyme is known as Kgp. It has been identified as a single 105 kDa band on SDS-PAGE prior to denaturation by heat however, after boiling, it yields bands at 60, 44, 27 and 17 kDa. Since both gingipains produce smaller size protein bands following heat denaturation the main difference between the gingipains is represented by their highest molecular weight upon heating, i.e. ~50kDa for RgpB and ~60kDa for Kgp. The study presented here focused on these highest molecular weight bands thought to contain the enzymatically active components ^{426, 526, 543, 544}.

4.6.1 Comparison of *P.gingivalis* W83 and HG66 derived cysteine proteases

Identification of microorganisms associated with PD has been the focus of significant research. While 500 species of bacteria have been identified in the oral cavity, only a

relatively small number of bacteria have been classified as virulent based on their strong relationship with periodontitis. Notably, these virulent strains show a strong relationship with disease phenotypes characterised by periodontal pocket depth and bleeding on probing^{52, 107}. The virulence of periodontal bacteria has been proposed to be based on three characteristics: i) adherence capacity⁵⁴⁵; ii) the ability to evade the host immune system by producing proteolytic enzymes,⁵⁴⁶; and iii) inhibition of phagocyte functions by degrading complement factors or inactivating cytokine secretions^{520, 521}. The work presented in this thesis will be highlighting ii) and iii). When considering bacterial species associated with periodontal disease, *P.gingivalis* was identified as the species which satisfied all three of these criteria. Belonging to the family of Porphyromonadaceae, *P.gingivalis* is known to invade gingival epithelial cells following their colonisation in the subgingival region. Notably, these gingival epithelial cells modulate oral health by adapting and responding to the infection by regulating the local inflammatory response^{60, 547}. The main effect of this bacterium, however, is to disrupt tissue homeostasis within the gingival environment resulting in advancement from gingivitis to more generalised periodontal disease which ultimately leads to alveolar bone loss²⁰⁰. Many diverse strains of *P.gingivalis* have been identified from orally infected patients including W50, A7A1, 381, ATCC 33277, and ATCC 49417⁵⁴⁸. However, it is unclear to what extent strain variability is associated with bacterial virulence in periodontal disease. It is also unclear as to what degree genetic variation within the host or other factors may be involved in driving PD responses.

The wild-type strain, W83, is the most frequently studied *P.gingivalis* strain and it has been used in earlier studies to extract membrane-associated proteolytic enzymes^{171, 549}. However, strain HG66 is known to secrete soluble forms of proteolytic enzymes into the GCF^{94, 164}. When studied here both strains, W83 and HG66, showed similar appearance of black pigmented colonies and a characteristic malodour following anaerobic growth on blood agar (figure 13, Materials and Methods). The proto-heme present in erythrocytes in blood agar enables the bacteria to grow by forming black pigmented colonies, due to deposits of heme - μ -oxo dimers present in the bacterial cell surface⁵⁵⁰. Depending on the strain, the colour and virulence of the bacterial colonies vary in appearance⁵⁵⁰. However, most *P.gingivalis* strains or variants are known to produce volatile sulphur compounds (VSCs), such as hydrogen sulphide (H₂S), methyl mercaptan (CH₃SH), and dimethyl sulphide which initiate the metabolism of the sulphur amino acids causing the oral malodour⁵⁵¹. Furthermore, the absence of black pigmented colonies in *P.gingivalis* was observed in heme-deprived blood agar medium indicating that the presence of heme plays a major role in colony pigmentation⁵⁵²⁻⁵⁵⁴. The growth and the virulence of the *P.gingivalis* bacteria are dependent upon the ability to acquire iron and protoporphyrin IX

from the host system and these function as essential nutrients. Notably, earlier studies have indicated that RgpA, RgpB, and Kgp from both the strains W83 and HG66 bind to iron or heme-containing compounds in the host system⁵⁵⁵.

At 48h, black pigmented colonies were inoculated into FAB broth to enable generation of bacterial growth curves for the W83 and HG66 strains. HG66 demonstrated faster growth compared with the W83 strain under anaerobic conditions (figure 34). However, both of the bacterial strains cultured generated a dark brown fluid, indicating the presence of haemin, though, this was comparatively low in strain HG66 at the 24h log-phase bacterial culture point. One of the possible means by which haemin can be eliminated is by using gel filtration chromatography, which was used in this study. Additionally, dialysis was undertaken overnight to remove the majority of the haemin.

Preliminary experiments measured cysteine protease activity for both the W83 and HG66 strains. During the purification process, amidolytic activity and SDS-PAGE analysis were performed. Analysis of the cell pellets and culture supernatants obtained from strains W83 and HG66 enabled identification of the most productive strain based on the level of proteolytic activity. The data presented in figures 35 and 36 demonstrated that both strains produced cell-bound and extracellular enzyme activity. However, cell-bound activity was higher in strain W83 while HG66 secreted more activity in soluble forms. This observation is in agreement with earlier studies which reported that major cysteine protease proteins were present in the outer membrane of the W83 bacteria strain⁵⁵⁶.

Previous studies report that different strains of *P.gingivalis* express multiple proteolytic enzymes and all of them differ in their molecular mass and specificity for peptide bonds^{202, 526}. Eight different endopeptidases and numerous exopeptidases have been documented with molecular weights ranging from 29 to 110kDa. Two of these proteins belong to the group of serine and metallopeptidases enzymes while the rest are cysteine proteases with specificity for Bz-L-Arg-pNA⁵²⁵. The data presented (figure 35) demonstrate that the W83 strain produced RgpB-specific aminopeptidase activity with a weaker expression for Kgp-specific aminopeptidase activity (figure 35A). Notably the HG66 strain expressed both RgpB and Kgp-specific aminopeptidase activity (figure 35B). Additionally, figure 36B highlighted data demonstrating that proteins with a wide range of molecular weights were present in both the cell pellet and culture supernatant derived from HG66. However, W83 extracts showed distinct bands at ~50kDa and at ~100kDa (figure 36A), which were presumed to be RgpA (~95kDa). Studies on comparison of W83 and HG66 reports that both strains express identical Rgp and Kgp protein sequence^{94, 185}.

Existing literature presents conflicting views on the various forms of cysteine proteases from *P.gingivalis* with different molecular masses and specificity for peptide bonds being

reported⁹⁴. To date, it is understood that there are 3 forms of gingipain, each of which can be distinguished on SDS-PAGE gels by the pattern of lower molecular mass bands produced. RgpA can exist in different molecular masses depending on the domains present. For RgpB this is ~50kDa due to the absence of hemagglutinin adhesion domains. However, when the hemagglutinin adhesion domains are present the size is reported to be 90~110kDa, which is comparable to RgpA^{94, 557}. Lysine gingipain has been shown to have a molecular mass of ~60 kDa with hemagglutinins (HA1, HA2, HA3, and HA4) present¹⁶⁰. Currently, there is a consensus of opinion that RgpB has a 50kDa molecular mass with some smaller molecular weight bands, while Kgp tends to be present from ~60-70kDa.

The variation of the molecular masses is notable for different isoforms of gingipains⁵⁴⁹. It is unclear where the variation in molecular mass of the different forms is derived from and whether this is affected by or related to the growth kinetics of the different clinical strains of *P.gingivalis*. However research has demonstrated that gingipains are produced by most strains of *P.gingivalis*^{179, 193, 558, 559}. The gingipains are classified as cysteine proteases containing an N-terminal C25 (catalytic cysteine residue) domain. Gingipains exhibit unique primary protein structures when compared with other cysteine proteolytic enzymes present in the databases, suggesting that gingipains comprise a distinct group of proteolytic enzymes. However further study is needed to better understand their biochemical properties and their specialised functions in causing periodontal tissue destruction⁵⁶⁰.

In addition to amidolytic activity (figure 35) and SDS-PAGE (figure 36) size determination, the isolated proteins were tested for cysteine protease activity (figure 37). Cysteine acts as a reducing agent for the activation of both gingipains (RgpB and Kgp)⁵⁶¹. This is in agreement with the data presented here (figure 37) showing that cysteine was necessary for complete activation of the amidolytic activity in both gingipains (RgpB or Kgp). Indeed in the absence of the cysteine, the enzyme activity decreased, indicating their absolute dependence for full activity. These data are consistent with a previous study which has shown that increasing concentrations of cysteine stimulate higher levels of total gingipain enzyme activity⁴²⁶. Notably 50mM of cysteine has been proposed as the highest concentration required for the total activation of gingipains, and this amount was applied here (figure 37). Above this concentration of cysteine, enzyme denaturation may occur resulting in no further activation⁴²⁶. Notably, Chen *et al.* reports that in the absence of cysteine in the lysine gingipain, enzyme stability was maintained at the pH range 5-9 however in the presence of cysteine the activity rapidly decreases⁵²⁵. While cysteine activates gingipain activity the report suggests that cysteine prepares the lysine gingipain

to lose activity rapidly. For this reason, gingipains were used in the absence of cysteine in order to avoid loss of stability of the proteolytic activity during experimental assays.

Additionally, the presence of calcium was shown to be essential for stabilisation of the enzyme at 4°C within a pH range 4.5 to 7.5 whilst in the absence of calcium the activity decreased⁵²⁵. Calcium (5mM) was used in this study in the enzyme buffer when measuring the amidolytic activity, in addition, it was added to the dialysis buffer to eliminate unwanted salts from the purified gingipains from HG66. The physiological level of calcium concentration in GCF of normal adults is reported to be 2.5mM⁵⁶². It is interesting to note that at 37°C the stability of the enzyme is maintained in the presence of calcium as most of the studies performed here were undertaken at this temperature⁵²⁵.

Given the amidolytic activity and molecular weight of cysteine proteases present in W83 and HG66, W83 exhibited increased levels of proteins in the cell-bound form, making further isolation of gingipains from this strain difficult. Notably, isolating cell-bound proteins from Gram-negative bacteria can result in significant LPS contamination from the outer membrane which may hinder the activity of cysteine proteases and this can interfere with downstream analysis.

It was therefore important to remove LPS from cysteine protease preparations especially as previous reports have shown that LPS from *P.gingivalis* has a significant impact on gingival cells and causes elevated inflammatory responses³²⁷. While the LPS contamination used by previous study report 5pg/ml the study here, shows 0.2ng/ml using the same method⁵⁶³. The results in chapter 6 shows that *Pg* LPS induced TNF- α in macrophages only at 1 μ g/ml indicating that LPS contamination had no effect on the macrophages. A key aspect of this study was to analyse whether cysteine proteases in isolation have the ability to inhibit the resolution of inflammation and to test this hypothesis it was therefore necessary to obtain relatively pure preparations of gingipains. For this reason, it was decided that isolation of proteins from HG66 culture supernatant would be preferable for application in downstream studies. Additionally, data obtained here indicate that both amidolytic activity (figure 35) and SDS-PAGE (figure 36) detectable proteins were released from HG66 indicating that this strain represents an appropriate source of extracellular cysteine proteases. Taken together these factors suggested that strain HG66 would be the more appropriate strain for gingipain isolation for use in the subsequent studies which were undertaken as part of this thesis.

4.6.2 Purified gingipain activity from the strain HG66

Affinity chromatography on arginine-Sepharose was preferred over other modes of purification, e.g. anion exchange, as this approach separates enzymes based on selective binding and subsequent elution of intact functioning proteins from the column. Here

arginine was used to elute fractions exhibiting activity for Bz-L-Arg-pNA and lysine was used to elute fractions exhibiting activity for Z-L-Lys-pNA (figure 38). Additionally, NaCl was used as a preliminary elution step to remove other proteins that might be bound non-specifically to the affinity column. The net effect of these sequential elution steps resulted in the isolation of separate fractions containing protein specificity for ARG and LYS. Notably, the yield of the desired enzyme obtained from 1-litre of culture medium was concentrated to ~1.5 ml in the final eluted protein step, generating ~0.5 mg of protein per ml. Additional purification steps might have removed further traces of other proteins however this might also have reduced the overall yield of the enzyme and was therefore not undertaken. Interestingly, Pike *et al.* further purified the gingipain proteins using anion-exchange chromatography to remove lower molecular mass molecules and reported the recovery of gingipain activity as 18% in the final eluted protein ⁴²⁶.

The data presented here show that proteins recovered from the culture medium of strain HG66, purified by gel filtration on Sephadex G-150 followed by affinity chromatography on arginine-Sepharose exhibit relatively high levels of RgpB and Kgp activity (figure 39) as demonstrated by the cleavage of substrates Bz-L-Arg-pNA and Z-L-LYS-pNA specific for Rgp and Kgp, respectively. In order to differentiate between RgpB from RgpA, molecular weight analysis was undertaken using SDS-PAGE. The data presented in figure 40 reveal the presence of 50kDa and 60kDa molecular weight bands indicative of RgpB and Kgp gingipains isolated from the soluble fractions of the culture supernatant of HG66. Though HG66 reported to express RgpA here (figure 36) and elsewhere the activity appeared to be lost on further purification steps ^{94, 185}. These data are in agreement with previous studies demonstrating similar molecular weight profiles ^{426, 525, 526, 532}. RgpA and Kgp have been shown to be the most potent virulence factors of *P.gingivalis* due to their hemagglutinin adhesion domains which enable the organism to colonise periodontal pockets and the gingival sulcus ^{564, 565}. These molecules also enable the organisms to acquire iron from erythrocytes ¹⁷⁷. Notably, inactivation of RgpB has been shown to affect RgpA function via post-translational modification events causing aberrant glycosylation processing of the arginine gingipains ⁵⁶⁶.

Having established appropriate molecular weights for the isolated proteins the presence of cysteine protease activity was confirmed using specific inhibitors (figure 41). These data strongly supported the notion that the isolated proteins were the relevant cysteine proteases sought, i.e. the gingipains. Various inhibitors have been used in previous studies, such as iodoacetamide, E-64, leupeptin, EDTA, p-aminobenzamidine, and all of these agents showed inhibition only for RgpB activity. TLCK was used here as this molecule has been shown to inhibit both of the enzymes, effectively suggesting that many active-cysteine sites might be expressed in the HG66 *P.gingivalis* strain ⁴²⁶. These data

are in agreement with that presented in figure 41, as the addition of TLCK reduced total enzyme activity to 50%, suggesting that the isolated proteins were indeed gingipains, i.e. cysteine proteases. While TLCK inhibited only 50% of cysteine protease activity, the inhibition is not complete indicating that either the presence of active-cysteine groups in the eluted proteases are less reactive to TLCK or different forms of cysteine groups exist. Inhibitors of Papain, superfamily of cysteine proteases show to inhibit only Rgp but not Kgp indicating that active-cysteine residues present in the Kgp were less reactive to depending on the inhibitors ⁴²⁶. Interestingly, the inhibition of both arginine and lysine gingipain by TLCK were also reported to prevent apoptosis in endothelial cells by inactivating caspase-3 enzymes ⁵⁶⁷. Additionally, TLCK was shown to inhibit the cleavage of CD99 on RgpA or Kgp-treated human umbilical vein endothelial cells ²⁰⁴.

The final confirmatory test used to identify the presence of gingipains from the isolated fractions from the *P.gingivalis* strain HG66 used here was mass spectrometry following in-gel digestion of the purified proteins. Data confirmed that both RgpB and KgpA were present within the isolated bands as they exhibited the highest identification score of cross correlation (XCorr>1000) (Table 7). This outcome was regarded as being definitive proof that the most abundant proteins within the bands were identified as gingipains, with coverage for the presence of both RgpB and Kgp being 28 %.

Interestingly, the presence of the major fimbrium subunit FimC and peptidylarginine deiminase enzyme activity were also observed in the Mass Spectrometry analysis (identification scores of XCorr <500 (table 7). Their role reported in the literature has been in mediating bacterial and host interactions as well as protein citrullination production which may be involved in rheumatoid arthritis pathogenesis. Hence they may also play a role in any downstream effects detected when studying the final eluted proteins ^{568, 569}. Furthermore, the analysis of the gel bands for protein identification also reported the presence of serine hydroxymethyltransferase, phosphoenolpyruvate carboxykinase, hydroxylamine reductase and other outer membrane proteins, albeit at very low amounts. Combined, these results confirm that the proteins isolated by gel filtration and affinity chromatography were enriched for cysteine proteases identified as gingipains specific for ARG and LYS amino acids.

4.7 Conclusion

Gingipains have been identified as principal components of the proteolytic enzymes produced by *P.gingivalis* and have been widely studied for their direct involvement in periodontal tissue destruction and modulation of host immune responses. Reportedly they may also play causative roles in other chronic inflammatory diseases associated with PD such as rheumatoid arthritis. Given the potential importance of gingipains in disease

pathogenesis, it is necessary to isolate them relatively purely to enable mechanistic studies, such as in determining their involvement in AC clearance. Indeed, while many studies have analysed the impact of *P.gingivalis* on phagocytic immune cells such as on NØ, monocytes, and MØ few studies have thus far reported on the effects of gingipains on AC clearance. Subsequently, the gingipains purified here can be analysed for their involvement in triggering inflammatory mediators, affecting chemotaxis and inflammation resolution. Outcomes from these studies might aid our understanding of the pathophysiology of periodontal diseases and their link to other systemic diseases.

Chapter 5

Result 3: Gingipain selectively cleaves CD14 leading to MØ hypo-responsiveness towards AC

5.1 Introduction

For phagocytes to discriminate a viable cell from an AC, the presence of specific AC ligands that are bound by MØ receptors are required in order to decide whether they have to be eaten by professional phagocytes or left to perform cellular functions in the biological system⁵⁷⁰. The discovery of phospholipid asymmetry and translocation from the inner leaflet to the outer leaflet of the plasma membrane is one of the early cell surface modulations undertaken by a dying cell. This translocation of phospholipids in AC guides the phagocytes to recognise and engulf them thereby preventing the activation of the adaptive immune system^{510, 571, 572}. AC clearance receptors are therefore critical players in innate immunity as they aid in the uptake of AC, which is a non-inflammatory process and results in resolution of inflammation and promotion of wound healing³³⁶.

This study addresses how *P. gingivalis* gingipains interferes with the host immune system by modifying AC clearance receptors on MØ and thereby reducing MØ uptake of dying cells. The first step in disturbing tissue homeostasis is to cleave essential receptors specific for the 'tether and tickle' mechanism of AC clearance^{280, 479}. A wide range of receptors (Table 8) has been suggested to be involved in the clearance of dying cells, acting either directly or through bridging molecules recognised by the phagocytes.

In addition to the receptors discussed, factors such as pro-resolving lipid mediators, nucleotides, fractalkine (CX3CL1), tRNA synthetases and ribosome components are also said to participate in mediating the clearance of dying or dead cells^{460, 573, 574}. The clearance of apoptotic NØ has been widely studied due to their role in infection and causing chronic inflammatory diseases^{21, 471, 575, 576}. Here, the study address how AC NØ are cleared by gingipain-treated MØ when exposed to periodontal pathogens. **Hence, the aim of this chapter was to analyse whether gingipains inhibit the clearance of AC by modifying MØ migration towards dying cells and reducing their interaction with primary AC NØ and whether this is dependent on specific AC receptors present on MØ.**

Receptors	References
Phosphatidylserine receptors	510, 577, 578
Class A scavenger receptor	514, 579
CD14	324, 325, 418
CD31	337, 580
CD47	339, 581, 582
CD91	300, 301
CD68	583, 584
$\alpha_v\beta_5$ and $\alpha_v\beta_3$	585-587
ATP-binding cassette transporter 1	588, 589
Complement receptors	40, 590

Table 8: List of receptors that participate in AC clearance

The above-listed receptors present on the surface of phagocytes have been suggested to act as bridging molecules important in the uptake and phagocytosis of dying cells.

5.2 Gingipains fail to induce apoptosis in primary NØ and THP-1 MØ

Apoptosis is prevalent in periodontal tissues and in the gingival sites infected with complex polymicrobial organisms¹⁰⁷. Upon constant exposure to bacterial biofilm, inflammation is induced causing bleeding and, in advanced stages of disease, alveolar bone destruction⁵⁹¹⁻⁵⁹⁴. AC death within the inflamed periodontal tissue contributes to the inflammatory environment either by modulating phagocyte function or by inhibiting their cell death resulting in the perpetuation of the chronic inflammatory lesion and frustrated healing⁵⁹⁵.

To check whether *P.gingivalis* gingipains influence apoptosis in phagocytes (MØ and NØ), THP-1 MØ were exposed to either RgpB or Kgp for 1h at 37°C. One hour incubation was chosen as most of the experiments performed in this study utilised phagocytes (THP-1 differentiated MØ) that were pre-treated with protease for 1h prior to the analysis of phagocyte function. E.g. in recognition and interaction with AC. Consequently, cell viability studies were performed in either MØ (Figure 42 & 43) or primary human NØ (Figure 44 & 45). The phagocytes were exposed to gingipains prior to assessment of cell death with annexin V FITC (to determine apoptotic death) and PI (to measure cell necrosis) using flow cytometry. The results for gingipain-treated THP-1 MØ are shown in figure 42.

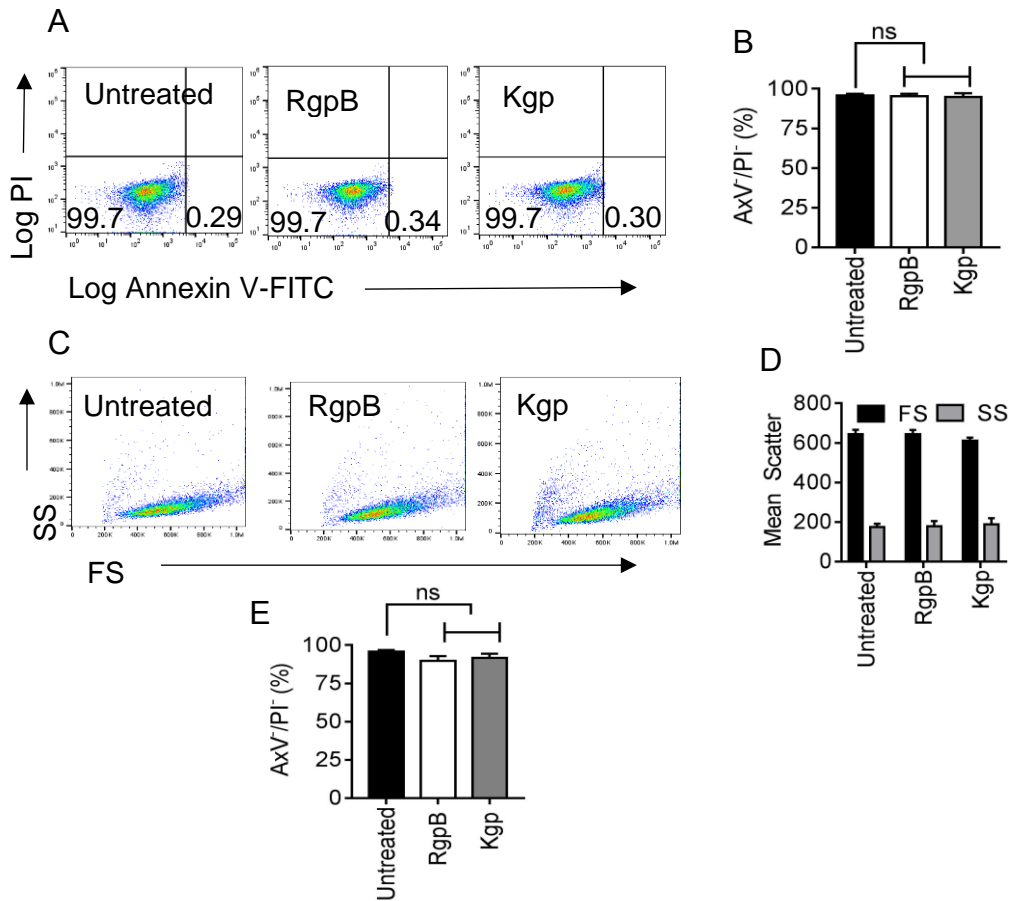


Figure 42: Measurement of cell viability, size, and granularity of gingipain-treated THP-1 MØ

THP-1 VD3 differentiated MØ were treated with RgpB or Kgp (5µg/ml) (as described in section 2.7.11) or left untreated for 1 h or 16 h at 37°C. Untreated or treated MØ were washed and stained with annexin V FITC or PI to assess cell viability using flow cytometry (as described in section 2.5.3.1). A) Flow cytometry plots showing MØ stained for annexin V FITC and PI to reveal the viability of cells following 1h treatment. B) Histogram showing percentage of cells negative for annexin V (i.e.viable) stain in 1h treatment. C) Flow cytometry plots showing forward (FS) and side (SS) scatter of MØ to reveal the size and granularity of cells following 1h treatment. D) Histogram showing the mean of forward and side scatter for untreated and treated MØ following 1h. E) Histogram showing percentage of cells negative for annexin V (i.e. positive for viable) stain following 16h treatment. Data shown are mean ± SEM for three independent experiments. Statistical analysis was conducted using ANOVA followed by Dunnett’s post-test: no significant (ns) differences were noted between treated and untreated cell. Data shown in A and C are representative whilst data shown in B, D and E are mean ± SEM of three independent experiments.

As shown in figure 42, MØ remain negative for annexin V and propidium iodide (i.e. viable – figure 42 A&B) following gingipain treatment indicating that gingipains do not induce apoptosis within one hour of treatment. Size and granularity were also measured (forward scatter and side scatter respectively) using flow cytometry. Untreated MØ, show large cells with low granularity (figure 42C) as revealed by high forward scatter and low side scatter. Gingipain-treated MØ remain similar to untreated MØ based on their size and granularity (figure 42 C&D). MØ were also incubated with gingipains for extended time

periods and checked for viability using AxV and PI after 16h (figure 42E). The data figure 42E shows that gingipains do not induce apoptosis with longer incubation times on MØ.

To confirm this finding using alternative method, nuclear morphology of untreated or 1h gingipain (RgpB or Kgp) treated THP-1 VD3 stimulated MØ were assessed by confocal microscopy following cell nuclear staining with acridine orange (10µg/ml). The results are shown in figure 43.

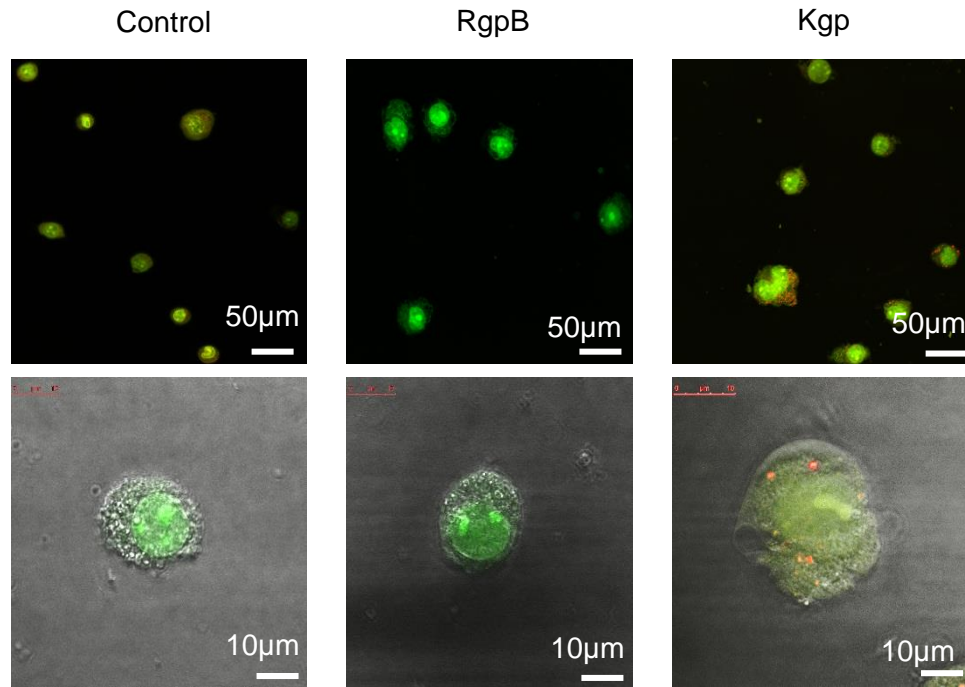


Figure 43: Confocal analysis of cell and nuclear morphology of gingipain-treated MØ

THP-1 VD3 MØ were either treated with RgpB or Kgp (5µg/ml) (as described in section 2.7.11) or left untreated (control) for 1h or 12h at 37°C. Cells were washed with PBS and stained with acridine orange (10µg/ml) (as described in section 2.5.3.2) and observed using confocal microscopy to detect nuclear changes in the MØ. Top panel shows the microscopic image of untreated or gingipain-treated MØ for 1h with the fluorescence stain (scale bar 50µm). Below panel shows the microscopic image of untreated or gingipain-treated MØ for 12h with the fluorescence stain (scale bar 10µm). Data shown are representative of three independent experiments.

Careful analysis to detect any nuclear changes in the gingipain-treated cells revealed that cells remained healthy and viable exhibiting intact cell membranes and nuclei with all nuclei emitting a similar pattern of green fluorescence indicating that gingipain treatment of cells does not alter the morphology of MØ (figure 43).

NØ are the most recruited immune cells in patients with PD and have been widely studied for their pathogenic role in causing advanced lesions in humans^{351, 435, 596-598}. With a short life span, NØ are classically characterised as phagocytic cells contributing to the inflammation induced by extracellular pathogens by producing antimicrobial mediators leading to acute inflammation and NØ death promotes the resolution of this acute

inflammation^{33, 599, 600}. However, in PD if the response of NØ to biofilm formation in the subgingival microorganism-infected regions is either prolonged or the resolution inhibited, the NØ may cause extended local inflammatory response triggering amplification of inflammation leading to chronic diseases^{191, 601, 602}. Delayed NØ apoptosis has been reported in chronic periodontitis patients, which is linked with disturbance of the extrinsic apoptotic pathway contributing to systemic inflammation¹⁹⁰. Additionally, increased GM-CSF and TNF- α in the gingival tissue of adult periodontitis patients are reported to inhibit NØ apoptosis by modulating BAX expression¹⁹⁰. Here, NØ viability was observed after treating cells with purified gingipains to assess the impact of NØ viability. NØ were treated with either RgpB or Kgp, for 1h at 37°C and stained with annexin V FITC (figure 44) for PS exposure and PI for nuclear morphology. The results are shown in figure 44 and 45.

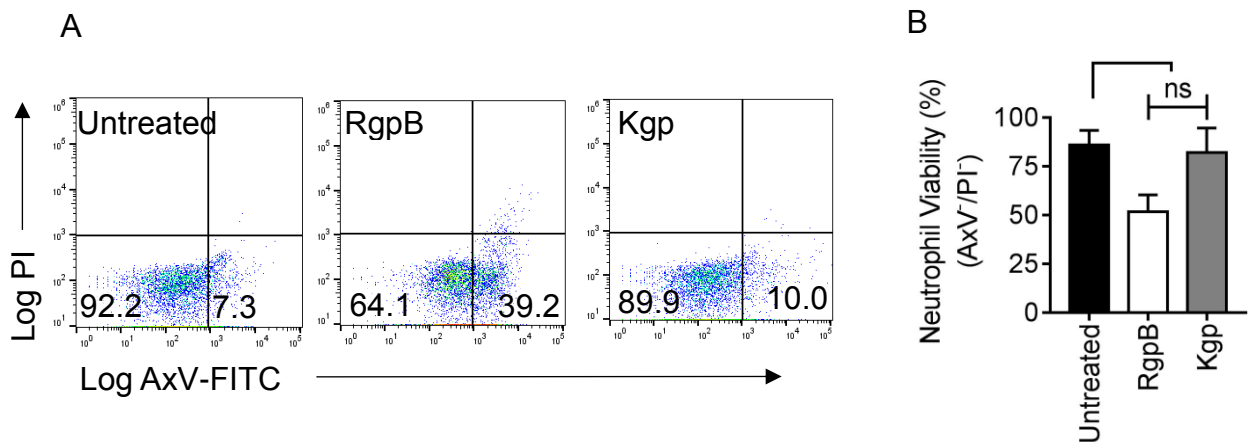


Figure 44: Measurement of cell viability, size, and granularity of gingipain-treated primary NØ

Primary NØ were treated with RgpB or Kgp (5 μ g/ml) or untreated for 1h at 37°C (as described in section 2.7.11). Untreated or treated NØ were washed and stained with annexin V FITC or PI to assess cell viability using flow cytometry (as described in section 2.5.3.1). A) Flow cytometry plots showing NØ stained for annexin V FITC and PI to reveal the viability of cells. Data shown are representative of three independent experiments B) Histogram showing percentage of cells negative for annexin V (i.e. positive for viable) stain. Data shown are mean \pm SEM for three independent experiments Statistical analysis was conducted using ANOVA followed by Dunnetts post-test: ns- not-significant compared to untreated.

The data in figure 44 shows that similar to THP-1 MØ, NØ maintained their viability after 1h treatment with either of the gingipains incubated at 37°C. Though Kgp-treated MØ cells remained negative for both annexin V and propidium iodide, RgpB treatment however, showed a trend with a shift of cells staining positive for annexin V (i.e. apoptotic) compared to untreated NØ (Figure 44A). However, no significant difference was observed in RgpB-treated NØ compared to untreated NØ.

To further support this work, nuclear morphology (figure 45) of untreated or 1h gingipain (RgpB or Kgp)-treated primary NØ was assessed by confocal microscopy following staining of cells with DAPI (100ng/ml). The results are shown in figure 45.

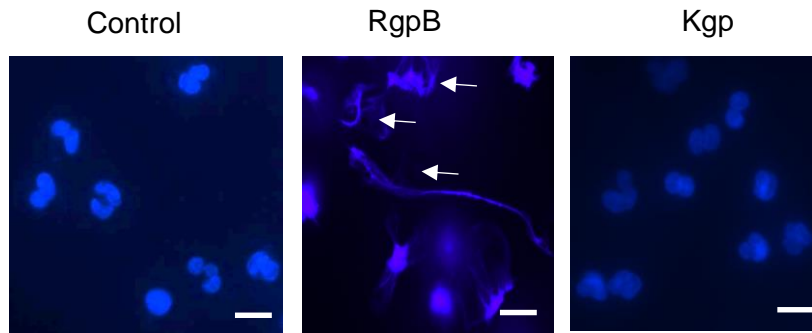


Figure 45: Fluorescent images of gingipain-treated primary NØ

Primary NØ were either treated with RgpB or Kgp (5µg/ml) (as described in section 2.7.11) or left untreated for 1h at 37°C. Cells were washed with PBS and stained with DAPI (as described in section 2.4.4.3) and observed using fluorescent microscopy to detect nuclear changes in the NØ. The microscopic image shows untreated or gingipain-treated NØ with the fluorescence stain (scale bar 50µm). Arrow indicates the formation of NETs in RgpB treated NØ. Data shown are representative of three independent experiments.

The data in figure 45 shows representative fluorescent images of DAPI stained NØ either treated with gingipains or left untreated for 1h at 37°C in a sfRPMI medium with 0.15%BSA (control). RgpB treated cells appear to show the formation of NETs following gingipain-treatment whereas Kgp treatment does not appear to induce NETs formation. Nevertheless, viable nuclei were noticeable in Kgp-treated NØ, similar to untreated NØ. Compared to untreated NØ, RgpB-treated NØ lacked prominent shaped nuclei in order to produce NETs.

5.3 Gingipain cleaves CD14, an AC clearance receptor

CD14, is an important innate immune receptor expressed as a membrane-associated CD14 (mCD14) and soluble form (sCD14). mCD14 is a protein anchored glycosylphosphatidylinositol (GPI) and is highly-expressed on differentiation of circulating monocytes to mature MØ^{328, 603}. sCD14 is synthesised either from the intracellular pools or via proteolysis of mCD14⁶⁰⁴. Both forms of CD14 mediate responses to LPS, from Gram-negative bacteria and can initiate shock^{143, 604, 605}. Traditionally, the mCD14 receptor was considered as an LPS receptor. LPS-LBP complexes induce immune responses by transferring LPS monomers to cell surface receptors such as CD14 and TLRs¹⁴². Conversely, cells that lack mCD14 such as endothelial and epithelial cells use sCD14 to respond to LPS by binding to additional surface receptors (e.g. integrin) to generate inflammatory responses in the host¹⁴¹.

Preliminary experiments were conducted to assess if *P.gingivalis* LPS stimulation of THP-1 differentiated MØ leads to loss of CD14 through shedding. Initial experiments involved two models of THP-1 monocytes i) THP-1 VD3 MØ or ii) THP-1 DS MØ for 48h. These models were used to determine cell viability (using Annexin V-FITC and PI) and CD14 expression using immunofluorescence and flow cytometry following LPS-stimulation (1h at 37°C). The results are shown in figure 46. Earlier experiments show that VD3 stimulated MØ expressed higher CD14 levels compared to DS MØ (figure 19). However, CD14 expression on DS MØ was detected also. They responded strongly to LPS producing increased cytokine levels³⁶ and also in future experiments (chapter 6).

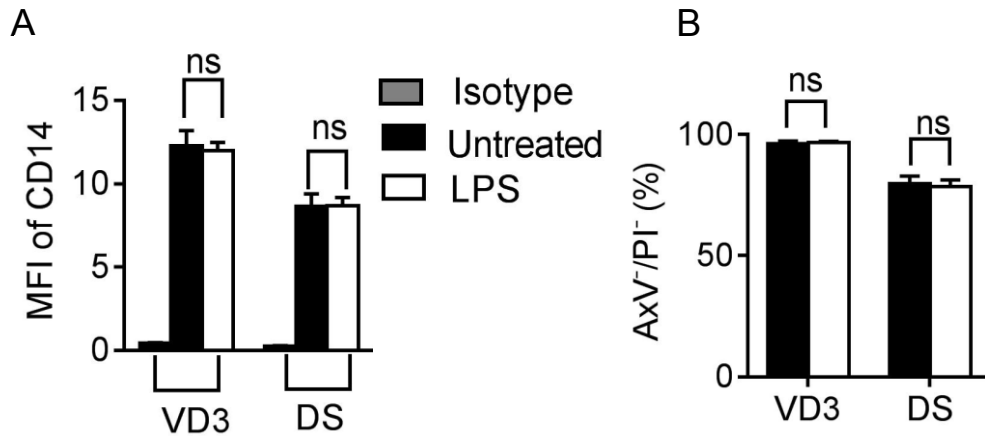


Figure 46: Quantification of CD14 expression on *P.gingivalis* LPS treated THP-1 MØ THP-1 cells were differentiated either with VD3 or DS for 48h at 37°C. MØ were either treated with LPS from *P.gingivalis* or untreated for 1h at 37°C. Cells were stained with mouse anti-human CD14 mAb 63D3 and analysed using flow cytometry. A) Histogram showing MFI of CD14 expression on differentiated MØ (VD3 and DS). B) Histogram showing percentage of cells negative for annexin V staining (i.e. viable cells). Data shown are mean \pm SEM for three independent experiments. Statistical analysis was conducted using ANOVA followed by Dunnett's post-test: no statistical significance (ns) was noted in CD14 expression after LPS treatment.

The results shown in figure 46 demonstrate that, following LPS stimulation, there was no reduction in CD14 receptor expression in either of the MØ models used (VD3 alone or DS). In addition, cells stained negative for Annexin V indicates cell viability (Figure 46B) compared to untreated MØ. These data indicate that CD14 receptor levels and cell viability are unaffected by LPS treatment.

Having observed that LPS stimulation of THP-1 MØ does not reduce levels of CD14 expression, MØ expression of CD14 following treatment with purified gingipains was assessed. The results are shown in figure 47.

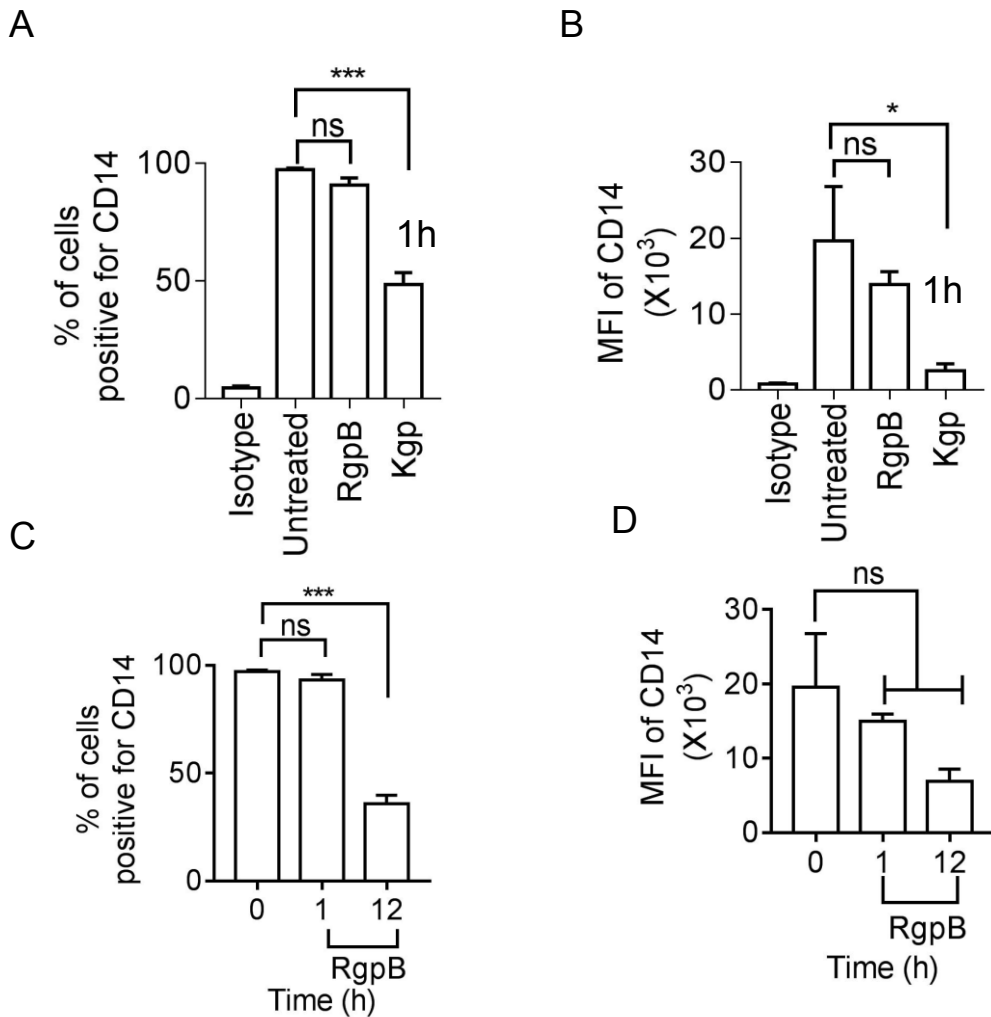


Figure 47: CD14 surface expression on THP-1 MØ treated with gingipains

THP-1 VD3 MØ were treated 5µg/ml with Kgp for 1h or with RgpB with 12h (as described in section 2.7.11) or untreated at 37°C prior to indirect immunofluorescence staining for CD14 using the the established mAb 63D3 and flow cytometry (as described in section 2.3.6.1). A) Histogram showing the percentage of cells positive for CD14 expression and B) MFI after 1h of either RgpB or Kgp treatment. C) Histogram showing the percentage of cells positive for CD14 expression at various time points 0, 1, 12h and D) their MFI after 1h of RgpB treatment. Flow data shown are collected from at least 10000 events. Data presented are mean ± SEM of at least three independent experiments. Statistical analysis was performed using ANOVA followed by Dunnett's post-test. * $P < 0.05$, *** $P < 0.001$, not significant (ns) compared with untreated cells.

The flow cytometry-based analyses (figure 47) confirm a significant decrease ($P < 0.001$) in CD14 receptor levels on VD3 stimulated MØ treated with Kgp, but not Rgp, compared to untreated cells in 1h treatment at 37°C. These data suggest that Kgp treatment of MØ decreases CD14 expression detected either as percentage of cell positive for CD14 (figure 47A) or MFI of CD14 expression on all cells (figure 47B). RgpB treated cells do not appear to show reduced CD14 expression after 1h of treatment (figure 47A & B). However, an extended treatment of MØ with RgpB causes a slower decrease in CD14 expression

at 12h compared to untreated (figure 47C, D), with reduced percentage of cells positive for CD14 and a trend towards reduced MFI (i.e. CD14 levels per cell).

Previous studies show that CD14 expression on human monocytes differs greatly from that on NØ. Monocytes have approximately 45,000 – 110,000 CD14 surface receptors per cell as compared to NØ which express significantly lower levels, estimated to be below 5000 receptors per cell^{304, 305, 501, 606, 607}. In a manner similar to that seen in MØ, NØ CD14 mediates binding of LPS through LBP forming a complex that triggers the innate immune inflammatory responses in humans³⁰⁵. Given the ability of gingipains RgpB and Kgp to reduce CD14, most likely by cleaving CD14 receptor from MØ cells, the CD14 expression on gingipain-treated primary NØ was also studied. The results are shown in figure 48.

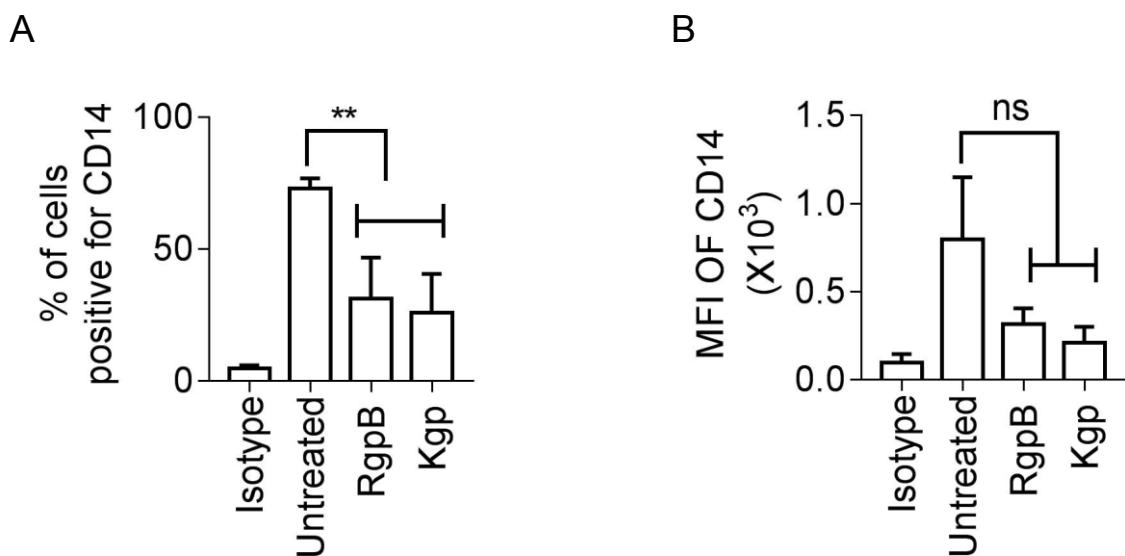


Figure 48: CD14 surface expression on primary NØ treated with gingipains

Primary human NØ were treated with either RgpB or Kgp (5µg/ml) (as described in section 2.7.11) or untreated for 1h at 37°C prior to indirect immunofluorescence staining for anti-CD14 using established mAb 63D3 using flow cytometry (as described in section 2.3.6.1). A) Histogram showing the percentage of cells positive for CD14 expression and B) mean fluorescence intensity (MFI). Data presented are mean ± SEM of three independent experiments. Statistical analysis was performed using ANOVA followed by a Dunnett's post-test. ** $P < 0.01$, not significant (ns) compared with untreated cells.

The data reveal that NØ express relatively low CD14 (figure 48B) compared to MØ (figure 47B). The data also reveal that both RgpB and Kgp cleave CD14 from the surface of primary NØ compared to untreated cells (figure 48). A significant effect of gingipain treatment ($P < 0.01$) can be observed in the percentage of NØ expressing CD14 with NØ treated with either of the gingipains compared to untreated cells. However, no significant effect was observed in the MFI of the untreated and treated NØ.

5.4 TLCK inhibits CD14 cleavage in THP-1 MØ

To assess whether the reduction in MØ CD14 noted above was due to cleavage by gingipains, TLCK, a cysteine protease inhibitor, was used. MØ were stained for CD14 expression following Kgp treatment in the presence or absence of TLCK and cell surface receptor expression was determined by immunofluorescence staining and flow cytometry. The results are shown in figure 49.

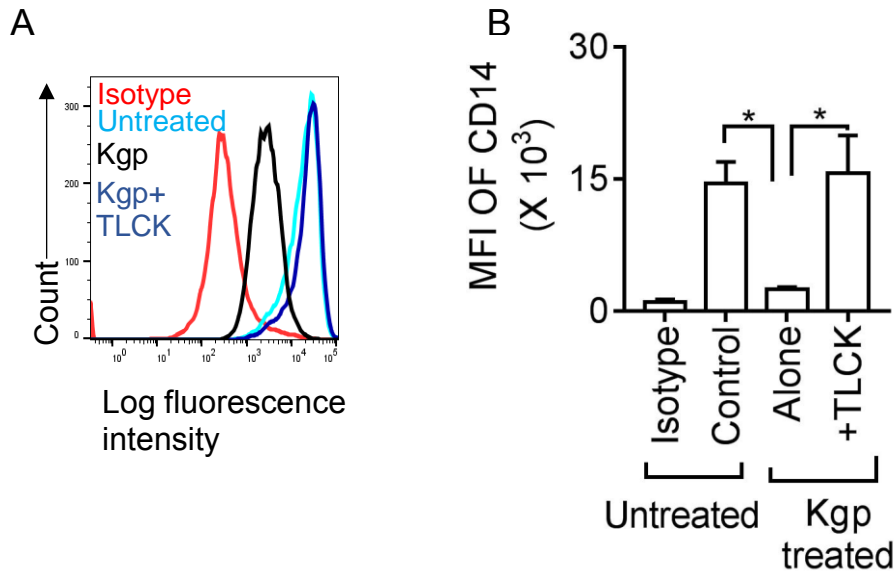


Figure 49: TLCK inhibits CD14 reduction on Kgp gingipain-treated THP-1 MØ

THP-1 VD3 MØ were treated with Kgp (5µg/ml) (as described in section 2.7.11) in the presence or absence of TLCK, cysteine inhibitor (as described in section 2.7.12) or left untreated for 1h at 37°C. Treated or untreated MØ were studied by indirect immunofluorescence staining with anti-CD14 and analysed using flow cytometry (as described in section 2.3.6.1). A) Representative overlay plots showing CD14 expression on MØ either untreated (light blue) or Kgp-treated for 1h (black) or Kgp and TLCK-treated for 1h (dark blue) and MØ stained with MOPC21 isotype negative control (red). B) Histogram showing MFI for the anti-CD14 stained cells. Data shown are mean ± SEM of three independent experiments. Statistical analysis was performed using ANOVA followed by a Bonferroni post-test (* $P < 0.05$). Data shown in A and B are representative.

The MFI extracted from the flow cytometric plots (figure 49A) suggests that CD14 expression was preserved on MØ treated with Kgp in the presence of the TLCK (figure 49B). Whereas compared to untreated cells, Kgp-treated MØ without TLCK treatment exhibited a rapid decrease ($P < 0.05$) in CD14 expression (figure 49B) in line with previous experiments (figure 48).

5.5 Expression of AC clearance receptors on gingipain-treated THP-1 MØ and primary NØ

Emerging research suggests that a wide range of receptors participate in the clearance of dying cells^{35, 608, 609}. The extracellular matrix glycoprotein, thrombospondin-1 (TSP-1) synthesized by both MØ and NØ binds to mediator $\alpha_v\beta_3$ integrin to form a complex with

MØ CD36 to clear AC ²⁹⁴. Additionally, calreticulin, an endoplasmic reticulum protein which is highly expressed on AC, signals to phagocytes to uptake dying cells using CD91 and involving other mediators such as collectins and low-density lipoprotein receptor-related protein present on phagocytic cells ^{275, 300}. Additionally, ICAM-3, another well-described ligand facilitates MØ migration to AC and binding to phagocytes ^{37, 281, 384}. These important receptors and ligands were studied for their expression on gingipain-treated phagocytic cells to assess whether their expression was altered in response to the proteases from *P. gingivalis*. The results are shown in figure 50. Alterations in expression of these receptors may affect AC clearance.

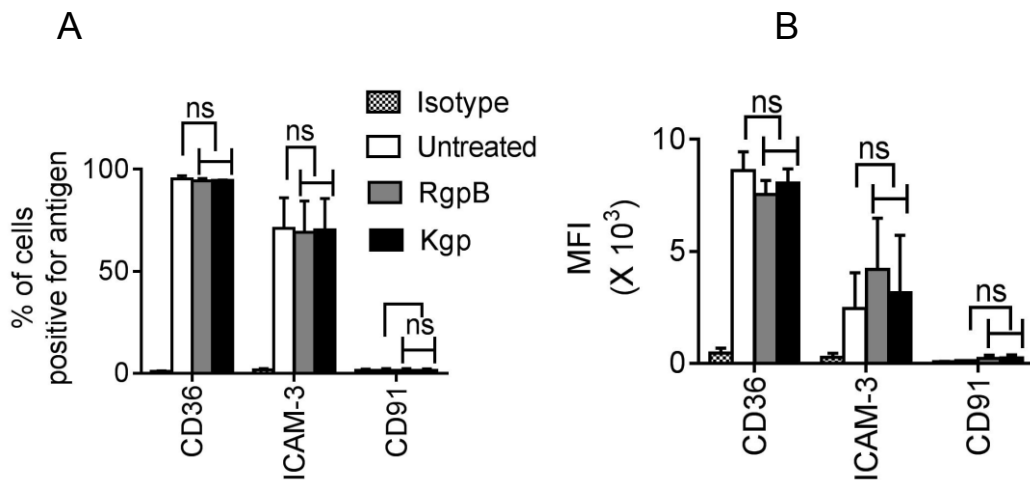


Figure 50: Gingipain treatment of MØ does not alter the expression of CD36, ICAM-3 or CD91

THP-1 MØ (VD3 or DS) were incubated with RgpB or Kgp for 1h (as described in section 2.7.11) at 37°C and stained with antibody to the indicated antigen (CD36, ICAM-3 or CD91) followed by secondary antibody FITC/PE and analysed using flow cytometry to determine receptor expression (as described in section 2.3.6.1 and 2.3.6.2). Data shown are A) percentage of cells positive for antigen and B) their MFI. Data presented are mean \pm SEM of three independent experiments. Statistical analysis was performed using ANOVA followed by Dunnett's post-test; no significant difference in antigen expression was noted with gingipain treatment.

The results in figure 50 suggest 1h treatment of gingipain (RgpB or Kgp) on THP-1 MØ fails to reduce significantly the percentage of cells expressing CD36, ICAM-3 or CD91 compared to untreated cells. Additionally, the MFI measure (figure 50B) shows that CD91 was expressed at low levels, ICAM-3 showed moderate expression compared to CD36 with the highest expression on MØ.

These receptor and ligand molecules were also studied for their expression on gingipain-treated human NØ to assess for the modulation of receptors in response to the proteases from *P.gingivalis*. The results are shown in figure 51.

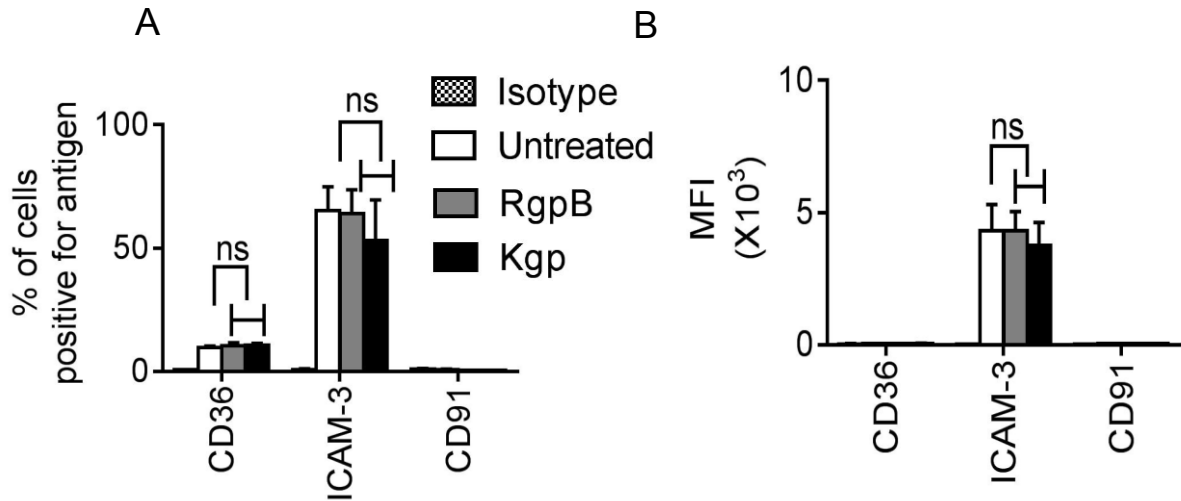


Figure 51: Gingipain treatment of primary NØ does not alter the expression of CD36, ICAM-3 or CD91

Primary NØ were incubated with RgpB or Kgp (5µg/ml) for 1h at 37°C (as described in section 2.7.11) and stained with antibody to the indicated antigen (CD36, ICAM-3 or CD91) followed by secondary antibody FITC/PE and analysed using flow cytometry to determine receptor expression (as described in section 2.3.6.1 and 2.3.6.2). Data shown is A) percentage of cells positive for antigen and their B) MFI respectively. Data presented are mean ± SEM of three independent experiments. Statistical analysis was performed using ANOVA followed by Dunnett's post-test; no significant difference in antigen expression was noted with gingipain treatment.

These studies with primary human NØ, suggest higher ICAM-3 expression compared to CD36, CD91 appeared poorly expressed with only weak fluorescence on primary NØ (figure 51B). However similar to THP-1 MØ, no cleavage of receptors was observed on gingipain-treated NØ compared to untreated cells.

To prevent uptake by phagocytes, viable cells use 'don't eat me' signals in order to avoid ingestion by phagocytes. CD31 (PECAM-1), is one such signal vital for leukocyte motility and cell-cell adhesion molecule. However due to inactivation of CD31 'don't eat me' signals on AC, CD31 initiates binding of AC to phagocytes and phagocytosis³³⁸. To assess gingipains' ability to cleave the CD31, MØ were treated with either RgpB or Kgp for 1h or 16h at 37°C and assessed for cell surface receptor using anti- CD31 and analysed via flow cytometry. The results are shown in figure 52.

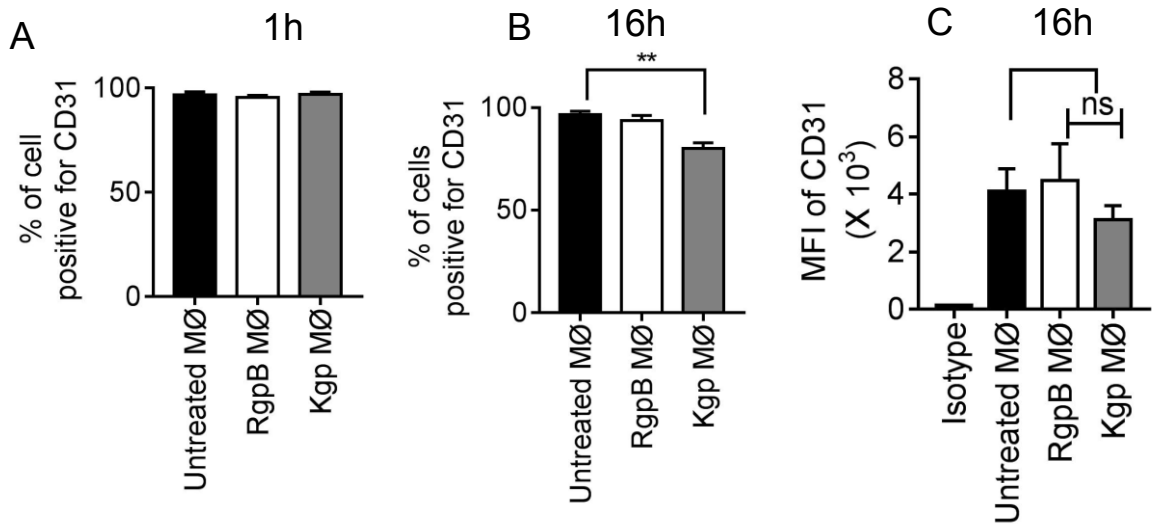


Figure 52: CD31 expression on gingipain-treated THP-1 MØ at various time points
 THP-1 VD3 MØ were incubated with RgpB or Kgp (5µg/ml) for 1h (as described in section 2.7.11) or 16 h at 37°C and stained with anti- CD31 and analysed by flow cytometry for cells positive for receptor expression (as described in section 2.3.6.2). Data shown is A) The percentage of cells positive for CD31 at 1h incubation B) The percentage of cells positive for CD31 at 16 h incubation. C) MFI for CD31 at 16 h. Data presented are mean ± SEM of three independent experiments. Statistical analysis was performed using ANOVA followed by a Dunnetts post-test; ** $P < 0.01$ compared with untreated cells.

The results in figure 52 suggest that RgpB fails to cleave CD31 on MØ even with extended time incubation. However, Kgp reduces CD31 expression only following 16h incubation (figure 52B) though no significant difference was observed in the MFI (figure 52C).

An identical approach was taken to study the effect of gingipains on another 'don't eat me' signal, CD47 is also expressed on viable cells to prevent uptake by phagocytes. CD47 is an integrin-associated protein and is a receptor for SIRPα, expressed mainly on phagocytes such as MØ and dendritic cells⁵⁸⁵. AC lose CD47 during the process of programmed cell death. Viable cells losing CD47 are unable to serve as a ligand for SIRPα leading to reduction of tyrosine phosphorylation of SHP-1 allowing the phagocytes to remove AC by engulfment^{16, 275, 341}. To assess gingipains' ability to cleave the CD47, THP-1 differentiated MØ were treated with gingipains (RgpB or Kgp) for 1h at 37°C and assessed for cell surface receptor using anti-CD47 and analysed via flow cytometry. The results are shown in figure 53.

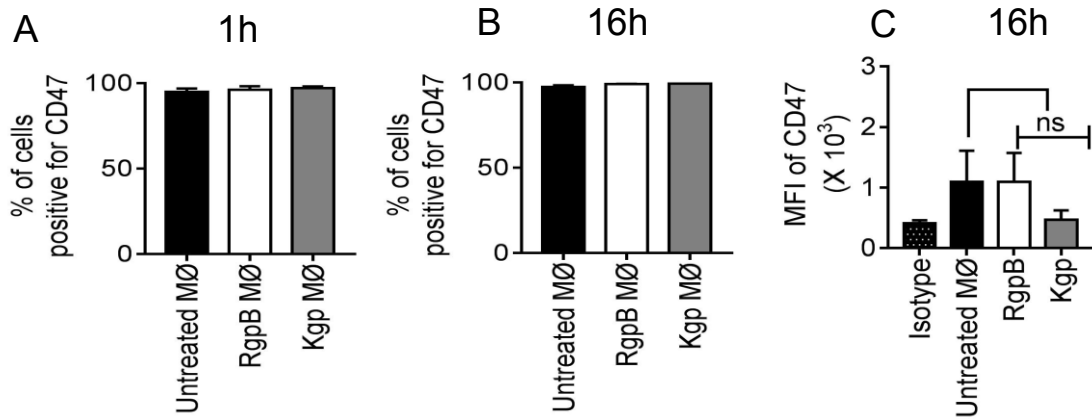


Figure 53: CD47 expression on gingipain-treated THP-1 MØ at various time points

THP-1 VD3 MØ were incubated with RgpB or Kgp (5µg/ml) for 1h (as described in section 2.7.11) or 16 h at 37°C and stained with anti-CD47 and analysed by flow cytometry for cells positive for receptor expression. Data shown is A) The percentage of cells positive for CD47 at 1h incubation B) The percentage of cells positive for CD47 at 16h incubation. C) MFI for CD47 at 16h incubation. Data presented is mean ± SEM of three independent experiments. Statistical analysis was performed using ANOVA followed by a Dunnett's post-test; no significant differences were noted compared with untreated MØ.

The results in figure 53 reveal that viable MØ express CD47 and no reduction in the CD47 receptor is observed after treatment with gingipains (either RgpB or Kgp) even at extended time points (16h) (figure 53B & C). Previous work has found that LPS from *P.gingivalis* induce enhanced production of TSP-1 on THP-1 cells⁶¹⁰. TSP-1 has shown earlier to interact with CD47 on MØ inducing osteoclastogenesis and bone resorption via an unknown mechanism thereby modulating the inflammatory responses resulting in damage of alveolar bone in periodontitis patients⁶¹¹.

CD31 is reported to bind homotypically i.e. CD31 on MØ binding to CD31 on AC. AC NØ have been shown to exhibit reduced CD31 in order to differentiate them from viable NØ and to allow this phagocytosis by MØ³³⁸. In order to assess if CD31 levels may be altered on viable and AC NØ, and in response to gingipains, flow cytometry was used. The level of CD31 expression was analysed in viable and AC NØ in addition to gingipain-treated NØ for 1h at 37°C and assessed for cell surface receptor using anti- CD31 and analysed via flow cytometry. The results are shown in figure 54.

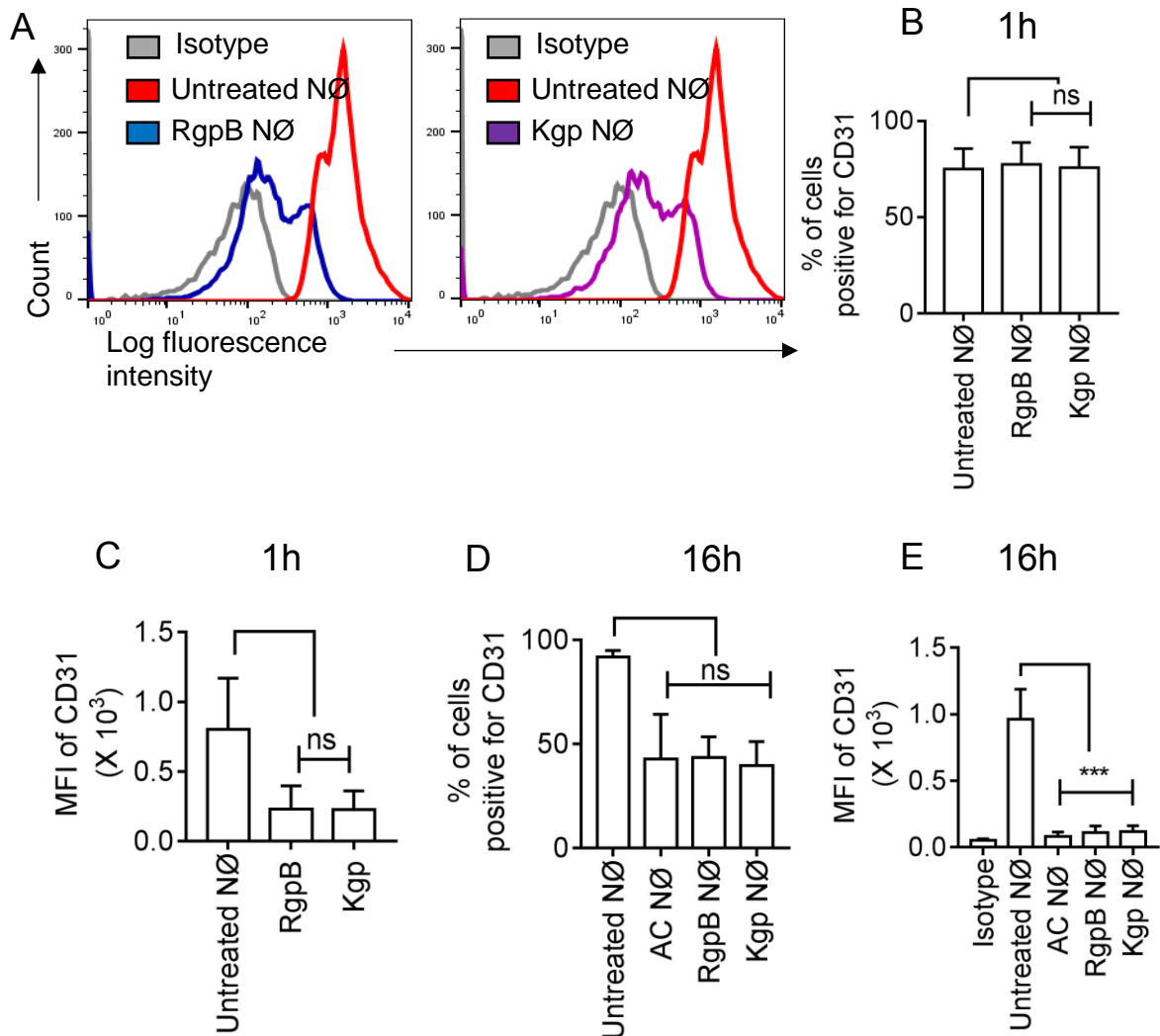


Figure 54: CD31 expression on gingipain-treated primary viable and AC NØ treatment at different time points

Human viable NØ were incubated either with RgpB or Kgp (5µg/ml) for 1h or 16h at 37°C (as described in section 2.7.11) or allowed to undergo spontaneous apoptosis for 16h at 37°C (as described in section 2.5.1.2), NØ were stained with anti-CD31 and analysed by flow cytometry for CD31 expression. Data shown is A) Representative flow cytometric plots of NØ stained for anti-CD31 detected using indirect immunofluorescence, showing overlay plots of CD31 surface expression for untreated viable NØ (red) or RgpB treated NØ (blue) or Kgp-treated NØ (purple) at 16h and their matched isotype control (grey). B) The percentage of cells positive for CD31 at 1h incubation C) MFI of CD31 at 1h time point. D) The percentage of cells positive for CD31 at 16h incubation E) MFI of CD31 at the 16h time point. Data shown are representative of three independent experiments for (A) and mean ± SEM of three independent experiments for (B, C, D, and E). Statistical analysis was performed using ANOVA followed by a Dunnett's post-test. *** $P < 0.001$ or not significant (ns) compared with untreated viable NØ (control).

The flow cytometric plots in figure 54 reveal that untreated viable NØ express a higher level of CD31 on their surface (figure 54A- red line) compared to RgpB (figure 54A- blue line) or Kgp-treated NØ at 16h (figure 54A- violet line). No significant difference was observed in the percentage of viable NØ positive for CD31 (figure 54B) or their MFI (figure

54C) following gingipain treatment despite a trend of reduced CD31, compared to untreated NØ at 1h and 16h (figure 54D). However, the MFI of CD31 of spontaneous AC NØ and gingipain-treated NØ after 16h exhibited a tremendous reduction compared to untreated viable NØ (figure 54E).

Another inhibitor for 'eat me' receptors, CD47 was also analysed in viable and AC NØ and gingipain-treated NØ for 1h at 37°C. The resulting cells were assessed for CD47 cell surface receptor levels using anti- CD47 using flow cytometry. The results are shown in figure 55.

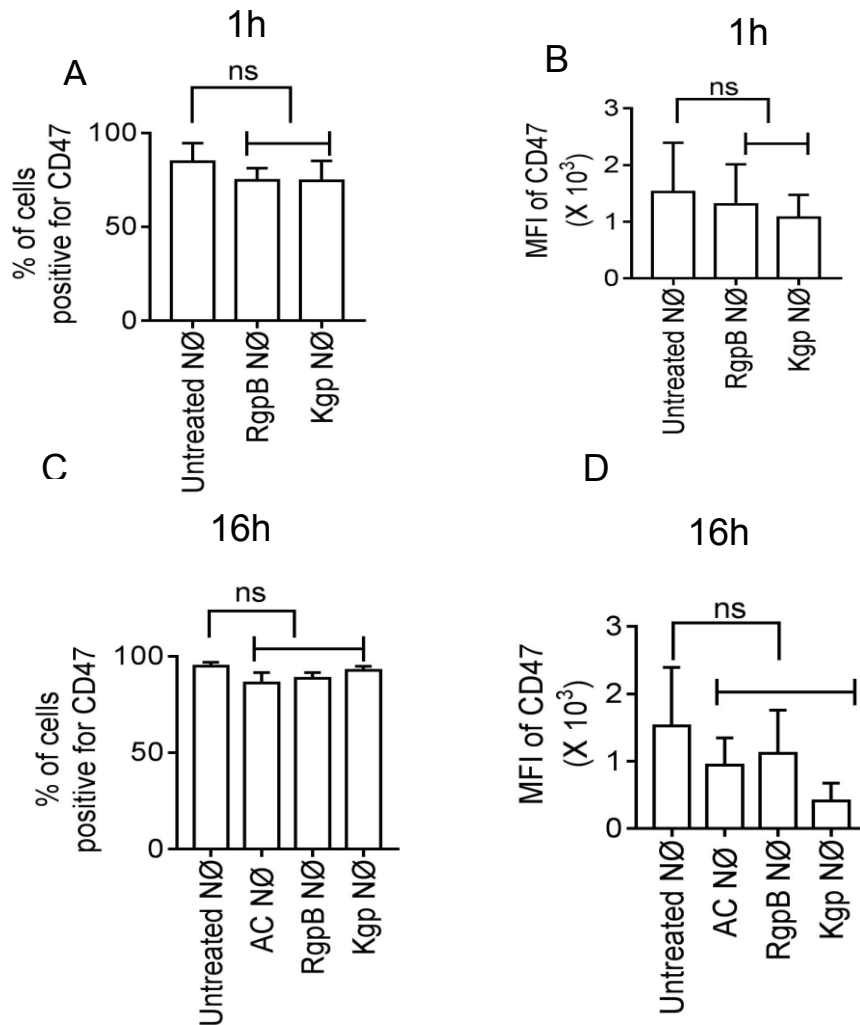


Figure 55: CD47 expression on gingipain-treated primary viable and AC NØ treatment at different time points

Human viable NØ were either incubated with RgpB or Kgp (5µg/ml) for 1h or 16h at 37°C (as described in section 2.7.11) or allowing to undergo spontaneous apoptosis for 16h at 37°C (as described in section 2.5.1.2) NØ were stained with anti-CD47 and analysed by flow cytometry for CD31 expression. Data shown is A) the percentage of cells positive for CD47 at 1h incubation B) MFI of CD47 at 1h time point C) The percentage of cells positive for CD47 at 16h incubation and D) MFI of CD47 at the 16h time point. Data shown are representative of three independent experiments for (A) and mean ± SEM of three independent experiments for (B, C, D, and E). Statistical analysis was performed using

ANOVA followed by a Dunnett's post-test. Not-significant (ns) compared with untreated cells.

The result in figure 55C indicate that CD47 was expressed at both viable and AC NØ. Additionally, no significant difference was observed in CD47 levels on NØ treated (1h or 16h) with the proteases compared to untreated NØ (figure 55B&D).

5.6 Gingipains inhibit the directional migration of phagocytes to AC

Having characterised a panel of 'eat me' and 'don't eat me' receptors important for AC clearance, the THP-1 derived MØ were used to assess for their migrational abilities in gingipain-exposed environments using an *in vitro* migration mode system. Phagocyte migration in response to the attractive mediators released by the AC is considered to be an essential step in the removal of dying cells. The prompt clearance of AC induces immunological tolerance and subsequent biological responses in the infected tissue of the host ⁶⁰⁹. The impact of gingipains on this is unknown. Preliminary results suggest that THP-1 VD3 MØ demonstrate efficient migration towards both AC B and AC NØ using an established Dunn chemotaxis chamber assay (figure 25D & 28D). To determine whether gingipains can inhibit phagocyte migration to AC, possibly through cleavage of receptors CD14, THP-1 VD3 MØ were treated with gingipains and analysed for migrational abilities. Kgp was chosen over RgpB to treat the MØ due to the rapid reduction of CD14 levels on Kgp-treated MØ (figure 47). THP-1 VD3 MØ grown on glass slides were treated with Kgp gingipain for 1h and sealed in a Dunn chamber prior to addition of AC as an attractant. The migration of the protease-treated MØ was recorded for 2h at 37°C using time-lapse video microscopy. The results are shown in figure 56.

The results in figure 56 show MØ migration towards AC B and this appears reduced for gingipain-treated MØ. The chemotaxis plots (figure 56A) shows the migration of 40 selected MØ, the count recommended by the chemotaxis and migrational tool assay V2.0 were standardised at the centre of the plot ⁴⁶⁹. MØ migration in the absence of a gradient (i.e. medium alone in the outer well) serves as a negative control and non-protease MØ migration towards AC B serves as a positive control ³⁷. Kgp-treated MØ appear to show some directional movement towards AC B, similar to untreated MØ. However, using the measure yFMI, as a measure of directional migration for all cells, the data suggest Kgp treatment of MØ causes a significant decrease in the directional migration of MØ towards dying cells ($P<0.01$) compared to non-protease treated MØ. These data suggest that gingipains may cause the delayed clearance of dying cells and their debris resulting in prolonged inflammation and tissue destruction.

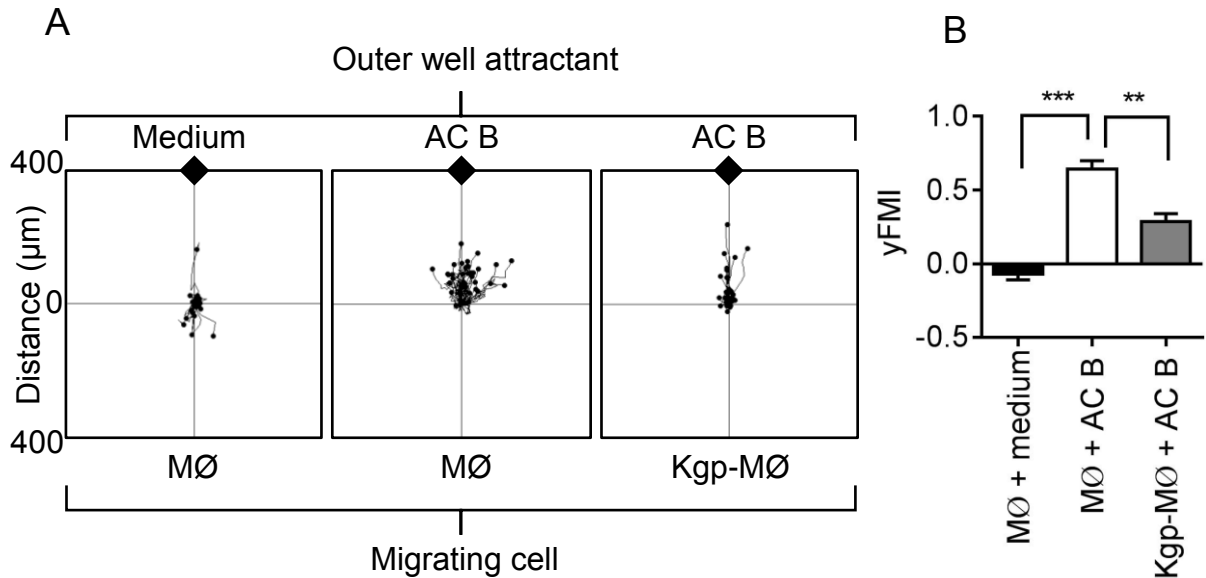


Figure 56: Gingipains inhibit MØ migration towards AC B cells

THP-1 cell-derived VD3 MØ were exposed to AC B in a horizontal migration assay. MØ were seeded on glass coverslips and treated or untreated with gingipains before loading to a Dunn horizontal chamber and exposed to putative attractants (as described in section 2.6.2.1). MØ migration was monitored for 2h at 37°C using time-lapse video microscopy. Migration of 40 cells per assay was measured using Image J and Ibidi Chemotaxis and Migration Tool (V2.0). The MØ route of travel is shown by a line from the starting point (set at the cross hairs of the plots) to the final MØ position after 2h (black dot). The relative location of AC was at the top of the plot (black diamond). (A) Representative plots showing: Left panel: Untreated MØ migration with control, cell-free medium as a putative attractant to reveal basal levels of MØ migration. Centre panel: Untreated MØ migration with AC B as an attractant. Right panel: Kgp-treated MØ (Kgp-MØ) migration with AC B cells as an attractant. (B) Forward migration index (yFMI) to quantify MØ migration in the direction of the AC B. Data shown are representative of three independent experiments for (A) and mean \pm SEM of three independent experiments for (B). Statistical analysis was conducted using ANOVA followed by a Bonferroni post-test $**P < 0.01$, $***P < 0.001$ compared to MØ + B cells.

From the data plots (figure 56A), other measurements of migration were extracted using image J and chemotaxis and migration tool. Parameters measured included Euclidean and accumulated distance, velocity, and angle. The results are shown in figure 57.

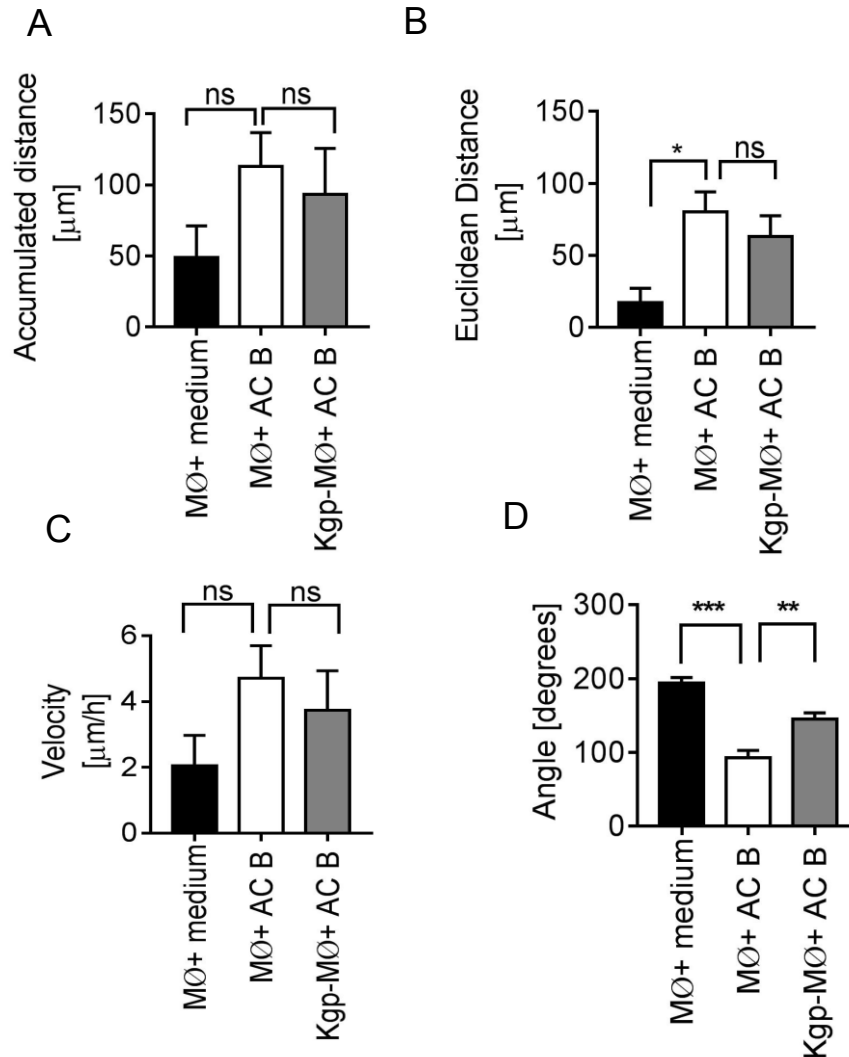


Figure 57: Gingipain treatment of THP-1 MØ does not affect distance, velocity or angle of migration towards AC B cells

THP-1 VD3 MØ with or without gingipain treatment were exposed to AC B in a horizontal migration assay (as described in section 2.6.2.1). MØ migration was monitored for 2h at 37°C using time-lapse video microscopy. Quantitative measurement of migrated MØ was analysed using Image J and Ibidi Chemotaxis and Migration Tool (V2.0). 40 cells per assay were tracked for their migration towards the chemoattractant and extrapolated the measurements from the data plots in figure 56. Data shown is A) Accumulated distance B) Euclidean distance C) velocity and D) angle measurement of Kgp-treated and untreated MØ moving towards AC B or medium alone. Data shown are the mean \pm SEM of three independent experiment. Statistical analysis was conducted using ANOVA followed by Bonferroni post-test; * $P < 0.05$, ** $P < 0.01$, *** $P < 0.001$ or not significant compared to MØ + AC B.

The results in figure 57 show that other than angle of migration, the other measures were unaffected, while the angle travelled alone suggests a significant difference ($P < 0.01$) between Kgp-treated MØ compared to untreated MØ. This indicates that the Kgp-treated MØ travelled in a less uniform manner compared to untreated MØ. Taken together, these data suggest that gingipain-treated MØ can be stimulated by AC such that the distance

and speed migrated by MØ are not significantly different to that of non-protease treated MØ, suggesting that chemokinesis is unaffected. However, directionality is reduced by gingipain treatment (figure 56B).

The VD3 stimulated THP-1 MØ were similarly used to assess for their migrational abilities in gingipain-exposed environment towards AC NØ using a Dunn chemotaxis chamber. The results are shown in figure 58.

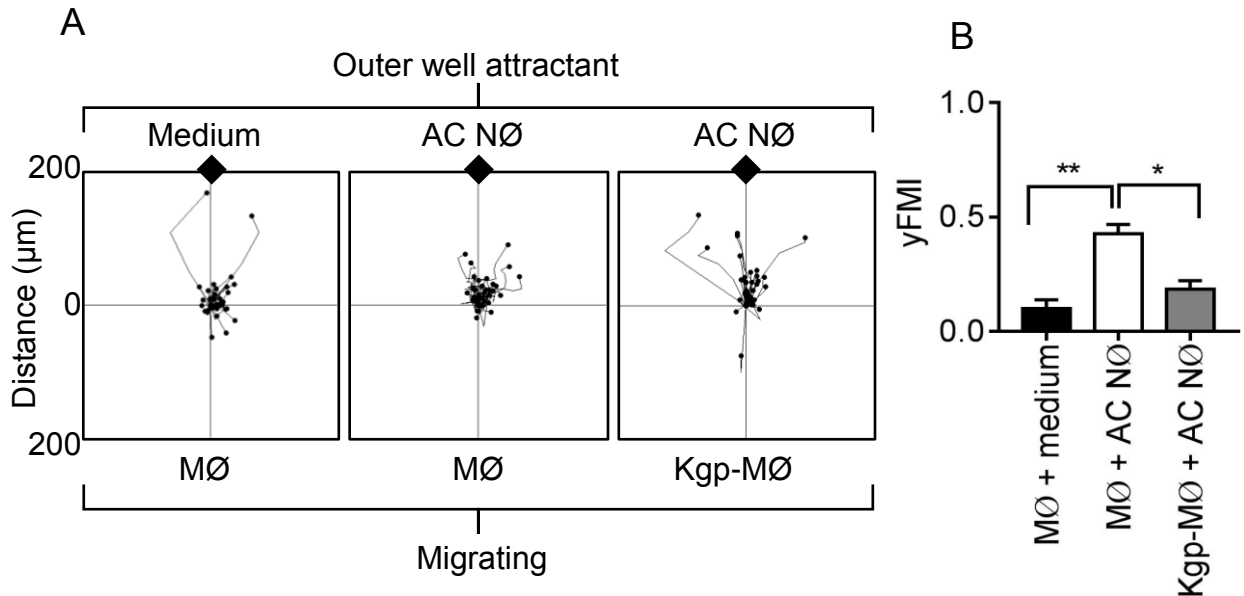


Figure 58: Gingipains inhibit MØ migration towards AC NØ

THP-1 VD3 MØ with or without gingipain treatment were exposed to AC NØ in a horizontal migration assay (as described in section 2.6.2.1). MØ migration was monitored for 2h at 37°C using time-lapse video microscopy. Migration of 40 cells per assay was measured using Image J and Ibidi Chemotaxis and Migration Tool (V2.0). The MØ route of travel is shown by a line from the starting point (set at the cross hairs of the plots) to the final MØ position after 2h (black dot). The relative location of AC was at the top of the plot (black diamond). (A) Representative plots showing: Left panel: Untreated MØ migration with control, cell-free medium as a putative attractant to reveal basal levels of MØ migration. Centre panel: Untreated MØ migration with AC NØ as an attractant. Right panel: Kgp-treated MØ (Kgp-MØ) migration with AC NØ as an attractant. (B) Forward migration index (yFMI) to quantify MØ migration in the direction of the AC NØ. Data shown are representative of 4 distinct experiments for (A) and mean ± SEM of three independent experiments for (B). Statistical analysis was conducted using ANOVA followed by Bonferroni post-test * $P < 0.05$, ** $P < 0.01$ compared to MØ + AC NØ.

Similar to previous experiment with AC B, migrational movement of gingipain-treated MØ towards AC NØ appeared similar to that of untreated MØ (figure 58A) however, a reduced yFMI for Kgp-treated MØ ($P < 0.05$) was noticed compared to untreated cells (MØ + AC NØ) (figure 58B).

The data plots in figure 58 were used to extract other quantitative measurements to assess further the migrational abilities of MØ towards AC NØ. The results are shown in figure 59.

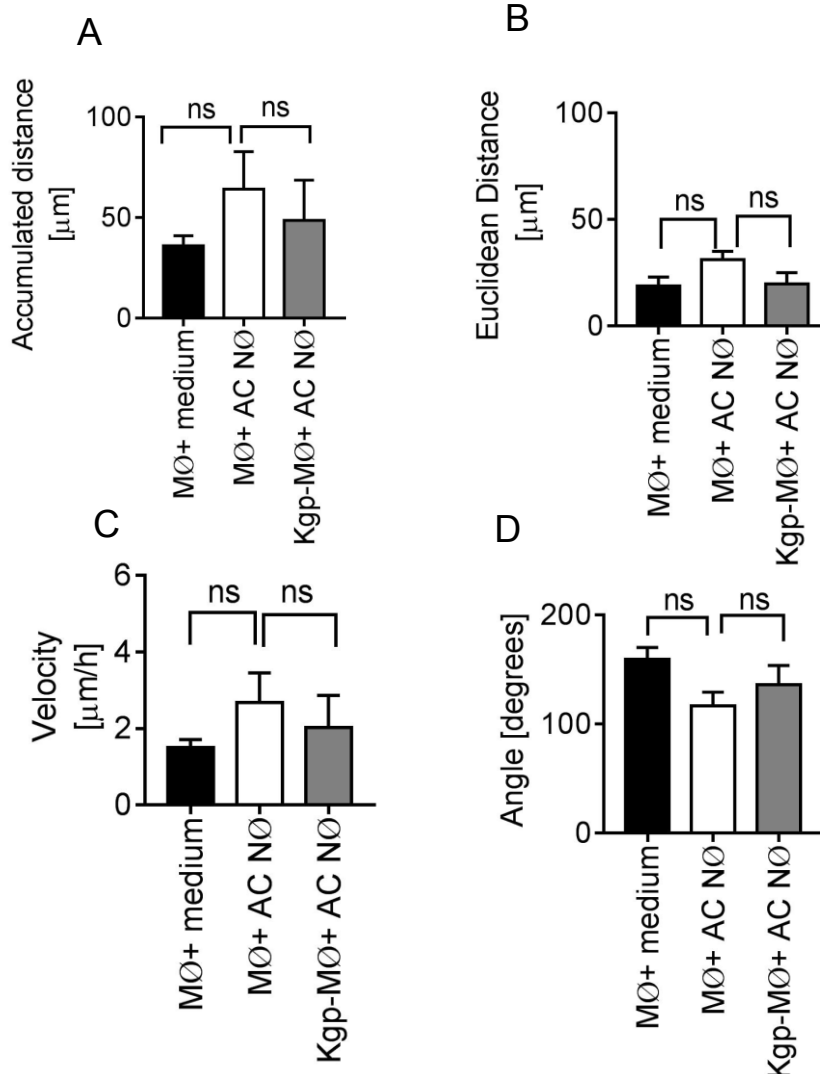


Figure 59: Gingipain treatment of THP-1 MØ does not affect distance, velocity or angle of migration towards AC NØ

THP-1 VD3 MØ were exposed to AC NØ in a horizontal migration assay. MØ were seeded on glass coverslips and treated or untreated with gingipains before loading to a Dunn horizontal chamber and exposed to AC NØ (as described in section 2.6.2.1). MØ migration was monitored for 2h at 37°C using time-lapse video microscopy. Quantitative measurement of migrated MØ was analysed using Image J and Ibidi Chemotaxis and Migration Tool (V2.0). 40 cells per assay were tracked for their migration towards the chemoattractant and extrapolated the measurements from the data plots in figure 58. Data shown is A) Accumulated distance B) Euclidean distance C) velocity and D) angle measurement of treated and untreated MØ movement towards AC NØ or medium on its own. Data shown are the mean \pm SEM of 4 distinct experiments. Statistical analysis was conducted using ANOVA followed by Bonferroni post-test. Not-significant (ns) compared to MØ + AC NØ.

The results in figure 59 suggest no significant difference in any of the quantitative measurements (Euclidean distance, accumulated distance, velocity or angle). Failed clearance of apoptotic NØ has been previously reported in periodontitis resulting in necrotic cell death of NØ and a consequent release of toxic intracellular contents into the periodontal tissues causing local tissue damage characteristic of PD³⁵⁶. Moreover, GCF

samples from chronic periodontitis patients' have been shown to contain hydrolytic enzymes from NØ^{612, 613}. Together, these data suggest that gingipain-treated MØ can be stimulated by AC NØ such that the distance and speed migrated by MØ are not significantly different to that of non-protease treated MØ, suggesting that chemokinesis is unaffected. Though, directionality is reduced by gingipain treatment.

5.7 Rgp and Kgp inhibits MØ migration towards AC NØ in a vertical cell migration assay

THP-1 MØ were also studied for their migration towards AC NØ following gingipain-treatment within an automated vertical Cell IQ-based assay. Since the Cell-IQ allows tracking of cells over a longer time period, MØ migration following RgpB treatment was also studied here as Rgp showed cleavage of CD14 at later time points (figure 47). This model assays MØ migrated from an upper well (the transwell) to a lower well, across a 0.8 µm pore membrane, performed in a 24 well plate. Throughout the assay and up to the end of the assay, the number of MØ migrated to the lower well, containing putative chemoattractant, was counted in an automated fashion using the Cell-IQ software. This vertical model is strongly influenced by gravity (cells can only move down) and the gradient is a 'step' gradient (i.e. no attractant in the top well and all attractant in the bottom well). Thus, in order to study true migration, in some cases AC NØ were also added to the upper transwell, to destroy the step gradient. This is shown in earlier results (figure 32) demonstrating that migration of MØ was reduced when the attractant was added to both upper and lower wells (i.e. the gradient was destroyed). This revealed true migration of MØ.

Two forms of AC were extracted and used 1) whole culture apoptotic B cells (AC B) or apoptotic NØ (AC NØ) where, after inducing apoptosis, the culture was used directly as a source of attractants; 2) whole culture AC (either B or NØ) centrifuged (2000xg for 20 minutes) to remove whole cells and their debris, leaving only the supernatant containing cell secretomes termed apoptotic B cell-derived AS (AS B) or apoptotic NØ-derived AS (AS NØ). This is performed in order to determine the effective recruitment of MØ and the 2000xg supernatant provides an attractant that is easier to apply to the Cell-IQ automated assays. The earlier result (figure 32) showed that AS NØ were more attractive than the whole culture apoptotic NØ using the vertical cell-IQ model.

Initial experiments were carried out for 4h to observe any effect in the gingipain-treated MØ migration towards AC B or AS B cells using the vertical migration model. The results are shown in figure 60.

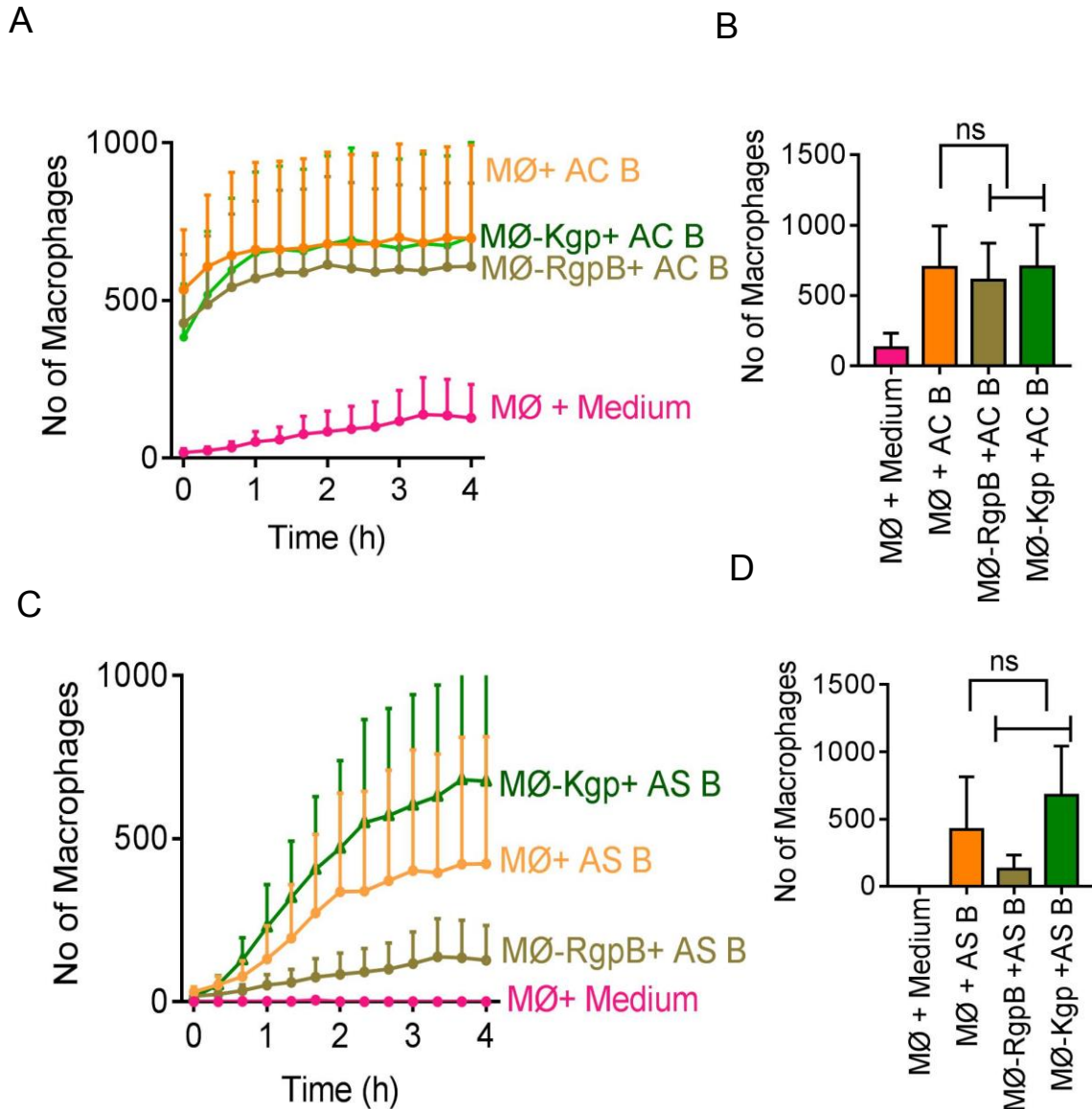


Figure 60: Gingipains does not inhibit vertical migration of MØ towards AC B or AS B cells

THP-1 VD3 MØ were either treated with gingipains (5µg/ml) (as described in section 2.7.11) or left untreated for 1h at 37°C and were seeded to a transwell (as described in section 2.6.2.2) placed over a lower well containing either AC B or AS B (as described in section 2.5.1.1) or medium in a 24-well plate. MØ migration from transwell to the lower chamber was assessed at the end of 4h by Cell-IQ software. (A) The graph shows the number of MØ migrated towards AC B or (C) AS B at different time points. (B) The histogram shows number of MØ migrated towards AC B or (D) AS B at 4h. Data shown are the mean ± SEM of three independent experiments with three replicates in each experiment. Statistical analysis was conducted using ANOVA followed by Dunnett's post-test. Not-significant (ns) compared to untreated.

The result in figure 60 shows that no significant difference was observed on gingipain-treated MØ migration compared to untreated MØ at the end of the 4h assay period (figure 60B and D). However, RgpB-treated MØ showed a trend towards reduced migration

towards AS B cells (figure 60C) though no significant difference was observed with untreated MØ (figure 60D).

Since the earlier experiment (figure 60) showed no inhibition of MØ migration towards AC B or AS B cells the ability of protease-treated MØ migration towards AC NØ or AS NØ was observed by extending the assay to 12h. The results are shown in figure 61.

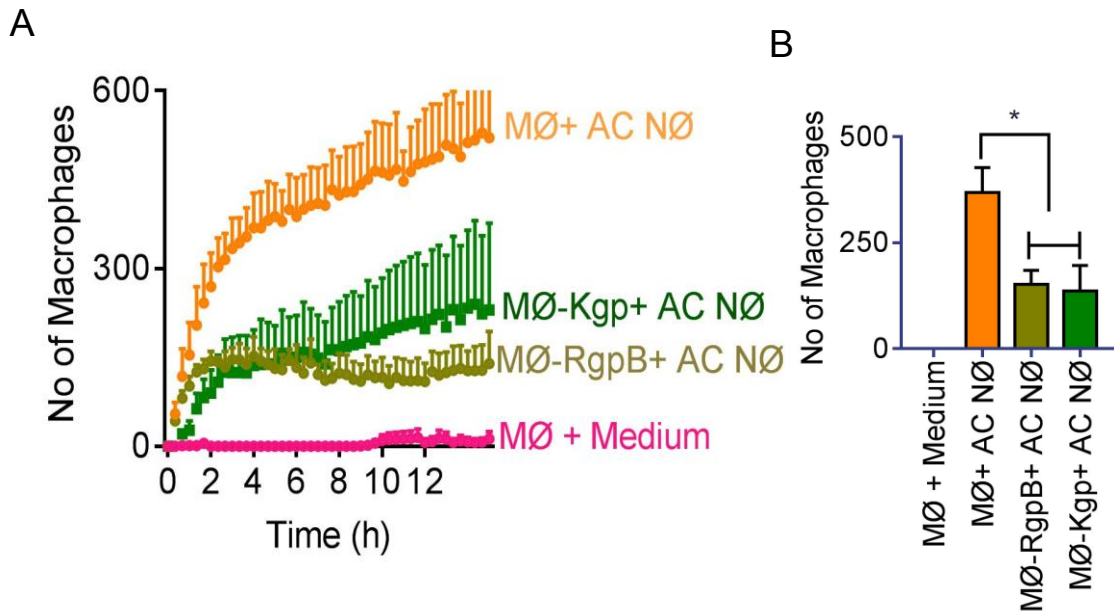


Figure 61: Gingipain treatment of MØ inhibits MØ migration towards AC NØ using vertical assay

THP-1 VD3 MØ were either treated with gingipains (5µg/ml) (as described in section 2.7.11) or left untreated for 1h at 37°C and were seeded to a transwell (as described in section 2.6.2.2) placed over a lower well containing either AC NØ (as described in section 2.5.1.2) or medium in a 24-well plate. MØ migration from transwell to the lower chamber was assessed at the end of 12h by cell-IQ software. (A) The graph shows the number of MØ migrated at different time points. (B) The histogram shows a number of MØ migrated at 4h time points. Data shown are the mean ± SEM of three independent experiments with three replicates in each experiment. Statistical analysis was conducted using ANOVA followed by Dunnett's post-test. * $P < 0.05$ compared to untreated.

Here, MØ treated with either Rgp or Kgp exhibited reduced migration to AC NØ at the end of the 12h period compared to untreated MØ migration towards whole culture AC NØ (figure 61). Untreated MØ were rapidly recruited to the lower well containing attractant, demonstrating significantly increased migration over gingipain-treated MØ. These differences were noticeable from 1-2h and for the duration of the assay.

The result in figure 61 demonstrates the RgpB or Kgp gingipain-treated MØ showed reduced migration to AC NØ compared to untreated MØ. The effects were similarly assessed for gingipain-treated MØ migration towards AS NØ. The results are shown in figure 62.

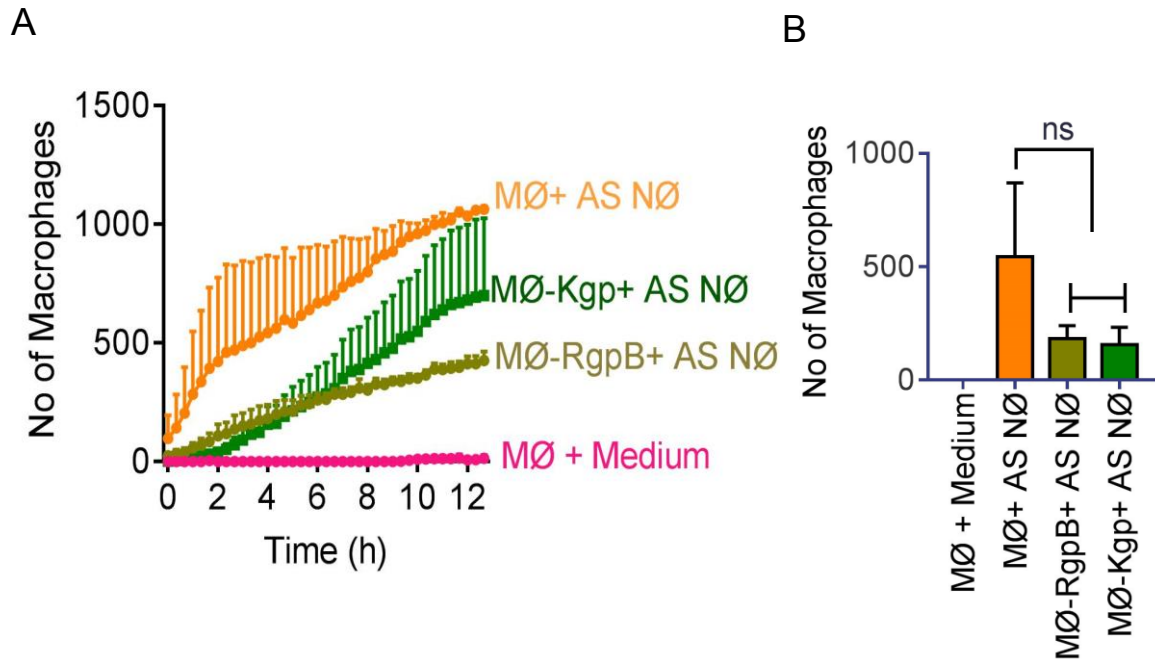


Figure 62: Gingipain does not inhibit vertical migration of MØ migration towards AS NØ

THP-1 VD3 MØ were either treated with gingipains (5µg/ml) (as described in section 2.7.11) or left untreated for 1h at 37°C and were seeded to a transwell (as described in section 2.6.2.2) placed over a lower well containing either AS NØ (as described in section 2.5.1.2) or medium in a 24-well plate. MØ migration from transwell to the lower chamber were assessed at the end of 12h by cell-IQ software. (A) The graph shows the number of MØ migrated at different time points. (B) The histogram shows a number of MØ migrated at 4h time points. Data shown are the mean ± SEM of three independent experiments. Statistical analysis was conducted using ANOVA followed by Dunnett's post-test. Not-significant (ns) compared to untreated.

The results in figure 62A show similar trends to MØ migration towards AC NØ. However, no significant difference was observed between the protease-treated and untreated MØ migration at the 4h time point (figure 62B). The AS NØ served as a stronger attractant with more MØ recruited (figure 62) comparison to whole culture AC NØ (figure 61).

5.8 Gingipains inhibit interaction of MØ with AC

Given the implication that gingipain-treated MØ are less able to migrate towards AC (either B or NØ) (figure 56 and 58), the effect of MØ interaction with phagocytes treated with gingipains was also assessed as a key point in the AC clearance process. Earlier results show (figure 33) that THP-1-derived MØ are able to interact with AC NØ or AC B individually. Additionally, the result also showed that MØ do not interact with viable MØ in the control, where only weaker interaction can be seen (figure 33).

Of all the receptor assessed, only a reduction in CD14 expression was noted on gingipain-treated MØ where Kgp was rapid in cleaving CD14 receptors from the MØ surface at 1h of treatment compared to RgpB which required an extended (12h) period (figure 47). Taking into account, which is CD14 is cleaved by the gingipains and the established importance

of CD14 as a tethering receptor for AC⁴¹⁸ the impact of gingipains on the ability of MØ to interact with AC was determined. THP-1 MØ or gingipain-treated MØ were co-cultured with AC B (used as a positive control) for 1h at 37°C and stained with Jenner–Giemsa staining and scored by microscopy for MØ interaction with AC. In this assay, interaction is defined as a MØ that has bound or phagocytosed an AC. The results are shown in figure 63.

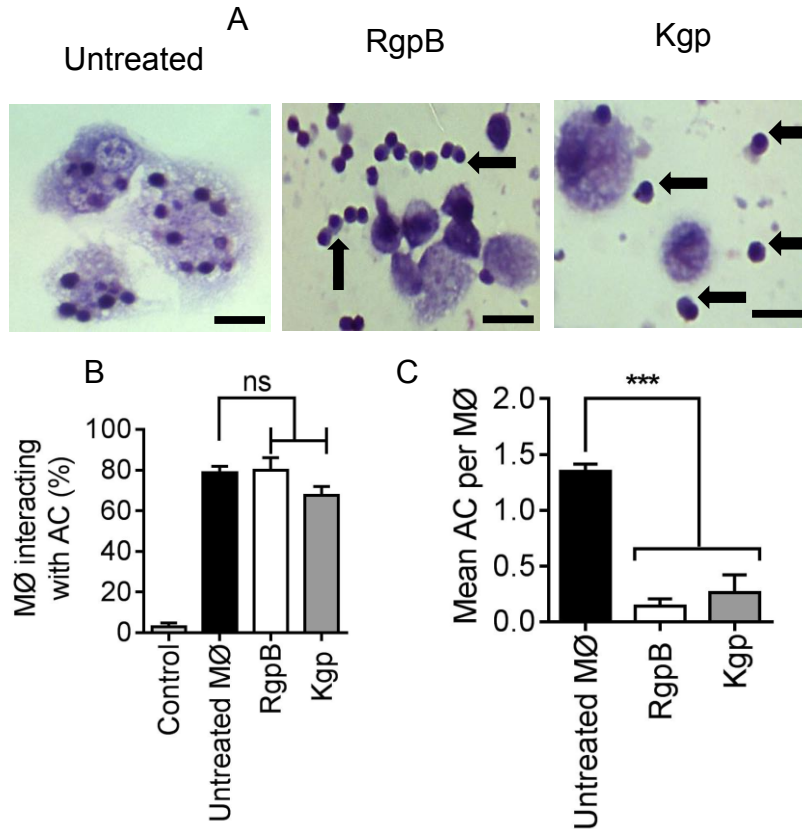


Figure 63: Gingipain treatment of MØ inhibits the interaction of MØ with AC B

THP-DS MØ (as described in 2.3.5 section) were treated or untreated with gingipains (5µg/ml) for 1h at 37°C (as described in section 2.7.11) prior to co-culture with apoptotic B cells for 1h (as described in section 2.6.1). A) Photomicrographs of Jenner-Giemsa stained untreated or gingipain-treated THP-1 DS MØ interacting with AC B cells. Untreated THP-1 MØ showing tethering and phagocytosing of AC B (left panel) and gingipain-treated (RgpB/Kgp) THP-1 MØ showing interaction with fewer AC B (middle and right panel). THP-1 MØ can be seen in light blue and AC are stained with intense blue. The arrow indicates the AC B cells that are not up taken by MØ. Magnification 40X. B) Histograms showing the percentage of MØ (with or without gingipain treatment) interacting (binding or phagocytosing) with AC B. C) The mean number of AC B cells interacting per MØ with or without gingipain treatment. Data shown are mean ± SEM of three independent experiments. Statistical analysis was conducted using ANOVA followed by Dunnett’s post-test: *** $P < 0.001$ or not significant (ns) compared to untreated. The photomicrographs are representative of three independent experiments.

The results in figure 63 suggest that many apoptotic B cells (arrow) are not taken up by the gingipain-treated (either RgpB or Kgp-treated) MØ compared to untreated MØ where AC can be seen internalised by the MØ (figure 63A). However, the percentage of MØ

interacting with AC remains unaffected by gingipain treatment (figure 63B). However, it was clearly visible under the microscope that many AC were left without uptake by MØ and that the numbers of AC per MØ appeared to be reduced. The nature of the scoring method used was not initially designed to detect the level of AC binding. So, the number of AC interacting per MØ was scored and the mean number of AC per MØ presented (figure 63C). As a result of the alternative scoring method, scoring the mean number of AC interacting per MØ exhibits a robust decrease in the level of interaction by gingipain-treated MØ (figure 63C). This may suggest that a reduction in CD14 or other receptors may lead to reduced AC clearance. Perhaps surprisingly, RgpB treatment reduced AC clearance after only 1h of treatment – a time when CD14 is not significantly cleaved by RgpB-perhaps suggesting that CD14 is not the sole mediator responsible for this effect. RgpB treated MØ show reduced CD14 only at 12h time point (figure 47D) however a trend to reduced MFI was noticed in 1h treatment (figure 47B).

Next, using a similar experimental approach, the ability of gingipain-treated MØ to interact with AC NØ in co-culture was assayed to determine the level of interaction with phagocytes. The results are shown in figure 64.

The results in figure 64 show a similar effect to that seen with AC B. Both RgpB and Kgp-treated MØ showed significantly reduced uptake of AC NØ (figure 64A). However, unlike with AC B, gingipain-treated MØ showed both a decreased percentage of interaction with apoptotic NØ (figure 64B) and a significant decrease in the mean number of AC NØ interacting per gingipain-treated MØ (figure 64C).

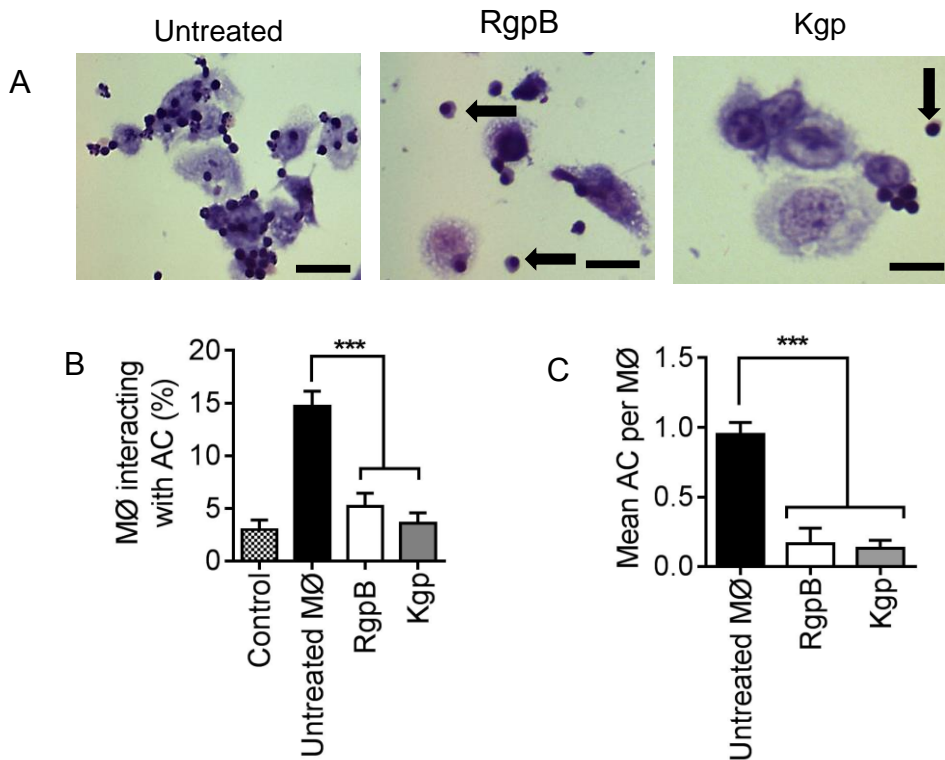


Figure 64: Gingipain treatment of MØ inhibits interaction of MØ with AC NØ

THP-1-DS MØ (as described in 2.3.5 section) were treated or untreated with gingipains (5µg/ml) for 1h at 37°C (as described in section 2.7.11) prior to co-culture with apoptotic NØ for 1h (as described in section 2.6.1). A) Photomicrographs of Jenner-Giemsa stained untreated or gingipain-treated THP-1 DS MØ interacting with AC NØ. Untreated THP-1 MØ showing tethering and phagocytosing of AC NØ (left panel) and gingipain-treated (RgpB/Kgp) THP-1 MØ showing interacting with fewer AC NØ (middle and right panel). THP-1 MØ can be seen in light blue and AC are stained with intense blue. The arrow indicates the AC B cells that are not up taken by MØ. Magnification 40X. B) Histograms showing the percentage of MØ with or without gingipain treatment interacting (binding or phagocytosing) with AC NØ C) The mean number of AC NØ interacting per MØ with or without gingipain treatment. Data shown are mean ± SEM of three independent experiments. Statistical analysis was conducted using ANOVA followed by Dunnett's post-test: *** $P < 0.001$ compared to untreated. The Photomicrographs are representative of three independent experiments.

5.9 Discussion

A wide range of receptors associated with phagocytes, AC, and soluble bridging molecules are involved in recognition and engulfment of AC ⁵⁷⁰. Before phagocyte recognition of an AC takes place, the AC undergoes several morphological changes resulting in the release of factors and alterations to the dying cell surface which ultimately lead to receptor-mediated recognition ⁶⁰⁹. The released signals enhance phagocyte migration, and subsequent recognition of, interaction with and engulfment of the dying cells. In addition, AC-derived vesicles have also been reported to recruit phagocytes and promote anti-inflammatory cytokines ^{37, 614, 615}.

'Find me' signals secreted in the form of soluble factors such as nucleotides ATP and UTP can promote recruitment of microglial cells⁶¹⁶. Also, the lipid LPC secreted from dying MCF7 breast cancer cells attracts THP-1 monocytes suggesting that 'find me' signals act also to promote MØ recruitment²⁵⁸. If phagocytes and dying cells are in close proximity, the need for 'find me' signals may be reduced when compared to phagocytes that are some significant distance from the dying cell. It may also be that different 'find me' signals act over different distances. Sphingosine 1-phosphate (S1P), a sphingolipid metabolite is proposed to be another 'find me' signal, acting via sphingosine 1-phosphate receptors (S1PRs), recruiting lymphocytes through various receptors⁶¹⁷. The chemotaxis of immune cells is reported to be regulated by S1PR1 via phosphoinositide (PI) 3-kinase- and Rac enzymes. Additionally, S1PR4 induces NØ chemotaxis towards FMLP from the blood to tissue⁶¹⁸.

Once phagocytes are recruited to dying cells, 'eat me' signals come into play. The most studied 'eat me' signal is PS, found in the outer leaflet of the plasma membrane of an AC, it has been shown to bind soluble proteins such as GAS6, protein S and MFGE8 in order to facilitate AC uptake by phagocytes^{46, 47, 332, 619}. Additionally, annexin I released from dying cells binds to PS marking them as apoptotic⁶²⁰. The 'Tether and tickle' mechanism proposed by Hoffman *et al.* is an important complex relationship as several ligands expressed by AC bind to appropriate phagocyte receptors for direct recognition and to stimulate uptake²⁸⁰. Specific antibodies used to block the exposed PS result in the decreased AC uptake, suggesting a key role for PS in the engulfment process⁴⁷. Conversely, treatment of healthy viable NØ with gingipain R were reported to enhance the uptake by MØ in a non-dependent PS exposure¹⁸⁸. However, it is unclear whether PS-R present on the phagocytes recognised PS as a naked molecule which is on its own or in combination with other soluble proteins⁶²¹. However, Park *et al.* identified that BAI1 expressed on the phagocytes can stereo-specifically bind to PS on AC suggesting that BAI1 act as a PS-R molecule to facilitate clearance²⁷⁶.

Inhibitory signals are also necessary to prevent clearance of viable cells. CD31 expressed by both viable and AC, functions to enable phagocytes to discriminate a viable target cell from a dying cell. The engulfing phagocyte also expresses CD31 receptors which bind CD31 on the target cell to tether to the surface. Viable cells initially tether and switch to a repulsive mode whereas dying cells tether and fail to repulse, instead switch on the adhesive mode until engulfed by the phagocytes³³⁸.

Once recognised, AC are taken via engulfment in two ways: (1) phagocytes engulf whole AC, if the encountered AC size is similar to phagocyte (e.g. professional phagocytes engulf AC NØ or apoptotic thymocytes as intact whole cells)^{235, 236}; (2) If the target AC varies is large relative to the phagocytes, then engulfment occurs in "bite-size" fragments.

In inflamed adipose tissue multiple phagocytes, have been reported to ingest smaller fragments of single apoptotic adipocytes^{609, 622}. In situation 2, the dismantling of AC into apoptotic bodies enables this to happen.

To explore potential therapeutic approaches to the treatment of chronic inflammatory diseases, such as periodontitis, it is necessary to understand how AC clearance is affected by pathogens and disease. The work in this chapter studied how *P. gingivalis* derivatives –gingipains interfere with AC clearance.

5.9.1 Gingipain modulation of CD14 on MØ

CD14 is a receptor for multiple ligands including endotoxin, PAMPs and also identified as an AC clearance receptor. It is involved in stimulating both pro-inflammatory responses to PAMPs and anti-inflammatory responses to AC through phagocytosis and immunosuppressive process^{142, 329, 418, 440, 623}. Expressed in myeloid cells, CD14 is well documented for its role in monocytes, MØ, and NØ^{324, 418}. However, recently a CD14 role on non-myeloid cells was reported in a range of cells (HELA, MCF-7, H400, B-2B, HPF, and Calu-3) which were studied for their ability to rapidly bind dying cells mediating clearance³⁶. This work also suggests a primary role for CD14 in regulating airway inflammation e.g. inhibition of AC clearance by airway cells in smokers causing respiratory infections⁶²⁴.

In light of the established CD14 receptor role in AC clearance, from our laboratory^{36, 418, 469} and elsewhere^{281, 326, 625}, here, CD14 function was studied in AC clearance and the influence of gingipains was assessed. A panel of cell clearance receptors was studied here and of those studied (CD14, ICAM-3, CD36, and CD91), CD14 was the only molecule cleaved by gingipains. This was cleaved rapidly from THP-1 VD3 MØ by Kgp (1h) and more slowly by Rgp (12h) (figure 47) without inducing apoptosis (figure 42 and 43). This is in agreement with previous studies which report that CD14 cleavage is apparent from gingipain-treated mouse peritoneal MØ⁶²⁶; human monocytes⁶²⁷ and from gingival fibroblasts⁶²⁸. However, gingipains have been shown to induce apoptosis in human gingival epithelial cells by activating mitochondria, FAS, TNFR and IL-R apoptosis signals suggesting that gingipain affects both intrinsic and extrinsic pathways in gingival epithelial cells¹⁸⁷. Apoptosis by gingipain was also observed in endothelial cells and lymphocytes^{629, 630}. Yet, the work presented here show that the gingipain does not induce apoptosis in MØ and NØ.

CD14 cleavage on THP-1 VD3 MØ was rapid on treatment with Kgp compared to Rgp (figure 47). This could be due to the presence of hemagglutinin/adhesion domains in Kgp that are lacking in RgpB. The hemagglutinin/adhesion domains have been reported to bind to the phospholipids and activating factor X in the blood coagulation system to

stimulate thrombin, an activating factor which has been associated with periodontitis infection by binding with haemoglobin and haem present in the host^{164, 183}. This suggests that the hemagglutinin/adhesion domains might be responsible for binding to the immune cells and thereby aiding bacterial attachment to immune cells to promote CD14 cleavage.

The gingipain-mediated reduction in CD14 on MØ, without inducing apoptosis, demonstrates the potential inflammatory nature of these proteases carried by the bacteria at the infected gingival sites. Whilst the data here suggest that gingipains cleave CD14 (figure 47) it is also possible that gingipains might simply have cleaved the epitope of the mAb that recognises CD14 leaving CD14 still on the surface of MØ. Potential future work may address this by staining gingipain-treated MØ with a range of CD14 antibodies that bind elsewhere on the CD14 molecule, and if the CD14 reduction was still observed, the chances are that gingipains actually cleaved CD14. Additionally, detection of released i.e. soluble CD14 by ELISA analysis might further confirm the cleavage of CD14 by gingipains. Increased levels of sCD14 are observed in the sera of periodontitis patients compared with the healthy controls, it seems likely that the reduction in CD14 is due to cleavage and that this is relevant to disease in patients⁶³¹.

Additionally, a previous study showed on human monocytes stained with the anti-CD14 mAb, MY4, that following exposure to gingipains MY4 binding was reduced and CD14 fragments were detected in the culture medium by western blot analysis. This resulted in downregulation of LPS-induced TNF- α production⁶²⁷. Furthermore, CD14 cleavage is also detected in human gingival fibroblasts, a dominant cell type in periodontal connective tissue, on exposure to arginine-specific cysteine proteinases. This led to LPS hyporesponsiveness (i.e. decreased IL-8 production)⁶²⁸. Reduced IL-8 production has been linked with inhibitory NØ phagocytosis function^{432, 632}. Additionally, increased CD14 levels were reported in the serum and saliva of *P.gingivalis* induced adult periodontitis patients suggesting that gingipains might contribute to the cleavage of CD14^{631, 633}. Whilst these results might suggest cleavage of CD14 would be anti-inflammatory, this doesn't consider the consequence of reduced CD14 on AC clearance as studied here and the impact this has on generating inflammation seen in periodontal disease.

The concentration of gingipains within the GCF in chronic periodontitis patients has been determined to be $\leq 1.5 \mu\text{M}$ and the concentration of gingipains used in this study was $5\mu\text{g/ml}$ which is therefore highly efficient in cleaving the CD14 on MØ and NØ⁶³⁴. An earlier study reported that using the same method used here to isolate gingipains in addition to anion-exchange chromatography 5mg of gingipain was isolated from 1 litre HG66 bacterial culture. The difference of concentration might be due to alteration in growth of the bacteria or the purification steps used here might be the reason for the variation in gingipain concentration.

However, within *in vivo* conditions, *P.gingivalis* secretes gingipains both as a membrane-bound and soluble form and as vesicles from bacterial outer membranes. It is therefore conceivable that higher concentrations of gingipains are released, from bacteria residing at the gingival sites or in the periodontal pocket to the circulating or recruited phagocytic cells leading to a local reduction of CD14 expression on MØ^{426, 526, 635-637}. Soluble gingipains from HG66 or W83 supernatants have been used previously for studying CD14 levels on phagocytes^{626, 627}. This raises the question whether cell membrane-bound gingipains interact with CD14 on monocytes/MØ but this remains unclear. However, vesicles from the outer membrane of *P.gingivalis* promote shedding of CD14 from the surface of human U937 MØ-like cells⁶³⁸ implying that membrane-associated cysteine proteases might participate to evade the host immune system.

Various gingipain inhibitors have been proposed to inhibit, to various degrees, all three gingipains²⁰². Here, TLCK, a cysteine protease active inhibitor was used to help confirm the gingipain role in CD14 cleavage. As mentioned earlier, TLCK is reported to inhibit both Rgp and Kgp proteases activity⁴²⁶. The data presented here (figure 49B) shows that TLCK blocked the loss of CD14 after treatment with Kgp, indicating that the isolated proteases were gingipains and that they were responsible for the CD14 cleavage seen. TLCK also inhibits thrombin in the blood coagulation defence system reported being associated with bone resorption by osteoclasts through a prostaglandin-dependent pathway this could be one of the reasons for alveolar bone resorption at periodontal sites^{544, 639}. Other inhibitors such as FPR-cmk and Z-FK-cmk specific for Rgp and Kgp respectively have shown to inhibit IL-8 production in human monocytic THP-1 cells treated with gingipains. This suggests that gingipains were the causative agent for the production of pro-inflammatory cytokines and their dependency on stimulating the enzyme activities on initiating destruction within periodontal region^{202, 640}.

5.9.2 CD14 on NØ

Having mentioned the importance of CD14 on monocytes/MØ in the inflammatory response, the ability of gingipain to cleave CD14 on primary NØ was also assessed. AC NØ have been used as a model for their participation in AC clearance in chronic inflammatory disease such as periodontitis^{190, 357}, rheumatoid arthritis^{641, 642}, cardiovascular disease^{643, 644} and other systemic diseases^{645, 646}. Before viable NØ become apoptotic, the efficiency of NØ to assist in clearance of microbial components will decide the nature of the inflammatory response. The action of gingipains to modulate NØ receptor levels as seen in MØ may impact pathogen or AC clearance in the infected tissue. The data presented here shows that both forms of gingipains (Rgp and Kgp) cleave CD14 on viable NØ in 1h of treatment (figure 48) without inducing apoptosis (figure 44). This is in agreement with a previous study showing that gingipains do not induce a

high level of apoptosis on NØ at 1h treatment¹⁸⁸. However, RgpB treated primary NØ showed viability only 60% (figure 44) which is correlated with the presence of NETs seen in figure 45. This might be a reason for the presence of NET's found in crevicular exudates of periodontitis patients indicating that NET's might be flushed out from the periodontal pocket to the GCF³⁷⁴.

It is interesting to note that the cleavage of CD14 observed with RgpB-treated NØ is much more rapid (1h) (figure 48A) compared to that in THP-1 MØ where RgpB cleaved after 12h (figure 47C). Though intermediate time points for Rgp treated THP-1 MØ were not analysed to detail the exact time point of cleavage, however, it is clear that Rgp fails to cleave CD14 on MØ in 1h treatment (figure 47A). This may be explained as data here shows that NØ express CD14 (figure 48) though to a lesser degree than MØ (figure 47). Previous studies agree that the GPI-anchored CD14 receptor is expressed on primary NØ^{501, 647}. Haziot *et al.* further demonstrate the presence of CD14 on NØ by digesting with PI-PLC, an enzyme that specifically cleaves the GPI anchor, suggesting that NØ express membrane-bound CD14⁶⁴⁷. Moreover, the same work demonstrates active participation of CD14 in releasing TNF- α upon interaction with LPS-LBP complexes indicating the direct participation of CD14 NØ in the acute inflammatory response. CD14 has been studied as a marker for inflammation on NØ for pulmonary infection in asthmatic children demonstrating reduced CD14 levels suggesting a poor response to bacterial components, such as LPS⁶⁴⁸. Inflammatory stimuli such as LPS and FMLP have been shown to increase the level of CD14 on the plasma membrane of NØ with an argument being made that the newly expressed CD14 is released from intracellular stores of the receptor⁶⁴⁹. Additionally, the same study showed that CD14 is expressed in vesicles secreted by the NØ and also in the azurophilic granules.

Again, the loss of CD14 from NØ might suggest that immune responses will be reduced following bacterial challenge. However, the impact of CD14 loss on the total immune response has not been considered i.e. the net effect of blocking responses to bacteria and reduced AC clearance.

5.9.3 Possible receptor modulation in periodontal disease

While CD14 levels are reduced on gingipain-treated THP-1 VD3 MØ here (figure 47), other studies have reported that TLR4 and TLR2 (co-receptors for CD14) are unaltered by gingipains on murine MØ^{146, 500, 626, 650-652}. Additionally, CHO reporter cells expressing CD14 and TLR2 respond to gingipain-deficient *P.gingivalis* through NF- κ B activation indicating that gingipains have no effect on TLR2 signaling pathways⁶⁵³. Gingipains' ability to cleave other GPI-anchored proteins, such as CD40, CD59, and CD157, suggests that CD14 is not the only GPI- anchored molecule cleaved by gingipains. However,

Sugawara *et al.* show that gingipains reduced CD59 by only 40% compared to a CD14 reduction of 80% on the surface of human gingival fibroblasts indicating CD14 as an efficient substrate for gingipains^{627, 628}.

The study here suggests that neither gingipain (RgpB or Kgp) cleave the AC clearance receptors CD36, ICAM-3, or CD91 from the surface of THP-1 MØ nor on primary NØ (figure 50 and 51) perhaps suggesting that the cleavage by gingipains doesn't affect all cell surface molecules. It remains possible that these other molecules are cleaved but that the mAB epitope remains unaffected. However, MØ and primary NØ exhibit very low levels of CD91 and primary NØ show low CD36 expression (figure 50B and 51B). Both cells (MØ and NØ) do however display significant ICAM-3 expression on their surface (figure 50B and 51B) and this remains unaffected by gingipain treatment. Interestingly, ICAM-3 shows high expression on both the phagocytes (MØ and NØ) confirming its role as a marker of leukocytes and this may suggest that this molecule could be important in facilitating AC clearance. Though the level of antigen does not necessarily correlate with its participation in AC clearance, earlier research shows that leukocytes undergoing apoptosis release ICAM-3 within their microparticles to promote recruitment of MØ and tethering to MØ³⁷. In both phagocytic cells (i.e. MØ and NØ) CD91 expression appeared weak and this might be a limitation of using THP-1 as a model for CD91, as primary human monocytes and their derived dendritic cells have been reported to express considerable amount of CD91⁶⁵⁴⁻⁶⁵⁶. However, work by Shaw *et al.* reported that freshly isolated NØ do not express CD91 but on turning apoptotic carry ecto- calreticulin to induce phagocytosis in a CD91- dependent mechanism on MØ^{657, 658}. THP-1 differentiated MØ and HMDM cells were reported to express increased amount of CD36 on their surface and use CD36 as a mediator to phagocytose apoptotic NØ^{288, 659, 660}. Further work could seek to assess the effect of gingipains on a broader range of AC clearance receptors and this could be perhaps addressed on a range of different cells including, for example, gingival fibroblasts that express CD14.

To avoid uptake and ingestion by MØ, viable cells express anti-phagocytic signals such as CD31, CD47 in order to differentiate them from the AC^{338, 582}. The data here show that both MØ and NØ express CD31 on viable cells (figures 52 and 54) and reduced CD31 was found on apoptotic NØ (figure 54E). This is in agreement with previous study explaining that NØ apoptosis disables CD31 switching off the repulsive mode which is active on viable NØ³³⁸. The same study explained that phagocytes, expressing CD31, use the disarmed CD31 signals on their target AC to tether and engulf dying cells. However, on exposure to Kgp, MØ CD31 was reduced compared to untreated cells at 16h (figure 52B) suggesting that gingipains may reduce CD31 which is otherwise essential to recognise AC. This would reduce the removal of dying cells. Additionally, both Rgp and

Kgp reduce CD31 on viable NØ at 16h (figure 54E). Possibilities that gingipain might have cleaved CD31 to a greater extent due to their weaker expression of CD31. This is in agreement with the previous study that demonstrated that RgpB cleaves CD31 on the NØ surface¹⁸⁸.

Spontaneous AC NØ and gingipain treatment both reduce CD31 NØ (figure 54E) which might promote the clearance by MØ. However, it is not clear whether gingipain cleaved CD31 or spontaneous apoptosis developed on NØ at 16h is responsible for CD31 cleavage. Earlier work shows NØ shed CD32 and CD16 receptors on turning apoptotic⁶⁶¹. Although CD31 is cleaved by gingipains, future experiments are needed to analyse whether the viable cells with cleaved CD31 are engulfed by the phagocytes and this would further address the bacterial clearance inhibition and promoted inflammation.

Whilst CD31 is cleaved by gingipains, CD47 expression was unaltered on the surface of the MØ and NØ by either of the gingipains over short time frames (figure 53 and 55). However, reduced CD47 expression was reported earlier in AC NØ but not other AC types such as apoptotic Jurkat T cells or apoptotic murine thymocytes^{275, 581}.

5.9.4 Gingipain-mediated alterations in MØ response in the migration to AC

The very first activity of phagocytes on sensing the pathogens is migration. Impaired NØ chemotaxis is well documented in chronic periodontitis patients⁶⁶²⁻⁶⁶⁸. Abnormal NØ chemotaxis was first recorded in the 1980s in localised juvenile periodontitis due to decreased chemotactic peptides such as C5a and FMLP found on the surface of NØ⁶⁶⁹. This might be one of the reasons why, despite the presence of numerous NØ numbers in the periodontal sites, elimination of pathogens or dead cells is ineffective^{667, 670}.

Gingipain modulation of IL-8, a potent NØ chemoattractant, has been shown to result in impaired NØ recruitment¹⁹³. The same study further explained the cleavage of 5- and 11-amino acids peptides by Rgp and 8-amino acids peptides by Kgp from the N-terminal portion of IL-8 resulted in a three-fold increase in priming and chemotactic abilities of IL-8 affecting directly NØ chemotaxis and thereby causing local tissue degradation. This has been proposed as one possible mechanism involved in *P.gingivalis* pathogenesis¹⁹³.

While these studies report mainly on defective NØ chemotaxis, here defective MØ chemotaxis was studied based on their migrational abilities following exposure to gingipain proteases. Based on the effect of the rapid cleavage of CD14 on Kgp-treated MØ compared to RgpB (figure 47), Kgp was chosen initially to study MØ chemotaxis assay using horizontal chemotaxis. The plots in figure 56 and 58 show that migrational activities of gingipain (Kgp)-treated MØ towards AC (either AC B cells or AC NØ) appear similar to untreated MØ (figure 56A and 58A). However, if the directional migration was

assessed quantitatively the yFMI measure shows a significant decrease on pre-treated MØ moving towards AC B cells ($P < 0.01$) (figure 56B) or AC NØ ($P < 0.05$) (figure 56B) compared to untreated MØ. Additionally, angle measures depict significant differences ($P < 0.01$) between Kgp-treated MØ compared to untreated cells moving towards AC B cells indicating less uniformity of movement by Kgp-treated MØ (figure 57D).

Though no significant difference was observed in various other measures of MØ migration to AC NØ (e.g. accumulated distance, Euclidean distance, velocity, and angle - figure 59), a significant variation was observed in the yFMI of Kgp-treated MØ compared to untreated MØ (figure 58B). This is in correlation with a previous study demonstrating defective directional accuracy on NØ migration, using another horizontal chemotaxis system: the Insall chamber, from PD patients⁶⁶². Moreover, the same study also observed a significant difference in the velocity of NØ from PD patients' displaying lower migration speed compared to healthy NØ migration towards CXCL8 and fMLP. It is unclear why the velocity showed no significant difference in gingipain-treated and untreated MØ using Dunn chamber. Taken together, the yFMI is considered as a true chemotaxis effect of all the measurements as explained in section 3.5.1.2 as the yFMI takes into account only these cells moving towards the putative chemoattractant while other measurements account all the cells in spite of their direction travelled.

For the effective MØ migration determination, gingipain-induced MØ were assessed for their migration abilities over a longer time frame using a vertical chemotaxis transwell system. This enabled counting over time to provide additional measures of migration. This system does not include a true gradient but it is a higher throughput assay which enables 24 well plates to be used. Initial experiments were observed for 4h using AC B or AS B as a positive control which has been used previously³⁷. The data in figure 60 shows that no significant difference was observed in gingipain (either RgpB or Kgp)-treated MØ compared to untreated MØ migrating towards AC or AS B cells. Though RgpB showed CD14 cleavage at later time points (figure 47) no effect in MØ chemotaxis was observed. This is interesting as in the Dunn chamber model, Kgp-treated MØ were inhibits yFMI, but not the distance travelled nor the speed of the MØ towards AC B. One of the limitations of using the Cell-IQ model is that other measurements cannot be extracted as the system is designed to count only cells on the transwell or bottom of a 24-well plate. It is possible that the movement of cells is sufficient for them to move through the transwell and, once through the transwell, they cannot ever move back up, so directionality is more difficult to measure in the vertical assay.

Conversely, a significant difference was seen in RgpB or Kgp-treated MØ migration towards AC NØ but not AS NØ compared to untreated MØ at 4h and extended later time points (figure 61 and 62). Additionally, Kgp-treated MØ performed better at the end of 12h

compared to RgpB-treated MØ migration towards AC NØ (figure 61). This indicates that CD14 might be not the only molecule involved in the defective migration as Kgp caused rapid CD14 cleavage compared to RgpB (figure 47) suggesting that other molecules might have undergone modulation for this migrational effect on MØ towards AC NØ. Additionally, increased levels of NØ elastase are correlated with increased gingipain secretion from *P.gingivalis*¹⁸⁴. NØ elastase has been reported to participate in inhibiting the clearance of apoptotic lymphocytes by cleaving CD14³⁷⁰. Hence the gingipains and the NØ elastase together may increase the inhibitory effects and drive inflammation in periodontitis patients. However, future experiments are required to directly assess any role for CD14 in migration by using anti-CD14.

NØ have been reported to use CD31 for directional migration through homotypic interaction with CD31-expressing human umbilical vein endothelial cells by guiding them for transmigration into the tissues⁶⁷¹. Perhaps not surprisingly, the same study observed that using anti-CD31 blocking antibodies impaired directional migration of NØ towards the chemoattractant. Alternatively, complement factors C5a and proteins molecules CXCL8, integrin β 1 were shown to regulate directional migration of the phagocytes. However, gingipains have been described to modulate C5a, CXCL8 and integrin β 1 expression on the immune cells^{179, 194, 567}. C5a enhances directional migration by acting as a chemoattractant protein for mouse MØ (J774A) and alveolar MØ^{672, 673}. On the other hand, IL-8 mediated NØ chemotaxis into the tissues through both phosphatidylinositol 3-kinase (PI3K)- γ - pathways, which has shown to be dysregulated by gingipain proteases⁶⁷⁴. Loss of integrin beta 1 signalling was observed on gingipain-treated endothelial cells and this degradation of integrin β 1 has been associated with upregulation of Bcl-2 expression in CHO cells preventing the cells from undergoing apoptosis^{567, 675}. Due to their adhesion functions, integrins mediate cell motility and aid in the directional migration of cells that have the flexibility to use either integrin-dependent and independent pathways and due to this mechanisms integrins have been proposed as a therapeutic strategy in the treatment of tumour invasion and metastasis mediated disease⁶⁷⁶. Similar approaches may be of use in the treatment of chronic inflammatory disease where cell recruitment is driving disease.

Aside from the above receptors, cytoskeletal actin filaments have been linked to MØ directional migration where actin proteins concentrate themselves at the edge of the MØ guiding them through filopodia - long parallel bundles form movements and lamellipodia - the branching filamentous networks like shape promoting flattening form of chemotaxis on MØ^{506, 677}. Gingipains-mediated degradation of actin filaments, observed in oral epithelial cells, suggests gingipains ability to reorganise the cytoskeleton by degrading the directional proteins^{678, 679}. Formation of actin filaments signals through a series of

molecules and receptors, such as guanosine triphosphate (GTP)-binding proteins (GTPases) and Cdc42, to activate Wiskott-Aldrich syndrome protein (WASP) to aid in the regulation of MØ by promoting directional migration towards various chemoattractants^{680, 681}. Additionally, PI3K and Protein Kinase B were also involved in directional sensing of phagocytes moving towards AC by regulating numerous phosphatidylinositol molecules^{506, 682}. PI3K activation mediates cell directional migration through WASP and Cdc42 molecules so inactivation of phosphatidylinositol 3-Kinase/Akt signalling, which has been observed in gingipain-induced gingival epithelial cells, might downregulate WASP and Cdc42 activation thereby affecting phagocyte chemotaxis^{683, 684}.

5.9.5 Gingipain-mediated alterations in MØ response in the clearance of AC

GPI- anchored CD14 (mCD14) has been widely researched for the uptake of AC however the involvement of the shed, soluble form of CD14 in the AC clearance process is unclear. Rey *et al.* showed that sCD14 binds to surface molecules of activated T cells isolated from PBMC and regulates negatively the activation and function of T lymphocytes by producing IL-2, IL-4, and IFN- γ suggesting that sCD14 might control the level of host inflammatory response by interacting with other negative regulators⁶⁸⁵. Also, a previous study showed that sCD14 binds to AC however, it is unknown whether sCD14 participates in promoting the clearance of AC^{418, 686}. Studies have found that treatment of human MØ with the CD14-specific monoclonal antibody 61D3 blocked the uptake of lipid-symmetric erythrocytes through PS-dependent mechanisms to inhibit the uptake the apoptotic lymphocytes indicating that CD14 might serve as a ligand for the anionic phospholipid phosphatidylserine on AC⁶⁸⁷. In contrast, Devitt *et al.* proposed CD14 as an unlikely receptor for PS on the AC by demonstrating PS-expressing liposomes showed no preferential blocking of apoptotic NØ clearance⁴¹⁸. Additionally, CD14 blocked by mAbs in human MØ or by genetic knockout in mice MØ, showed impaired binding (tethering) of apoptotic lymphocytes suggesting CD14 as a non-redundant tethering receptor for AC²⁸². This correlates with the data presented here shown in figure 63 and 64 that gingipain-treated MØ reveal an inability to bind to AC B or AC NØ and this is likely due to the reduction of CD14 receptors shown on Kgp-treated MØ at the 1h time point (figure 47). Subsequently, a previous study reported that gingipains cleave CD14 from gingival fibroblasts implying that gingipains might impair clearance of AC by CD14 expressing human fibroblast, as seen here in MØ (figure 63 and 64)⁶²⁸. However, RgpB-treated MØ also displayed defective interaction with AC B or AC NØ even when cleavage of CD14 was observed only at 16h (figure 47). These data suggest that CD14 can be made non-functional by gingipains long before it is removed from the cell surface or that other molecules that can be cleaved rapidly by gingipains, might be involved in the apoptotic clearance. Future work could seek to identify these other cleaved receptors.

Additionally, *P.gingivalis* gingipains can modify immune responses in other ways. They regulate the subversion of complement system through degradation of C3 components which are essential for mediating phagocytosis using effector molecules⁵²⁰. Furthermore, all three gingipains have been shown to digest and activate C1q component⁵²⁰. C1q components are demonstrated to be abnormal in patients suffering from lupus and failure of C1q to bind to AC resulted in impaired phagocytosis by monocytes^{688, 689}. Gingipains have also been reported to cleave C5a complement component which is involved in the recruitment and activation of inflammatory cells by inactivating C5a interaction with the anaphylatoxin receptor (C5aR) to form complex with TLR2²¹⁴. TLR2 on NØ has been shown to recognise *P.gingivalis* and regulates MYD88 ubiquitylation and degradation thereby inhibiting antimicrobial secretion by activated NØ^{690, 691}. Taken together, the above studies suggests that gingipains attack the phagocytosis process by degrading the complement factors essential to recognise and mediate the clearance mechanism.

5.10 Conclusion

Uptake of apoptotic NØ within acute inflammatory responses establishes a most important protection against inflammation^{188, 692}. If apoptotic NØ cells are not removed in an appropriate and timely manner, exacerbation of inflammation occurs as a result of cell necrosis. Taken together the data presented here reveal that gingipains may impact inflammation by interfering with the clearance of AC and that this may be mediated by at least two methods: 1. Inhibition of phagocyte migration towards AC, and 2. Inhibition of removal of AC at the level of tethering and engulfment. The net effect of these two points of inhibition would result in delayed AC removal that would be responsible for cell necrosis and associated prolonged inflammation. This work, therefore, raises the possibility that inhibition of gingipain activity may be a useful strategy for preventing or interrupting the chronic inflammation seen in periodontitis.

Chapter 6

Result 4: Regulation of pro and anti-inflammatory cytokines in RgpB and Kgp induced THP-1 MØ

6.1 Introduction

To protect the host from surgical trauma, sudden injury or from invading foreign organisms the host triggers an immune response in the form of release of mediators necessary for defence from the noxious agents ³³. The nature of the inflammatory mediators released during the “war” between the phagocytic cells and microorganism are self-limiting, to ensure there is no significant damage caused to the host ³³⁶. However, the released mediators, e.g. due to failed clearance of NØ in the later stages of an inflammatory response, can cause severe damage to local tissue due to the unintentional release of their destructive contents. Timely removal of AC therefore has to be controlled tightly ^{5, 693}. MØ, the main producer of endogenous modulators on exposure to inflammatory stimuli, produce protein mediators such as cytokines, which decide the nature of the downstream response ⁶⁹⁴. Usually the removal of AC generates an anti-inflammatory response. Phagocytosis of AC NØ is known increase production of anti-inflammatory mediators such as TGF- β and PGE2 ³²⁹. However if the uptake or ingestion of AC is delayed, pro-inflammatory mediators dominate ^{264, 460, 575, 695}. It is currently not clear whether, depending on the receptors that mediate the AC clearance, the level and type of the inflammatory mediators varies. However, Fadok *et al.* demonstrated that PS-mediated uptake of AC was similar to VnR and CD36 receptor-mediated recognition of AC which inhibit pro-inflammatory cytokine production. Additionally, β -glucan treated MØ, which utilised FcR or CR3 for the uptake of AC, also inhibited GM-CSF, IL-8, IL-10 and TNF- α expression and increased TGF- β production ^{329, 696, 697}.

The inflammatory cytokines elicited from microorganism infected immune cells have been widely studied and used as a model for destructive tissue damage and defective resolution of inflammation ^{193, 327, 329, 698}. Here, the oral microbiota serves as an excellent model system to study the inflammatory response provoked by bacteria residing in tissues surrounding the tooth during periodontitis. **Therefore, the aim of this chapter was to study gingipain-induced pro-inflammatory (TNF- α) and anti-inflammatory (TGF- β and IL-10) cytokine levels during protease-treated MØ phagocytosis of AC NØ.**

6.2 LPS-induced TNF- α production

TNF- α is the most commonly used marker of the pro-inflammatory response and is produced by monocytes or MØ treated with stimuli, such as LPS ^{310, 699}. However, clearance of AC has been shown to inhibit pro-inflammatory signals and trigger an anti-

inflammatory response, increasing levels of cytokines such as TGF- β via autocrine/paracrine mechanisms^{329, 697}. Conversely, following LPS stimulation, the phagocytosis process has been studied widely for the immunosuppressive effects by AC, turning off the inflammation induced by LPS stimuli on M \emptyset ⁴⁴⁰.

Preliminary assays were established to assess the dose of *E.coli* LPS (*Ec* LPS) (positive control) required to generate TNF- α production in M \emptyset . To determine the immune suppressive effect of AC B or AS B cells, preliminary experiments were conducted to establish an *Ec* LPS-induced inflammatory response in the THP-1 derived M \emptyset model. VD3 differentiated THP-1 M \emptyset were co-cultured with AC B or AS B cells for 18h. This was followed by *Ec* LPS stimulation for 4h. The TNF- α production was measured using ELISA analysis and results are presented in figure 65.

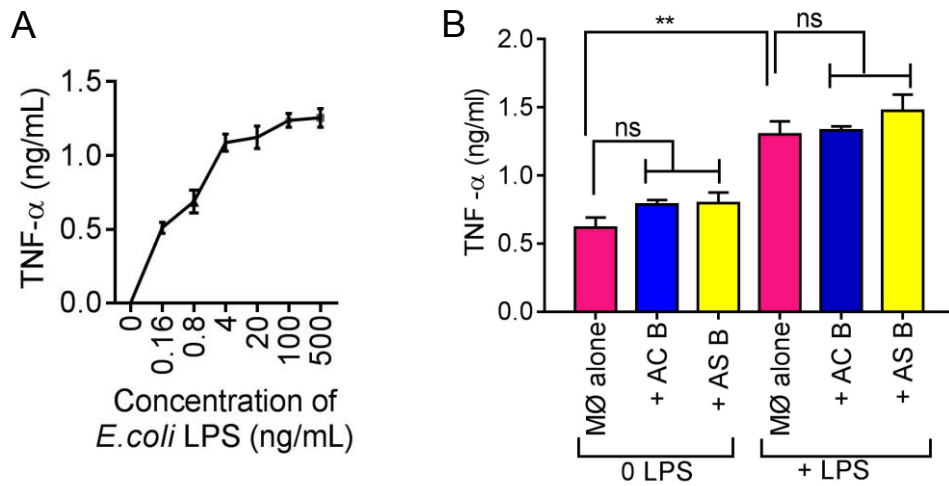


Figure 65: AC B or AS B cells fail to inhibit *E.coli* LPS -induced TNF- α production by M \emptyset

A) Titration of *Ec* LPS-induced TNF- α response of THP-1- derived VD3 M \emptyset . B) VD3 differentiated M \emptyset were either co-cultured with AC B or AS B cells (as described in section 2.5) for 18h at 37 $^{\circ}$ C or were untreated and stimulated with or without LPS (4ng/ml) from *Ec* for 4h at 37 $^{\circ}$ C to induce TNF- α production (as described in section 2.8.1.1 and 2.8.1.2). TNF- α release was quantified using ELISA (as described in section 2.8.3). Data shown are mean \pm SEM of three independent experiments. Statistical analysis was conducted using ANOVA followed by a Bonferroni post-test. ** P < 0.01 not significant (ns) compared with untreated cultures.

The data in figure 65A shows that M \emptyset respond to *Ec* LPS at a range of doses by producing TNF- α . Following titration, 4ng/ml *Ec* LPS was chosen to induce TNF- α production for future experiments as this dose showed a significant response for TNF- α while below 4ng/ml less response for TNF- α can be seen (figure 65A). Figure 65B shows that AC B or AS B cells fail to inhibit TNF- α production induced by 4ng/ml *Ec* LPS. No significant differences were observed in M \emptyset stimulated with LPS in the presence or absence of AC B or AS B. However a significant difference (P < 0.01) was observed in the LPS stimulated TNF- α response in M \emptyset compared with basal level (no LPS) M \emptyset

demonstrating the ability of the THP-1 model to respond by induction of inflammatory cytokine production. This data is in contrast to previous work which has shown that in the presence of AC B cells the LPS-induced inflammation was reduced compared with MØ that were stimulated with LPS alone ³⁶.

The immune suppressive effects of primary AC NØ or AS NØ were also studied in *Ec* LPS-induced inflammatory response in the THP-1 derived MØ model. The results are shown in figure 66.

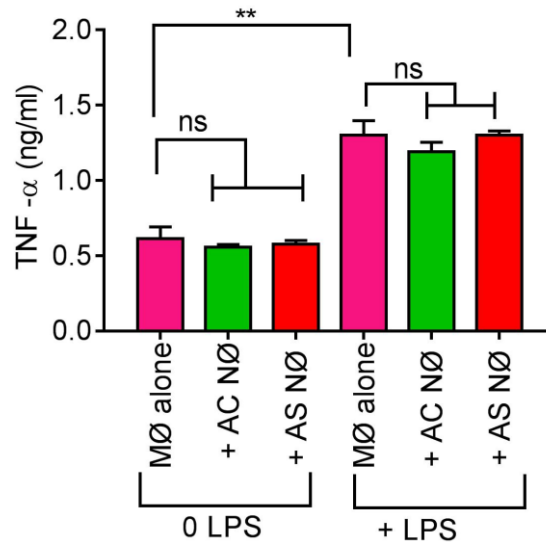


Figure 66: AC NØ or AS NØ cells fail to inhibit *E.coli* LPS -induced TNF- α production by MØ

VD3 differentiated MØ were either co-cultured with AC NØ or AS NØ (as described in section 2.5) cells for 18h at 37°C or were untreated and stimulated with or without LPS (4ng/ml) from *Ec* for 4h at 37°C to induce TNF- α production (as described in section 2.8.1.1 and 2.8.1.2). TNF- α release was quantified using ELISA (as described in section 2.8.1.3). Data shown are mean \pm SEM of three independent experiments. Statistical analysis was conducted using ANOVA followed by a Bonferroni post-test. ** $P < 0.01$ or not significant (ns) compared with untreated.

The data in figure 66 shows similar effects to that observed for AC B or AS B cell treatments. A significant difference ($P < 0.01$) was observed on LPS elicited TNF- α responses on MØ compared with untreated MØ indicating successful induction of TNF- α by LPS. However, again AC NØ or AS NØ failed to inhibit the inflammation induced by *Ec* LPS. Additionally, phagocytosis of AC NØ or AS NØ did not elicit significant TNF- α production compared with untreated MØ alone indicating that the phagocytosis response is generally an anti-inflammatory process, findings in agreement with ³²⁹.

The *P. gingivalis* LPS (*Pg* LPS)-induced signalling pathways remain unclear as conflicting evidence indicates that cell activation occurs through either TLR2 and/or TLR4 ^{120, 147, 150, 327, 700}. Notably however, *Ec* LPS responses are predominately mediated through TLR4 ¹⁴⁶.

⁷⁰¹, ⁷⁰². The LPS isolated from *Pg* used in this study was ultra-pure and obtained from InvivoGen and is reported as a TLR4 agonist ⁷⁰³⁻⁷⁰⁵.

Due to potential differences in the signalling pathways, two models of MØ were initially tested to determine the most appropriate model to elicit a robust TNF- α response in THP-1 derived MØ cells. The models studied were: i) THP-1 VD3 differentiated MØ; and ii) THP-1 DS MØ. The results of these analyses are shown in figure 67.

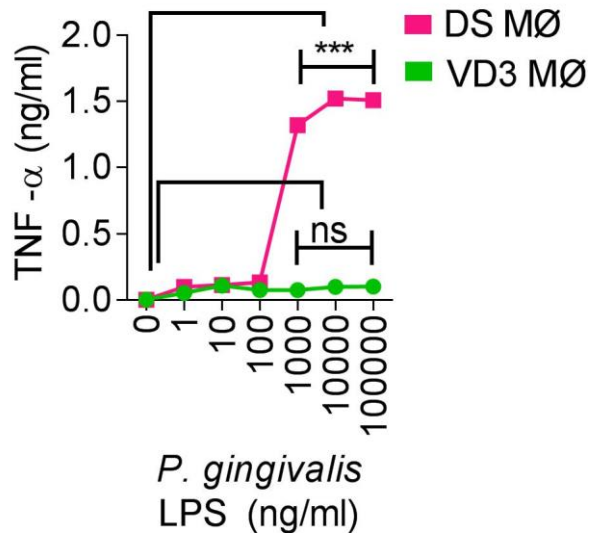


Figure 67: TNF- α response in an LPS (*P.gingivalis*) induced THP-1 derived MØ model

THP-1 cells were washed and suspended in cRPMI and seeded in 24 well plates (1×10^6). Cells were induced with stimulants either VD3 or DS for 48h (as described in section 2.3.5). Following this, *Pg* LPS ($1 \mu\text{g/ml}$) were induced at a range of concentrations for 4h at 37°C and the supernatants were collected and stored at -20°C until TNF- α response were quantified using ELISA (as described in section 2.8.1). Data shown are mean \pm SEM of three independent experiments with each experiment. Statistical analysis was conducted using ANOVA followed by a Bonferroni post-test. *** $P < 0.001$ or not significant (ns) compared with no (0) LPS.

VD3 stimulated MØ showed undetectable TNF- α response to *Pg* LPS stimulation (no significant difference compared with untreated MØ) for 4h (figure 67). However, DS MØ exhibited more robust responses to *Pg* LPS from $1 \mu\text{g/ml}$ by producing increased TNF- α ($P < 0.001$) compared with untreated DS MØ (figure 67). Hence $1 \mu\text{g/ml}$ of *Pg* LPS was chosen as an appropriate dose for use in further studies. Notably Thomas *et al.* showed detectable levels of TLR4 were expressed in DS stimulated THP-1 MØ compared with THP-1 VD3 derived MØ indicating that *Pg* LPS response could be mediated through TLR4 in this model ⁷⁰⁶.

Having observed that DS MØ expressed an enhanced response to *Pg* LPS (figure 67) the presence of AC (either B cells or primary NØ) in suppressing the pro-inflammatory cytokine response was assessed. The results of these studies are shown in figure 68.

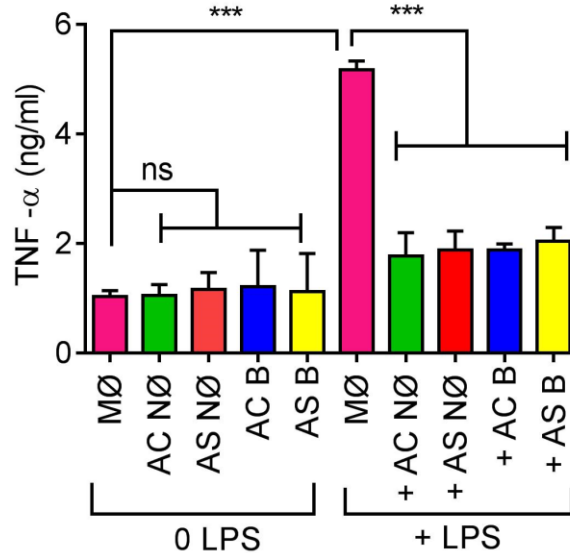


Figure 68: AC inhibit *Pg* LPS-induced TNF- α production

THP-1-derived DS MØ (VD3/PMA) were co-cultured with AC (B or NØ) or their derived AS (as described in section 2.5) for 18h prior to the addition of *Pg* LPS (1 μ g/ml). After 4h stimulation, TNF- α production was assessed using ELISA. Data shown were mean \pm SEM of three independent experiments. Statistical analysis was conducted using ANOVA followed by a Bonferroni post-test. *** P < 0.001 or not significant (ns) compared with untreated cultures.

ELISA data (figure 68) confirmed a significant difference (P < 0.001) in TNF- α production detected between *Pg* LPS-induced MØ compared with untreated MØ. Additionally, the presence of AC (AC B or AS B or AC NØ or AS NØ) significantly (P < 0.001) inhibited the inflammatory response induced by *Pg* LPS in MØ cultures. These data are in contrast to *Ec* LPS (figure 65 and 66) exposure where neither of the AC (B cells or NØ) inhibited the inflammatory response induced by *Ec* LPS (figures 65 and 66). Additionally, these results indicate that the phagocytosis of AC does not trigger further TNF- α release. Both the AS as well as the AC of both NØ and B cells reduced the inflammatory response equally. Previously AS from phagocytic cells have been shown to exhibit anti-inflammatory properties^{614, 615}. These data therefore suggest that *Pg* LPS-induced inflammation can be switched off by AC or their released factors (AS).

6.3 Gingipain induced TNF- α production

A possible mechanism used by pathogens to evade the host defence system is to dysregulate the cytokine networks²¹⁴. Gingipains are known to degrade cytokines such as membrane-bound and the soluble form of TNF- α ^{521, 626}. This process can contribute to deleterious effects such as bone resorption by activating osteoclasts and recruiting NØ causing inflamed periodontal tissues and apoptosis in gingival fibroblast^{707, 708}. Increased levels of TNF- α have been reported at the sites of gingival inflammation indicating that this cytokine might be an indicator for periodontal disease. Notably all forms of gingipains (HRGP, RgpB, and Kgp) have been demonstrated to cleave TNF- α ⁵²².

Whilst attempting to address the effect of gingipain treatment on MØ during inflammatory responses, significant unexpected TNF- α production was noted from MØ that were otherwise untreated. Initial experiments of gingipain treatment were performed in the two MØ model systems (similar to the LPS-induced TNF- α response shown in figure 67) to assess the ability of gingipains to elicit pro-inflammatory cytokine responses. The two models used were i) THP-1 VD3 differentiated MØ; and ii) THP-1 DS MØ. The differentiated MØ (VD3 or DS MØ) were incubated with either of the two gingipains (RgpB and Kgp) and assessed for TNF- α production. Results are shown in figure 69.

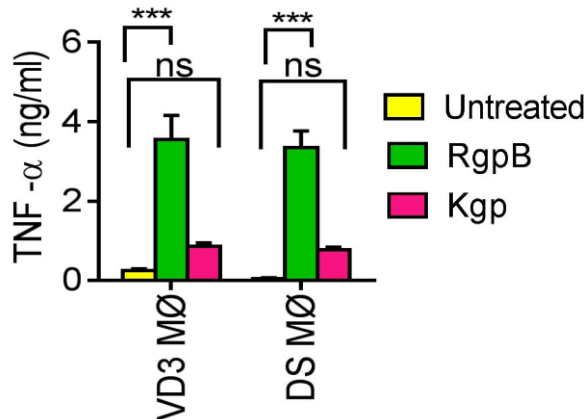


Figure 69: TNF- α release from gingipain-treated MØ

THP-1 derived MØ (VD3-differentiated THP-1 or DS-differentiated THP-1-Yellow) were treated with the gingipains (5 μ g/ml) (RgpB-Green and Kgp-Pink) for 1h at 37°C in a serum-free medium (as described in section 2.7.11) immediately prior to ELISA to measure TNF- α production (as described in section 2.8.1). Data shown are mean \pm SEM from three independent experiments. Statistical analysis was conducted using ANOVA followed by a Bonferroni post-test. *** P < 0.001 or not significant (ns) compared with untreated samples.

Both models (VD3 and DS MØ) produced increased TNF- α inflammation upon stimulation with gingipains following a 1h incubation at 37°C.

The data in figure 69 show that RgpB induces greater TNF- α release compared with Kgp treatment, in both MØ models. RgpB treated VD3 or DS MØ triggered higher TNF- α production (P < 0.01) compared with untreated MØ (controls in both model systems). However, no significant differences were observed between Kgp-treated and untreated MØ. This outcome could be due to the CD14 cleavage observed in Kgp-treated MØ which occurred within 1h of treatment at 37°C compared with RgpB which showed cleavage only at 16h (figure 47, chapter 3). Notably the results presented in figure 69 correlate with a previous study demonstrating that arginine gingipains were efficient in producing higher TNF- α compared with Kgp gingipains⁵²¹.

Having observed that both models of MØ released TNF- α in response to RgpB, the highly adherent DS MØ were used further to study the ability of AC (both B cells and NØ) to inhibit this inflammatory response. Since *P.gingivalis* LPS only induced a response to DS

MØ (figure 67) the same model was used to study gingipain inflammation to enable comparison. This is the first time that the impact of AC on gingipain-induced inflammation has been assessed.

THP-1 DS MØ were incubated with both types of AC (B cells or NØ) for 18h at 37°C. Following incubation, MØ were stimulated with gingipains (either RgpB or Kgp) at 37°C for 1h and the supernatants were collected and assayed for TNF-α measurement using ELISA. The results are shown in figure 70 and 71.

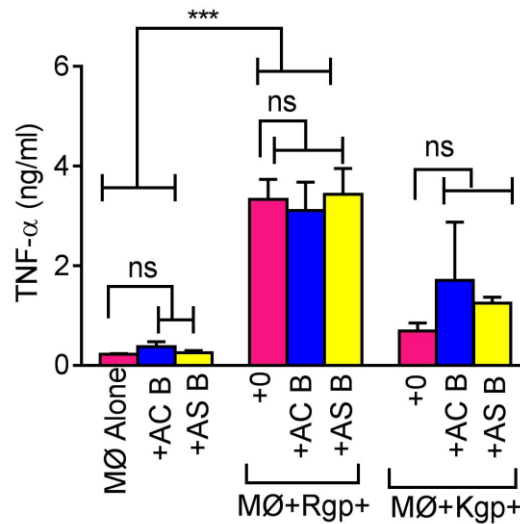


Figure 70: AC B or AS B cells fails to inhibit gingipain-induced TNF-α production

DS THP-1 MØ (VD3/PMA) were co-cultured with AC B or AS B (as described in section 2.5) for 18h prior to treatment with gingipain from *P. gingivalis* to induce TNF-α. Produced TNF-α levels were assessed using ELISA analysis. Data shown were mean ± SEM of three independent experiments. Statistical analysis was conducted using ANOVA followed by a Bonferroni post-test. *** $P < 0.001$ or not significant (ns) compared with untreated samples.

The results presented in figures 70 and 71 suggest that both AC types (B cells or NØ) fail to inhibit the inflammation induced by RgpB in MØ alone. Data presented in figure 69 indicate that Kgp failed to induce significant TNF-α levels. Together, these data (figure 70 and 71) indicate that the clearance of AC in the absence of gingipains can be anti-inflammatory in nature, however, the addition of RgpB alone induced inflammation in MØ and they are resistant to the effects of AC. Moreover, *Pg* LPS-induced inflammation is abrogated by AC (both B cells and NØ) and their derived AS (figure 68) whilst gingipain-induced inflammation is not. These data suggest that gingipains are significant pro-inflammatory modulators which may be key to driving chronic PD pathogenesis.

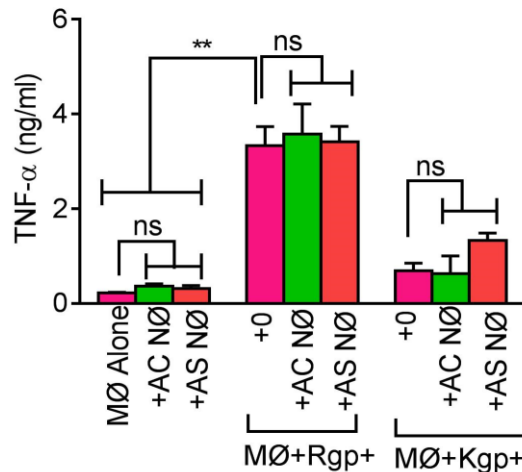


Figure 71: AC NØ or AS NØ cells failed to inhibit gingipain-induced TNF- α production

DS THP-1 MØ (VD3/PMA) were co-cultured with AC NØ or AS NØ (as described in section 2.5) for 18h prior to treatment with gingipain (5 μ g/ml) (as described in section 2.7.11) from *P.gingivalis* to induce TNF- α production. TNF- α levels were assessed using ELISA analysis (as described in section 2.8.1). Data shown were mean \pm SEM of three independent experiments. Statistical analysis was conducted using ANOVA followed by a Bonferroni post-test. ** P < 0.01 or not significant (ns) compared with untreated samples.

6.4 Inhibition of gene expression of TGF- β and IL-10 anti-inflammatory cytokines on gingipain-treated MØ

Clearance of AC is an immunologically silent process which activates anti-inflammatory cytokines via autocrine/paracrine mechanisms resulting in reduced pro-inflammatory mediators^{440, 709}. Notably engulfment of AC promotes the release anti-inflammatory mediators such as TGF- β ²⁷⁹, IL-10⁷¹⁰ as well as other cytokines³²⁹. AC themselves have also been reported to secrete IL-10⁷¹¹ and TGF- β ⁷¹² prior to them encountering MØ. Additionally, the AC use these secreted mediators to promote the activated MØ to engulf them^{713, 714}.

Having shown that RgpB gingipain increased the release of TNF- α from MØ with no apparent inhibitory effects of AC, (figures 70 and 71), the response of anti-inflammatory cytokines TGF- β and IL-10 was assessed at the mRNA level in MØ co-cultured with apoptotic NØ analysed using RT-PCR. VD3 stimulated THP-1 MØ were either co-cultured with apoptotic NØ or cultured alone for 6h at 37°C prior to incubation with gingipains (either RgpB or Kgp) for 1h at 37°C. Subsequently, supernatants were collected at 2000Xg for 10 minutes and the cell pellet was stored at -80°C until RNA isolation was performed.

6.4.1 Quality assessment of isolated RNA

Pelleted cells were treated using the E.Z.N.A total RNA kit I to isolate RNA (as described in the section 2.9.3). Table 9 shows quantified RNA from MØ or co-culture of MØ with AC NØ using the NanoDrop spectrophotometer. A 260/280 ratio was obtained to determine the RNA quality and to estimate the quantity isolated. Samples showing a 260/280 ratio of above 2 were further processed for PCR analysis. The 260/280 ratio was the primary measure for the purity of the nucleic acid and the 260/230 as the secondary measure. Subsequently, cDNA synthesis was performed using 100ng of RNA.

Samples	A ₂₆₀ /A ₂₈₀	A ₂₆₀ /A ₂₃₀	Concentration, ng/µl
MØ	2.18	1.88	217.8
MØ- RgpB	2.24	1.69	165.9
MØ-Kgp	2.14	2.06	338.8
MØ + AC NØ	2.17	1.84	336.7
MØ –RgpB + AC NØ	2.21	0.95	112.1
MØ –Kgp + AC NØ	2.20	1.71	172.4

Table 9: Quantification of RNA for PCR analysis using the NanoDrop 2000c

RNA was isolated using the E.Z.N.A total RNA kit from VD3 stimulated THP-1 MØ or MØ co-culture of with AC NØ. Isolated RNA was quantified using the NanoDrop spectrophotometer. 1µl of the RNA sample was added to the cleaned NanoDrop sample contact apparatus. The 260/280 ratio was determined to assess the purity of RNA. Samples showing 260/280 ratio of above 2 were further processed for PCR. 100ng of RNA was used to perform the downstream PCR analysis. Data shown are representative of three independent experiments. Data shown are mean of ± SEM of three independent experiments.

Having shown the purity of RNA samples using the NanoDrop, agarose gel electrophoresis was implemented as a secondary measure to assess the quality of the RNA. RNA integrity of the ribosomal RNA was evaluated in cells including gingipain-treated MØ and with the co-cultured AC NØ. To check for any signs of degradation of the total RNA, 1% denaturing agarose gel were stained with ethidium bromide (as described in section 2.9.4.2). RNA samples were treated according to the manufacturer's instructions. Samples were viewed under a UVP transilluminator at the end of the electrophoresis period. Results are presented in figure 72.

Intact total RNA was assumed when the rRNA bands were viewed clearly as in figure 72, as distinct 28S and 18S rRNA bands in all the RNA samples. The results presented in

figure 72 also indicate that gingipain treatment of cells did not result in degradation of the integrity of the RNA in the samples.

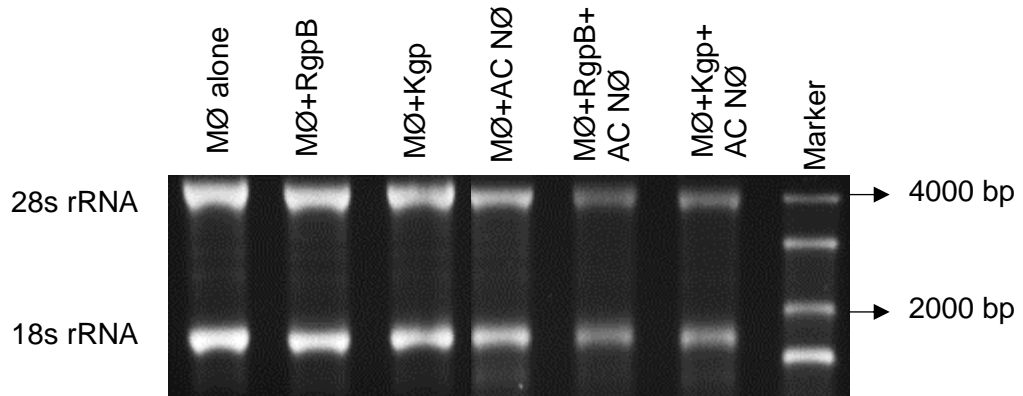


Figure 72: Quality assessment of isolated RNA using agarose gel electrophoresis
 RNA was isolated from the VD3 stimulated THP-1 MØ or from MØ co-cultured with AC NØ (as described in section 2.5.1.2) and incubated for 6h at 37°C followed by gingipain treatment for 1h at 37°C. The isolation of RNA was carried out according to E.Z.N.A total RNA kit I (as described in section 2.9.3). Isolated RNA samples were mixed with 2X sample buffer and incubated for 5 mins at 95°C. Samples were incubated on ice for 1-minute prior to loading in 1% agarose gels (as described in section 2.9.4.2). Gels were electrophoresed for 30 minutes at 60 Volts, 120 Watts at 250 mA and viewed using a UVP transilluminator. Data shown are representative of three independent experiments.

6.4.2 Relative mRNA expression level of TGF-β and IL-10

To assess the level of anti-inflammatory cytokine gene expression at a transcriptional level, purified RNA samples were reverse transcribed to cDNA and the resulting synthesized cDNA were then amplified using specific primers for TGF-β or IL-10 using Syber Green as a fluorescent nucleic acid stain to enable detection of amplified DNA. The housekeeping gene assay used for comparison was β-actin. The amplified DNA represents threshold cycle (Ct) values in the amplification curve obtained from the MxPro-Mx3000P SYBR Green software. The obtained fluorescence Ct values were standardised by setting the baselines and thresholds at the same level to remove background noise from the analysis.

Using a comparative Δ Ct method, (as described in section 2.9.6.3) co-cultured untreated MØ with AC NØ were compared with gingipain-treated (either RgpB or Kgp) co-cultured cells. Results are shown in figure 73.

The data presented in figure 73 show that interaction phagocytosis of AC NØ by MØ provokes increased TGF-β expression ($P<0.001$) compared with MØ on their own indicating that AC promote anti-inflammatory cytokine expression. These data are in agreement with previous findings³²⁹. The results in figure 73 also suggest that a threefold reduction in TGF-β mRNA expression ($P<0.001$) occurred in gingipain (either RgpB or Kgp) treated-MØ co-cultured with AC NØ compared with untreated co-cultured cells.

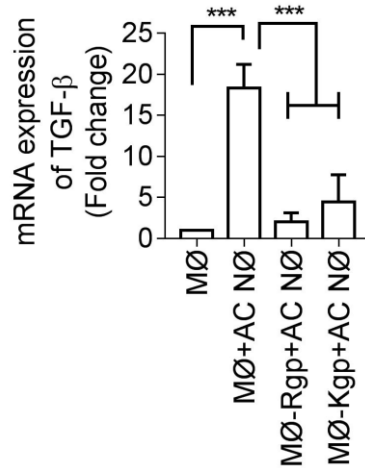


Figure 73: Relative gene expression of TGF- β in gingipain-treated MØ using PCR analysis

VD3 stimulated THP-1 MØ or MØ co-cultured with AC NØ (as described in section 2.5.1.2) incubated for 6h at 37°C followed by gingipain (5 μ g/ml) treatment for 1h at 37°C. RNA was isolated according to E.Z.N.A total RNA kit I (as described in section 2.9.3). Isolated RNA was transcribed to cDNA using the primer design RT-nanoscript. The synthesised cDNA was amplified using specific primers for TGF- β (10 μ M) with human β -actin (100 μ M) used as an internal control (as described in section 2.9.5 and 2.9.6). The histogram shows the mRNA expression of TGF- β in fold change for untreated MØ alone and MØ either treated with gingipain (5 μ g/ml) or untreated and co-cultured with AC NØ for 18h (as described in section 2.7.11). Data shown are mean \pm SEM of three independent experiments. Statistical analysis was conducted using ANOVA followed by a Bonferroni post-test. *** P <0.001 compared to untreated.

IL-10, another anti-inflammatory cytokine-triggered by AC clearance by MØ also participates in enabling tissue homeostasis⁷¹⁵. *In vivo* studies performed in IL-10-deficient mice show that IL-10 regulates the suppression of pro-inflammatory mediators by restricting the inflammatory responses generated by the host defence system⁷¹⁶. The level of the IL-10 anti-inflammatory cytokine was also assessed at a transcriptional level using the purified RNA samples. These were reverse transcribed to cDNA and the resulting synthesized cDNA then amplified using specific primers for IL-10. The results are shown in figure 74.

The data in figure 74 show that AC NØ, in addition to TGF- β , were also able to induce IL-10 expression (P <0.001) in MØ compared with MØ alone. The results also show that gingipains (both RgpB and Kgp) prevent the induction of IL-10 mRNA similar to that observed for TGF- β in the treated MØ (figure 73). Both gingipains exhibited less than a five-fold change in IL-10 expression (P <0.001) compared with untreated MØ with AC NØ exerting a 20 fold-change.

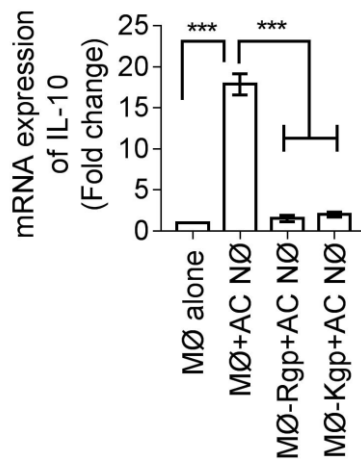


Figure 74: Relative gene expression of IL-10 in gingipain-treated MØ using PCR analysis

VD3 stimulated THP-1 MØ or MØ co-cultured with AC NØ (as described in section 2.5.1.2) incubated for 6h at 37°C followed by gingipain (5µg/ml) treatment for 1h at 37°C. RNA was isolated according to E.Z.N.A total RNA kit I (as described in section 2.9.3). Isolated RNA was transcribed to cDNA using primer design RT-nanoscript. The synthesised cDNA was amplified using specific primers for IL-10 (10µM) with human β-actin (100µM) used as an internal control (as described in section 2.9.5 and 2.9.6). The histogram shows the mRNA expression of IL-10 in fold change for untreated MØ alone and MØ either treated with gingipain (5µg/ml) or untreated and then co-cultured with AC NØ for 18h (as described in section 2.7.11). Data shown are mean ± SEM of three independent experiments. Statistical analysis was conducted using ANOVA followed by a Bonferroni post-test. *** $P < 0.001$ compared to untreated samples.

6.5 Discussion

The classically activated MØ, i.e. M1 phenotype MØ, have been reported to be associated with several systemic diseases compared to M2-anti-inflammatory MØ phenotype^{41, 717-723}. The role of MØ phenotypes at the mRNA level was investigated in the mouse gingival tissues for their participation in PD and studies found that excess generation of M1 markers (nitric oxide synthase, TNF-α, IL-1β, IL-6 and C-reactive protein) were upregulated while M2 markers (CD206 and IL-10) were downregulated^{406, 724, 725}. Activation of monocytes/MØ in the periodontitis rat model was found to elevate TNF-α receptors in MØ, thereby triggering the initial pathogenesis of atherosclerosis causing aortic inflammatory responses⁴⁰⁶. Here, the work aimed to dissect whether gingipains inhibit the production of pro- and anti-inflammatory cytokines at the protein and mRNA levels.

6.5.1 TNF-α production by LPS and gingipains from *P.gingivalis*

Ingestion of AC by MØ has been reported previously to result in decreased TNF-α and IL-8 at the transcription level indicating that removal of AC inhibits pro-inflammatory mediators⁶⁷⁴. This correlates with the findings presented here (figure 68) which show that AC prevent the inflammation by suppressing TNF-α protein production.

To discuss in detail, firstly, the model used for *Ec* LPS was VD3 differentiated MØ (figure 65) which have been shown earlier in this study to express higher CD14 levels (figure 19) and reported elsewhere to express very low TLR4 levels and detectable TLR2 levels^{445, 706}. Additionally, the model used here for *Pg* LPS studies was DS MØ as LPS from *Pg* did not induce responses in VD3 MØ (figure 67). DS MØ showed clear expression of CD14 (figure 19) and a detectable level of TLR4⁷⁰⁶. The similarity between these MØ models is that both models show increased CD14 expression (figure 19) compared to THP-1 cells, though DS MØ show stronger expression of detectable levels of TLR4 while VD3 MØ revealed marked TLR2 receptors^{445, 706}. Whilst studies have shown that TLR4-deficient mice are hyporesponsive to *Ec* LPS, TNF- α production has also been shown to be regulated through TLR-2 receptors in MØ treated with *Ec* LPS suggesting that TLR2 might also be a signalling component for *Ec* LPS endotoxins^{146, 726}.

Sadeghi *et al.* showed, using RT-PCR analysis, the VD3 upon differentiating THP-1 monocytes diminish the TLR4 and TLR2 levels whilst CD14 remained unaltered⁴⁴⁶. This raises the possibility that *Pg* LPS might require either TLR4 or TLR2 presence to stimulate the pro-inflammatory TNF- α production in MØ. This might be a reason for *Pg* LPS inducing responses in DS MØ (which have been reported to express TLR4) but not VD3 MØ. Additionally, a recent study explained that of all the THP-1 differentiated models, PMA-differentiated MØ and DS-MØ, expressed higher TNF- α responses and this might be a consequence of PMA-induced differentiation³⁶. Taken together, the above studies suggest that CD14 and TLR's regulate LPS-associated responses and that cellular differences in receptor expression may explain the different ability of *Pg* and *Ec* LPS to induce inflammatory responses^{500, 700}.

Previously published research investigated two different isoforms of *Pg* LPS, based on their lipid A mass ions, *Pg* LPS1435/1449 and *Pg* LPS1690 and characterised the TNF- α protein levels in the serum of mice stimulated with *Pg* LPS (1435/1449 and 1690) showing variability in the TNF- α response⁷²⁷. Additionally, the same study found that *Ec* LPS induced higher TNF- α levels compared to these two *Pg* isoforms suggesting that *Ec* LPS is more potent compared to *Pg* LPS. This strength of response could be one reason why AC were able to turn off the inflammation induced by *Pg* LPS but remained resistant to *Ec* LPS (figure 65, 66, 68). Both human monocytes and gingival fibroblasts are reported to express both TLR2 and TLR4 and *Pg* LPS acts both as an agonist and antagonist in both these cells for the secretion of inflammatory cytokines^{728, 729}. Subsequently, another study found that *Pg* LPS and *Ec* LPS regulate differentially the production of IL-6 by human gingival fibroblast which expresses both TLR2 and TLR4 suggesting that, depending on the presence of TLR, the LPS from *Pg* or *Ec* controls the production of inflammatory mediators in the gingival tissues⁷⁰⁰.

In LPS, the lipid A core is a highly conserved amphipathic molecule linked to a hydrophilic phosphorylated D-glucosamine disaccharide by hydrophobic fatty acid chains (C12-C14). It is the biologically potent component of LPS. It is also responsible for LPS' non-specific interaction with host cells via fusion with the phospholipid membrane which has been considered as a possible mechanism of action in activating immune cells ⁷³⁰⁻⁷³². *Pg* lipid A contains fatty acids composed of 16–17 carbon atoms however, the absence of an ester-linked phosphate group at the 4' position and fatty acids at positions 3 and 3' and differences in the core sugar composition marks them as a unique structure compared to *Ec* lipid A structure (figure 75) ^{733, 734}. For this reason, low endotoxic activity is reported for *Pg* LPS compared to *Ec* LPS in human monocytes ^{138, 735}. This is consistent with the study shown here (figure 65 and 67) revealing maximal TNF- α production from M \emptyset stimulated with only 4ng/ml for *Ec* LPS but at 1 μ g/ml for *Pg* LPS.

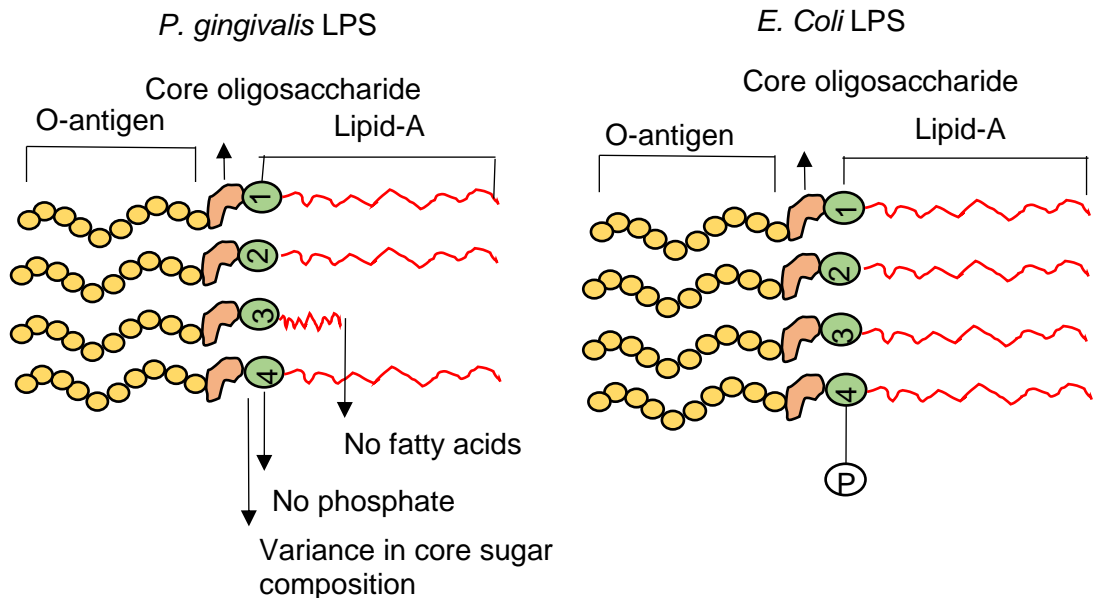


Figure 75: Structure of *Pg* LPS and *Ec* LPS

The diagram depicts the major components of, LPS. *Pg* LPS is composed of three main subunits, O-antigen, core oligosaccharides that attaches to lipid A through sugars, which has been varied in the *Pg* LPS compared to *Ec* LPS. Followed by sugars, Lipid A components in *Pg* LPS varies in fatty acids at 3 position along with absence of phosphate group at 4 position compared to *Ec* LPS. While *Ec* LPS displays all the major components without missing sugars, fatty acids and phosphate groups. Adapted from ⁷³³

The amino-terminal region of CD14 on M \emptyset provides several different locations for *Ec* LPS binding sites ⁷³⁶. In human CD14, three leucine-rich domains are reported to be responsible for *Ec* LPS binding and activation of host cells ⁷³⁷. Additionally, highly hydrophilic regions of four CD14 proteins in addition to region 3 and 4 of CD14 were reported to participate in *Ec* LPS binding which was characterised by mAb epitope mapping using multiple alanine replacement mutations ⁷³⁸⁻⁷⁴⁰. Notably, region 1 of CD14 was described to be involved in *Ec* LPS signaling ⁷³⁷.

Studies have revealed the binding sites of *Pg* LPS in CD14 differs from *Ec* LPS CD14 binding sites⁷³⁶. *Pg* LPS fails to elicit E-selectin expression on non-myeloid cells such as human endothelial cells due to reduced or no expression of CD14. However, *Ec* LPS facilitates E-selectin expression both on myeloid and non-myeloid cells⁷⁴¹. This is explained by CD14-dependent pathways theory that CD14 uses electrostatic interactions to capture different microbial ligands using their charged residues (hydrophilic region) on their surface. Also, to support the explanation that *Pg* LPS and *Ec* LPS binds to different regions of CD14 a series of CD14 proteins were analysed⁷³⁶. The outcome of the studies identified that residues E11K of CD14 partially reduced and D59K of CD14 completely inhibited the *Pg* LPS binding compared to wildtype CD14 confirming *Pg* LPS have moderate affinity towards E11 residues of CD14. However no difference in *Ec* LPS binding to both E11 and D59 were observed compared to wildtype CD14 suggesting that *Ec* LPS have higher affinity towards both residues⁷³⁶.

Subsequently, studies using anti-CD14 mAbs on MØ showed prevention of AC binding to CD14^{324, 418}. Earlier, the same mAbs MEM-18 was shown to inhibit LPS recognition of CD14⁷³⁹. Taken together, Devitt *et al.* proposed that the binding sites for LPS and AC on CD14 were either identical or close³²⁴. Later, Thomas *et al.* investigated the binding of apoptotic lymphocytes to HeLa cells expressing CD14 mutants³⁶. These studies also revealed glutamic acid residue 11 (E11) as an apoptotic recognition site on CD14. Earlier studies suggested that E11 may bind *Pg* LPS but perhaps not *Ec* LPS⁷³⁶.

Together, the above theory supports the data presented here, that AC NØ were able to prevent the inflammation induced by *Pg* LPS (figure 68) but not from *Ec* LPS (figure 65 and 66). This may be the result of competition for CD14 as both *Pg* LPS and AC might have similar CD14 binding patterns. However, *Ec* LPS may have a different binding site on CD14 and so may be unaffected.

The results presented here in figure 69 suggests that low TNF- α was found in Kgp-compared to RgpB-induced MØ cells. This might be due to the cleaved CD14 demonstrated in VD3 MØ (figure 47) within 1h by Kgp and later time points (16h) by RgpB at 37°C (figure 47) perhaps suggesting a requirement for CD14 in regulating TNF- α production. Additionally, *Pg* LPS induced TNF- α inflammation only in the DS MØ (figure 67) while RgpB induced TNF- α both on VD3 and DS MØ (figure 69) suggesting that gingipain-induced inflammation is not as a result of LPS contamination.

The possible CD14 cleavage sites for Rgp and Kgp are reported to be 21 Arg-X and 9 LYS-X bonds respectively and for TLR4 29 Arg and 35 Lys amino acid sequence^{627, 628, 742, 743}. Moreover, deletion of amino acids 9-12 and 35-39 both singly, or in combination, within the N-terminal 65 amino acid region of CD14 have been demonstrated to eliminate

the binding of the mAb MY4 which blocks LPS binding and therefore has been used as an indicator of the LPS binding site^{627, 744}. Followed by this, Sugawara *et al.* proposed that gingipains might cleave CD14, eliminating MY4 binding and hence resulting in reduced LPS-induced TNF- α response.

Interestingly, AC N \emptyset , which were able to turn off the TNF- α inflammation induced by LPS from *Pg* (figure 68), failed to prevent the inflammation induced from gingipains both RgpB and Kgp (figure 70 & 71). Though the same M \emptyset model (DS differentiated M \emptyset) was used to induce TNF- α responses by LPS or gingipains, the difference in inhibiting the inflammation, by AC N \emptyset or their derived AS, suggests that gingipains may be the most potent mediators of inflammation and that this may be resistant to usual mechanisms of control (e.g. by AC). This also suggests that gingipains may be more significant in causing or driving PD than LPS. It is also important to note that, despite RgpB treatment of DS M \emptyset being only 1h and *Pg* LPS treatment was for 4h, the level of released TNF- α response induced by the *Pg* LPS (figure 67) and RgpB (figure 69) was similar, again supporting the idea that RgpB may be an extremely potent driver of inflammation in periodontal disease.

6.5.2 Role of anti-inflammatory cytokines in PD

Enhanced anti-inflammatory and immunosuppressive cytokines are reported to be produced from monocytes cultured with AC and following LPS stimulation, AC reduce pro-inflammatory responses⁴⁴⁰. Interaction of M \emptyset with apoptotic N \emptyset for 1h increased by 40% the release of TGF- β 1 cytokine and when left for 18h this increased to three times the expression of TGF- β compared to control³²⁹. These correlate with the results shown in figure 73, where M \emptyset fed with AC N \emptyset produced increased TGF- β 1 mRNA compared to untreated M \emptyset indicating that AC may stimulate the expression of anti-inflammatory cytokines. Additionally, M \emptyset treated with gingipains, either Rgp or Kgp, did not increase TGF- β mRNA in response to AC N \emptyset (figure 73). This reduced TGF- β mRNA level correlates with the reduced AC clearance seen following gingipain treatment. Together, these suggest that TGF- β induction is linked closely to AC binding and uptake. Future work could seek to address that gingipains might have destabilised TGF- β mRNA in the phagocytes.

Additionally, upregulated TGF- β expression was found in *Pg* LPS- induced human gingival fibroblasts compared to *Pg* LPS-induced periodontal ligament suggesting that gingival fibroblasts might be the likely source⁷⁴⁵. Consequently, it was reported that greater production of TGF- β stimulates the release of IL-6 from T helper cells and together these cytokines produce massive amounts of IL-17 which have been associated with alveolar bone loss in chronic periodontitis patients^{597, 746}. Moreover, *Pg* has been reported to regulate human aortic smooth muscle cells through activation of TGF- β and stimulating

the human aortic smooth muscle cells to bind to LDL thereby causing cardiovascular disease⁷⁴⁷.

Similar to TGF- β , mRNA for IL-10, another significant anti-inflammatory cytokine, was downregulated in the gingipain-stimulated M ϕ phagocytosing AC N ϕ (figure 74). This correlates with previous findings that reduced IL-10 is found in periodontal lesions compared to healthy gingival tissues⁷⁴⁸. In contrast, IL-10 levels were found to be significantly higher in gingivitis patients compared to those who progressed to periodontitis⁷⁴⁹. This suggests that in initial stages of inflammation IL-10 may be induced. However, on progressing to advanced PD the bacterial factors such as gingipains may modulate IL-10 expression leading to reduced effects. Together, reduction in the mRNA levels of TGF- β and IL-10 indicates that gingipain might have affected the transcription of the phagocytes inhibiting mRNA stability thereby affecting the production of these cytokines.

Studies addressing cytokine levels in PD have demonstrated that no difference in IL-10 is observed in human gingival fibroblasts or periodontal ligament cells treated with LPS (*P.gingivalis*) compared to untreated cells⁷⁴⁵. This suggests that LPS is a weaker stimulant compared to the gingipains (both RgpB and Kgp) which reduced IL-10 mRNA expression in M ϕ (figure 74). *In vivo* studies using IL-10 knockout mice reveal severe bone loss suggesting that IL-10 could be an important mediator of alveolar bone homeostasis⁷⁵⁰⁻⁷⁵⁴. Moreover, IL-10 has been proposed as a potential therapeutic strategy for bone resorption to improve osteoporosis by dental implantation in osteoporotic periodontitis patients⁷⁵⁴.

The uptake and ingestion of the AC N ϕ by M ϕ are important, as they may be sufficient to induce protective anti-inflammatory responses. However, the data presented here (figure 73) suggests that impaired clearance might lead to reduced TGF- β expression. Previous study stated that in *in vivo* CD14^{-/-} mice showed reduced AC clearance but no evidence of inflammation suggesting that the AC even when not eaten are enough to induce anti-inflammatory cytokine production⁴¹⁸. Additionally, a knock out study demonstrated that dendritic cells derived from the bone marrow of IL-10 deficient mice on stimulation with LPS inhibited ingestion of AC suggesting that the presence of IL-10 is essential to mediate efficient phagocytosis⁷⁵⁵.

Taken together, these data suggest gingipains inhibit both TGF- β and IL-10 gene expression at the mRNA level (figure 73 and 74) and increase, in the case of RgpB, pro-inflammatory cytokines (TNF- α) as shown in this chapter (figure 67) suggesting that gingipains evade the host immune system by inhibiting the production of anti-inflammatory mediators. This could be a possible underlying mechanism contributing to the pathogenesis of chronic periodontal disease.

6.5.3 Other cytokine levels in periodontal diseases

While this work has focused on TNF- α , TGF- β and IL-10, alterations in other cytokines may also affect PD. Studies show that IL-1 β , a primary pro-inflammatory cytokine was found to be elevated in the GCF of periodontitis patients compared to healthy controls ⁷⁵⁶. Human gingival epithelial cells challenged with live *Pg* induced increased IL-1 β ⁷⁵⁷. Additionally, the same work investigated gingipain-deficient *Pg* mutant bacteria (lacking both Arg and Lys) and revealed that they were unable to induce IL-1 β , IL-6 and IL-8 degradation. Lys-gingipain-deficient *Pg* (Kgp⁻) mutants completely lacked the ability compared to Arg-gingipain-deficient (Rgp⁻) *Pg* mutant. These data indicate that Kgp is a potent inflammatory activator in *Pg* compared to Rgp. However, the study presented here show that RgpB as a potent inducer of TNF- α inflammation compared to Kgp suggesting that modulation in cytokines level might have varied depending on the stimulants.

Previous work has shown that IFN- γ and GM-CSF are activators of M ϕ in response to bacterial infections, playing an important regulatory role in mediating innate and adaptive immunity ⁷⁵⁸. Fitzpatrick *et al.* investigated the cDNA array of human M ϕ exposed to gingipains and found increased levels of IFN- γ and GM-CSF in addition to IL-1 β cytokines ⁴²⁹. The activation of phosphorylated p38 α MAPK has been linked to increased TNF- α and IL-8 on human M ϕ stimulated with gingipains, resulting in modulation of chemokines ⁵⁶³, ⁷⁵⁹. Other components of *Pg*, such as fimbriae, have been shown to participate in contributing to IL-1 β , IL-6, and TNF- α production in murine peritoneal M ϕ , and have been shown to be responsible for forming resorption pits on the dentine slices ⁷⁶⁰.

6.6 Conclusion

Overall, the work in this chapter suggests that M ϕ fed AC N ϕ have suppressed production of pro-inflammatory cytokines (TNF- α) in response to LPS from *Pg*. This may be mediated by the AC-induced anti-inflammatory cytokines (TGF- β and IL-10), which are increased at the mRNA levels. However, on gingipain treatment, the cytokine levels were altered. The role of cleaved CD14 has been suggested for LPS hypo responsiveness shown in Kgp-mediated M ϕ while, RgpB-treated M ϕ showed hyper responsiveness to produce TNF- α suggesting that CD14 might be a mediator responsible for TNF- α production. Additionally, AC N ϕ are able to prevent the inflammation induced by *Pg* LPS but not from gingipains. This needs further analyses to elucidate the factors released by AC, by determining the presence of other immune modifying factors (e.g. presence of lipid mediators produced by M ϕ fed AC) and their level of contribution in inhibiting gingipain-mediated or LPS-mediated inflammation.

Taken together, the above findings may suggest that, along with gingipains other components of *Pg* bacteria might also promote aberrant inflammation in PD and thereby

contributing to the inflamed gingival crevice. Importantly, the work in this chapter suggests that RgpB appears to be a strong driver of inflammation (TNF- α). Perhaps providing Rgp inhibitors locally might help to break the significant pro-inflammatory responses such that the normal anti-inflammatory mechanisms associated with normal AC clearance might function to resolve the inflammation.

Chapter 7

7 Discussion

Following tissue injury and activation of the inflammatory cascade, there is a rapid effort to resolve inflammation by eradicating the pathogens, infected cells and the resultant AC by professional phagocytes. This is undertaken through a rapidly changing pro-inflammatory to anti-inflammatory response which promotes normal healing⁶⁰⁸. Thus the inflammatory response is a vital protective mechanism that regulates complex defence factors in the host, allowing them to gain access to infected or damaged sites and finally to restore tissue homeostasis. It is a collective response of white blood cells, cytokines, chemokines and other soluble factors to establish a healed and repaired milieu.

A central event in this is the apoptotic death of inflammatory cells. Clearance of dying and dead cells is regarded as a nonphlogistic phenomenon associated with the immunomodulatory and anti-inflammatory process and this promotes the turning off of pro-inflammatory responses^{35, 329}. Indeed the importance of this process can be seen when it fails. Deficient or failed clearance of AC by MØ leads to necrosis and this is connected with pro-inflammatory consequences resulting in auto-immune disease^{43, 286}. A series of PRRs recognise both PAMPs and AC, identified by innate immune receptor ligation studies²⁸² and knockout mice work^{284, 285, 761} demonstrating that inefficient clearance of AC promote secondary necrosis contributing to the progression of chronic inflammatory diseases in the host system. One such inflammatory disease is periodontitis. Though initiated by oral pathogens, aberrant inflammatory responses occur in susceptible individuals and this is the key to the progression to PD⁸. Thus PD provides an interesting model in which it is possible to try to understand the complex relationships between host-pathogen interaction, inflammation, and resolution of inflammation, as studied here. It also serves as a model to understand systemic diseases initiated by the inflammatory mediators.

P.gingivalis is a major microorganism strongly associated with chronic PD and it promotes advanced periodontal lesions by proliferating to a high cell number within the gingival region resulting in bone resorption and ultimately in tooth loss¹⁰⁷. The components of *P.gingivalis* that promote this pathogenesis have been studied recently in regard to evasion of the immune system^{118, 121, 147, 172} and this research underlines that the proteases, gingipains, synthesised by *P.gingivalis* are responsible for inhibition of the immune system and exacerbating the inflammatory response in the host^{94, 202, 526}.

Due to the enormous number of NØ present at the gingival crevice/epithelium, it is clear that these cells play a major role in the pathogenic mechanisms in PD by deciding the fate

of inflammation (chronic inflammation or resolution). Increased amounts of necrotic NØ³⁵⁶ and destructive hydrolytic enzymes indicate that their timely removal is essential to chronic periodontitis disease resolution¹⁹⁰. However, this process has never been fully studied thus far and hence the work presented here sought to address this knowledge gap. It is known that various chemoattractants, such as CXCL12, IL-8, IL-1 β , C5a, and exogenous signals recruit NØ to the crevicular region leading to an unwanted and continued infiltration of cells that subsequently become necrotic^{351, 358}. Indeed impaired NØ chemotaxis⁶⁶² or reduced NØ phagocytic activity have also been suggested as a cause for tissue destruction at periodontal sites⁷⁶². While a number of studies have examined NØ function and their chemotaxis ability, there has not been a strong focus on MØ clearance of AC NØ in a periodontal inflammation context. As such, this study also provides new and additional insights into MØ clearance of AC, including studies on their migration and interaction with AC NØ, in addition to the ability of AC NØ to turn off the inflammation by stimulating the release of anti-inflammatory mediators in a gingipain-affected environment. This thesis therefore builds on and contributes to work in the field of AC clearance within the PD context.

7.1 MØ phagocytosis mechanisms in human periodontal disease

Differentiated tissue MØ are activated in response to an infection and have been simplistically viewed as a professional scavenger of pathogens and AC. However, they use a cascade of molecules and biochemical reactions to rapidly eradicate unwanted cells and restore homeostasis³⁵. The appearance of AC and their released apoptotic bodies within MØ is a sure indication that MØ are the professional “eaters”⁷⁶³. While MØ clearance of AC is regarded as non-inflammatory³²⁹, the persistence of AC due to defective uptake by MØ *in vivo* can result in the absence of pro-inflammatory consequences however this is likely a consequence of a specific clearance defect²⁸². Notably, clearance of necrotic cells is associated with pro-inflammatory and an immune-stimulatory response⁷⁶⁴⁻⁷⁶⁶ and failure of AC clearance is widely linked with autoimmunity and chronic inflammatory diseases^{43, 348, 471, 576, 767}. Currently it is not clear as to whether periodontitis pathogenesis is associated with autoimmune mechanisms, however, its relationship with rheumatoid arthritis suggests that the immunological and pathological links are identical in both diseases⁷⁶⁸. Inflammatory NØ are regarded as one of the main drivers of the destruction seen in the periodontal tissues and a deficiency in AC clearance mechanisms has recently been suggested as a major reason for the persistent inflammation in PD^{190, 191, 356, 662}. However, the precise defects in AC clearance remain ill-defined.

The THP-1 model used previously within the Devitt Laboratory provides an excellent model for studying the clearance of AC cells and AC B cells acted as a positive control in

this study with clearance of human AC NØ as a primary target ^{36, 37, 444}. The data presented here demonstrated that the differentiated THP-1 MØ migration towards, and interaction with, human AC NØ, a novel effect were comparatively lower than to AC B cells. This latter limitation has also been previously shown in HMDM ⁴¹⁸. Additionally, THP-1 differentiated MØ responses to microbial stimuli (i.e. LPS and gingipains) showed higher cytokine expression suggesting their ability to generate pro-inflammatory and suppress anti-inflammatory responses. Collectively, the data presented indicate that the THP-1 MØ model system provides a good model system for studying AC NØ clearance.

This thesis tested the hypothesis: **In the presence of *P. gingivalis* factors, MØ lose their ability to migrate and phagocytose the AC due to the cleavage of AC clearance receptors prompting a dominant pro-inflammatory response that may contribute to chronic inflammation and tissue destruction in periodontal disease.** The data presented support the premise that defective AC clearance might be a mechanism underpinning the pathophysiology of the periodontal disease.

Evidence 1 - CD14 is a preferred substrate for gingipains

Hoffman *et al.* proposed a “tether and tickle” hypothesis to describe the interaction between phagocytes and AC suggesting a two-part model whereby the initial binding of AC (tether), induced (tickled) a phagocytotic response and anti-inflammatory signalling, that was essential for successful clearance of AC. Furthermore, the study explained that PS exposure alone is not sufficient for the uptake of AC, with additional receptors on the phagocytes (e.g. CD14, CD68, CD36, and $\alpha_v\beta_3$ integrin) being required for the binding to promote the engulfment process ²⁸⁰. In order to study the AC clearance in PD, here, a list of AC clearance receptors on the MØ exposed to gingipains was studied.

Of the gingipains RgpB and Kgp, Kgp elicited rapid cleavage of CD14 on MØ compared with RgpB which demonstrated CD14 degradation only at 16h. This might be due to the presence of hemagglutinin/adhesion domain in Kgp which is absent in RgpB. Notably, the adhesion and binding capacity of the hemagglutinin/adhesion domain for haemoglobin and haem, might underpin the ability to lyse the epithelial cell barrier causing bleeding and swelling in the gums ^{164, 183, 544}. This adhesion and binding capability of Kgp might also be the reason for the rapid action of Kgp targeted against MØ by degrading CD14 compared, with RgpB which lacks these domains.

In addition to CD14, CD31 cleavage has also been noticed on MØ and NØ. Nevertheless, CD14 cleavage was rapid compared to CD31 suggesting that CD14 might be a crucial substrate for gingipains in driving PD. Though Kgp reduced CD31 on MØ it is not clear whether reduction of CD31 in NØ is due to spontaneous apoptosis or to the effect of gingipains. However, previous findings suggests that RgpB cleaves CD31 on the cell

surface of both viable and AC NØ¹⁸⁸. It is also important to note that that cleavage of these receptors i.e. both CD31 and CD14 were reduced on both the phagocytes i.e. MØ and NØ at same time points. Taking into consideration that gingipains cleaved CD14 and CD31 on the MØ and NØ their role on promoting migration and engulfment has been discussed further.

Evidence 2 - Impact of gingipains on MØ migration and phagocytosis

The initial activity after MØ sensing the chemoattractants is to migrate to AC. Based on the data obtained in this study suggests that both RgpB and Kgp affects the phagocytes directionality resulting in poor recruitment to AC, which is seen in using horizontal chemotaxis assays. It is not clear whether CD14 participates in regulating directional migration of phagocytes. Though CD14 knock out studies propose that CD14 acts as an important tethering receptor to AC, yet to date no study confirmed CD14 role on promoting migration³²⁴.

However, *in vivo* studies studying immune cells from calves revealed higher expression of CD14 on monocytes recruited to lymph nodes at the onset of inflammation suggesting that CD14 might be responsible for sensing the inflammatory mediators and thereby enabling prompt transmigration activities of monocytes⁷⁶⁹. However, it is unclear whether CD14 increased expression is a consequence of the transmigration. Furthermore, CD31 is known to participate in the directional migration of viable NØ via homotypic interaction of CD31-CD31 between NØ and endothelial cells. CD31 blocking antibodies are known to reduce directional NØ migration but not velocity towards the chemoattractant⁶⁷¹. Studies using CD31-deficient mice demonstrated overall normal transmigration activity of NØ however, NØ were specifically trapped between the endothelium and basement membrane signifying the non-directional movement of CD31 lacking NØ^{770, 771}

Following migration, the macrophages tether and uptake the AC. Devitt *et al.* observed that CD14-deficient mouse MØ showed reduced binding and phagocytosis of AC B cells and subsequently proposed that CD14 acts as a tethering receptor facilitating the uptake of AC²⁸². Similarly, CD14-dependent phagocytosis of Gram-negative bacteria by human monocytes and THP-1 cells, reveals a requirement for CD14 in not only clearing AC but also bacterial compounds^{772, 773}. Data presented here show poor interaction and phagocytosis of AC B cells or AC NØ in gingipain-treated MØ (both RgpB and Kgp-treated) suggesting that cleavage of CD14 inhibits the tethering capacity which, in turn, prevents the phagocytosis by MØ. Additionally, CD31, 'don't eat me' signals are also proposed as a tethering receptor essential to discriminate a viable from an AC, switching from a repulsive mode (on viable cells) to an adhesion mode (on AC)³³⁸. Kgp cleaved CD31 on MØ at 16h suggesting that gingipain dysregulates CD31 signals by inhibiting

homotypic interactions essential for tethering to AC through their CD31-adhesive mode signals. Also, reduced CD31 by Kgp on viable MØ might be the reason for poor recruitment to AC NØ seen in vertical chemotaxis assay. However, a previous study reported that the cleavage of CD31 alone might not be sufficient for cell uptake but may also require exposure of PS at the surface of AC NØ ¹⁸⁸.

Collectively these data correlate with those presented here, which have been validated using a series of established AC clearance receptors CD14, CD36, ICAM-3 and CD91. Though the presence of other AC clearance receptors was found on MØ, the absence of CD14 due to the gingipain cleavage might be an explanation for poor AC clearance reported in PD patients. In addition, CD31 might have also participated in migrational events of the phagocytes with some of the previous studies specifically underscoring CD31 for the ability to regulate directional migration. Together, these receptors might have played a possible mechanism for the presence of relatively high number of necrotic NØ compared with AC NØ reported in the gingival crevice and periodontal pockets in PD patients ³⁵⁶. Of course, it is possible that gingipains also cleave other receptors that have not yet been identified but which function in apoptotic cell clearance.

Evidence 3 – Impact of gingipains on MØ inflammatory mediators

The data presented here suggest that both LPS and gingipains from *P.gingivalis* induce similar levels of TNF- α , however, LPS from *P.gingivalis* only induces responses in THP-1 DS MØ whereas gingipains induced responses in both the THP-1 VD3 and THP-1 DS MØ models. This might be due to a difference in expression pattern recognition receptors present in the THP-1 models. For example, TLR4 is more readily detectable in DS MØ compared with THP-1 or THP-1 VD3 MØ and this may explain why *P.gingivalis* LPS induces responses only in those models expressing TLR4. However similar levels of CD14 expression were previously observed in both the differentiated MØ models ⁷⁰⁶. Interestingly, multiple reports have proposed that TLR2 rather than TLR4 may be critical for host response to infection with *P. gingivalis* ^{119, 774}. Furthermore, due to the highly heterogeneous nature of the lipid A of *P.gingivalis* LPS, activated primary bone marrow cells obtained from both TLR2 and TLR4 knockout mice suggest a functional interaction of *P.gingivalis* LPS with both TLR2 and TLR4 ¹⁴⁷. In addition previously it has been reported that TLR2 is downregulated on both VD3 and PMA alone differentiated MØ derived from THP-1 cells ⁴⁴⁵. Collectively, these data may indicate that *P.gingivalis* LPS-mediated responses may be regulated through TLR4 rather than TLR2 in the THP1-derived MØ used in this study.

Previous studies confirm that both TLR4 and TLR2 levels are unaffected on gingipain-treated murine MØ and for TLR4 levels on human monocytes ^{626, 627}. These previous

finding may support with the data presented here which suggests that gingipains elicit TNF- α expression in both THP-1 M ϕ models indicating the effect might be both TLR4- and TLR2-independent. Notably, gingipain responses might be dependent on CD14 for inducing inflammation, as Kgp-treated M ϕ exhibit a lower production of TNF- α compared with RgpB-treated M ϕ suggesting a rapid clearance of CD14 proteolytically by Kgp might downregulate synthesis of TNF- α . This may agree with previous findings that indicate a CD14 reduction on human monocytes treated with gingipains also induced lower TNF- α production following LPS stimulation⁶²⁷. Taken together, the data here further support the hypothesis that M ϕ CD14 cleavage by gingipains attenuates cellular recognition of bacterial components in addition to reducing the tethering and migration capacity of phagocytes compelling them to mediate a dominant inflammatory response in the host immune system.

7.2 Mechanistic differences in AC N ϕ response to LPS and gingipains

M ϕ ingestion of AC N ϕ inhibits production of pro-inflammatory mediators and enhances anti-inflammatory cytokine production through autocrine/paracrine mechanisms³²⁹. This is in agreement with the findings presented in this study which suggest that AC N ϕ ingested by M ϕ mediate increased TGF- β and IL-10, at the mRNA level, and reduced TNF- α at the protein level. Interestingly, AC N ϕ inhibit TNF- α levels induced by *Pg* LPS but not gingipains. Similar results were seen using LPS/gingipain-induced TNF- α inflammation in M ϕ ingesting AC B cells. This highlights that gingipains being inflammatory the AC fails to turn off the inflammation unlike in LPS-induced M ϕ . Subsequently AC might act differentially in regulating the modulation of pro-inflammatory cytokines in LPS compared with gingipain-induced inflammation in M ϕ .

Persistence of AC in CD14-deficient mice fails to elicit a pro-inflammatory response, however, the study also suggested that anti-inflammatory ticking is still present in spite of reduced tethering and removal of AC²⁸². This suggests that AC binding can be separated from the ability of AC to exert anti-inflammatory effects (i.e. it is possible to separate the “tether” and “tickle”). However, the data obtained here indicate that CD14 cleaved gingipain-treated M ϕ ingestion of AC N ϕ lose anti-inflammatory cytokines. This suggests that gingipains may inhibit the production of anti-inflammatory cytokines through CD14 or other receptors cleavage on M ϕ in response to AC and thus results in the persistence of a pro-inflammatory condition. Taken together, the data presented here suggest that AC N ϕ may regulate M ϕ responses through CD14 for triggering both pro- and anti-inflammatory properties to prevent the inflammation induced by *P.gingivalis* components and that this might be a reason for the dominant TNF- α response in periodontitis patients which is reported.

Figure 76 summarises the function of MØ in a gingipain-exposed environment where phagocytes are either altered, through modifying their AC clearance receptors or their phagocytic activity, thereby governing aberrant inflammatory response in PD patients.

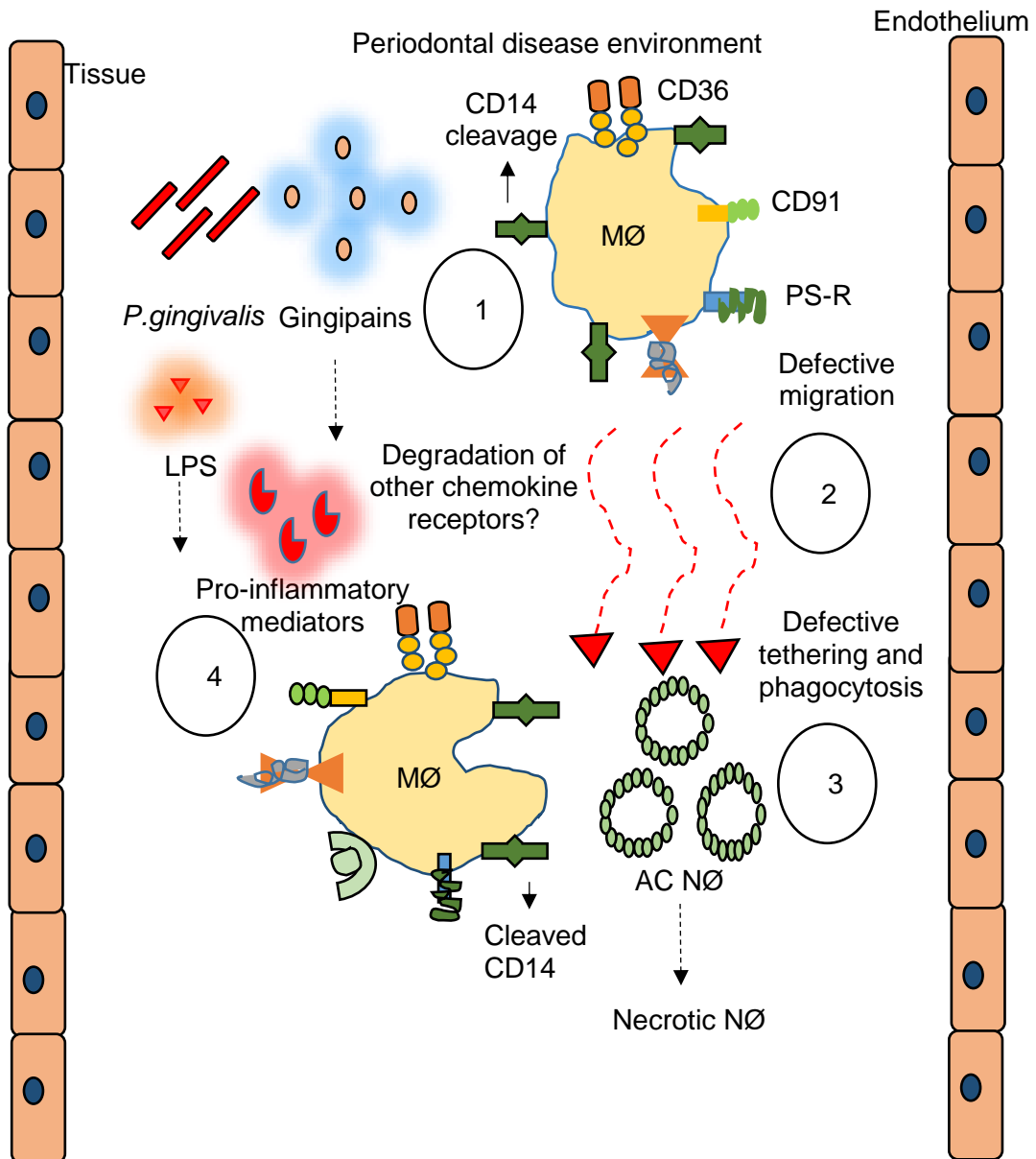


Figure 76: Possible defective AC clearance mechanism involved in PD

1. Gingipains from *P.gingivalis* cleave CD14 from MØ. 2. The cleavage of CD14 receptor together with degradation of other chemokine (e.g. IL-8) receptors on MØ modulates MØ migration towards AC. 3. Reduction of CD14 inhibits tethering and phagocytosis of AC by MØ resulting in AC becoming necrotic. 4. Failure of clearance of AC together with the inflammation induced by LPS and gingipains might contribute to enhanced and chronic inflammation within the PD patients'.

7.3 Conclusion

This thesis originally proposed the hypothesis that in the periodontitis tissue microenvironment, MØ are defective for migration, tethering and phagocytosing AC via cleavage of receptors associated with recognition and phagocytosis by MØ, leading to a dominant inflammatory response in PD patients. This study used an *in vitro* AC clearance model utilising THP-1 differentiated MØ and primary AC NØ to study the effect of the *P.gingivalis* virulent proteases, gingipains, on MØ function. This was to model the context of destructive PD. The data presented here suggest that among a panel of AC clearance receptors gingipains preferentially cleaved CD14 at the surface of MØ as well as CD31, a 'don't-eat me'/tethering receptor. Additionally, gingipain-treated MØ demonstrate poor directional migration and phagocytosis activity (i.e. tethering and uptake) towards AC NØ. This might be due to the lack of CD14 on MØ exposed to gingipain regulating the tethering capacity on MØ though the reason for defective migration is still not clear. Furthermore the findings are in agreement with previous work which indicate that CD14 acts as a tethering receptor for AC. Notably the dominant inflammatory response in gingipain-treated MØ fails to be turned off by AC even though AC NØ prevent LPS-induced inflammatory responses in phagocytes. In an inflammatory capacity, AC NØ might regulate anti-inflammatory responses in MØ through CD14-dependent ingestion of AC. Hence the work done here contributes to the literature of defective AC clearance in chronic inflammatory PD and advances current knowledge of the pathophysiology of the periodontal disease. The profound effect of CD14 degradation by Kgp on MØ migration is also a route by which *in vivo* gingipains may support defective AC clearance.

The findings from this work are of interest in the study of the complex process of CD14-mediated inflammation and CD14-mediated resolution of inflammation in physiology and pathophysiology. Future work will build on the data obtained here to apply this knowledge to understanding various inflammatory and autoimmune diseases and, in so doing, may contribute to the development of new therapeutic strategies.

7.4 Future work

Whilst the work presented here extends significantly the knowledge in the field, there are a number of areas where additional research may address gaps in knowledge that remain. Further research could be conducted in the following areas:

- 1) The discovery that anti-CD14 blocking antibodies (MEM-18 and 61D3) applied to phagocytes inhibit MØ ligand-binding responses of AC and also LPS binding suggests that both LPS and AC binding patterns share the same epitopes or neighbouring sites on CD14³²⁴. Additionally, using a panel of anti-CD14 blocking antibodies or point mutations has identified the crucial CD14 regions involved in

the AC binding to MØ³⁶. With this knowledge in mind, a direct analysis can be performed to study whether gingipains bind CD14 and, if so, do they share identical or nearby epitopes on MØ CD14. The work presented here and previous work suggest that gingipain cleaved CD14 MØ caused hyporesponsivity for the production of pro-inflammatory cytokines⁶²⁶. Therefore, gingipain effects on CD14 signalling partners to induce cellular responses could be further characterised.

- 2) The data presented here indicate that TLCK inhibits the proteolytic activity of gingipains in CD14 cleavage. Furthermore, the knowledge from previous studies predicts that 21 Arg and 9 Lys bonds are the possible cleavage sites in CD14^{627, 628, 742}. Therefore, proteomic studies using mass spectrometry might provide an understanding of the specific cleavage sites in CD14. If the identification of the cleaved peptides confirms the specific cleavage sites, investigation of this peptide region in MØ chemotaxis and related biological activity could be undertaken.
- 3) The work within this study indicates that Kgp induces less TNF- α compared with RgpB treatment and that AC NØ fail to prevent the inflammation induced from either of the gingipains. This is despite CD14 presence in RgpB treated MØ compared with Kgp at 1h. Earlier studies have shown that CD14-deficient mice, despite the chronic presence of AC, exhibited no overt TNF- α production²⁸². Therefore, CD14-mediated inflammatory signalling should be further explored to determine the role of CD14-dependent stimulation on inflammatory mediators in response to AC.
- 4) While mCD14 has been studied widely for its clearance role, CD14 proteolysis by gingipains might also function to release the sCD14. The participation of sCD14 in triggering or blocking the clearance of AC is unknown. However previous studies have shown that gingipains degrade both mCD14 and sCD14 from human monocytes. Notably, sCD14 acts as a soluble mediator in AC tethering to enable their uptake by MØ^{282, 627}. Another study also demonstrated that on exposure to *P.gingivalis* fimbriae, human gingival epithelial cells failed to stimulate cytokines due to the weaker expression of mCD14 and their inability to utilise sCD14⁷⁷⁵. Therefore, sCD14 detection in the culture supernatant of MØ treated with gingipains would be valuable. Further, it would be important to analyse whether 1) sCD14 promotes AC clearance and 2) if gingipains bind to sCD14 and whether this acts as an anti-inflammatory or pro-inflammatory strategy mediating AC clearance.
- 5) Similar to AC NØ, the AS derived from apoptotic NØ also inhibit the inflammation induced by *P.gingivalis* LPS on MØ in this study. Characterisation of the pro-resolving mediators derived from AC NØ or their AS which modulate inflammation might provide a broad view of the mechanisms involved in achieving the resolution

phase of inflammation for application in periodontal therapy and other NØ related pathologies.

- 6) *In vivo* studies using *P.gingivalis*-infected mice with specific gingipain inhibitors resulted in improved periodontal health with reduced bone resorption and tissue destruction⁷⁷⁶⁻⁷⁷⁹. Therefore, using a combined CD14-mediated therapy along with the existing gingipain treatment might act as a possible approach which targets the reprogramming of the inflammatory cascade in periodontal disease. Indeed it would also be useful to ensure that gingipain inhibitors restore effective AC clearance *in vivo* and potentially clinical trials in this area could be undertaken.

References

1. Lawrence, T., D.A. Willoughby&D.W. Gilroy, Anti-inflammatory lipid mediators and insights into the resolution of inflammation. *Nat Rev Immunol*, 2002. **2**(10): p. 787-795.
2. Barton, G.M., A calculated response: Control of inflammation by the innate immune system. *Journal of Clinical Investigation*, 2008. **118**(2): p. 413-420.
3. Mogensen, T.H., Pathogen recognition and inflammatory signaling in innate immune defenses. *Clin Microbiol Rev*, 2009. **22**(2): p. 240-73, Table of Contents.
4. Serhan, C.N.&J. Savill, Resolution of inflammation: the beginning programs the end. *Nat Immunol*, 2005. **6**(12): p. 1191-7.
5. Serhan, C.N., S.D. Brain, C.D. Buckley, D.W. Gilroy, C. Haslett, L.A. O'Neill, M. Perretti, A.G. Rossi&J.L. Wallace, Resolution of inflammation: state of the art, definitions and terms. *Faseb j*, 2007. **21**(2): p. 325-32.
6. Maskrey, B.H., I.L. Megson, P.D. Whitfield&A.G. Rossi, Mechanisms of resolution of inflammation: a focus on cardiovascular disease. *Arterioscler Thromb Vasc Biol*, 2011. **31**(5): p. 1001-6.
7. Trowbridge, H.O., & Emling, R. C., *Inflammation: a review of the process*. 1989, Chicago: Quintessence Pub. Co.
8. Cekici, A., A. Kantarci, H. Hasturk&T.E. Van Dyke, Inflammatory and immune pathways in the pathogenesis of periodontal disease. *Periodontol 2000*, 2014. **64**(1): p. 57-80.
9. McInnes, I.B.&G. Schett, Cytokines in the pathogenesis of rheumatoid arthritis. *Nat Rev Immunol*, 2007. **7**(6): p. 429-442.
10. Ito, T.&U. Ikeda, Inflammatory cytokines and cardiovascular disease. *Curr Drug Targets Inflamm Allergy*, 2003. **2**(3): p. 257-65.
11. Libby, P., P.M. Ridker&A. Maseri, Inflammation and Atherosclerosis. *Circulation*, 2002. **105**(9): p. 1135-1143.
12. Amor, S., F. Puentes, D. Baker&P. van der Valk, Inflammation in neurodegenerative diseases. *Immunology*, 2010. **129**(2): p. 154-69.
13. Hotamisligil, G.S., Inflammation and metabolic disorders. *Nature*, 2006. **444**(7121): p. 860-867.
14. McDaniel, M.L., G. Kwon, J.R. Hill, C.A. Marshall&J.A. Corbett, Cytokines and nitric oxide in islet inflammation and diabetes. *Proc Soc Exp Biol Med*, 1996. **211**(1): p. 24-32.
15. McCracken, J.M.&L.-A.H. Allen, Regulation of Human Neutrophil Apoptosis and Lifespan in Health and Disease. *Journal of Cell Death*, 2014. **7**: p. 15-23.
16. Erwig, L.P.&P.M. Henson, Clearance of apoptotic cells by phagocytes. *Cell Death Differ*, 2007. **15**(2): p. 243-250.
17. Kurihara, T., G. Warr, J. Loy&R. Bravo, Defects in Macrophage Recruitment and Host Defense in Mice Lacking the CCR2 Chemokine Receptor. *The Journal of Experimental Medicine*, 1997. **186**(10): p. 1757-1762.
18. Kono, H.&K.L. Rock, How dying cells alert the immune system to danger. *Nature reviews. Immunology*, 2008. **8**(4): p. 279-289.
19. Bianchi, M.E., HMGB1 loves company. *J Leukoc Biol*, 2009. **86**(3): p. 573-6.
20. Das, S.T., L. Rajagopalan, A. Guerrero-Plata, J. Sai, A. Richmond, R.P. Garofalo&K. Rajarathnam, Monomeric and Dimeric CXCL8 Are Both Essential for In Vivo Neutrophil Recruitment. *PLoS ONE*, 2010. **5**(7): p. e11754.
21. Kolaczowska, E.&P. Kuberski, Neutrophil recruitment and function in health and inflammation. *Nat Rev Immunol*, 2013. **13**(3): p. 159-75.
22. Muller, W.A., Getting Leukocytes to the Site of Inflammation. *Veterinary pathology*, 2013. **50**(1): p. 7-22.
23. Ley, K., C. Laudanna, M.I. Cybulsky&S. Nourshargh, Getting to the site of inflammation: the leukocyte adhesion cascade updated. *Nat Rev Immunol*, 2007. **7**(9): p. 678-689.
24. Segal, A.W., How Neutrophils Kill Microbes. *Annu Rev Immunol*, 2005. **23**: p. 197-223.
25. Reeves, E.P., M. Nagl, J. Godovac-Zimmermann&A.W. Segal, Reassessment of the microbicidal activity of reactive oxygen species and hypochlorous acid with reference to the phagocytic vacuole of the neutrophil granulocyte. *Journal of medical microbiology*, 2003. **52**(Pt 8): p. 643-651.
26. Gazendam, R.P., J.L. van Hamme, A.T. Tool, M. van Houdt, P.J. Verkuijlen, M. Herbst, J.G. Liese, F.L. van de Veerdonk, D. Roos, T.K. van den Berg&T.W. Kuijpers, Two independent killing mechanisms of *Candida albicans* by human neutrophils: evidence from innate immunity defects. *Blood*, 2014. **124**(4): p. 590-7.

References

27. Brinkmann, V., U. Reichard, C. Goosmann, B. Fauler, Y. Uhlemann, D.S. Weiss, Y. Weinrauch & A. Zychlinsky, Neutrophil Extracellular Traps Kill Bacteria. *Science*, 2004. **303**(5663): p. 1532-1535.
28. Krautgartner, W.D., M. Klappacher, M. Hannig, A. Obermayer, D. Hartl, V. Marcos & L. Vitkov, Fibrin mimics neutrophil extracellular traps in SEM. *Ultrastruct Pathol*, 2010. **34**(4): p. 226-31.
29. De, Y., Q. Chen, A.P. Schmidt, G.M. Anderson, J.M. Wang, J. Wooters, J.J. Oppenheim & O. Chertov, LI-37, the Neutrophil Granule–And Epithelial Cell–Derived Cathelicidin, Utilizes Formyl Peptide Receptor–Like 1 (Fpr1) as a Receptor to Chemoattract Human Peripheral Blood Neutrophils, Monocytes, and T Cells. *The Journal of Experimental Medicine*, 2000. **192**(7): p. 1069-1074.
30. Chertov, O., H. Ueda, L.L. Xu, K. Tani, W.J. Murphy, J.M. Wang, O.M.Z. Howard, T.J. Sayers & J.J. Oppenheim, Identification of Human Neutrophil-derived Cathepsin G and Azurocidin/CAP37 as Chemoattractants for Mononuclear Cells and Neutrophils. *The Journal of Experimental Medicine*, 1997. **186**(5): p. 739-747.
31. Awad, A.S., G.R. Kinsey, K. Khutsishvili, T. Gao, W.K. Bolton & M.D. Okusa, Monocyte/macrophage chemokine receptor CCR2 mediates diabetic renal injury. *American Journal of Physiology - Renal Physiology*, 2011. **301**(6): p. F1358-F1366.
32. Varin, A., S. Mukhopadhyay, G. Herbein & S. Gordon, Alternative activation of macrophages by IL-4 impairs phagocytosis of pathogens but potentiates microbial-induced signalling and cytokine secretion. *Blood*, 2010. **115**(2): p. 353-62.
33. Serhan, C.N., N. Chiang & T.E. Van Dyke, Resolving inflammation: dual anti-inflammatory and pro-resolution lipid mediators. *Nature reviews. Immunology*, 2008. **8**(5): p. 349-361.
34. Maddox, J.F., M. Hachicha, T. Takano, N.A. Petasis, V.V. Fokin & C.N. Serhan, Lipoxin A4 stable analogs are potent mimetics that stimulate human monocytes and THP-1 cells via a G-protein-linked lipoxin A4 receptor. *J Biol Chem*, 1997. **272**(11): p. 6972-8.
35. Gregory, C.D. & A. Devitt, The macrophage and the apoptotic cell: an innate immune interaction viewed simplistically? *Immunology*, 2004. **113**(1): p. 1-14.
36. Thomas, L., A. Bielemeier, P.A. Lambert, R.P. Darveau, L.J. Marshall & A. Devitt, The N-terminus of CD14 acts to bind apoptotic cells and confers rapid-tethering capabilities on non-myeloid cells. *PLoS One*, 2013. **8**(7): p. e70691.
37. Torr, E.E., D.H. Gardner, L. Thomas, D.M. Goodall, A. Bielemeier, R. Willetts, H.R. Griffiths, L.J. Marshall & A. Devitt, Apoptotic cell-derived ICAM-3 promotes both macrophage chemoattraction to and tethering of apoptotic cells. *Cell Death Differ*, 2012. **19**(4): p. 671-9.
38. Cairns, A.P., A.D. Crockard & A.L. Bell, CD36-mediated apoptotic cell clearance in SLE. *Lupus*, 2001. **10**(9): p. 656-7.
39. Miyanishi, M., K. Tada, M. Koike, Y. Uchiyama, T. Kitamura & S. Nagata, Identification of Tim4 as a phosphatidylserine receptor. *Nature*, 2007. **450**(7168): p. 435-9.
40. Mevorach, D., J.O. Mascarenhas, D. Gershov & K.B. Elkon, Complement-dependent Clearance of Apoptotic Cells by Human Macrophages. *The Journal of Experimental Medicine*, 1998. **188**(12): p. 2313-2320.
41. Lee, W.J., S. Tateya, A.M. Cheng, N. Rizzo-DeLeon, N.F. Wang, P. Handa, C.L. Wilson, A.W. Clowes, I.R. Sweet, K. Bomsztyk, M.W. Schwartz & F. Kim, M2 Macrophage Polarization Mediates Anti-inflammatory Effects of Endothelial Nitric Oxide Signaling. *Diabetes*, 2015. **64**(8): p. 2836-2846.
42. Lawrence, T. & D.W. Gilroy, Chronic inflammation: a failure of resolution? *International Journal of Experimental Pathology*, 2007. **88**(2): p. 85-94.
43. Hanayama, R., M. Tanaka, K. Miyasaka, K. Aozasa, M. Koike, Y. Uchiyama & S. Nagata, Autoimmune disease and impaired uptake of apoptotic cells in MFG-E8-deficient mice. *Science*, 2004. **304**(5674): p. 1147-50.
44. Soehnlein, O. & L. Lindbom, Phagocyte partnership during the onset and resolution of inflammation. *Nat Rev Immunol*, 2010. **10**(6): p. 427-39.
45. Pittman, K. & P. Kubes, Damage-Associated Molecular Patterns Control Neutrophil Recruitment. *Journal of Innate Immunity*, 2013. **5**(4): p. 315-323.
46. Hanayama, R., M. Tanaka, K. Miwa, A. Shinohara, A. Iwamatsu & S. Nagata, Identification of a factor that links apoptotic cells to phagocytes. *Nature*, 2002. **417**(6885): p. 182-7.
47. Fadok, V.A., D.L. Bratton, S.C. Frasch, M.L. Warner & P.M. Henson, The role of phosphatidylserine in recognition of apoptotic cells by phagocytes. *Cell Death Differ*, 1998. **5**(7): p. 551-62.
48. Gershov, D., S. Kim, N. Brot & K.B. Elkon, C-Reactive protein binds to apoptotic cells, protects the cells from assembly of the terminal complement components, and sustains an

- antiinflammatory innate immune response: implications for systemic autoimmunity. *J Exp Med*, 2000. **192**(9): p. 1353-64.
49. Voll, R.E., M. Herrmann, E.A. Roth, C. Stach, J.R. Kaldeh&I. Girkontaite, Immunosuppressive effects of apoptotic cells. *Nature*, 1997. **390**(6658): p. 350-351.
 50. Laskin, D.L.&K.J. Pendino, Macrophages and inflammatory mediators in tissue injury. *Annu Rev Pharmacol Toxicol*, 1995. **35**: p. 655-77.
 51. Hanes, P.J.&R. Krishna, Characteristics of inflammation common to both diabetes and periodontitis: are predictive diagnosis and targeted preventive measures possible? *The EPMA Journal*, 2010. **1**(1): p. 101-116.
 52. Pihlstrom, B.L., B.S. Michalowicz&N.W. Johnson, Periodontal diseases. *Lancet*, 2005. **366**(9499): p. 1809-20.
 53. White, D., N. Pitts, J. Steele, K. Sadler&B. Chadwick. Disease and related disorders – a report from the Adult Dental Health Survey 2009 2011.
 54. Watt, R.G., J.G. Steele, E.T. Treasure, D.A. White, N.B. Pitts&J.J. Murray, Adult Dental Health Survey 2009: implications of findings for clinical practice and oral health policy. *Br Dent J*, 2013. **214**(2): p. 71-5.
 55. Kreshover, S.J.&A.L. Russell, Periodontal Disease. *The Journal of the American Dental Association*. **56**(5): p. 625-629.
 56. Russell, A.L., The Periodontal Index. *Journal of Periodontology*, 1967. **38**(6 Part II): p. 585-591.
 57. Goodson, J.M., A.C. Tanner, A.D. Haffajee, G.C. Sornberger&S.S. Socransky, Patterns of progression and regression of advanced destructive periodontal disease. *Journal of Clinical Periodontology*, 1982. **9**(6): p. 472-481.
 58. Prayitno, S.W., M. Addy&W.G. Wade, Does gingivitis lead to periodontitis in young adults? *Lancet*, 1993. **342**(8869): p. 471-2.
 59. Shah, N., N. Bansal&A. Logani, Recent advances in imaging technologies in dentistry. *World Journal of Radiology*, 2014. **6**(10): p. 794-807.
 60. Tribble, G.D.&R.J. Lamont, Bacterial invasion of epithelial cells and spreading in periodontal tissue. *Periodontology 2000*, 2010. **52**(1): p. 68-83.
 61. Dale, B.A., Periodontal epithelium: a newly recognized role in health and disease. *Periodontol 2000*, 2002. **30**: p. 70-8.
 62. Michalowicz, B.S., D. Aeppli, J.G. Virag, D.G. Klump, J.E. Hinrichs, N.L. Segal, T.J. Bouchard Jr&B.L. Pihlstrom, Periodontal findings in adult twins. *Journal of Periodontology*, 1991. **62**(5): p. 293-299.
 63. Loe, H., The role of bacteria in periodontal diseases. *Bulletin of the World Health Organization*, 1981. **59**(6): p. 821-825.
 64. Sorsa, T., L. Tjäderhane, Y.T. Konttinen, A. Lauhio, T. Salo, H.M. Lee, L.M. Golub, D.L. Brown&P. Mäntylä, Matrix metalloproteinases: Contribution to pathogenesis, diagnosis and treatment of periodontal inflammation. *Annals of Medicine*, 2006. **38**(5): p. 306-321.
 65. Noguchi, K.&I. Ishikawa, The roles of cyclooxygenase-2 and prostaglandin E2 in periodontal disease. *Periodontology 2000*, 2007. **43**(1): p. 85-101.
 66. Hikiji, H., T. Takato, T. Shimizu&S. Ishii, The roles of prostanoids, leukotrienes, and platelet-activating factor in bone metabolism and disease. *Progress in Lipid Research*, 2008. **47**(2): p. 107-126.
 67. Yucel-Lindberg, T.&T. Bage, Inflammatory mediators in the pathogenesis of periodontitis. *Expert Rev Mol Med*, 2013. **15**: p. e7.
 68. Dias, I.H., J.B. Matthews, I.L. Chapple, H.J. Wright, C.R. Dunston&H.R. Griffiths, Activation of the neutrophil respiratory burst by plasma from periodontitis patients is mediated by pro-inflammatory cytokines. *J Clin Periodontol*, 2011. **38**(1): p. 1-7.
 69. Page, R.C., Milestones in periodontal research and the remaining critical issues. *Journal of Periodontal Research*, 1999. **34**(7): p. 331-339.
 70. Engebretson, S.P., J.T. Grbic, R. Singer&I.B. Lamster, GCF IL-1beta profiles in periodontal disease. *J Clin Periodontol*, 2002. **29**(1): p. 48-53.
 71. Yucel, O.O., E. Berker, L. Mescil, K. Eratalay, E. Tepe&I. Tezcan, Association of interleukin-1 beta (+3954) gene polymorphism and gingival crevicular fluid levels in patients with aggressive and chronic periodontitis. *Genet Couns*, 2013. **24**(1): p. 21-35.
 72. Noh, M.K., M.I.N. Jung, S.H. Kim, S.R. Lee, K.H. Park, D.H. Kim, H.H. Kim&Y.G. Park, Assessment of IL-6, IL-8 and TNF- α levels in the gingival tissue of patients with periodontitis. *Experimental and Therapeutic Medicine*, 2013. **6**(3): p. 847-851.
 73. Varghese, S.S., H. Thomas, N.D. Jayakumar, M. Sankari&R. Lakshmanan, Estimation of salivary tumor necrosis factor-alpha in chronic and aggressive periodontitis patients. *Contemporary Clinical Dentistry*, 2015. **6**(Suppl 1): p. S152-S156.

References

74. Singh, P., N.D. Gupta, A. Bey&S. Khan, Salivary TNF-alpha: A potential marker of periodontal destruction. *Journal of Indian Society of Periodontology*, 2014. **18**(3): p. 306-310.
75. Wright, H.J., J.B. Matthews, I.L. Chapple, N. Ling-Mountford&P.R. Cooper, Periodontitis associates with a type 1 IFN signature in peripheral blood neutrophils. *J Immunol*, 2008. **181**(8): p. 5775-84.
76. Dutzan, N., R. Vernal, M. Hernandez, A. Dezerega, O. Rivera, N. Silva, J.C. Aguillon, J. Puente, P. Pozo&J. Gamonal, Levels of interferon-gamma and transcription factor T-bet in progressive periodontal lesions in patients with chronic periodontitis. *J Periodontol*, 2009. **80**(2): p. 290-6.
77. Papanthanasίου, E., F. Teles, T. Griffin, E. Arguello, M. Finkelman, J. Hanley&T.C. Theoharides, Gingival crevicular fluid levels of interferon-gamma, but not interleukin-4 or -33 or thymic stromal lymphopoietin, are increased in inflamed sites in patients with periodontal disease. *J Periodontal Res*, 2014. **49**(1): p. 55-61.
78. Liao, C.-H., W. Fei, Z.-H. Shen, M.-P. Yin&C. Lu, Expression and distribution of TNF- α and PGE2 of periodontal tissues in rat periodontitis model. *Asian Pacific Journal of Tropical Medicine*, 2014. **7**(5): p. 412-416.
79. Båge, T., A. Kats, B.S. Lopez, G. Morgan, G. Nilsson, I. Burt, M. Korotkova, L. Corbett, A.J. Knox, L. Pino, P.-J. Jakobsson, T. Mod  er&T. Yucel-Lindberg, Expression of Prostaglandin E Synthases in Periodontitis: Immunolocalization and Cellular Regulation. *The American Journal of Pathology*, 2011. **178**(4): p. 1676-1688.
80. Sanchez, G.A., V.A. Miozza, A. Delgado&L. Busch, Salivary IL-1beta and PGE2 as biomarkers of periodontal status, before and after periodontal treatment. *J Clin Periodontol*, 2013. **40**(12): p. 1112-7.
81. Gursoy, U.K., E. Kononen, S. Huuonen, T. Tervahartiala, P.J. Pussinen, A.L. Suominen&T. Sorsa, Salivary type I collagen degradation end-products and related matrix metalloproteinases in periodontitis. *J Clin Periodontol*, 2013. **40**(1): p. 18-25.
82. Sorsa, T., U.K. Gursoy, S. Nwhator, M. Hernandez, T. Tervahartiala, J. Leppil  hti, M. Gursoy, E. Kononen, G. Emingil, P.J. Pussinen&P. Mantyla, Analysis of matrix metalloproteinases, especially MMP-8, in gingival crevicular fluid, mouthrinse and saliva for monitoring periodontal diseases. *Periodontol* 2000, 2016. **70**(1): p. 142-63.
83. Leppil  hti, J.M., P.A. Hernandez-Rios, J.A. Gamonal, T. Tervahartiala, R. Brignardello-Petersen, P. Mantyla, T. Sorsa&M. Hernandez, Matrix metalloproteinases and myeloperoxidase in gingival crevicular fluid provide site-specific diagnostic value for chronic periodontitis. *J Clin Periodontol*, 2014. **41**(4): p. 348-56.
84. Gutierrez-Venegas, G., O. Alonso Luna, J.A. Ventura-Arroyo&C. Hernandez-Bermudez, Myricetin suppresses lipoteichoic acid-induced interleukin-1beta and cyclooxygenase-2 expression in human gingival fibroblasts. *Microbiol Immunol*, 2013. **57**(12): p. 849-56.
85. Ishii, K., H. Hamamoto, K. Imamura, T. Adachi, M. Shoji, K. Nakayama&K. Sekimizu, *Porphyromonas gingivalis* Peptidoglycans Induce Excessive Activation of the Innate Immune System in Silkworm Larvae. *The Journal of Biological Chemistry*, 2010. **285**(43): p. 33338-33347.
86. Khalaf, H., J. Lonn&T. Bengtsson, Cytokines and chemokines are differentially expressed in patients with periodontitis: possible role for TGF-beta1 as a marker for disease progression. *Cytokine*, 2014. **67**(1): p. 29-35.
87. Alpagot, T., K. Konopka, M. Bhattacharyya, S. Gebremedhin&N. Duzgunes, The association between gingival crevicular fluid TGF-beta1 levels and periodontal status in HIV-1(+) patients. *J Periodontol*, 2008. **79**(1): p. 123-30.
88. Mize, T.W., K.P. Sundararaj, R.S. Leite&Y. Huang, Increased and Correlated Expression of CTGF and TGF β 1 in Surgically Removed Periodontal Tissues with Chronic Periodontitis. *Journal of periodontal research*, 2015. **50**(3): p. 315-319.
89. Lagdive, S.S., P.P. Marawar, G. Byakod&S.B. Lagdive, Evaluation and comparison of interleukin-8 (IL-8) level in gingival crevicular fluid in health and severity of periodontal disease: a clinico-biochemical study. *Indian J Dent Res*, 2013. **24**(2): p. 188-92.
90. Goutoudi, P., E. Diza&M. Arvanitidou, Effect of periodontal therapy on crevicular fluid interleukin-6 and interleukin-8 levels in chronic periodontitis. *Int J Dent*, 2012. **2012**: p. 362905.
91. Issaranggun Na Ayuthaya, B., P. Satravaha&P. Pavasant, Interleukin-12 modulates the immunomodulatory properties of human periodontal ligament cells. *Journal of Periodontal Research*, 2017. **52**(3): p. 546-555.

References

92. Na Ayuthaya, B.I., V. Everts&P. Pavasant, Interleukin-12 (IL-12) Induces Receptor Activator of Nuclear Factor Kappa-B Ligand (RANKL) Expression by Human Periodontal Ligament Cells. *J Periodontol*, 2017: p. 1-19.
93. Van Dyke, T.E., The management of inflammation in periodontal disease. *Journal of Periodontology*, 2008. **79**(8 SUPPL.): p. 1601-1608.
94. Potempa, J., A. Banbula&J. Travis, Role of bacterial proteinases in matrix destruction and modulation of host responses. *Periodontol 2000*, 2000. **24**: p. 153-92.
95. How, K.Y., K.P. Song&K.G. Chan, Porphyromonas gingivalis: An Overview of Periodontopathic Pathogen below the Gum Line. *Frontiers in Microbiology*, 2016. **7**: p. 53.
96. Di Benedetto, A., I. Gigante, S. Colucci&M. Grano, Periodontal Disease: Linking the Primary Inflammation to Bone Loss. *Clinical and Developmental Immunology*, 2013. **2013**: p. 7.
97. Carvalho, R.P., J.S. Mesquita, A. Bonomo, P.X. Elsas&A.P. Colombo, Relationship of neutrophil phagocytosis and oxidative burst with the subgingival microbiota of generalized aggressive periodontitis. *Oral Microbiol Immunol*, 2009. **24**(2): p. 124-32.
98. Wang, M., J.L. Krauss, H. Domon, K.B. Hosur, S. Liang, P. Magotti, M. Triantafilou, K. Triantafilou, J.D. Lambris&G. Hajishengallis, Microbial Hijacking of Complement–Toll-like Receptor Crosstalk. *Science signaling*, 2010. **3**(109): p. ra11-ra11.
99. Gyurko, R., G. Boustany, P.L. Huang, A. Kantarci, T.E. Van Dyke, C.A. Genco&F.C. Gibson Iii, Mice Lacking Inducible Nitric Oxide Synthase Demonstrate Impaired Killing of Porphyromonas gingivalis. *Infection and Immunity*, 2003. **71**(9): p. 4917-4924.
100. Imatani, T., T. Kato&K. Okuda, Production of inflammatory cytokines by human gingival fibroblasts stimulated by cell-surface preparations of Porphyromonas gingivalis. *Oral Microbiol Immunol*, 2001. **16**(2): p. 65-72.
101. van Winkelhoff, A.J., T.E. Rams&J. Slots, Systemic antibiotic therapy in periodontics. *Periodontol 2000*, 1996. **10**: p. 45-78.
102. Page, R.C., Current understanding of the aetiology and progression of periodontal disease. *International dental journal*, 1986. **36**(3): p. 153-161.
103. Paster, B.J., S.K. Boches, J.L. Galvin, R.E. Ericson, C.N. Lau, V.A. Levanos, A. Sahasrabudhe&F.E. Dewhirst, Bacterial diversity in human subgingival plaque. *Journal of Bacteriology*, 2001. **183**(12): p. 3770-3783.
104. Finlay, B.B.&S. Falkow, Common themes in microbial pathogenicity revisited. *Microbiol Mol Biol Rev*, 1997. **61**(2): p. 136-69.
105. Miller, J.F., J.J. Mekalanos&S. Falkow, Coordinate regulation and sensory transduction in the control of bacterial virulence. *Science*, 1989. **243**(4893): p. 916-22.
106. Maurelli, A.T., Temperature regulation of virulence genes in pathogenic bacteria: a general strategy for human pathogens? *Microb Pathog*, 1989. **7**(1): p. 1-10.
107. Socransky, S.S., A.D. Haffajee, M.A. Cugini, C. Smith&R.L. Kent, Jr., Microbial complexes in subgingival plaque. *J Clin Periodontol*, 1998. **25**(2): p. 134-44.
108. Duncan, M.J., Oral microbiology and genomics. *Periodontol 2000*, 2005. **38**: p. 63-71.
109. Lamont, R.J.&H.F. Jenkinson, Life Below the Gum Line: Pathogenic Mechanisms of Porphyromonas gingivalis. *Microbiology and Molecular Biology Reviews*, 1998. **62**(4): p. 1244-1263.
110. Curtis, M.A., C. Zenobia&R.P. Darveau, The relationship of the oral microbiota to periodontal health and disease. *Cell Host Microbe*, 2011. **10**(4): p. 302-6.
111. Darveau, R.P., G. Hajishengallis&M.A. Curtis, Porphyromonas gingivalis as a Potential Community Activist for Disease. *Journal of Dental Research*, 2012. **91**(9): p. 816-820.
112. Li, L., R. Michel, J. Cohen, A. Decarlo&E. Kozarov, Intracellular survival and vascular cell-to-cell transmission of Porphyromonas gingivalis. *BMC Microbiol*, 2008. **8**: p. 26.
113. Olsen, I.&A. Progulsk-Fox, Invasion of Porphyromonas gingivalis strains into vascular cells and tissue. *Journal of Oral Microbiology*, 2015. **7**: p. 10.3402/jom.v7.28788.
114. Lamont, R.J., A. Chan, C.M. Belton, K.T. Izutsu, D. Vassel&A. Weinberg, Porphyromonas gingivalis invasion of gingival epithelial cells. *Infect Immun*, 1995. **63**(10): p. 3878-85.
115. Pan, C., J. Liu, H. Wang, J. Song, L. Tan&H. Zhao, Porphyromonas gingivalis can invade periodontal ligament stem cells. *BMC Microbiology*, 2017. **17**: p. 38.
116. Amornchat, C., S. Rassameemasmaung, W. Sripairojthikoon&S. Swasdison, Invasion of Porphyromonas gingivalis into human gingival fibroblasts in vitro. *J Int Acad Periodontol*, 2003. **5**(4): p. 98-105.
117. Deshpande, R.G., M.B. Khan&C.A. Genco, Invasion of aortic and heart endothelial cells by Porphyromonas gingivalis. *Infect Immun*, 1998. **66**(11): p. 5337-43.
118. Wang, M., M.A. Shakhathreh, D. James, S. Liang, S. Nishiyama, F. Yoshimura, D.R. Demuth&G. Hajishengallis, Fimbrial proteins of porphyromonas gingivalis mediate in vivo

- virulence and exploit TLR2 and complement receptor 3 to persist in macrophages. *J Immunol*, 2007. **179**(4): p. 2349-58.
119. Hajishengallis, G., P. Ratti&E. Harokopakis, Peptide mapping of bacterial fimbrial epitopes interacting with pattern recognition receptors. *J Biol Chem*, 2005. **280**(47): p. 38902-13.
 120. Le Sage, F., O. Meilhac&M.P. Gonthier, Porphyromonas gingivalis lipopolysaccharide induces pro-inflammatory adipokine secretion and oxidative stress by regulating Toll-like receptor-mediated signaling pathways and redox enzymes in adipocytes. *Mol Cell Endocrinol*, 2017.
 121. Holden, J.A., T.J. Attard, K.M. Laughton, A. Mansell, N.M. O'Brien-Simpson&E.C. Reynolds, Porphyromonas gingivalis lipopolysaccharide weakly activates M1 and M2 polarized mouse macrophages but induces inflammatory cytokines. *Infect Immun*, 2014. **82**(10): p. 4190-203.
 122. Imamura, T., A. Banbula, P.J.B. Pereira, J. Travis&J. Potempa, Activation of Human Prothrombin by Arginine-specific Cysteine Proteinases (Gingipains R) from Porphyromonas gingivalis *. *Journal of Biological Chemistry*, 2001. **276**(22): p. 18984-18991.
 123. Genco, C.A., B.M. Odusanya, J. Potempa, J. Mikolajczyk-Pawlinska&J. Travis, A peptide domain on gingipain R which confers immunity against Porphyromonas gingivalis infection in mice. *Infect Immun*, 1998. **66**(9): p. 4108-14.
 124. Loubakos, A., J. Potempa, J. Travis, M.R. D'Andrea, P. Andrade-Gordon, R. Santulli, E.J. Mackie&R.N. Pike, Arginine-specific protease from Porphyromonas gingivalis activates protease-activated receptors on human oral epithelial cells and induces interleukin-6 secretion. *Infect Immun*, 2001. **69**(8): p. 5121-30.
 125. Chen, T.&M.J. Duncan, Gingipain adhesin domains mediate Porphyromonas gingivalis adherence to epithelial cells. *Microb Pathog*, 2004. **36**(4): p. 205-9.
 126. Li, N., P. Yun, C.M. Jeffries, D. Langley, R. Gamsjaeger, W.B. Church, N. Hunter&C.A. Collyer, The modular structure of haemagglutinin/adhesin regions in gingipains of Porphyromonas gingivalis. *Mol Microbiol*, 2011. **81**(5): p. 1358-73.
 127. Veith, P.D., Y.Y. Chen, D.G. Gorasia, D. Chen, M.D. Glew, N.M. O'Brien-Simpson, J.D. Cecil, J.A. Holden&E.C. Reynolds, Porphyromonas gingivalis outer membrane vesicles exclusively contain outer membrane and periplasmic proteins and carry a cargo enriched with virulence factors. *J Proteome Res*, 2014. **13**(5): p. 2420-32.
 128. Hiratsuka, K., Y. Abiko, M. Hayakawa, T. Ito, H. Sasahara&H. Takiguchi, Role of Porphyromonas gingivalis 40-kDa outer membrane protein in the aggregation of P. gingivalis vesicles and Actinomyces viscosus. *Arch Oral Biol*, 1992. **37**(9): p. 717-24.
 129. Veith, P.D., G.H. Talbo, N. Slakeski, S.G. Dashper, C. Moore, R.A. Paolini&E.C. Reynolds, Major outer membrane proteins and proteolytic processing of RgpA and Kgp of Porphyromonas gingivalis W50. *Biochem J*, 2002. **363**(Pt 1): p. 105-15.
 130. Maeda, K., G.D. Tribble, C.M. Tucker, C. Anaya, S. Shizukuishi, J.P. Lewis, D.R. Demuth&R.J. Lamont, A Porphyromonas gingivalis Tyrosine Phosphatase is a Multifunctional Regulator of Virulence Attributes. *Molecular microbiology*, 2008. **69**(5): p. 1153-1164.
 131. Curtis, M.A., J. Aduse-Opoku&M. Rangarajan, Cysteine proteases of Porphyromonas gingivalis. *Crit Rev Oral Biol Med*, 2001. **12**(3): p. 192-216.
 132. de Diego, I., F. Veillard, M.N. Sztukowska, T. Guevara, B. Potempa, A. Pomowski, J.A. Huntington, J. Potempa&F.X. Gomis-Ruth, Structure and mechanism of cysteine peptidase gingipain K (Kgp), a major virulence factor of Porphyromonas gingivalis in periodontitis. *J Biol Chem*, 2014. **289**(46): p. 32291-302.
 133. Restaino, C.G., A. Chaparro, M.A. Valenzuela, A.M. Kettlun, R. Vernal, A. Silva, J. Puente, M.P. Jaque, R. Leon&J. Gamonal, Stimulatory response of neutrophils from periodontitis patients with periodontal pathogens. *Oral Dis*, 2007. **13**(5): p. 474-81.
 134. Wang, P.L.&K. Ohura, Porphyromonas gingivalis lipopolysaccharide signaling in gingival fibroblasts-CD14 and Toll-like receptors. *Crit Rev Oral Biol Med*, 2002. **13**(2): p. 132-42.
 135. Bengtsson, T., A. Khalaf&H. Khalaf, Secreted gingipains from Porphyromonas gingivalis colonies exert potent immunomodulatory effects on human gingival fibroblasts. *Microbiological Research*, 2015. **178**: p. 18-26.
 136. McCoy, S.A., H.R. Creamer, M. Kawanami&D.F. Adams, The concentration of lipopolysaccharide on individual root surfaces at varying times following in vivo root planing. *J Periodontol*, 1987. **58**(6): p. 393-9.
 137. Moore, J., M. Wilson&J.B. Kieser, The distribution of bacterial lipopolysaccharide (endotoxin) in relation to periodontally involved root surfaces. *J Clin Periodontol*, 1986. **13**(8): p. 748-51.

References

138. Shapira, L., S. Takashiba, S. Amar&T.E. Van Dyke, Porphyromonas gingivalis lipopolysaccharide stimulation of human monocytes: dependence on serum and CD14 receptor. *Oral Microbiol Immunol*, 1994. **9**(2): p. 112-7.
139. Darveau, R.P., M.D. Cunningham, T. Bailey, C. Seachord, K. Ratcliffe, B. Bainbridge, M. Dietsch, R.C. Page&A. Aruffo, Ability of bacteria associated with chronic inflammatory disease to stimulate E-selectin expression and promote neutrophil adhesion. *Infect Immun*, 1995. **63**(4): p. 1311-7.
140. Jersmann, H.P.A., C.S.T. Hii, G.L. Hodge&A. Ferrante, Synthesis and Surface Expression of CD14 by Human Endothelial Cells. *Infection and Immunity*, 2001. **69**(1): p. 479-485.
141. Pugin, J., C.C. Schürer-Maly, D. Leturcq, A. Moriarty, R.J. Ulevitch&P.S. Tobias, Lipopolysaccharide activation of human endothelial and epithelial cells is mediated by lipopolysaccharide-binding protein and soluble CD14. *Proceedings of the National Academy of Sciences of the United States of America*, 1993. **90**(7): p. 2744-2748.
142. Wright, S.D., R.A. Ramos, P.S. Tobias, R.J. Ulevitch&J.C. Mathison, CD14, a receptor for complexes of lipopolysaccharide (LPS) and LPS binding protein. *Science*, 1990. **249**(4975): p. 1431-3.
143. Landmann, R., H.P. Knopf, S. Link, S. Sansano, R. Schumann&W. Zimmerli, Human monocyte CD14 is upregulated by lipopolysaccharide. *Infection and Immunity*, 1996. **64**(5): p. 1762-1769.
144. Vaure, C.&Y. Liu, A Comparative Review of Toll-Like Receptor 4 Expression and Functionality in Different Animal Species. *Frontiers in Immunology*, 2014. **5**: p. 316.
145. Needham, B.D.&M.S. Trent, Fortifying the barrier: the impact of lipid A remodelling on bacterial pathogenesis. *Nat Rev Micro*, 2013. **11**(7): p. 467-481.
146. Hoshino, K., O. Takeuchi, T. Kawai, H. Sanjo, T. Ogawa, Y. Takeda, K. Takeda&S. Akira, Cutting edge: Toll-like receptor 4 (TLR4)-deficient mice are hyporesponsive to lipopolysaccharide: evidence for TLR4 as the Lps gene product. *J Immunol*, 1999. **162**(7): p. 3749-52.
147. Darveau, R.P., T.T. Pham, K. Lemley, R.A. Reife, B.W. Bainbridge, S.R. Coats, W.N. Howald, S.S. Way&A.M. Hajjar, Porphyromonas gingivalis lipopolysaccharide contains multiple lipid A species that functionally interact with both toll-like receptors 2 and 4. *Infect Immun*, 2004. **72**(9): p. 5041-51.
148. Hirschfeld, M., J.J. Weis, V. Toshchakov, C.A. Salkowski, M.J. Cody, D.C. Ward, N. Qureshi, S.M. Michalek&S.N. Vogel, Signaling by Toll-Like Receptor 2 and 4 Agonists Results in Differential Gene Expression in Murine Macrophages. *Infection and Immunity*, 2001. **69**(3): p. 1477-1482.
149. Darveau, R.P., S. Arbabi, I. Garcia, B. Bainbridge&R.V. Maier, Porphyromonas gingivalis lipopolysaccharide is both agonist and antagonist for p38 mitogen-activated protein kinase activation. *Infect Immun*, 2002. **70**(4): p. 1867-73.
150. Ogawa, T., Y. Asai, M. Hashimoto, O. Takeuchi, T. Kurita, Y. Yoshikai, K. Miyake&S. Akira, Cell activation by Porphyromonas gingivalis lipid A molecule through Toll-like receptor 4- and myeloid differentiation factor 88-dependent signaling pathway. *Int Immunol*, 2002. **14**(11): p. 1325-32.
151. Putnins, E.E., A.R. Sanaie, Q. Wu&J.D. Firth, Induction of keratinocyte growth factor 1 Expression by lipopolysaccharide is regulated by CD-14 and toll-like receptors 2 and 4. *Infect Immun*, 2002. **70**(12): p. 6541-8.
152. Martin, M., J. Katz, S.N. Vogel&S.M. Michalek, Differential induction of endotoxin tolerance by lipopolysaccharides derived from Porphyromonas gingivalis and Escherichia coli. *J Immunol*, 2001. **167**(9): p. 5278-85.
153. Aida, Y., K. Kusumoto, K. Nakatomi, H. Takada, M.J. Pabst&K. Maeda, An analogue of lipid A and LPS from Rhodobacter sphaeroides inhibits neutrophil responses to LPS by blocking receptor recognition of LPS and by depleting LPS-binding protein in plasma. *J Leukoc Biol*, 1995. **58**(6): p. 675-82.
154. Roberts, F.A., G.J. Richardson&S.M. Michalek, Effects of Porphyromonas gingivalis and Escherichia coli lipopolysaccharides on mononuclear phagocytes. *Infect Immun*, 1997. **65**(8): p. 3248-54.
155. Eichinger, A., H.G. Beisel, U. Jacob, R. Huber, F.J. Medrano, A. Banbula, J. Potempa, J. Travis&W. Bode, Crystal structure of gingipain R: an Arg-specific bacterial cysteine proteinase with a caspase-like fold. *Embo j*, 1999. **18**(20): p. 5453-62.
156. Guo, Y., K.-A. Nguyen&J. Potempa, Dichotomy of gingipains action as virulence factors: from cleaving substrates with the precision of a surgeon's knife to a meat chopper-like brutal degradation of proteins. *Periodontology* 2000, 2010. **54**(1): p. 15-44.

References

157. Imamura, T., The role of gingipains in the pathogenesis of periodontal disease. *J Periodontol*, 2003. **74**(1): p. 111-8.
158. Okamoto, K., T. Kadowaki, K. Nakayama&K. Yamamoto, Cloning and sequencing of the gene encoding a novel lysine-specific cysteine proteinase (Lys-gingipain) in *Porphyromonas gingivalis*: structural relationship with the arginine-specific cysteine proteinase (Arg-gingipain). *J Biochem*, 1996. **120**(2): p. 398-406.
159. Okamoto, K., K. Nakayama, T. Kadowaki, N. Abe, D.B. Ratnayake&K. Yamamoto, Involvement of a lysine-specific cysteine proteinase in hemoglobin adsorption and heme accumulation by *Porphyromonas gingivalis*. *J Biol Chem*, 1998. **273**(33): p. 21225-31.
160. Pavloff, N., P.A. Pemberton, J. Potempa, W.C. Chen, R.N. Pike, V. Prochazka, M.C. Kiefer, J. Travis&P.J. Barr, Molecular cloning and characterization of *Porphyromonas gingivalis* lysine-specific gingipain. A new member of an emerging family of pathogenic bacterial cysteine proteinases. *J Biol Chem*, 1997. **272**(3): p. 1595-600.
161. Barkocy-Gallagher, G.A., N. Han, J.M. Patti, J. Whitlock, A. Progulske-Fox&M.S. Lantz, Analysis of the prtP gene encoding porphypain, a cysteine proteinase of *Porphyromonas gingivalis*. *J Bacteriol*, 1996. **178**(10): p. 2734-41.
162. Slakeski, N., P.S. Bhogal, N.M. O'Brien-Simpson&E.C. Reynolds, Characterization of a second cell-associated Arg-specific cysteine proteinase of *Porphyromonas gingivalis* and identification of an adhesin-binding motif involved in association of the prtR and prtK proteinases and adhesins into large complexes. *Microbiology*, 1998. **144** (Pt 6): p. 1583-92.
163. Nakayama, K., Domain-specific rearrangement between the two Arg-gingipain-encoding genes in *Porphyromonas gingivalis*: possible involvement of nonreciprocal recombination. *Microbiol Immunol*, 1997. **41**(3): p. 185-96.
164. Li, N.&C.A. Collyer, Gingipains from *Porphyromonas gingivalis* – Complex domain structures confer diverse functions. *European Journal of Microbiology & Immunology*, 2011. **1**(1): p. 41-58.
165. Allaker, R.P., J. Aduse-Opoku, J.E. Batten&M.A. Curtis, Natural variation within the principal arginine-specific protease gene, prpR1, of *Porphyromonas gingivalis*. *Oral Microbiol Immunol*, 1997. **12**(5): p. 298-302.
166. Mikolajczyk-Pawlinska, J., T. Kordula, N. Pavloff, P.A. Pemberton, W.C. Chen, J. Travis&J. Potempa, Genetic variation of *Porphyromonas gingivalis* genes encoding gingipains, cysteine proteinases with arginine or lysine specificity. *Biol Chem*, 1998. **379**(2): p. 205-11.
167. NM, O.B.-S., P.D. Veith, S.G. Dashper&E.C. Reynolds, *Porphyromonas gingivalis* gingipains: the molecular teeth of a microbial vampire. *Curr Protein Pept Sci*, 2003. **4**(6): p. 409-26.
168. Chen, T., K. Nakayama, L. Belliveau&M.J. Duncan, *Porphyromonas gingivalis* gingipains and adhesion to epithelial cells. *Infect Immun*, 2001. **69**(5): p. 3048-56.
169. Nguyen, K.A., A.A. DeCarlo, M. Paramaesvaran, C.A. Collyer, D.B. Langley&N. Hunter, Humoral responses to *Porphyromonas gingivalis* gingipain adhesin domains in subjects with chronic periodontitis. *Infect Immun*, 2004. **72**(3): p. 1374-82.
170. Chu, L., T.E. Bramanti, J.L. Ebersole&S.C. Holt, Hemolytic activity in the periodontopathogen *Porphyromonas gingivalis*: kinetics of enzyme release and localization. *Infect Immun*, 1991. **59**(6): p. 1932-40.
171. Shah, H.N.&S.E. Gharbia, Lysis of erythrocytes by the secreted cysteine proteinase of *Porphyromonas gingivalis* W83. *FEMS Microbiol Lett*, 1989. **52**(1-2): p. 213-7.
172. Weinberg, A., C.M. Belton, Y. Park&R.J. Lamont, Role of fimbriae in *Porphyromonas gingivalis* invasion of gingival epithelial cells. *Infect Immun*, 1997. **65**(1): p. 313-6.
173. Okuda, K.&T. Kato, Hemagglutinating activity of lipopolysaccharides from subgingival plaque bacteria. *Infection and Immunity*, 1987. **55**(12): p. 3192-3196.
174. Du, L., P. Pellen-Mussi, F. Chandad, C. Mouton&M. Bonnaure-Mallet, Fimbriae and the hemagglutinating adhesin HA-Ag2 mediate adhesion of *Porphyromonas gingivalis* to epithelial cells. *Infection and Immunity*, 1997. **65**(9): p. 3875-3881.
175. Smalley, J.W., A.J. Birss, B. Szmigielski&J. Potempa, The HA2 haemagglutinin domain of the lysine-specific gingipain (Kgp) of *Porphyromonas gingivalis* promotes micro-oxo bishaem formation from monomeric iron(III) protoporphyrin IX. *Microbiology*, 2006. **152**(Pt 6): p. 1839-45.
176. Sakai, E., M. Naito, K. Sato, H. Hotokezaka, T. Kadowaki, A. Kamaguchi, K. Yamamoto, K. Okamoto&K. Nakayama, Construction of recombinant hemagglutinin derived from the gingipain-encoding gene of *Porphyromonas gingivalis*, identification of its target protein on erythrocytes, and inhibition of hemagglutination by an interdomain regional peptide. *J Bacteriol*, 2007. **189**(11): p. 3977-86.

References

177. DeCarlo, A.A., M. Paramaesvaran, P.L. Yun, C. Collyer & N. Hunter, Porphyrim-mediated binding to hemoglobin by the HA2 domain of cysteine proteinases (gingipains) and hemagglutinins from the periodontal pathogen *Porphyromonas gingivalis*. *J Bacteriol*, 1999. **181**(12): p. 3784-91.
178. Lewis, J.P., J.A. Dawson, J.C. Hannis, D. Muddiman & F.L. Macrina, Hemoglobinase activity of the lysine gingipain protease (Kgp) of *Porphyromonas gingivalis* W83. *J Bacteriol*, 1999. **181**(16): p. 4905-13.
179. Jayaprakash, K., H. Khalaf & T. Bengtsson, Gingipains from *Porphyromonas gingivalis* play a significant role in induction and regulation of CXCL8 in THP-1 cells. *BMC Microbiol*, 2014. **14**: p. 193.
180. Palm, E., H. Khalaf & T. Bengtsson, *Porphyromonas gingivalis* downregulates the immune response of fibroblasts. *BMC Microbiol*, 2013. **13**: p. 155.
181. Imamura, T., R.N. Pike, J. Potempa & J. Travis, Pathogenesis of periodontitis: a major arginine-specific cysteine proteinase from *Porphyromonas gingivalis* induces vascular permeability enhancement through activation of the kallikrein/kinin pathway. *Journal of Clinical Investigation*, 1994. **94**(1): p. 361-367.
182. Moreau, M.E., N. Garbacki, G. Molinaro, N.J. Brown, F. Marceau & A. Adam, The kallikrein-kinin system: current and future pharmacological targets. *J Pharmacol Sci*, 2005. **99**(1): p. 6-38.
183. Imamura, T., S. Tanase, T. Hamamoto, J. Potempa & J. Travis, Activation of blood coagulation factor IX by gingipains R, arginine-specific cysteine proteinases from *Porphyromonas gingivalis*. *Biochemical Journal*, 2001. **353**(Pt 2): p. 325-331.
184. Mikolajczyk-Pawlinska, J., J. Travis & J. Potempa, Modulation of interleukin-8 activity by gingipains from *Porphyromonas gingivalis*: implications for pathogenicity of periodontal disease. *FEBS Lett*, 1998. **440**(3): p. 282-6.
185. Sheets, S.M., J. Potempa, J. Travis, H.M. Fletcher & C.A. Casiano, Gingipains from *Porphyromonas gingivalis* W83 synergistically disrupt endothelial cell adhesion and can induce caspase-independent apoptosis. *Infect Immun*, 2006. **74**(10): p. 5667-78.
186. Desta, T. & D.T. Graves, Fibroblast apoptosis induced by *Porphyromonas gingivalis* is stimulated by a gingipain and caspase-independent pathway that involves apoptosis-inducing factor. *Cell Microbiol*, 2007. **9**(11): p. 2667-75.
187. Stathopoulou, P.G., J.C. Galicia, M.R. Benakanakere, C.A. Garcia, J. Potempa & D.F. Kinane, *Porphyromonas gingivalis* induce apoptosis in human gingival epithelial cells through a gingipain-dependent mechanism. *BMC Microbiol*, 2009. **9**: p. 107.
188. Guzik, K., M. Bzowska, J. Smagur, O. Krupa, M. Sieprawska, J. Travis & J. Potempa, A new insight into phagocytosis of apoptotic cells: proteolytic enzymes divert the recognition and clearance of polymorphonuclear leukocytes by macrophages. *Cell Death Differ*, 2007. **14**(1): p. 171-82.
189. Castro, S.A., R. Collighan, P.A. Lambert, I.H. Dias, P. Chauhan, C.E. Bland, I. Milic, M.R. Milward, P.R. Cooper & A. Devitt, *Porphyromonas gingivalis* gingipains cause defective macrophage migration towards apoptotic cells and inhibit phagocytosis of primary apoptotic neutrophils. *Cell Death Dis*, 2017. **8**(3): p. e2644.
190. Gamonal, J., M. Sanz, A. O'Connor, A. Acevedo, I. Suarez, A. Sanz, B. Martinez & A. Silva, Delayed neutrophil apoptosis in chronic periodontitis patients. *J Clin Periodontol*, 2003. **30**(7): p. 616-23.
191. Matthews, J.B., H.J. Wright, A. Roberts, P.R. Cooper & I.L. Chapple, Hyperactivity and reactivity of peripheral blood neutrophils in chronic periodontitis. *Clin Exp Immunol*, 2007. **147**(2): p. 255-64.
192. Hiroi, M., T. Shimojima, M. Kashimata, T. Miyata, H. Takano, M. Takahama & H. Sakagami, Inhibition by *Porphyromonas gingivalis* LPS of apoptosis induction in human peripheral blood polymorphonuclear leukocytes. *Anticancer Res*, 1998. **18**(5a): p. 3475-9.
193. Dias, I.H.K., L. Marshall, P.A. Lambert, I.L.C. Chapple, J.B. Matthews & H.R. Griffiths, Gingipains from *Porphyromonas gingivalis* Increase the Chemotactic and Respiratory Burst-Priming Properties of the 77-Amino-Acid Interleukin-8 Variant. *Infection and Immunity*, 2008. **76**(1): p. 317-323.
194. Jagels, M.A., J.A. Ember, J. Travis, J. Potempa, R. Pike & T.E. Hugli, Cleavage of the human C5A receptor by proteinases derived from *Porphyromonas gingivalis*: cleavage of leukocyte C5a receptor. *Adv Exp Med Biol*, 1996. **389**: p. 155-64.
195. Hartmann, K., B.M. Henz, S. Kruger-Krasagakes, J. Kohl, R. Burger, S. Guhl, I. Haase, U. Lippert & T. Zuberbier, C3a and C5a stimulate chemotaxis of human mast cells. *Blood*, 1997. **89**(8): p. 2863-70.

References

196. Nigrovic, P.A., O. Malbec, B. Lu, M.M. Markiewski, C. Kepley, N. Gerard, C. Gerard, M. Daëron&D.M. Lee, C5a receptor enables participation of mast cells in immune complex arthritis independent of Fc γ receptor modulation. *Arthritis and rheumatism*, 2010. **62**(11): p. 3322-3333.
197. Kitamura, Y., S. Matono, Y. Aida, T. Hirofujii&K. Maeda, Gingipains in the culture supernatant of *Porphyromonas gingivalis* cleave CD4 and CD8 on human T cells. *J Periodontal Res*, 2002. **37**(6): p. 464-8.
198. Giacaman, R.A., A.C. Asrani, K.F. Ross&M.C. Herzberg, Cleavage of protease-activated receptors on an immortalized oral epithelial cell line by *Porphyromonas gingivalis* gingipains. *Microbiology*, 2009. **155**(Pt 10): p. 3238-3246.
199. Sharlow, E.R., C.S. Paine, L. Babiarz, M. Eisinger, S. Shapiro&M. Seiberg, The protease-activated receptor-2 upregulates keratinocyte phagocytosis. *J Cell Sci*, 2000. **113** (Pt 17): p. 3093-101.
200. Herath, T.D., R.P. Darveau, C.J. Seneviratne, C.Y. Wang, Y. Wang&L. Jin, Heterogeneous *Porphyromonas gingivalis* LPS modulates immuno-inflammatory response, antioxidant defense and cytoskeletal dynamics in human gingival fibroblasts. *Sci Rep*, 2016. **6**: p. 29829.
201. Zhu, X.Q., W. Lu, Y. Chen, X.F. Cheng, J.Y. Qiu, Y. Xu&Y. Sun, Effects of *Porphyromonas gingivalis* Lipopolysaccharide Tolerized Monocytes on Inflammatory Responses in Neutrophils. *PLoS One*, 2016. **11**(8): p. e0161482.
202. Potempa, J., R. Pike&J. Travis, Titration and mapping of the active site of cysteine proteinases from *Porphyromonas gingivalis* (gingipains) using peptidyl chloromethanes. *Biol Chem*, 1997. **378**(3-4): p. 223-30.
203. Ekici, O.D., M.G. Gotz, K.E. James, Z.Z. Li, B.J. Rukamp, J.L. Asgian, C.R. Caffrey, E. Hansell, J. Dvorak, J.H. McKerrow, J. Potempa, J. Travis, J. Mikolajczyk, G.S. Salvesen&J.C. Powers, Aza-peptide Michael acceptors: a new class of inhibitors specific for caspases and other clan CD cysteine proteases. *J Med Chem*, 2004. **47**(8): p. 1889-92.
204. Yun, P.L., A.A. Decarlo, C.C. Chapple&N. Hunter, Functional implication of the hydrolysis of platelet endothelial cell adhesion molecule 1 (CD31) by gingipains of *Porphyromonas gingivalis* for the pathology of periodontal disease. *Infect Immun*, 2005. **73**(3): p. 1386-98.
205. Curtis, M.A., J.M. Slaney, R.J. Carman&P.A. Pemberton, Interaction of a trypsin-like enzyme of *Porphyromonas gingivalis* W83 with antithrombin III. *FEMS Microbiol Lett*, 1993. **108**(2): p. 169-74.
206. Gron, H., R. Pike, J. Potempa, J. Travis, I.B. Thogersen, J.J. Enghild&S.V. Pizzo, The potential role of alpha 2-macroglobulin in the control of cysteine proteinases (gingipains) from *Porphyromonas gingivalis*. *J Periodontal Res*, 1997. **32**(1 Pt 1): p. 61-8.
207. Blankenvoorde, M.F., W. van't Hof, E. Walgreen-Weterings, T.J. van Steenberg, H.S. Brand, E.C. Veerman&A.V. Nieuw Amerongen, Cystatin and cystatin-derived peptides have antibacterial activity against the pathogen *Porphyromonas gingivalis*. *Biol Chem*, 1998. **379**(11): p. 1371-5.
208. Umemoto, T., Y. Naito, M. Li, I. Suzuki&I. Namikawa, Growth inhibition of a human oral bacterium *Porphyromonas gingivalis* by rat cysteine proteinase inhibitor cystatin S. *Lett Appl Microbiol*, 1996. **23**(3): p. 151-3.
209. Hajshengallis, G., M. Wang, E. Harokopakis, M. Triantafilou&K. Triantafilou, *Porphyromonas gingivalis* Fimbriae Proactively Modulate β (2) Integrin Adhesive Activity and Promote Binding to and Internalization by Macrophages. *Infection and Immunity*, 2006. **74**(10): p. 5658-5666.
210. Sharp, L., S. Poole, K. Reddi, J. Fletcher, S. Nair, M. Wilson, M. Curtis, B. Henderson&P. Tabona, A lipid A-associated protein of *Porphyromonas gingivalis*, derived from the haemagglutinating domain of the RI protease gene family, is a potent stimulator of interleukin 6 synthesis. *Microbiology*, 1998. **144** (Pt 11): p. 3019-26.
211. Laine, M.L., B.J. Appelmelk&A.J. van Winkelhoff, Prevalence and distribution of six capsular serotypes of *Porphyromonas gingivalis* in periodontitis patients. *J Dent Res*, 1997. **76**(12): p. 1840-4.
212. Singh, A., T. Wyant, C. Anaya-Bergman, J. Aduse-Opoku, J. Brunner, M.L. Laine, M.A. Curtis&J.P. Lewis, The Capsule of *Porphyromonas gingivalis* Leads to a Reduction in the Host Inflammatory Response, Evasion of Phagocytosis, and Increase in Virulence. *Infection and Immunity*, 2011. **79**(11): p. 4533-4542.
213. Maeba, S., S. Otake, J. Namikoshi, Y. Shibata, M. Hayakawa, Y. Abiko&M. Yamamoto, Transcutaneous immunization with a 40-kDa outer membrane protein of *Porphyromonas gingivalis* induces specific antibodies which inhibit coaggregation by *P. gingivalis*. *Vaccine*, 2005. **23**(19): p. 2513-21.

References

214. Hajshengallis, G., Periodontitis: from microbial immune subversion to systemic inflammation. *Nat Rev Immunol*, 2015. **15**(1): p. 30-44.
215. THE WHO group, Integrated chronic disease prevention and control. 2002.
216. Southerland, J.H., G.W. Taylor, K. Moss, J.D. Beck&S. Offenbacher, Commonality in chronic inflammatory diseases: periodontitis, diabetes, and coronary artery disease. *Periodontol* 2000, 2006. **40**: p. 130-43.
217. Taylor, G.W., B.A. Burt, M.P. Becker, R.J. Genco, M. Shlossman, W.C. Knowler&D.J. Pettitt, Severe periodontitis and risk for poor glycemic control in patients with non-insulin-dependent diabetes mellitus. *J Periodontol*, 1996. **67**(10 Suppl): p. 1085-93.
218. Pacios, S., O. Andriankaja, J. Kang, M. Alnammary, J. Bae, B. de Brito Bezerra, H. Schreiner, D.H. Fine&D.T. Graves, Bacterial Infection Increases Periodontal Bone Loss in Diabetic Rats through Enhanced Apoptosis. *The American Journal of Pathology*, 2013. **183**(6): p. 1928-1935.
219. Preshaw, P.M., A.L. Alba, D. Herrera, S. Jepsen, A. Konstantinidis, K. Makrilakis&R. Taylor, Periodontitis and diabetes: a two-way relationship. *Diabetologia*, 2012. **55**(1): p. 21-31.
220. Gomes, M.S., P. Chagas, D.M. Padilha, P. Caramori, F.N. Hugo, C.H. Schwanke&J.B. Hilgert, Association between self-reported oral health, tooth loss and atherosclerotic burden. *Braz Oral Res*, 2012. **26**(5): p. 436-42.
221. DeCarlo, A.A., Jr., L.J. Windsor, M.K. Bodden, G.J. Harber, B. Birkedal-Hansen&H. Birkedal-Hansen, Activation and novel processing of matrix metalloproteinases by a thiol-proteinase from the oral anaerobe *Porphyromonas gingivalis*. *J Dent Res*, 1997. **76**(6): p. 1260-70.
222. Galkina, E.&K. Ley, Immune and Inflammatory Mechanisms of Atherosclerosis. *Annual review of immunology*, 2009. **27**: p. 165-197.
223. Valtonen, V.V., Role of infections in atherosclerosis. *American Heart Journal*, 1999. **138**(5, Supplement): p. S431-S433.
224. Hubacek, J.A., G. Rothe, J. Pit'ha, Z. Skodova, V. Stanek, R. Poledne&G. Schmitz, C(-260)-->T polymorphism in the promoter of the CD14 monocyte receptor gene as a risk factor for myocardial infarction. *Circulation*, 1999. **99**(25): p. 3218-20.
225. Ford, P.J., E. Gemmell, A. Chan, C.L. Carter, P.J. Walker, P.S. Bird, M.J. West, M.P. Cullinan&G.J. Seymour, Inflammation, heat shock proteins and periodontal pathogens in atherosclerosis: an immunohistologic study. *Oral Microbiol Immunol*, 2006. **21**(4): p. 206-11.
226. Choi, C.H., R. Spooner, J. DeGuzman, T. Koutouzis, D.M. Ojcius&Ö. Yilmaz, P. gingivalis-Nucleoside-diphosphate-kinase Inhibits ATP-Induced Reactive-Oxygen-Species via P2X(7) Receptor/NADPH-Oxidase Signaling and Contributes to Persistence. *Cellular microbiology*, 2013. **15**(6): p. 961-976.
227. Ekuni, D., T. Tomofuji, T. Sanbe, K. Irie, T. Azuma, T. Maruyama, N. Tamaki, J. Murakami, S. Koikeguchi&T. Yamamoto, Periodontitis-induced lipid peroxidation in rat descending aorta is involved in the initiation of atherosclerosis. *Journal of Periodontal Research*, 2009. **44**(4): p. 434-442.
228. Bartold, P.M., V. Marino, M. Cantley&D.R. Haynes, Effect of *Porphyromonas gingivalis*-induced inflammation on the development of rheumatoid arthritis. *J Clin Periodontol*, 2010. **37**(5): p. 405-11.
229. Kinloch, A.J., S. Alzabin, W. Brintnell, E. Wilson, L. Barra, N. Wegner, D.A. Bell, E. Cairns&P.J. Venables, Immunization with *Porphyromonas gingivalis* enolase induces autoimmunity to mammalian alpha-enolase and arthritis in DR4-IE-transgenic mice. *Arthritis Rheum*, 2011. **63**(12): p. 3818-23.
230. Harre, U., D. Georgess, H. Bang, A. Bozec, R. Axmann, E. Ossipova, P.-J. Jakobsson, W. Baum, F. Nimmerjahn, E. Szarka, G. Sarmay, G. Krumbholz, E. Neumann, R. Toes, H.-U. Scherer, A.I. Catrina, L. Klareskog, P. Jurdic&G. Schett, Induction of osteoclastogenesis and bone loss by human autoantibodies against citrullinated vimentin. *The Journal of Clinical Investigation*, 2012. **122**(5): p. 1791-1802.
231. Wang, Y., M. Li, S. Stadler, S. Correll, P. Li, D. Wang, R. Hayama, L. Leonelli, H. Han, S.A. Grigoryev, C.D. Allis&S.A. Coonrod, Histone hypercitrullination mediates chromatin decondensation and neutrophil extracellular trap formation. *J Cell Biol*, 2009. **184**(2): p. 205-13.
232. Wegner, N., R. Wait, A. Sroka, S. Eick, K.A. Nguyen, K. Lundberg, A. Kinloch, S. Culshaw, J. Potempa&P.J. Venables, Peptidylarginine deiminase from *Porphyromonas gingivalis* citrullinates human fibrinogen and alpha-enolase: implications for autoimmunity in rheumatoid arthritis. *Arthritis Rheum*, 2010. **62**(9): p. 2662-72.

References

233. Elmore, S., Apoptosis: A Review of Programmed Cell Death. *Toxicologic pathology*, 2007. **35**(4): p. 495-516.
234. Elliott, M.R.&K.S. Ravichandran, Clearance of apoptotic cells: implications in health and disease. *J Cell Biol*, 2010. **189**(7): p. 1059-70.
235. Wood, W., M. Turmaine, R. Weber, V. Camp, R.A. Maki, S.R. McKercher&P. Martin, Mesenchymal cells engulf and clear apoptotic footplate cells in macrophageless PU.1 null mouse embryos. *Development*, 2000. **127**(24): p. 5245-52.
236. Parnaik, R., M.C. Raff&J. Scholes, Differences between the clearance of apoptotic cells by professional and non-professional phagocytes. *Curr Biol*, 2000. **10**(14): p. 857-60.
237. Distelhorst, C.W., Recent insights into the mechanism of glucocorticosteroid-induced apoptosis. *Cell Death Differ*, 2002. **9**(1): p. 6-19.
238. Schumacher, B., K. Hofmann, S. Boulton&A. Gartner, The C. elegans homolog of the p53 tumor suppressor is required for DNA damage-induced apoptosis. *Curr Biol*, 2001. **11**(21): p. 1722-7.
239. Borges, H.L., R. Linden&J.Y.J. Wang, DNA damage-induced cell death: lessons from the central nervous system. *Cell research*, 2008. **18**(1): p. 17-26.
240. Salinas, L.S., E. Maldonado&R.E. Navarro, Stress-induced germ cell apoptosis by a p53 independent pathway in *Caenorhabditis elegans*. *Cell Death Differ*, 2006. **13**(12): p. 2129-39.
241. Schumacher, B., C. Schertel, N. Wittenburg, S. Tuck, S. Mitani, A. Gartner, B. Conradt&S. Shaham, C. elegans ced-13 can promote apoptosis and is induced in response to DNA damage. *Cell Death Differ*, 2005. **12**(2): p. 153-61.
242. Kerr, J.F., A.H. Wyllie&A.R. Currie, Apoptosis: a basic biological phenomenon with wide-ranging implications in tissue kinetics. *Br J Cancer*, 1972. **26**(4): p. 239-57.
243. Hacker, G., The morphology of apoptosis. *Cell Tissue Res*, 2000. **301**(1): p. 5-17.
244. Nakagawa, T., H. Zhu, N. Morishima, E. Li, J. Xu, B.A. Yankner&J. Yuan, Caspase-12 mediates endoplasmic-reticulum-specific apoptosis and cytotoxicity by amyloid- β . *Nature*, 2000. **403**(6765): p. 98-103.
245. Chen, M., Y. Xing, A. Lu, W. Fang, B. Sun, C. Chen, W. Liao&G. Meng, Internalized *Cryptococcus neoformans* Activates the Canonical Caspase-1 and the Noncanonical Caspase-8 Inflammasomes. *The Journal of Immunology*, 2015. **195**(10): p. 4962.
246. Colussi, P.A., N.L. Harvey&S. Kumar, Prodomain-dependent Nuclear Localization of the Caspase-2 (Nedd2) Precursor: A NOVEL FUNCTION FOR A CASPASE PRODOMAIN. *Journal of Biological Chemistry*, 1998. **273**(38): p. 24535-24542.
247. Enari, M., H. Sakahira, H. Yokoyama, K. Okawa, A. Iwamatsu&S. Nagata, A caspase-activated DNase that degrades DNA during apoptosis, and its inhibitor ICAD. *Nature*, 1998. **391**(6662): p. 43-50.
248. Ashkenazi, A., Directing cancer cells to self-destruct with pro-apoptotic receptor agonists. *Nat Rev Drug Discov*, 2008. **7**(12): p. 1001-1012.
249. Scoltock, A.B.&J.A. Cidlowski, Activation of intrinsic and extrinsic pathways in apoptotic signaling during UV-C-induced death of Jurkat cells: the role of caspase inhibition. *Exp Cell Res*, 2004. **297**(1): p. 212-23.
250. Crow, M.T., K. Mani, Y.J. Nam&R.N. Kitsis, The mitochondrial death pathway and cardiac myocyte apoptosis. *Circ Res*, 2004. **95**(10): p. 957-70.
251. Woo, M., R. Hakem, M.S. Soengas, G.S. Duncan, A. Shahinian, D. Kägi, A. Hakem, M. McCurrach, W. Khoo, S.A. Kaufman, G. Senaldi, T. Howard, S.W. Lowe&T.W. Mak, Essential contribution of caspase 3/CPP32 to apoptosis and its associated nuclear changes. *Genes & Development*, 1998. **12**(6): p. 806-819.
252. Sprick, M.R., M.A. Weigand, E. Rieser, C.T. Rauch, P. Juo, J. Blenis, P.H. Krammer&H. Walczak, FADD/MORT1 and Caspase-8 Are Recruited to TRAIL Receptors 1 and 2 and Are Essential for Apoptosis Mediated by TRAIL Receptor 2. *Immunity*, 2000. **12**(6): p. 599-609.
253. Li, H., H. Zhu, C.-j. Xu&J. Yuan, Cleavage of BID by Caspase 8 Mediates the Mitochondrial Damage in the Fas Pathway of Apoptosis. *Cell*, 1998. **94**(4): p. 491-501.
254. Fink, S.L.&B.T. Cookson, Caspase-1-dependent pore formation during pyroptosis leads to osmotic lysis of infected host macrophages. *Cell Microbiol*, 2006. **8**(11): p. 1812-25.
255. Cullen, S.P.&S.J. Martin, Caspase activation pathways: some recent progress. *Cell Death Differ*, 2009. **16**(7): p. 935-8.
256. Rao, L., D. Perez&E. White, Lamin proteolysis facilitates nuclear events during apoptosis. *J Cell Biol*, 1996. **135**(6 Pt 1): p. 1441-55.

257. Buendia, B., A. Santa-Maria&J.C. Courvalin, Caspase-dependent proteolysis of integral and peripheral proteins of nuclear membranes and nuclear pore complex proteins during apoptosis. *J Cell Sci*, 1999. **112** (Pt 11): p. 1743-53.
258. Lauber, K., E. Bohn, S.M. Krober, Y.J. Xiao, S.G. Blumenthal, R.K. Lindemann, P. Marini, C. Wiedig, A. Zobywalski, S. Baksh, Y. Xu, I.B. Autenrieth, K. Schulze-Osthoff, C. Belka, G. Stuhler&S. Wesselborg, Apoptotic cells induce migration of phagocytes via caspase-3-mediated release of a lipid attraction signal. *Cell*, 2003. **113**(6): p. 717-30.
259. Gonzalez, O.A., M. John Novak, S. Kirakodu, A.J. Stromberg, S. Shen, L. Orraca, J. Gonzalez-Martinez&J.L. Ebersole, Effects of aging on apoptosis gene expression in oral mucosal tissues. *Apoptosis*, 2013. **18**(3): p. 249-259.
260. Li, J.&J. Yuan, Caspases in apoptosis and beyond. *Oncogene*, 2008. **27**(48): p. 6194-206.
261. Gamonal, J., A. Bascones, A. Acevedo, E. Blanco&A. Silva, Apoptosis in Chronic Adult Periodontitis Analyzed by in Situ DNA Breaks, Electron Microscopy, and Immunohistochemistry. *Journal of Periodontology*, 2001. **72**(4): p. 517-525.
262. Tennant, I., J.D. Pound, L.A. Marr, J.J.L.P. Willems, S. Petrova, C.A. Ford, M. Paterson, A. Devitt&C.D. Gregory, Innate recognition of apoptotic cells: novel apoptotic cell-associated molecular patterns revealed by crossreactivity of anti-LPS antibodies. *Cell Death and Differentiation*, 2013. **20**(5): p. 698-708.
263. Savill, J., I. Dransfield, N. Hogg&C. Haslett, Vitronectin receptor-mediated phagocytosis of cells undergoing apoptosis. *Nature*, 1990. **343**(6254): p. 170-173.
264. Lucas, M., L.M. Stuart, A. Zhang, K. Hodivala-Dilke, M. Febbraio, R. Silverstein, J. Savill&A. Lacy-Hulbert, Requirements for apoptotic cell contact in regulation of macrophage responses. *J Immunol*, 2006. **177**(6): p. 4047-54.
265. Vance, J.E., Phosphatidylserine and phosphatidylethanolamine in mammalian cells: two metabolically related aminophospholipids. *J Lipid Res*, 2008. **49**(7): p. 1377-87.
266. Appelt, U., A. Sheriff, U.S. Gaipl, J.R. Kalden, R.E. Voll&M. Herrmann, Viable, apoptotic and necrotic monocytes expose phosphatidylserine: cooperative binding of the ligand Annexin V to dying but not viable cells and implications for PS-dependent clearance. *Cell Death Differ*, 2005. **12**(2): p. 194-6.
267. Callahan, M.K., P. Williamson&R.A. Schlegel, Surface expression of phosphatidylserine on macrophages is required for phagocytosis of apoptotic thymocytes. *Cell Death Differ*, 2000. **7**(7): p. 645-53.
268. Thery, C., L. Zitvogel&S. Amigorena, Exosomes: composition, biogenesis and function. *Nat Rev Immunol*, 2002. **2**(8): p. 569-579.
269. Dillon, S.R., M. Mancini, A. Rosen&M.S. Schlissel, Annexin V binds to viable B cells and colocalizes with a marker of lipid rafts upon B cell receptor activation. *J Immunol*, 2000. **164**(3): p. 1322-32.
270. Frasch, S.C., P.M. Henson, J.M. Kailey, D.A. Richter, M.S. Janes, V.A. Fadok&D.L. Bratton, Regulation of phospholipid scramblase activity during apoptosis and cell activation by protein kinase Cdelta. *J Biol Chem*, 2000. **275**(30): p. 23065-73.
271. Datta, R., H. Kojima, K. Yoshida&D. Kufe, Caspase-3-mediated cleavage of protein kinase C theta in induction of apoptosis. *J Biol Chem*, 1997. **272**(33): p. 20317-20.
272. Verhoven, B., R.A. Schlegel&P. Williamson, Mechanisms of phosphatidylserine exposure, a phagocyte recognition signal, on apoptotic T lymphocytes. *J Exp Med*, 1995. **182**(5): p. 1597-601.
273. Zhao, J., Q. Zhou, T. Wiedmer&P.J. Sims, Level of expression of phospholipid scramblase regulates induced movement of phosphatidylserine to the cell surface. *J Biol Chem*, 1998. **273**(12): p. 6603-6.
274. Bratton, D.L., V.A. Fadok, D.A. Richter, J.M. Kailey, L.A. Guthrie&P.M. Henson, Appearance of phosphatidylserine on apoptotic cells requires calcium-mediated nonspecific flip-flop and is enhanced by loss of the aminophospholipid translocase. *J Biol Chem*, 1997. **272**(42): p. 26159-65.
275. Gardai, S.J., K.A. McPhillips, S.C. Frasch, W.J. Janssen, A. Starefeldt, J.E. Murphy-Ullrich, D.L. Bratton, P.A. Oldenborg, M. Michalak&P.M. Henson, Cell-surface calreticulin initiates clearance of viable or apoptotic cells through trans-activation of LRP on the phagocyte. *Cell*, 2005. **123**(2): p. 321-34.
276. Park, D., A.C. Tosello-Tramont, M.R. Elliott, M. Lu, L.B. Haney, Z. Ma, A.L. Klibanov, J.W. Mandell&K.S. Ravichandran, BAI1 is an engulfment receptor for apoptotic cells upstream of the ELMO/Dock180/Rac module. *Nature*, 2007. **450**(7168): p. 430-4.
277. Wu, Y., N. Tibrewal&R.B. Birge, Phosphatidylserine recognition by phagocytes: a view to a kill. *Trends Cell Biol*, 2006. **16**(4): p. 189-97.

References

278. Ravichandran, K.S.&U. Lorenz, Engulfment of apoptotic cells: signals for a good meal. *Nat Rev Immunol*, 2007. **7**(12): p. 964-74.
279. Huynh, M.L., V.A. Fadok&P.M. Henson, Phosphatidylserine-dependent ingestion of apoptotic cells promotes TGF-beta1 secretion and the resolution of inflammation. *J Clin Invest*, 2002. **109**(1): p. 41-50.
280. Hoffmann, P.R., A.M. deCathelineau, C.A. Ogden, Y. Leverrier, D.L. Bratton, D.L. Daleke, A.J. Ridley, V.A. Fadok&P.M. Henson, Phosphatidylserine (PS) induces PS receptor-mediated macropinocytosis and promotes clearance of apoptotic cells. *J Cell Biol*, 2001. **155**(4): p. 649-59.
281. Moffatt, O.D., A. Devitt, E.D. Bell, D.L. Simmons&C.D. Gregory, Macrophage recognition of ICAM-3 on apoptotic leukocytes. *J Immunol*, 1999. **162**(11): p. 6800-10.
282. Devitt, A., K.G. Parker, C.A. Ogden, C. Oldreive, M.F. Clay, L.A. Melville, C.O. Bellamy, A. Lacy-Hulbert, S.C. Gangloff, S.M. Goyert&C.D. Gregory, Persistence of apoptotic cells without autoimmune disease or inflammation in CD14(-/-) mice. *The Journal of Cell Biology*, 2004. **167**(6): p. 1161-1170.
283. Stuart, L.M., K. Takahashi, L. Shi, J. Savill&R.A. Ezekowitz, Mannose-binding lectin-deficient mice display defective apoptotic cell clearance but no autoimmune phenotype. *J Immunol*, 2005. **174**(6): p. 3220-6.
284. Ramirez-Ortiz, Z.G., W.F. Pendergraft, 3rd, A. Prasad, M.H. Byrne, T. Iram, C.J. Blanchette, A.D. Luster, N. Hacohen, J. El Khoury&T.K. Means, The scavenger receptor SCARF1 mediates the clearance of apoptotic cells and prevents autoimmunity. *Nat Immunol*, 2013. **14**(9): p. 917-26.
285. Botto, M., C. Dell'Agnola, A.E. Bygrave, E.M. Thompson, H.T. Cook, F. Petry, M. Loos, P.P. Pandolfi&M.J. Walport, Homozygous C1q deficiency causes glomerulonephritis associated with multiple apoptotic bodies. *Nat Genet*, 1998. **19**(1): p. 56-9.
286. Szondy, Z., Z. Sarang, P. Molnár, T. Németh, M. Piacentini, P.G. Mastroberardino, L. Falasca, D. Aeschlimann, J. Kovács, I. Kiss, É. Szegezdi, G. Lakos, É. Rajnavölgyi, P.J. Birckbichler, G. Melino&L. Fésüs, Transglutaminase 2(-/-) mice reveal a phagocytosis-associated crosstalk between macrophages and apoptotic cells. *Proceedings of the National Academy of Sciences of the United States of America*, 2003. **100**(13): p. 7812-7817.
287. Pepino, M.Y., O. Kuda, D. Samovski&N.A. Abumrad, Structure-Function of CD36 and Importance of Fatty Acid Signal Transduction in Fat Metabolism. *Annual review of nutrition*, 2014. **34**: p. 281-303.
288. Fadok, V.A., M.L. Warner, D.L. Bratton&P.M. Henson, CD36 is required for phagocytosis of apoptotic cells by human macrophages that use either a phosphatidylserine receptor or the vitronectin receptor (alpha v beta 3). *J Immunol*, 1998. **161**(11): p. 6250-7.
289. Greenberg, M.E., M. Sun, R. Zhang, M. Febbraio, R. Silverstein&S.L. Hazen, Oxidized phosphatidylserine-CD36 interactions play an essential role in macrophage-dependent phagocytosis of apoptotic cells. *The Journal of Experimental Medicine*, 2006. **203**(12): p. 2613-2625.
290. Silverstein, R.L.&R.L. Nachman, Thrombospondin binds to monocytes-macrophages and mediates platelet-monocyte adhesion. *Journal of Clinical Investigation*, 1987. **79**(3): p. 867-874.
291. Silverstein, R.L., L.L. Leung&R.L. Nachman, Thrombospondin: a versatile multifunctional glycoprotein. *Arteriosclerosis*, 1986. **6**(3): p. 245-53.
292. Jaffe, E.A., L.L.K. Leung, R.L. Nachman, R.I. Levin&D.F. Mosher, Thrombospondin is the endogenous lectin of human platelets. *Nature*, 1982. **295**(5846): p. 246-248.
293. Silverstein, R.L., A.S. Asch&R.L. Nachman, Glycoprotein IV mediates thrombospondin-dependent platelet-monocyte and platelet-U937 cell adhesion. *Journal of Clinical Investigation*, 1989. **84**(2): p. 546-552.
294. Savill, J., N. Hogg, Y. Ren&C. Haslett, Thrombospondin cooperates with CD36 and the vitronectin receptor in macrophage recognition of neutrophils undergoing apoptosis. *J Clin Invest*, 1992. **90**(4): p. 1513-22.
295. Ren, Y., R.L. Silverstein, J. Allen&J. Savill, CD36 gene transfer confers capacity for phagocytosis of cells undergoing apoptosis. *J Exp Med*, 1995. **181**(5): p. 1857-62.
296. Podrez, E.A., D. Schmitt, H.F. Hoff&S.L. Hazen, Myeloperoxidase-generated reactive nitrogen species convert LDL into an atherogenic form in vitro. *Journal of Clinical Investigation*, 1999. **103**(11): p. 1547-1560.
297. Podrez, E.A., M. Febbraio, N. Sheibani, D. Schmitt, R.L. Silverstein, D.P. Hajjar, P.A. Cohen, W.A. Frazier, H.F. Hoff&S.L. Hazen, Macrophage scavenger receptor CD36 is the

References

- major receptor for LDL modified by monocyte-generated reactive nitrogen species. *Journal of Clinical Investigation*, 2000. **105**(8): p. 1095-1108.
298. Febbraio, M., D.P. Hajjar&R.L. Silverstein, CD36: a class B scavenger receptor involved in angiogenesis, atherosclerosis, inflammation, and lipid metabolism. *Journal of Clinical Investigation*, 2001. **108**(6): p. 785-791.
299. Febbraio, M., E.A. Podrez, J.D. Smith, D.P. Hajjar, S.L. Hazen, H.F. Hoff, K. Sharma&R.L. Silverstein, Targeted disruption of the class B scavenger receptor CD36 protects against atherosclerotic lesion development in mice. *Journal of Clinical Investigation*, 2000. **105**(8): p. 1049-1056.
300. Ogden, C.A., A. deCathelineau, P.R. Hoffmann, D. Bratton, B. Ghebrehiwet, V.A. Fadok&P.M. Henson, C1q and Mannose Binding Lectin Engagement of Cell Surface Calreticulin and Cd91 Initiates Macropinocytosis and Uptake of Apoptotic Cells. *The Journal of Experimental Medicine*, 2001. **194**(6): p. 781-796.
301. Vandivier, R.W., C.A. Ogden, V.A. Fadok, P.R. Hoffmann, K.K. Brown, M. Botto, M.J. Walport, J.H. Fisher, P.M. Henson&K.E. Greene, Role of surfactant proteins A, D, and C1q in the clearance of apoptotic cells in vivo and in vitro: calreticulin and CD91 as a common collectin receptor complex. *J Immunol*, 2002. **169**(7): p. 3978-86.
302. Gardai, S.J., Y.-Q. Xiao, M. Dickinson, J.A. Nick, D.R. Voelker, K.E. Greene&P.M. Henson, By Binding SIRP α or Calreticulin/CD91, Lung Collectins Act as Dual Function Surveillance Molecules to Suppress or Enhance Inflammation. *Cell*, 2003. **115**(1): p. 13-23.
303. Donnelly, S., W. Roake, S. Brown, P. Young, H. Naik, P. Wordsworth, D.A. Isenberg, K.B. Reid&P. Eggleton, Impaired recognition of apoptotic neutrophils by the C1q/calreticulin and CD91 pathway in systemic lupus erythematosus. *Arthritis Rheum*, 2006. **54**(5): p. 1543-56.
304. Van Voorhis, W.C., R.M. Steinman, L.S. Hair, J. Luban, M.D. Witmer, S. Koide&Z.A. Cohn, Specific antimono-nuclear phagocyte monoclonal antibodies. Application to the purification of dendritic cells and the tissue localization of macrophages. *J Exp Med*, 1983. **158**(1): p. 126-45.
305. Wright, S.D., R.A. Ramos, A. Hermanowski-Vosatka, P. Rockwell&P.A. Detmers, Activation of the adhesive capacity of CR3 on neutrophils by endotoxin: dependence on lipopolysaccharide binding protein and CD14. *J Exp Med*, 1991. **173**(5): p. 1281-6.
306. Kusunoki, T., E. Hailman, T.S. Juan, H.S. Lichenstein&S.D. Wright, Molecules from *Staphylococcus aureus* that bind CD14 and stimulate innate immune responses. *J Exp Med*, 1995. **182**(6): p. 1673-82.
307. Weidemann, B., J. Schletter, R. Dziarski, S. Kusumoto, F. Stelter, E.T. Rietschel, H.D. Flad&A.J. Ulmer, Specific binding of soluble peptidoglycan and muramyldipeptide to CD14 on human monocytes. *Infection and Immunity*, 1997. **65**(3): p. 858-864.
308. Zhang, Y., M. Doerfler, T.C. Lee, B. Guillemin&W.N. Rom, Mechanisms of stimulation of interleukin-1 beta and tumor necrosis factor-alpha by *Mycobacterium tuberculosis* components. *Journal of Clinical Investigation*, 1993. **91**(5): p. 2076-2083.
309. Espevik, T., M. Otterlei, G. Skjak-Braek, L. Ryan, S.D. Wright&A. Sundan, The involvement of CD14 in stimulation of cytokine production by uronic acid polymers. *Eur J Immunol*, 1993. **23**(1): p. 255-61.
310. Soell, M., E. Lett, F. Holveck, M. Scholler, D. Wachsmann&J.P. Klein, Activation of human monocytes by streptococcal rhamnose glucose polymers is mediated by CD14 antigen, and mannan binding protein inhibits TNF-alpha release. *J Immunol*, 1995. **154**(2): p. 851-60.
311. van der Bruggen, T., S. Nijenhuis, E. van Raaij, J. Verhoef&B. Sweder van Asbeck, Lipopolysaccharide-Induced Tumor Necrosis Factor Alpha Production by Human Monocytes Involves the Raf-1/MEK1-MEK2/ERK1-ERK2 Pathway. *Infection and Immunity*, 1999. **67**(8): p. 3824-3829.
312. Piehler, A.P., R.M. Grimholt, R. Ovstebø&J.P. Berg, Gene expression results in lipopolysaccharide-stimulated monocytes depend significantly on the choice of reference genes. *BMC Immunol*, 2010. **11**: p. 21.
313. Elizur, A., T.L. Adair-Kirk, D.G. Kelley, G.L. Griffin, D.E. Demello&R.M. Senior, Tumor necrosis factor-alpha from macrophages enhances LPS-induced clara cell expression of keratinocyte-derived chemokine. *Am J Respir Cell Mol Biol*, 2008. **38**(1): p. 8-15.
314. Xiong, Y.&D.B. Hales, Expression, regulation, and production of tumor necrosis factor-alpha in mouse testicular interstitial macrophages in vitro. *Endocrinology*, 1993. **133**(6): p. 2568-73.
315. Moreno, C., J. Merino, N. Ramírez, A. Echeverría, F. Pastor&A. Sánchez-Ibarrola, Lipopolysaccharide needs soluble CD14 to interact with TLR4 in human monocytes depleted of membrane CD14. *Microbes and Infection*, 2004. **6**(11): p. 990-995.

References

316. Landmann, R., A.M. Reber, S. Sansano&W. Zimmerli, Function of soluble CD14 in serum from patients with septic shock. *J Infect Dis*, 1996. **173**(3): p. 661-8.
317. Frey, E.A., D.S. Miller, T.G. Jahr, A. Sundan, V. Bazil, T. Espevik, B.B. Finlay&S.D. Wright, Soluble CD14 participates in the response of cells to lipopolysaccharide. *J Exp Med*, 1992. **176**(6): p. 1665-71.
318. Loppnow, H., F. Stelter, U. Schonbeck, C. Schluter, M. Ernst, C. Schutt&H.D. Flad, Endotoxin activates human vascular smooth muscle cells despite lack of expression of CD14 mRNA or endogenous membrane CD14. *Infect Immun*, 1995. **63**(3): p. 1020-6.
319. Hailman, E., T. Vasselon, M. Kelley, L.A. Busse, M.C. Hu, H.S. Lichenstein, P.A. Detmers&S.D. Wright, Stimulation of macrophages and neutrophils by complexes of lipopolysaccharide and soluble CD14. *J Immunol*, 1996. **156**(11): p. 4384-90.
320. Isaza-Guzman, D.M., D. Aristizabal-Cardona, M.C. Martinez-Pabon, H. Velasquez-Echeverri&S.I. Tobon-Arroyave, Estimation of sCD14 levels in saliva obtained from patients with various periodontal conditions. *Oral Dis*, 2008. **14**(5): p. 450-6.
321. Fassbender, K., S. Walter, S. Kuhl, R. Landmann, K. Ishii, T. Bertsch, A.K. Stalder, F. Muehlhauser, Y. Liu, A.J. Ulmer, S. Rivest, A. Lentschat, E. Gulbins, M. Jucker, M. Staufenbiel, K. Brechtel, J. Walter, G. Multhaup, B. Penke, Y. Adachi, T. Hartmann&K. Beyreuther, The LPS receptor (CD14) links innate immunity with Alzheimer's disease. *Faseb j*, 2004. **18**(1): p. 203-5.
322. Amano, S., K. Kawakami, H. Iwahashi, S. Kitano&S. Hanazawa, Functional role of endogenous CD14 in lipopolysaccharide-stimulated bone resorption. *J Cell Physiol*, 1997. **173**(3): p. 301-9.
323. Jersmann, H.P., Time to abandon dogma: CD14 is expressed by non-myeloid lineage cells. *Immunol Cell Biol*, 2005. **83**(5): p. 462-7.
324. Devitt, A., O.D. Moffatt, C. Raykundalia, J.D. Capra, D.L. Simmons&C.D. Gregory, Human CD14 mediates recognition and phagocytosis of apoptotic cells. *Nature*, 1998. **392**(6675): p. 505-9.
325. Gregory, C.D., CD14-dependent clearance of apoptotic cells: relevance to the immune system. *Curr Opin Immunol*, 2000. **12**(1): p. 27-34.
326. Schlegel, R.A., S. Kraehling, M.K. Callahan&P. Williamson, CD14 is a component of multiple recognition systems used by macrophages to phagocytose apoptotic lymphocytes. *Cell Death Differ*, 1999. **6**(6): p. 583-92.
327. Diya, Z., C. Lili, L. Shenglai, G. Zhiyuan&Y. Jie, Lipopolysaccharide (LPS) of *Porphyromonas gingivalis* induces IL-1beta, TNF-alpha and IL-6 production by THP-1 cells in a way different from that of *Escherichia coli* LPS. *Innate Immun*, 2008. **14**(2): p. 99-107.
328. Dentener, M.A., V. Bazil, E.J. Von Asmuth, M. Ceska&W.A. Buurman, Involvement of CD14 in lipopolysaccharide-induced tumor necrosis factor-alpha, IL-6 and IL-8 release by human monocytes and alveolar macrophages. *J Immunol*, 1993. **150**(7): p. 2885-91.
329. Fadok, V.A., D.L. Bratton, A. Konowal, P.W. Freed, J.Y. Westcott&P.M. Henson, Macrophages that have ingested apoptotic cells in vitro inhibit proinflammatory cytokine production through autocrine/paracrine mechanisms involving TGF-beta, PGE2, and PAF. *J Clin Invest*, 1998. **101**(4): p. 890-8.
330. Ishimoto, Y., K. Ohashi, K. Mizuno&T. Nakano, Promotion of the uptake of PS liposomes and apoptotic cells by a product of growth arrest-specific gene, gas6. *J Biochem*, 2000. **127**(3): p. 411-7.
331. Balasubramanian, K., J. Chandra&A.J. Schroit, Immune clearance of phosphatidylserine-expressing cells by phagocytes. The role of beta2-glycoprotein I in macrophage recognition. *J Biol Chem*, 1997. **272**(49): p. 31113-7.
332. Anderson, H.A., C.A. Maylock, J.A. Williams, C.P. Paweletz, H. Shu&E. Shacter, Serum-derived protein S binds to phosphatidylserine and stimulates the phagocytosis of apoptotic cells. *Nat Immunol*, 2003. **4**(1): p. 87-91.
333. Borisenko, G.G., S.L. Iverson, S. Ahlberg, V.E. Kagan&B. Fadeel, Milk fat globule epidermal growth factor 8 (MFG-E8) binds to oxidized phosphatidylserine: implications for macrophage clearance of apoptotic cells. *Cell Death Differ*, 2004. **11**(8): p. 943-5.
334. Azuma, Y., Y. Inami&K. Matsumoto, Alterations in cell surface phosphatidylserine and sugar chains during apoptosis and their time-dependent role in phagocytosis by macrophages. *Biol Pharm Bull*, 2002. **25**(10): p. 1277-81.
335. Fadeel, B.&D. Xue, The ins and outs of phospholipid asymmetry in the plasma membrane: roles in health and disease. *Critical reviews in biochemistry and molecular biology*, 2009. **44**(5): p. 264-277.
336. Ravichandran, K.S., Find-me and eat-me signals in apoptotic cell clearance: progress and conundrums. *The Journal of Experimental Medicine*, 2010. **207**(9): p. 1807-1817.

337. Muller, W.A., S.A. Weigl, X. Deng&D.M. Phillips, PECAM-1 is required for transendothelial migration of leukocytes. *J Exp Med*, 1993. **178**(2): p. 449-60.
338. Brown, S., I. Heinisch, E. Ross, K. Shaw, C.D. Buckley&J. Savill, Apoptosis disables CD31-mediated cell detachment from phagocytes promoting binding and engulfment. *Nature*, 2002. **418**(6894): p. 200-3.
339. Oldenborg, P.A., CD47: A Cell Surface Glycoprotein Which Regulates Multiple Functions of Hematopoietic Cells in Health and Disease. *ISRN Hematol*, 2013. **2013**: p. 614619.
340. Oldenborg, P.A., A. Zheleznyak, Y.F. Fang, C.F. Lagenaur, H.D. Gresham&F.P. Lindberg, Role of CD47 as a marker of self on red blood cells. *Science*, 2000. **288**(5473): p. 2051-4.
341. Gardai, S.J., D.L. Bratton, C.A. Ogden&P.M. Henson, Recognition ligands on apoptotic cells: a perspective. *J Leukoc Biol*, 2006. **79**(5): p. 896-903.
342. Cooper, D., F.P. Lindberg, J.R. Gamble, E.J. Brown&M.A. Vadas, Transendothelial migration of neutrophils involves integrin-associated protein (CD47). *Proceedings of the National Academy of Sciences of the United States of America*, 1995. **92**(9): p. 3978-3982.
343. Liu, Y., D. Merlin, S.L. Burst, M. Pochet, J.L. Madara&C.A. Parkos, The role of CD47 in neutrophil transmigration. Increased rate of migration correlates with increased cell surface expression of CD47. *J Biol Chem*, 2001. **276**(43): p. 40156-66.
344. Lindberg, F.P., D.C. Bullard, T.E. Caver, H.D. Gresham, A.L. Beaudet&E.J. Brown, Decreased resistance to bacterial infection and granulocyte defects in IAP-deficient mice. *Science*, 1996. **274**(5288): p. 795-8.
345. Senior, R.M., H.D. Gresham, G.L. Griffin, E.J. Brown&A.E. Chung, Entactin stimulates neutrophil adhesion and chemotaxis through interactions between its Arg-Gly-Asp (RGD) domain and the leukocyte response integrin. *Journal of Clinical Investigation*, 1992. **90**(6): p. 2251-2257.
346. Elward, K., M. Griffiths, M. Mizuno, C.L. Harris, J.W. Neal, B.P. Morgan&P. Gasque, CD46 plays a key role in tailoring innate immune recognition of apoptotic and necrotic cells. *J Biol Chem*, 2005. **280**(43): p. 36342-54.
347. Chaplin, D.D., Overview of the Immune Response. *The Journal of allergy and clinical immunology*, 2010. **125**(2 Suppl 2): p. S3-23.
348. McCubbrey, A.L.&J.L. Curtis, Efferocytosis and lung disease. *Chest*, 2013. **143**(6): p. 1750-1757.
349. Devitt, A.&L.J. Marshall, The innate immune system and the clearance of apoptotic cells. *Journal of Leukocyte Biology*, 2011. **90**(3): p. 447-457.
350. Krysko, D.V., G. Denecker, N. Festjens, S. Gabriels, E. Parthoens, K. D'Herde&P. Vandenabeele, Macrophages use different internalization mechanisms to clear apoptotic and necrotic cells. *Cell Death Differ*, 2006. **13**(12): p. 2011-2022.
351. Scott, D.A.&J.L. Krauss, Neutrophils in periodontal inflammation. *Frontiers of Oral Biology*, 2012. **15**: p. 56-83.
352. Borregaard, N., O.E. Sorensen&K. Theilgaard-Monch, Neutrophil granules: a library of innate immunity proteins. *Trends Immunol*, 2007. **28**(8): p. 340-5.
353. Ishikawa, F.&S. Miyazaki, New biodefense strategies by neutrophils. *Archivum Immunologiae et Therapiae Experimentalis*, 2005. **53**(3): p. 226-233.
354. Ivanyi, L.&T. Lehner, Stimulation of lymphocyte transformation by bacterial antigens in patients with periodontal disease. *Archives of Oral Biology*, 1970. **15**(11): p. 1089-1096.
355. Lavine, W.S., E.G. Maderazo, J. Stolman, P.A. Ward, R.B. Cogen, I. Greenblatt&P.B. Robertson, Impaired neutrophil chemotaxis in patients with juvenile and rapidly progressing periodontitis. *J Periodontal Res*, 1979. **14**(1): p. 10-9.
356. Crawford, J.M., J.M. Wilton&P. Richardson, Neutrophils die in the gingival crevice, periodontal pocket, and oral cavity by necrosis and not apoptosis. *J Periodontol*, 2000. **71**(7): p. 1121-9.
357. Shivanaikar, S.S., M. Faizuddin&K. Bhat, Effect of smoking on neutrophil apoptosis in chronic periodontitis: an immunohistochemical study. *Indian J Dent Res*, 2013. **24**(1): p. 147.
358. Havens, A.M., E. Chiu, M. Taba, J. Wang, Y. Shiozawa, Y. Jung, L.S. Taichman, N.J. D'Silva, R. Gopalakrishnan, C. Wang, W.V. Giannobile&R.S. Taichman, Stromal-derived factor-1alpha (CXCL12) levels increase in periodontal disease. *J Periodontol*, 2008. **79**(5): p. 845-53.
359. Guarnieri, C., G. Melandri, I. Caldarera, M. Scheda, A. Ligabue, S. Guizzardi&A. Branzi, Reduced oxidative activity of circulating neutrophils in patients after myocardial infarction. *Cell Biochem Funct*, 1990. **8**(3): p. 157-62.
360. Brock, G.R., C.J. Butterworth, J.B. Matthews&I.L. Chapple, Local and systemic total antioxidant capacity in periodontitis and health. *J Clin Periodontol*, 2004. **31**(7): p. 515-21.

References

361. Chapple, I.L.&J.B. Matthews, The role of reactive oxygen and antioxidant species in periodontal tissue destruction. *Periodontol* 2000, 2007. **43**: p. 160-232.
362. Matthews, J.B., H.J. Wright, A. Roberts, N. Ling-Mountford, P.R. Cooper&I.L. Chapple, Neutrophil hyper-responsiveness in periodontitis. *J Dent Res*, 2007. **86**(8): p. 718-22.
363. Gümüş, P., G. Emingil, V.-Ö. Öztürk, G.N. Belibasakis&N. Bostanci, Oxidative stress markers in saliva and periodontal disease status: modulation during pregnancy and postpartum. *BMC Infectious Diseases*, 2015. **15**: p. 261.
364. Ahmadi-Motamayel, F., M.T. Goodarzi, Z. Jamshidi&R. Kebriaei, Evaluation of Salivary and Serum Antioxidant and Oxidative Stress Statuses in Patients with Chronic Periodontitis: A Case-Control Study. *Frontiers in Physiology*, 2017. **8**: p. 189.
365. Asif, K.&S.V. Kothiwale, Phagocytic activity of peripheral blood and crevicular phagocytes in health and periodontal disease. *J Indian Soc Periodontol*, 2010. **14**(1): p. 8-11.
366. Gomez-Cambronero, J., E. Wang, G. Johnson, C.K. Huang&R.I. Sha'afi, Platelet-activating factor induces tyrosine phosphorylation in human neutrophils. *Journal of Biological Chemistry*, 1991. **266**(10): p. 6240-6245.
367. Van Dyke, T.E., H.U. Horoszewicz, L.J. Cianciola&R.J. Genco, Neutrophil chemotaxis dysfunction in human periodontitis. *Infection and Immunity*, 1980. **27**(1): p. 124-132.
368. Guentsch, A., M. Puklo, P.M. Preshaw, E. Glockmann, W. Pfister, J. Potempa&S. Eick, Neutrophils in chronic and aggressive periodontitis in interaction with *Porphyromonas gingivalis* and *Aggregatibacter actinomycetemcomitans*. *Journal of Periodontal Research*, 2009. **44**(3): p. 368-377.
369. Nibali, L., M. O'Dea, G. Bouma, M. Parkar, A.J. Thrasher, S. Burns&N. Donos, Genetic variants associated with neutrophil function in aggressive periodontitis and healthy controls. *Journal of Periodontology*, 2010. **81**(4): p. 527-534.
370. Henriksen, P.A., A. Devitt, Y. Kotelevtsev&J.M. Sallenave, Gene delivery of the elastase inhibitor elafin protects macrophages from neutrophil elastase-mediated impairment of apoptotic cell recognition. *FEBS Lett*, 2004. **574**(1-3): p. 80-4.
371. Carneiro, V.M.A., A.C.B. Bezerra, M.C.M. Guimarães&M.I. Muniz-Junqueira, Decreased phagocytic function in neutrophils and monocytes from peripheral blood in periodontal disease. *Journal of Applied Oral Science*, 2012. **20**(5): p. 503-509.
372. Nussbaum, G.&L. Shapira, How has neutrophil research improved our understanding of periodontal pathogenesis? *J Clin Periodontol*, 2011. **38 Suppl 11**: p. 49-59.
373. Vitkov, L., M. Klappacher, M. Hannig&W.D. Krautgartner, Neutrophil fate in gingival crevicular fluid. *Ultrastruct Pathol*, 2010. **34**(1): p. 25-30.
374. Vitkov, L., M. Klappacher, M. Hannig&W.D. Krautgartner, Extracellular neutrophil traps in periodontitis. *J Periodontal Res*, 2009. **44**(5): p. 664-72.
375. Delbosc, S., J.-M. Alsac, C. Journe, L. Louedec, Y. Castier, M. Bonnaure-Mallet, R. Ruimy, P. Rossignol, P. Bouchard, J.-B. Michel&O. Meilhac, *Porphyromonas gingivalis* Participates in Pathogenesis of Human Abdominal Aortic Aneurysm by Neutrophil Activation. Proof of Concept in Rats. *PLoS ONE*, 2011. **6**(4): p. e18679.
376. Belaouaj, A., Neutrophil elastase-mediated killing of bacteria: lessons from targeted mutagenesis. *Microbes Infect*, 2002. **4**(12): p. 1259-64.
377. Ujii, Y., S. Oida, K. Gomi, T. Arai&M. Fukae, Neutrophil elastase is involved in the initial destruction of human periodontal ligament. *J Periodontal Res*, 2007. **42**(4): p. 325-30.
378. Matheson, S., H. Larjava&L. Hakkinen, Distinctive localization and function for lumican, fibromodulin and decorin to regulate collagen fibril organization in periodontal tissues. *J Periodontal Res*, 2005. **40**(4): p. 312-24.
379. Young, R.E., R.D. Thompson, K.Y. Larbi, M. La, C.E. Roberts, S.D. Shapiro, M. Perretti&S. Nourshargh, Neutrophil elastase (NE)-deficient mice demonstrate a nonredundant role for NE in neutrophil migration, generation of proinflammatory mediators, and phagocytosis in response to zymosan particles in vivo. *J Immunol*, 2004. **172**(7): p. 4493-502.
380. Nemoto, E., S. Kanaya, M. Minamibuchi&H. Shimauchi, Cleavage of PDGF receptor on periodontal ligament cells by elastase. *J Dent Res*, 2005. **84**(7): p. 629-33.
381. Rodriguez-Prados, J.C., P.G. Traves, J. Cuenca, D. Rico, J. Aragonés, P. Martín-Sanz, M. Cascante&L. Bosca, Substrate fate in activated macrophages: a comparison between innate, classic, and alternative activation. *J Immunol*, 2010. **185**(1): p. 605-14.
382. Pioli, P.A., L.K. Weaver, T.M. Schaefer, J.A. Wright, C.R. Wira&P.M. Guyre, Lipopolysaccharide-induced IL-1 beta production by human uterine macrophages up-regulates uterine epithelial cell expression of human beta-defensin 2. *J Immunol*, 2006. **176**(11): p. 6647-55.
383. Page, R.C., The role of inflammatory mediators in the pathogenesis of periodontal disease. *J Periodontal Res*, 1991. **26**(3 Pt 2): p. 230-42.

References

384. Gregory, C.D., A. Devitt&O. Moffatt, Roles of ICAM-3 and CD14 in the recognition and phagocytosis of apoptotic cells by macrophages. *Biochem Soc Trans*, 1998. **26**(4): p. 644-9.
385. Zadeh, H.H., F.C. Nichols&K.T. Miyasaki, The role of the cell-mediated immune response to *Actinobacillus actinomycetemcomitans* and *Porphyromonas gingivalis* in periodontitis. *Periodontol 2000*, 1999. **20**: p. 239-88.
386. Chapple, C.C., M. Srivastava&N. Hunter, Failure of macrophage activation in destructive periodontal disease. *J Pathol*, 1998. **186**(3): p. 281-6.
387. Gemmell, E., C.L. Carter&G.J. Seymour, Mast cells in human periodontal disease. *J Dent Res*, 2004. **83**(5): p. 384-7.
388. Martinez, F.O., A. Sica, A. Mantovani&M. Locati, Macrophage activation and polarization. *Front Biosci*, 2008. **13**: p. 453-61.
389. Bullon, P., H.N. Newman&M. Battino, Obesity, diabetes mellitus, atherosclerosis and chronic periodontitis: a shared pathology via oxidative stress and mitochondrial dysfunction? *Periodontol 2000*, 2014. **64**(1): p. 139-53.
390. Page, R.C.&H.E. Schroeder, Pathogenesis of inflammatory periodontal disease: a summary of current work. *Laboratory Investigation*, 1976. **34**(3): p. 235-249.
391. Fatemi, K., M. Radvar, A. Rezaee, H. Rafatpanah, H. Azangoo khiavi, Y. Dadpour&N. Radvar, Comparison of relative TLR-2 and TLR-4 expression level of disease and healthy gingival tissue of smoking and non-smoking patients and periodontally healthy control patients. *Aust Dent J*, 2013. **58**(3): p. 315-20.
392. Pauletto, N.C., K. Liede, A. Nieminen, H. Larjava&V.J. Uitto, Effect of cigarette smoking on oral elastase activity in adult periodontitis patients. *J Periodontol*, 2000. **71**(1): p. 58-62.
393. de Heens, G.L., R. Kikkert, L.A. Aarden, U. van der Velden&B.G. Loos, Effects of smoking on the ex vivo cytokine production in periodontitis. *J Periodontal Res*, 2009. **44**(1): p. 28-34.
394. Axtelius, B., B. Soderfeldt, A. Nilsson, S. Edwardsson&R. Attstrom, Therapy-resistant periodontitis. Psychosocial characteristics. *J Clin Periodontol*, 1998. **25**(6): p. 482-91.
395. Mengel, R., M. Bacher&L. Flores-De-Jacoby, Interactions between stress, interleukin-1beta, interleukin-6 and cortisol in periodontally diseased patients. *J Clin Periodontol*, 2002. **29**(11): p. 1012-22.
396. Johannsen, A., G. Rylander, B. Soder&M. Asberg, Dental plaque, gingival inflammation, and elevated levels of interleukin-6 and cortisol in gingival crevicular fluid from women with stress-related depression and exhaustion. *J Periodontol*, 2006. **77**(8): p. 1403-9.
397. Michalowicz, B.S., S.R. Diehl, J.C. Gunsolley, B.S. Sparks, C.N. Brooks, T.E. Koertge, J.V. Califano, J.A. Burmeister&H.A. Schenkein, Evidence of a substantial genetic basis for risk of adult periodontitis. *J Periodontol*, 2000. **71**(11): p. 1699-707.
398. Amorim, F., M. Depoli, G. Simões, B. Campagnaro, C. Tonini, I. Louro, J. Arruda, E. Vasquez&S. Meyrelles, Endothelial Nitric Oxide Synthase Gene Polymorphism and Periodontal Disease. *Journal of Blood Diseases*, 2012. **2**: p. 34-37.
399. Erciyas, K., S. Pehlivan, T. Sever&R. Orbak, Genetic Variation of Myeloperoxidase Gene Contributes to Aggressive Periodontitis: A Preliminary Association Study in Turkish Population. *Disease markers*, 2010. **28**(2): p. 95-99.
400. Cueno, M.E., K. Seki, K. Ochiai&K. Imai, Periodontal disease level-butyrac acid putatively contributes to the ageing blood: A proposed link between periodontal diseases and the ageing process. *Mechanisms of Ageing and Development*, 2017. **162**: p. 100-105.
401. Preshaw, P.M., K. Henne, J.J. Taylor, R.A. Valentine&G. Conrads, Age-related changes in immune function (immune senescence) in caries and periodontal diseases: a systematic review. *J Clin Periodontol*, 2017. **44 Suppl 18**: p. S153-s177.
402. Jeffcoat, M.K., N.C. Geurs, M.S. Reddy, S.P. Cliver, R.L. Goldenberg&J.C. Hauth, Periodontal infection and preterm birth: results of a prospective study. *J Am Dent Assoc*, 2001. **132**(7): p. 875-80.
403. Saini, R., S. Saini&S.R. Saini, Periodontitis: A risk for delivery of premature labor and low-birth-weight infants. *Journal of Natural Science, Biology, and Medicine*, 2010. **1**(1): p. 40-42.
404. Toomarian, L.&N. Hashemi, Periodontal manifestation of leukocyte adhesion deficiency type I. *Arch Iran Med*, 2010. **13**(4): p. 355-9.
405. Tewari, S., S. Tewari, R.K. Sharma, P. Abrol&R. Sen, Necrotizing stomatitis: a possible periodontal manifestation of deferiprone-induced agranulocytosis. *Oral Surgery, Oral Medicine, Oral Pathology, Oral Radiology, and Endodontology*, 2009. **108**(4): p. e13-e19.
406. Miyajima, S.-i., K. Naruse, Y. Kobayashi, N. Nakamura, T. Nishikawa, K. Adachi, Y. Suzuki, T. Kikuchi, A. Mitani, M. Mizutani, N. Ohno, T. Noguchi&T. Matsubara,

References

- Periodontitis-activated monocytes/macrophages cause aortic inflammation. *Scientific Reports*, 2014. **4**: p. 5171.
407. Shi, C.&E.G. Pamer, Monocyte recruitment during infection and inflammation. *Nature reviews. Immunology*, 2011. **11**(11): p. 762-774.
408. Hanazawa, S., Y. Kawata, A. Takeshita, H. Kumada, M. Okithu, S. Tanaka, Y. Yamamoto, T. Masuda, T. Umemoto&S. Kitano, Expression of monocyte chemoattractant protein 1 (MCP-1) in adult periodontal disease: increased monocyte chemotactic activity in crevicular fluids and induction of MCP-1 expression in gingival tissues. *Infect Immun*, 1993. **61**(12): p. 5219-24.
409. Gemmell, E., C.L. Carter&G.J. Seymour, Chemokines in human periodontal disease tissues. *Clinical and Experimental Immunology*, 2001. **125**(1): p. 134-141.
410. Kabashima, H., M. Yoneda, K. Nagata, T. Hirofujii&K. Maeda, The presence of chemokine (MCP-1, MIP-1alpha, MIP-1beta, IP-10, RANTES)-positive cells and chemokine receptor (CCR5, CXCR3)-positive cells in inflamed human gingival tissues. *Cytokine*, 2002. **20**(2): p. 70-7.
411. Madeira, M.F.M., C.M. Queiroz-Junior, G.M. Costa, P.C. Santos, E.M. Silveira, G.P. Garlet, P.S. Cisalpino, M.M. Teixeira, T.A. Silva&D.d.G. Souza, MIF induces osteoclast differentiation and contributes to progression of periodontal disease in mice. *Microbes and Infection*, 2012. **14**(2): p. 198-206.
412. Nowzari, H., S. Phamduong, J.E. Botero, M.C. Villacres&S.K. Rich, The profile of inflammatory cytokines in gingival crevicular fluid around healthy osseointegrated implants. *Clin Implant Dent Relat Res*, 2012. **14**(4): p. 546-52.
413. Bozkurt, F.Y., Z. Yetkin Ay, E. Berker, E. Tepe&S. Akkus, Anti-inflammatory cytokines in gingival crevicular fluid in patients with periodontitis and rheumatoid arthritis: a preliminary report. *Cytokine*, 2006. **35**(3-4): p. 180-5.
414. Offenbacher, S., S. Barros, L. Mendoza, S. Mauriello, J. Preisser, K. Moss, M. de Jager&M. Aspiras, Changes in Gingival Crevicular Fluid Inflammatory Mediator Levels during the Induction and Resolution of Experimental Gingivitis in Humans. *Journal of clinical periodontology*, 2010. **37**(4): p. 324-333.
415. Martinez-Pomares, L.&S. Gordon, Antigen Presentation the Macrophage Way. *Cell*. **131**(4): p. 641-643.
416. Nakajima, T., K. Ueki-Maruyama, T. Oda, Y. Ohsawa, H. Ito, G.J. Seymour&K. Yamazaki, Regulatory T-cells infiltrate periodontal disease tissues. *J Dent Res*, 2005. **84**(7): p. 639-43.
417. Gregory, C.D., M. Rowe&A.B. Rickinson, Different Epstein-Barr virus-B cell interactions in phenotypically distinct clones of a Burkitt's lymphoma cell line. *J Gen Virol*, 1990. **71 (Pt 7)**: p. 1481-95.
418. Devitt, A., S. Pierce, C. Oldreive, W.H. Shingler&C.D. Gregory, CD14-dependent clearance of apoptotic cells by human macrophages: the role of phosphatidylserine. *Cell Death Differ*, 2003. **10**(3): p. 371-82.
419. Keenan, T.M.&A. Folch, Biomolecular gradients in cell culture systems. *Lab on a chip*, 2008. **8**(1): p. 10.1039/b711887b.
420. Nelson, K.E., R.D. Fleischmann, R.T. DeBoy, I.T. Paulsen, D.E. Fouts, J.A. Eisen, S.C. Daugherty, R.J. Dodson, A.S. Durkin, M. Gwinn, D.H. Haft, J.F. Kolonay, W.C. Nelson, T. Mason, L. Tallon, J. Gray, D. Granger, H. Tettelin, H. Dong, J.L. Galvin, M.J. Duncan, F.E. Dewhirst&C.M. Fraser, Complete genome sequence of the oral pathogenic Bacterium porphyromonas gingivalis strain W83. *J Bacteriol*, 2003. **185**(18): p. 5591-601.
421. Loos, B.G., D.W. Dyer, T.S. Whittam&R.K. Selander, Genetic structure of populations of Porphyromonas gingivalis associated with periodontitis and other oral infections. *Infect Immun*, 1993. **61**(1): p. 204-12.
422. Menard, C.&C. Mouton, Clonal diversity of the taxon Porphyromonas gingivalis assessed by random amplified polymorphic DNA fingerprinting. *Infect Immun*, 1995. **63**(7): p. 2522-31.
423. Siddiqui, H., D.R. Yoder-Himes, D. Mizgalska, K.A. Nguyen, J. Potempa&I. Olsen, Genome Sequence of Porphyromonas gingivalis Strain HG66 (DSM 28984). *Genome Announc*, 2014. **2**(5).
424. Bartholomew, J.W.&T. Mittwer, THE GRAM STAIN. *Bacteriological Reviews*, 1952. **16**(1): p. 1-29.
425. Murakami, Y., M. Imai, H. Nakamura&F. Yoshimura, Separation of the outer membrane and identification of major outer membrane proteins from Porphyromonas gingivalis. *Eur J Oral Sci*, 2002. **110**(2): p. 157-62.

References

426. Pike, R., W. McGraw, J. Potempa&J. Travis, Lysine- and arginine-specific proteinases from *Porphyromonas gingivalis*. Isolation, characterization, and evidence for the existence of complexes with hemagglutinins. *J Biol Chem*, 1994. **269**(1): p. 406-11.
427. Nowakowski, A.B., W.J. Wobig&D.H. Petering, Native SDS-PAGE: High Resolution Electrophoretic Separation of Proteins With Retention of Native Properties Including Bound Metal Ions. *Metallomics : integrated biometal science*, 2014. **6**(5): p. 1068-1078.
428. Shevchenko, A., H. Tomas, J. Havlis, J.V. Olsen&M. Mann, In-gel digestion for mass spectrometric characterization of proteins and proteomes. *Nat. Protocols*, 2007. **1**(6): p. 2856-2860.
429. Fitzpatrick, R.E., A. Aprico, L.C. Wijeyewickrema, C.N. Pagel, D.M. Wong, J. Potempa, E.J. Mackie&R.N. Pike, High molecular weight gingipains from *Porphyromonas gingivalis* induce cytokine responses from human macrophage-like cells via a nonproteolytic mechanism. *J Innate Immun*, 2009. **1**(2): p. 109-17.
430. Silva, M.T.&M. Correia-Neves, Neutrophils and Macrophages: the Main Partners of Phagocyte Cell Systems. *Frontiers in Immunology*, 2012. **3**: p. 174.
431. Faurischou, M.&N. Borregaard, Neutrophil granules and secretory vesicles in inflammation. *Microbes and Infection*, 2003. **5**(14): p. 1317-1327.
432. Kunkel, S.L., T. Standiford, K. Kasahara&R.M. Strieter, Interleukin-8 (IL-8): the major neutrophil chemotactic factor in the lung. *Exp Lung Res*, 1991. **17**(1): p. 17-23.
433. Becker, S., J. Quay&J. Soukup, Cytokine (tumor necrosis factor, IL-6, and IL-8) production by respiratory syncytial virus-infected human alveolar macrophages. *J Immunol*, 1991. **147**(12): p. 4307-12.
434. Detmers, P.A., D.E. Powell, A. Walz, I. Clark-Lewis, M. Baggiolini&Z.A. Cohn, Differential effects of neutrophil-activating peptide 1/IL-8 and its homologues on leukocyte adhesion and phagocytosis. *J Immunol*, 1991. **147**(12): p. 4211-7.
435. Deas, D.E., S.A. Mackey&H.T. McDonnell, Systemic disease and periodontitis: manifestations of neutrophil dysfunction. *Periodontol 2000*, 2003. **32**: p. 82-104.
436. Darveau, R.P., Periodontitis: a polymicrobial disruption of host homeostasis. *Nat Rev Micro*, 2010. **8**(7): p. 481-490.
437. Gille, C., A. Leiber, B. Spring, V.A. Kempf, J. Loeffler, C.F. Poets&T.W. Orlikowsky, Diminished phagocytosis-induced cell death (PICD) in neonatal monocytes upon infection with *Escherichia coli*. *Pediatr Res*, 2008. **63**(1): p. 33-8.
438. Kobayashi, S.D., K.R. Braughton, A.R. Whitney, J.M. Voyich, T.G. Schwan, J.M. Musser&F.R. DeLeo, Bacterial pathogens modulate an apoptosis differentiation program in human neutrophils. *Proc Natl Acad Sci U S A*, 2003. **100**(19): p. 10948-53.
439. Fox, S., A.E. Leitch, R. Duffin, C. Haslett&A.G. Rossi, Neutrophil Apoptosis: Relevance to the Innate Immune Response and Inflammatory Disease. *Journal of Innate Immunity*, 2010. **2**(3): p. 216-227.
440. Voll, R.E., M. Herrmann, E.A. Roth, C. Stach, J.R. Kalden&I. Girkontaite, Immunosuppressive effects of apoptotic cells. *Nature*, 1997. **390**(6658): p. 350-1.
441. Webster, M., K.L. Witkin&O. Cohen-Fix, Sizing up the nucleus: nuclear shape, size and nuclear-envelope assembly. *Journal of Cell Science*, 2009. **122**(10): p. 1477-1486.
442. Önerci, T.M., *Nasal Physiology and Pathophysiology of Nasal Disorders*. 2013: Springer Berlin Heidelberg.
443. van Furth, R., Z.A. Cohn, J.G. Hirsch, J.H. Humphrey, W.G. Spector&H.L. Langevoort, The mononuclear phagocyte system: a new classification of macrophages, monocytes, and their precursor cells. *Bulletin of the World Health Organization*, 1972. **46**(6): p. 845-852.
444. Nadella, V., Z. Wang, T.S. Johnson, M. Griffin&A. Devitt, Transglutaminase 2 interacts with syndecan-4 and CD44 at the surface of human macrophages to promote removal of apoptotic cells. *Biochim Biophys Acta*, 2015. **1853**(1): p. 201-12.
445. Daigneault, M., J.A. Preston, H.M. Marriott, M.K. Whyte&D.H. Dockrell, The identification of markers of macrophage differentiation in PMA-stimulated THP-1 cells and monocyte-derived macrophages. *PLoS One*, 2010. **5**(1): p. e8668.
446. Sadeghi, K., B. Wessner, U. Laggner, M. Ploder, D. Tamandl, J. Friedl, U. Zugel, A. Steinmeyer, A. Pollak, E. Roth, G. Boltz-Nitulescu&A. Spittler, Vitamin D3 down-regulates monocyte TLR expression and triggers hyporesponsiveness to pathogen-associated molecular patterns. *Eur J Immunol*, 2006. **36**(2): p. 361-70.
447. Aldo, P.B., V. Craveiro, S. Guller&G. Mor, Effect of culture conditions on the phenotype of THP-1 monocyte cell line. *Am J Reprod Immunol*, 2013. **70**(1): p. 80-6.
448. Huh, H.Y., S.F. Pearce, L.M. Yesner, J.L. Schindler&R.L. Silverstein, Regulated expression of CD36 during monocyte-to-macrophage differentiation: potential role of CD36 in foam cell formation. *Blood*, 1996. **87**(5): p. 2020-8.

References

449. Ferracini, M., F.J. Rios, M. Pecenin&S. Jancar, Clearance of apoptotic cells by macrophages induces regulatory phenotype and involves stimulation of CD36 and platelet-activating factor receptor. *Mediators Inflamm*, 2013. **2013**: p. 950273.
450. Parthasarathy, S., A. Raghavamenon, M.O. Garelnabi&N. Santanam, Oxidized Low-Density Lipoprotein. *Methods in Molecular Biology (Clifton, N.j.)*, 2010. **610**: p. 403-417.
451. Nagahama, Y., T. Obama, M. Usui, Y. Kanazawa, S. Iwamoto, K. Suzuki, A. Miyazaki, T. Yamaguchi, M. Yamamoto&H. Itabe, Oxidized low-density lipoprotein-induced periodontal inflammation is associated with the up-regulation of cyclooxygenase-2 and microsomal prostaglandin synthase 1 in human gingival epithelial cells. *Biochem Biophys Res Commun*, 2011. **413**(4): p. 566-71.
452. Van Haastert, P.J.M.&P.N. Devreotes, Chemotaxis: signalling the way forward. *Nat Rev Mol Cell Biol*, 2004. **5**(8): p. 626-634.
453. Roussos, E.T., J.S. Condeelis&A. Patsialou, Chemotaxis in cancer. *Nature reviews. Cancer*, 2011. **11**(8): p. 573-587.
454. Condeelis, J., R.H. Singer&J.E. Segall, The great escape: when cancer cells hijack the genes for chemotaxis and motility. *Annu Rev Cell Dev Biol*, 2005. **21**: p. 695-718.
455. Aman, A.&T. Piotrowski, Cell migration during morphogenesis. *Developmental Biology*, 2010. **341**(1): p. 20-33.
456. Schneider, L., M. Cammer, J. Lehman, S.K. Nielsen, C.F. Guerra, I.R. Veland, C. Stock, E.K. Hoffmann, B.K. Yoder, A. Schwab, P. Satir&S.T. Christensen, Directional Cell Migration and Chemotaxis in Wound Healing Response to PDGF-AA are Coordinated by the Primary Cilium in Fibroblasts. *Cellular Physiology and Biochemistry*, 2010. **25**(2-3): p. 279-292.
457. Singer, M.&P.J. Sansonetti, IL-8 is a key chemokine regulating neutrophil recruitment in a new mouse model of Shigella-induced colitis. *J Immunol*, 2004. **173**(6): p. 4197-206.
458. Carrigan, S.O., D.B. Pink&A.W. Stadnyk, Neutrophil transepithelial migration in response to the chemoattractant fMLP but not C5a is phospholipase D-dependent and related to the use of CD11b/CD18. *J Leukoc Biol*, 2007. **82**(6): p. 1575-84.
459. Dixit, N.&S.I. Simon, Chemokines, selectins and intracellular calcium flux: temporal and spatial cues for leukocyte arrest. *Frontiers in Immunology*, 2012. **3**: p. 188.
460. Thorp, E.B., Mechanisms of failed apoptotic cell clearance by phagocyte subsets in cardiovascular disease. *Apoptosis : an international journal on programmed cell death*, 2010. **15**(9): p. 1124-1136.
461. Truman, L.A., C.A. Ford, M. Pasikowska, J.D. Pound, S.J. Wilkinson, I.E. Dumitriu, L. Melville, L.A. Melrose, C.A. Ogden, R. Nibbs, G. Graham, C. Combadiere&C.D. Gregory, CX3CL1/fractalkine is released from apoptotic lymphocytes to stimulate macrophage chemotaxis. *Blood*, 2008. **112**(13): p. 5026-36.
462. Segundo, C., F. Medina, C. Rodriguez, R. Martinez-Palencia, F. Leyva-Cobian&J.A. Brieva, Surface molecule loss and bleb formation by human germinal center B cells undergoing apoptosis: role of apoptotic blebs in monocyte chemotaxis. *Blood*, 1999. **94**(3): p. 1012-20.
463. Law, A.M.&M.D. Aitken, Continuous-flow capillary assay for measuring bacterial chemotaxis. *Appl Environ Microbiol*, 2005. **71**(6): p. 3137-43.
464. Kramer, N., A. Walzl, C. Unger, M. Rosner, G. Krupitza, M. Hengstschlager&H. Dolznig, In vitro cell migration and invasion assays. *Mutat Res*, 2013. **752**(1): p. 10-24.
465. Islam, L.N., I.C. McKay&P.C. Wilkinson, The use of collagen or fibrin gels for the assay of human neutrophil chemotaxis. *J Immunol Methods*, 1985. **85**(1): p. 137-51.
466. Breckenridge, M.T., T.T. Egelhoff&H. Baskaran, A microfluidic imaging chamber for the direct observation of chemotactic transmigration. *Biomed Microdevices*, 2010. **12**(3): p. 543-53.
467. Zicha, D., G. Dunn&G. Jones, Analyzing chemotaxis using the Dunn direct-viewing chamber. *Methods Mol Biol*, 1997. **75**: p. 449-57.
468. Zicha, D., G.A. Dunn&A.F. Brown, A new direct-viewing chemotaxis chamber. *J Cell Sci*, 1991. **99** (Pt 4): p. 769-75.
469. Hawkins, L.A.&A. Devitt, Current understanding of the mechanisms for clearance of apoptotic cells-a fine balance. *J Cell Death*, 2013. **6**: p. 57-68.
470. Asano, Y.&E. Horn, Visualization and Data Analysis of Chemotaxis and Migration Processes Chemotaxis and Migration Tool 2.0 2011.
471. Szondy, Z., É. Garabuczi, G. Joós, G.J. Tsay&Z. Sarang, Impaired Clearance of Apoptotic Cells in Chronic Inflammatory Diseases: Therapeutic Implications. *Frontiers in Immunology*, 2014. **5**: p. 354.

References

472. Gustafsson, A., H. Ito, B. Asman&K. Bergstrom, Hyper-reactive mononuclear cells and neutrophils in chronic periodontitis. *J Clin Periodontol*, 2006. **33**(2): p. 126-9.
473. Yoon, J., A. Terada&H. Kita, CD66b regulates adhesion and activation of human eosinophils. *J Immunol*, 2007. **179**(12): p. 8454-62.
474. Lakschevitz, F.S., S. Hassanpour, A. Rubin, N. Fine, C. Sun&M. Glogauer, Identification of neutrophil surface marker changes in health and inflammation using high-throughput screening flow cytometry. *Exp Cell Res*, 2016. **342**(2): p. 200-9.
475. Carlos, T.M.&J.M. Harlan, Leukocyte-endothelial adhesion molecules. *Blood*, 1994. **84**(7): p. 2068-101.
476. Chan, Y.-K., M.-H. Tsai, D.-C. Huang, Z.-H. Zheng&K.-D. Hung, Leukocyte nucleus segmentation and nucleus lobe counting. *BMC Bioinformatics*, 2010. **11**: p. 558-558.
477. Rowat, A.C., D.E. Jaalouk, M. Zwerger, W.L. Ung, I.A. Eydelnant, D.E. Olins, A.L. Olins, H. Herrmann, D.A. Weitz&J. Lammerding, Nuclear Envelope Composition Determines the Ability of Neutrophil-type Cells to Passage through Micron-scale Constrictions. *The Journal of Biological Chemistry*, 2013. **288**(12): p. 8610-8618.
478. Carvalho, L.O., E.N. Aquino, A.C. Neves&W. Fontes, The Neutrophil Nucleus and Its Role in Neutrophilic Function. *J Cell Biochem*, 2015. **116**(9): p. 1831-6.
479. Somersan, S.&N. Bhardwaj, Tethering and tickling: a new role for the phosphatidylserine receptor. *J Cell Biol*, 2001. **155**(4): p. 501-4.
480. Porter, A.G.&R.U. Janicke, Emerging roles of caspase-3 in apoptosis. *Cell Death Differ*, 1999. **6**(2): p. 99-104.
481. Weinmann, P., P. Gaehdgens&B. Walzog, Bcl-Xl- and Bax-alpha-mediated regulation of apoptosis of human neutrophils via caspase-3. *Blood*, 1999. **93**(9): p. 3106-15.
482. Pryde, J.G., A. Walker, A.G. Rossi, S. Hannah&C. Haslett, Temperature-dependent arrest of neutrophil apoptosis. Failure of Bax insertion into mitochondria at 15 degrees C prevents the release of cytochrome c. *J Biol Chem*, 2000. **275**(43): p. 33574-84.
483. Gregory, C.D.&A.E. Milner, Regulation of cell survival in Burkitt lymphoma: implications from studies of apoptosis following cold-shock treatment. *Int J Cancer*, 1994. **57**(3): p. 419-26.
484. Cheng, E.H., D.G. Kirsch, R.J. Clem, R. Ravi, M.B. Kastan, A. Bedi, K. Ueno&J.M. Hardwick, Conversion of Bcl-2 to a Bax-like death effector by caspases. *Science*, 1997. **278**(5345): p. 1966-8.
485. Dunkern, T.R., G. Fritz&B. Kaina, Ultraviolet light-induced DNA damage triggers apoptosis in nucleotide excision repair-deficient cells via Bcl-2 decline and caspase-3/-8 activation. *Oncogene*, 2001. **20**(42): p. 6026-38.
486. Schuler, M., E. Bossy-Wetzler, J.C. Goldstein, P. Fitzgerald&D.R. Green, p53 induces apoptosis by caspase activation through mitochondrial cytochrome c release. *J Biol Chem*, 2000. **275**(10): p. 7337-42.
487. Pongracz, J., P. Webb, K. Wang, E. Deacon, O.J. Lunn&J.M. Lord, Spontaneous neutrophil apoptosis involves caspase 3-mediated activation of protein kinase C-delta. *J Biol Chem*, 1999. **274**(52): p. 37329-34.
488. Chen, Y., H. Wu, W.R. Winnall, K.L. Loveland, Y. Makanji, D.J. Phillips, J.A. Smith&M.P. Hedger, Tumour necrosis factor-alpha stimulates human neutrophils to release preformed activin A. *Immunol Cell Biol*, 2011. **89**(8): p. 889-96.
489. Sabroe, I., S.K. Dower&M.K. Whyte, The role of Toll-like receptors in the regulation of neutrophil migration, activation, and apoptosis. *Clin Infect Dis*, 2005. **41 Suppl 7**: p. S421-6.
490. Sabroe, I., L.R. Prince, E.C. Jones, M.J. Horsburgh, S.J. Foster, S.N. Vogel, S.K. Dower&M.K. Whyte, Selective roles for Toll-like receptor (TLR)2 and TLR4 in the regulation of neutrophil activation and life span. *J Immunol*, 2003. **170**(10): p. 5268-75.
491. Feterowski, C., H. Weighardt, K. Emmanuilidis, T. Hartung&B. Holzmann, Immune protection against septic peritonitis in endotoxin-primed mice is related to reduced neutrophil apoptosis. *Eur J Immunol*, 2001. **31**(4): p. 1268-77.
492. Pillay, J., I. den Braber, N. Vriskoop, L.M. Kwast, R.J. de Boer, J.A. Borghans, K. Tesselaar&L. Koenderman, In vivo labeling with ²H₂O reveals a human neutrophil lifespan of 5.4 days. *Blood*, 2010. **116**(4): p. 625-7.
493. Mayadas, T.N., X. Cullere&C.A. Lowell, The Multifaceted Functions of Neutrophils. *Annual review of pathology*, 2014. **9**: p. 181-218.
494. Hou, F.F., J. Boyce, Y. Zhang&W.F. Owen, Jr., Phenotypic and functional characteristics of macrophage-like cells differentiated in pro-inflammatory cytokine-containing cultures. *Immunol Cell Biol*, 2000. **78**(3): p. 205-13.

References

495. Thomas, L., A. Bielemeier, P.A. Lambert, R.P. Darveau, L.J. Marshall & A. Devitt, The N-Terminus of CD14 Acts to Bind Apoptotic Cells and Confers Rapid-Tethering Capabilities on Non-Myeloid Cells. *PLoS ONE*, 2013. **8**(7).
496. Elliott, M.R., F.B. Chekeni, P.C. Trampont, E.R. Lazarowski, A. Kadl, S.F. Walk, D. Park, R.I. Woodson, M. Ostankovich, P. Sharma, J.J. Lysiak, T.K. Harden, N. Leitinger & K.S. Ravichandran, Nucleotides released by apoptotic cells act as a find-me signal to promote phagocytic clearance. *Nature*, 2009. **461**(7261): p. 282-6.
497. Omata, W., W.E.t. Ackerman, D.D. Vandre & J.M. Robinson, Trophoblast cell fusion and differentiation are mediated by both the protein kinase C and a pathways. *PLoS One*, 2013. **8**(11): p. e81003.
498. McNally, A.K. & J.M. Anderson, Macrophage fusion and multinucleated giant cells of inflammation. *Adv Exp Med Biol*, 2011. **713**: p. 97-111.
499. Triantafilou, K., M. Triantafilou & R.L. Dedrick, A CD14-independent LPS receptor cluster. *Nat Immunol*, 2001. **2**(4): p. 338-45.
500. Zanoni, I., R. Ostuni, L.R. Marek, S. Barresi, R. Barbalat, G.M. Barton, F. Granucci & J.C. Kagan, CD14 controls the LPS-induced endocytosis of Toll-like receptor 4. *Cell*, 2011. **147**(4): p. 868-80.
501. Antal-Szalmas, P., J.A. Strijp, A.J. Weersink, J. Verhoef & K.P. Van Kessel, Quantitation of surface CD14 on human monocytes and neutrophils. *J Leukoc Biol*, 1997. **61**(6): p. 721-8.
502. Genin, M., F. Clement, A. Fattaccioli, M. Raes & C. Michiels, M1 and M2 macrophages derived from THP-1 cells differentially modulate the response of cancer cells to etoposide. *BMC Cancer*, 2015. **15**: p. 577.
503. Cammer, M. & D. Cox, Chemotactic responses by macrophages to a directional source of a cytokine delivered by a micropipette. *Methods Mol Biol*, 2014. **1172**: p. 125-35.
504. Ploeger, D.T.A., N.A. Hosper, M. Schipper, J.A. Koerts, S. de Rond & R.A. Bank, Cell plasticity in wound healing: paracrine factors of M1/ M2 polarized macrophages influence the phenotypical state of dermal fibroblasts. *Cell Communication and Signaling : CCS*, 2013. **11**: p. 29-29.
505. Vogel, D.Y., J.E. Glim, A.W. Stavenuiter, M. Breur, P. Heijnen, S. Amor, C.D. Dijkstra & R.H. Beelen, Human macrophage polarization in vitro: maturation and activation methods compared. *Immunobiology*, 2014. **219**(9): p. 695-703.
506. Tang, Y., S. Wu, Q. Liu, J. Xie, J. Zhang, D. Han, Q. Lu & Q. Lu, Mertk Deficiency Affects Macrophage Directional Migration via Disruption of Cytoskeletal Organization. *PLoS ONE*, 2015. **10**(1): p. e0117787.
507. Kawagishi, C., K. Kurosaka, N. Watanabe & Y. Kobayashi, Cytokine production by macrophages in association with phagocytosis of etoposide-treated P388 cells in vitro and in vivo. *Biochimica et Biophysica Acta (BBA) - Molecular Cell Research*, 2001. **1541**(3): p. 221-230.
508. Scannell, M., M.B. Flanagan, A. deStefani, K.J. Wynne, G. Cagney, C. Godson & P. Maderna, Annexin-1 and peptide derivatives are released by apoptotic cells and stimulate phagocytosis of apoptotic neutrophils by macrophages. *J Immunol*, 2007. **178**(7): p. 4595-605.
509. Griffin, G.K., G. Newton, M.L. Tarrío, D.-x. Bu, E. Maganto-Garcia, V. Azcutia, P. Alcaide, N. Grabie, F.W. Luscinskas, K.J. Croce & A.H. Lichtman, IL-17 and TNF α Sustain Neutrophil Recruitment During Inflammation Through Synergistic Effects on Endothelial Activation. *Journal of Immunology (Baltimore, Md. : 1950)*, 2012. **188**(12): p. 6287-6299.
510. Fadok, V.A., D.R. Voelker, P.A. Campbell, J.J. Cohen, D.L. Bratton & P.M. Henson, Exposure of phosphatidylserine on the surface of apoptotic lymphocytes triggers specific recognition and removal by macrophages. *J Immunol*, 1992. **148**(7): p. 2207-16.
511. Balasubramanian, K., J. Chandra & A.J. Schroit, Immune Clearance of Phosphatidylserine-expressing Cells by Phagocytes THE ROLE OF β 2-GLYCOPROTEIN I IN MACROPHAGE RECOGNITION. *Journal of Biological Chemistry*, 1997. **272**(49): p. 31113-31117.
512. Duvall, E., A.H. Wyllie & R.G. Morris, Macrophage recognition of cells undergoing programmed cell death (apoptosis). *Immunology*, 1985. **56**(2): p. 351-8.
513. Dini, L., F. Autuori, A. Lentini, S. Oliverio & M. Piacentini, The clearance of apoptotic cells in the liver is mediated by the asialoglycoprotein receptor. *FEBS Lett*, 1992. **296**(2): p. 174-8.
514. Platt, N., H. Suzuki, Y. Kurihara, T. Kodama & S. Gordon, Role for the class A macrophage scavenger receptor in the phagocytosis of apoptotic thymocytes in vitro. *Proc Natl Acad Sci U S A*, 1996. **93**(22): p. 12456-60.
515. Basu, S., R.J. Binder, T. Ramalingam & P.K. Srivastava, CD91 is a common receptor for heat shock proteins gp96, hsp90, hsp70, and calreticulin. *Immunity*, 2001. **14**(3): p. 303-13.

References

516. Esmann, L., C. Idel, A. Sarkar, L. Hellberg, M. Behnen, S. Moller, G. van Zandbergen, M. Klinger, J. Kohl, U. Bussmeyer, W. Solbach&T. Laskay, Phagocytosis of apoptotic cells by neutrophil granulocytes: diminished proinflammatory neutrophil functions in the presence of apoptotic cells. *J Immunol*, 2010. **184**(1): p. 391-400.
517. Nagele, E.P., M. Han, N.K. Acharya, C. DeMarshall, M.C. Kosciuk&R.G. Nagele, Natural IgG Autoantibodies Are Abundant and Ubiquitous in Human Sera, and Their Number Is Influenced By Age, Gender, and Disease. *PLoS ONE*, 2013. **8**(4): p. e60726.
518. Mankovich, A.R., C.-Y. Lee&V. Heinrich, Differential Effects of Serum Heat Treatment on Chemotaxis and Phagocytosis by Human Neutrophils. *PLoS ONE*, 2013. **8**(1): p. e54735.
519. Curtis, M.A., H.K. Kuramitsu, M. Lantz, F.L. Macrina, K. Nakayama, J. Potempa, E.C. Reynolds&J. Aduse-Opoku, Molecular genetics and nomenclature of proteases of *Porphyromonas gingivalis*. *J Periodontal Res*, 1999. **34**(8): p. 464-72.
520. Popadiak, K., J. Potempa, K. Riesbeck&A.M. Blom, Biphasic effect of gingipains from *Porphyromonas gingivalis* on the human complement system. *J Immunol*, 2007. **178**(11): p. 7242-50.
521. Mezyk-Kopec, R., M. Bzowska, J. Potempa, M. Bzowska, N. Jura, A. Sroka, R.A. Black&J. Bereta, Inactivation of membrane tumor necrosis factor alpha by gingipains from *Porphyromonas gingivalis*. *Infect Immun*, 2005. **73**(3): p. 1506-14.
522. Calkins, C.C., K. Platt, J. Potempa&J. Travis, Inactivation of tumor necrosis factor-alpha by proteinases (gingipains) from the periodontal pathogen, *Porphyromonas gingivalis*. Implications of immune evasion. *J Biol Chem*, 1998. **273**(12): p. 6611-4.
523. Ferrero, E., M.E. Ferrero, R. Pardi&M.R. Zocchi, The platelet endothelial cell adhesion molecule-1 (PECAM1) contributes to endothelial barrier function. *FEBS Lett*, 1995. **374**(3): p. 323-6.
524. Rapala-Kozik, M., G. Bras, B. Chruscicka, J. Karkowska-Kuleta, A. Sroka, H. Herwald, K.A. Nguyen, S. Eick, J. Potempa&A. Kozik, Adsorption of components of the plasma kinin-forming system on the surface of *Porphyromonas gingivalis* involves gingipains as the major docking platforms. *Infect Immun*, 2011. **79**(2): p. 797-805.
525. Chen, Z., J. Potempa, A. Polanowski, M. Wikstrom&J. Travis, Purification and characterization of a 50-kDa cysteine proteinase (gingipain) from *Porphyromonas gingivalis*. *J Biol Chem*, 1992. **267**(26): p. 18896-901.
526. Potempa, J., R. Pike&J. Travis, The multiple forms of trypsin-like activity present in various strains of *Porphyromonas gingivalis* are due to the presence of either Arg-gingipain or Lys-gingipain. *Infect Immun*, 1995. **63**(4): p. 1176-82.
527. Sato, K., E. Sakai, P.D. Veith, M. Shoji, Y. Kikuchi, H. Yukitake, N. Ohara, M. Naito, K. Okamoto, E.C. Reynolds&K. Nakayama, Identification of a new membrane-associated protein that influences transport/maturation of gingipains and adhesins of *Porphyromonas gingivalis*. *J Biol Chem*, 2005. **280**(10): p. 8668-77.
528. Pike, R.N., J. Potempa, W. McGraw, T.H. Coetzer&J. Travis, Characterization of the binding activities of proteinase-adhesin complexes from *Porphyromonas gingivalis*. *J Bacteriol*, 1996. **178**(10): p. 2876-82.
529. Potempa, J., A. Sroka, T. Imamura&J. Travis, Gingipains, the major cysteine proteinases and virulence factors of *Porphyromonas gingivalis*: structure, function and assembly of multidomain protein complexes. *Curr Protein Pept Sci*, 2003. **4**(6): p. 397-407.
530. Vanterpool, E., F. Roy, L. Sandberg&H.M. Fletcher, Altered Gingipain Maturation in vimA- and vimE-Defective Isogenic Mutants of *Porphyromonas gingivalis*. *Infection and Immunity*, 2005. **73**(3): p. 1357-1366.
531. O'Brien-Simpson, N.M., R.A. Paolini, B. Hoffmann, N. Slakeski, S.G. Dashper&E.C. Reynolds, Role of RgpA, RgpB, and Kgp Proteinases in Virulence of *Porphyromonas gingivalis* W50 in a Murine Lesion Model. *Infection and Immunity*, 2001. **69**(12): p. 7527-7534.
532. Fujimura, S., K. Hirai, Y. Shibata, K. Nakayama&T. Nakamura, Comparative properties of envelope-associated arginine-gingipains and lysine-gingipain of *Porphyromonas gingivalis*. *FEMS Microbiol Lett*, 1998. **163**(2): p. 173-9.
533. Lantz, M.S., R.D. Allen, P. Bounelis, L.M. Switalski&M. Hook, *Bacteroides gingivalis* and *Bacteroides intermedius* recognize different sites on human fibrinogen. *J Bacteriol*, 1990. **172**(2): p. 716-26.
534. Lantz, M.S., R.D. Allen, T.A. Vail, L.M. Switalski&M. Hook, Specific cell components of *Bacteroides gingivalis* mediate binding and degradation of human fibrinogen. *J Bacteriol*, 1991. **173**(2): p. 495-504.
535. Wikstrom, M.&A. Linde, Ability of oral bacteria to degrade fibronectin. *Infect Immun*, 1986. **51**(2): p. 707-11.

References

536. Lantz, M.S., R.D. Allen, L.W. Duck, J.L. Blume, L.M. Switalski&M. Hook, Identification of Porphyromonas gingivalis components that mediate its interactions with fibronectin. J Bacteriol, 1991. **173**(14): p. 4263-70.
537. Birkedal-Hansen, H., R.E. Taylor, J.J. Zambon, P.K. Barwa&M.E. Neiders, Characterization of collagenolytic activity from strains of Bacteroides gingivalis. J Periodontal Res, 1988. **23**(4): p. 258-64.
538. Otsuka, M., J. Endo, D. Hinode, A. Nagata, R. Maehara, M. Sato&R. Nakamura, Isolation and characterization of protease from culture supernatant of Bacteroides gingivalis. J Periodontal Res, 1987. **22**(6): p. 491-8.
539. Sundqvist, G., J. Carlsson, B. Herrmann&A. Tarnvik, Degradation of human immunoglobulins G and M and complement factors C3 and C5 by black-pigmented Bacteroides. J Med Microbiol, 1985. **19**(1): p. 85-94.
540. Imamura, T., J. Potempa, R.N. Pike, J.N. Moore, M.H. Barton&J. Travis, Effect of free and vesicle-bound cysteine proteinases of Porphyromonas gingivalis on plasma clot formation: implications for bleeding tendency at periodontitis sites. Infection and Immunity, 1995. **63**(12): p. 4877-4882.
541. Nilsson, T., J. Carlsson&G. Sundqvist, Inactivation of key factors of the plasma proteinase cascade systems by Bacteroides gingivalis. Infect Immun, 1985. **50**(2): p. 467-71.
542. Grenier, D., G. Chao&B.C. McBride, Characterization of sodium dodecyl sulfate-stable Bacteroides gingivalis proteases by polyacrylamide gel electrophoresis. Infection and Immunity, 1989. **57**(1): p. 95-99.
543. Pavloff, N., J. Potempa, R.N. Pike, V. Prochazka, M.C. Kiefer, J. Travis&P.J. Barr, Molecular cloning and structural characterization of the Arg-gingipain proteinase of Porphyromonas gingivalis. Biosynthesis as a proteinase-adhesin polyprotein. J Biol Chem, 1995. **270**(3): p. 1007-10.
544. Imamura, T., A. Banbula, P.J. Pereira, J. Travis&J. Potempa, Activation of human prothrombin by arginine-specific cysteine proteinases (Gingipains R) from porphyromonas gingivalis. J Biol Chem, 2001. **276**(22): p. 18984-91.
545. Tokuda, M., M. Duncan, M.I. Cho&H.K. Kuramitsu, Role of Porphyromonas gingivalis protease activity in colonization of oral surfaces. Infect Immun, 1996. **64**(10): p. 4067-73.
546. Fleetwood, A.J., N.M. O'Brien-Simpson, P.D. Veith, R.S. Lam, A. Achuthan, A.D. Cook, W. Singleton, I.K. Lund, E.C. Reynolds&J.A. Hamilton, Porphyromonas gingivalis-derived RgpA-Kgp Complex Activates the Macrophage Urokinase Plasminogen Activator System: IMPLICATIONS FOR PERIODONTITIS. J Biol Chem, 2015. **290**(26): p. 16031-42.
547. Al-Taweel, F.B., C.W.I. Douglas&S.A. Whawell, The Periodontal Pathogen Porphyromonas gingivalis Preferentially Interacts with Oral Epithelial Cells in S Phase of the Cell Cycle. Infection and Immunity, 2016. **84**(7): p. 1966-1974.
548. Igboin, C.O., A.L. Griffen&E.J. Leys, Porphyromonas gingivalis Strain Diversity. Journal of Clinical Microbiology, 2009. **47**(10): p. 3073-3081.
549. Potempa, J., J. Mikolajczyk-Pawlinska, D. Brassell, D. Nelson, I.B. Thogersen, J.J. Enghild&J. Travis, Comparative properties of two cysteine proteinases (gingipains R), the products of two related but individual genes of Porphyromonas gingivalis. J Biol Chem, 1998. **273**(34): p. 21648-57.
550. Nakayama, K., Porphyromonas gingivalis and related bacteria: from colonial pigmentation to the type IX secretion system and gliding motility. Journal of Periodontal Research, 2015. **50**(1): p. 1-8.
551. Suzuki, N., T. Higuchi, M. Nakajima, A. Fujimoto, H. Morita, M. Yoneda, T. Hanioka&T. Hirofuji, Inhibitory Effect of Enterococcus faecium WB2000 on Volatile Sulfur Compound Production by Porphyromonas gingivalis. International Journal of Dentistry, 2016. **2016**: p. 8241681.
552. Smalley, J.W., M.F. Thomas, A.J. Birss, R. Withnall&J. Silver, A combination of both arginine- and lysine-specific gingipain activity of Porphyromonas gingivalis is necessary for the generation of the micro-oxo bishaem-containing pigment from haemoglobin. Biochem J, 2004. **379**(Pt 3): p. 833-40.
553. Smalley, J.W., J. Silver, P.J. Marsh&A.J. Birss, The periodontopathogen Porphyromonas gingivalis binds iron protoporphyrin IX in the mu-oxo dimeric form: an oxidative buffer and possible pathogenic mechanism. Biochem J, 1998. **331** (Pt 3): p. 681-5.
554. Smalley, J.W., A.J. Birss, R. Withnall&J. Silver, Interactions of Porphyromonas gingivalis with oxyhaemoglobin and deoxyhaemoglobin. Biochem J, 2002. **362**(Pt 1): p. 239-45.
555. Olczak, T., W. Simpson, X. Liu&C.A. Genco, Iron and heme utilization in Porphyromonas gingivalis. FEMS Microbiol Rev, 2005. **29**(1): p. 119-44.

References

556. Imai, M., Y. Murakami, K. Nagano, H. Nakamura & F. Yoshimura, Major outer membrane proteins from *Porphyromonas gingivalis*: strain variation, distribution, and clinical significance in periradicular lesions. *Eur J Oral Sci*, 2005. **113**(5): p. 391-9.
557. Rangarajan, M., J. Aduse-Opoku, J.M. Slaney, K.A. Young & M.A. Curtis, The prpR1 and prR2 arginine-specific protease genes of *Porphyromonas gingivalis* W50 produce five biochemically distinct enzymes. *Mol Microbiol*, 1997. **23**(5): p. 955-65.
558. Nadkarni, M.A., K.A. Nguyen, C.C. Chapple, A.A. DeCarlo, N.A. Jacques & N. Hunter, Distribution of *Porphyromonas gingivalis* biotypes defined by alleles of the *kgp* (Lys-gingipain) gene. *J Clin Microbiol*, 2004. **42**(8): p. 3873-6.
559. Maisetta, G., F.L. Brancatisano, S. Esin, M. Campa & G. Batoni, Gingipains produced by *Porphyromonas gingivalis* ATCC49417 degrade human-beta-defensin 3 and affect peptide's antibacterial activity in vitro. *Peptides*, 2011. **32**(5): p. 1073-7.
560. Barrett, A., J. Woessner & N. Rawlings, *Handbook of Proteolytic Enzymes*. 2 ed. 2004.
561. Imamura, T., K. Matsushita, J. Travis & J. Potempa, Inhibition of Trypsin-Like Cysteine Proteinases (Gingipains) from *Porphyromonas gingivalis* by Tetracycline and Its Analogues. *Antimicrobial Agents and Chemotherapy*, 2001. **45**(10): p. 2871-2876.
562. Staniec, D., M. Ksiazek, I.B. Thøgersen, J.J. Enghild, A. Sroka, D. Bryzek, M. Bogyo, M. Abrahamson & J. Potempa, Calcium Regulates the Activity and Structural Stability of Tpr, a Bacterial Calpain-like Peptidase. *The Journal of Biological Chemistry*, 2015. **290**(45): p. 27248-27260.
563. Grenier, D. & S.-i. Tanabe, *Porphyromonas gingivalis* Gingipains Trigger a Proinflammatory Response in Human Monocyte-derived Macrophages Through the p38 α Mitogen-activated Protein Kinase Signal Transduction Pathway. *Toxins*, 2010. **2**(3): p. 341-352.
564. Booth, V., F.P. Ashley & T. Lehner, Passive immunization with monoclonal antibodies against *Porphyromonas gingivalis* in patients with periodontitis. *Infect Immun*, 1996. **64**(2): p. 422-7.
565. Booth, V. & T. Lehner, Characterization of the *Porphyromonas gingivalis* antigen recognized by a monoclonal antibody which prevents colonization by the organism. *J Periodontal Res*, 1997. **32**(1 Pt 1): p. 54-60.
566. Rangarajan, M., A. Hashim, J. Aduse-Opoku, N. Paramonov, E.F. Hounsell & M.A. Curtis, Expression of Arg-Gingipain RgpB Is Required for Correct Glycosylation and Stability of Monomeric Arg-Gingipain RgpA from *Porphyromonas gingivalis* W50. *Infection and Immunity*, 2005. **73**(8): p. 4864-4878.
567. Sheets, S.M., J. Potempa, J. Travis, C.A. Casiano & H.M. Fletcher, Gingipains from *Porphyromonas gingivalis* W83 Induce Cell Adhesion Molecule Cleavage and Apoptosis in Endothelial Cells. *Infection and Immunity*, 2005. **73**(3): p. 1543-1552.
568. Mangat, P., N. Wegner, P.J. Venables & J. Potempa, Bacterial and human peptidylarginine deiminases: targets for inhibiting the autoimmune response in rheumatoid arthritis? *Arthritis Research & Therapy*, 2010. **12**(3): p. 209-209.
569. Enersen, M., K. Nakano & A. Amano, *Porphyromonas gingivalis* fimbriae. *Journal of Oral Microbiology*, 2013. **5**: p. 10.3402/jom.v5i0.20265.
570. Hochreiter-Hufford, A. & K.S. Ravichandran, Clearing the dead: apoptotic cell sensing, recognition, engulfment, and digestion. *Cold Spring Harb Perspect Biol*, 2013. **5**(1): p. a008748.
571. Krahling, S., M.K. Callahan, P. Williamson & R.A. Schlegel, Exposure of phosphatidylserine is a general feature in the phagocytosis of apoptotic lymphocytes by macrophages. *Cell Death Differ*, 1999. **6**(2): p. 183-9.
572. Akira, S., K. Takeda & T. Kaisho, Toll-like receptors: critical proteins linking innate and acquired immunity. *Nat Immunol*, 2001. **2**(8): p. 675-80.
573. Wakasugi, K. & P. Schimmel, Two distinct cytokines released from a human aminoacyl-tRNA synthetase. *Science*, 1999. **284**(5411): p. 147-51.
574. Horino, K., H. Nishiura, T. Ohsako, Y. Shibuya, T. Hiraoka, N. Kitamura & T. Yamamoto, A monocyte chemotactic factor, S19 ribosomal protein dimer, in phagocytic clearance of apoptotic cells. *Lab Invest*, 1998. **78**(5): p. 603-17.
575. Yun, J.H., P.M. Henson & R.M. Tuder, Phagocytic clearance of apoptotic cells: role in lung disease. *Expert review of respiratory medicine*, 2008. **2**(6): p. 753-765.
576. Hodge, S., G. Hodge, J. Ahern, H. Jersmann, M. Holmes & P.N. Reynolds, Smoking alters alveolar macrophage recognition and phagocytic ability: implications in chronic obstructive pulmonary disease. *Am J Respir Cell Mol Biol*, 2007. **37**(6): p. 748-55.
577. Li, M.O., M.R. Sarkisian, W.Z. Mehal, P. Rakic & R.A. Flavell, Phosphatidylserine receptor is required for clearance of apoptotic cells. *Science*, 2003. **302**(5650): p. 1560-3.

References

578. Henson, P.M., D.L. Bratton&V.A. Fadok, The phosphatidylserine receptor: a crucial molecular switch? *Nat Rev Mol Cell Biol*, 2001. **2**(8): p. 627-633.
579. Wermeling, F., Y. Chen, T. Pikkarainen, A. Scheynius, O. Winqvist, S. Izui, J.V. Ravetch, K. Tryggvason&M.C.I. Karlsson, Class A scavenger receptors regulate tolerance against apoptotic cells, and autoantibodies against these receptors are predictive of systemic lupus. *The Journal of Experimental Medicine*, 2007. **204**(10): p. 2259-2265.
580. Watt, S.M., S.E. Gschmeissner&P.A. Bates, PECAM-1: its expression and function as a cell adhesion molecule on hemopoietic and endothelial cells. *Leuk Lymphoma*, 1995. **17**(3-4): p. 229-44.
581. Tada, K., M. Tanaka, R. Hanayama, K. Miwa, A. Shinohara, A. Iwamatsu&S. Nagata, Tethering of apoptotic cells to phagocytes through binding of CD47 to Src homology 2 domain-bearing protein tyrosine phosphatase substrate-1. *J Immunol*, 2003. **171**(11): p. 5718-26.
582. Lv, Z., Z. Bian, L. Shi, S. Niu, B. Ha, A. Tremblay, L. Li, X. Zhang, J. Paluszynski, M. Liu, K. Zen&Y. Liu, Loss of Cell Surface CD47 Clustering Formation and Binding Avidity to SIRPalpha Facilitate Apoptotic Cell Clearance by Macrophages. *J Immunol*, 2015. **195**(2): p. 661-71.
583. Sambrano, G.R.&D. Steinberg, Recognition of oxidatively damaged and apoptotic cells by an oxidized low density lipoprotein receptor on mouse peritoneal macrophages: role of membrane phosphatidylserine. *Proc Natl Acad Sci U S A*, 1995. **92**(5): p. 1396-400.
584. Oka, K., T. Sawamura, K.-i. Kikuta, S. Itokawa, N. Kume, T. Kita&T. Masaki, Lectin-like oxidized low-density lipoprotein receptor 1 mediates phagocytosis of aged/apoptotic cells in endothelial cells. *Proceedings of the National Academy of Sciences of the United States of America*, 1998. **95**(16): p. 9535-9540.
585. Brown, E., Integrin-associated protein (CD47): an unusual activator of G protein signaling. *Journal of Clinical Investigation*, 2001. **107**(12): p. 1499-1500.
586. Chauss, D., L.A. Brennan, O. Bakina&M. Kantorow, Integrin alphaVbeta5-mediated Removal of Apoptotic Cell Debris by the Eye Lens and Its Inhibition by UV Light Exposure. *J Biol Chem*, 2015. **290**(51): p. 30253-66.
587. Finnemann, S.C.&E. Rodriguez-Boulan, Macrophage and Retinal Pigment Epithelium Phagocytosis: Apoptotic Cells and Photoreceptors Compete for $\alpha\beta 3$ and $\alpha\beta 5$ Integrins, and Protein Kinase C Regulates $\alpha\beta 5$ Binding and Cytoskeletal Linkage. *The Journal of Experimental Medicine*, 1999. **190**(6): p. 861-874.
588. Iadevaia, V., A. Rinaldi, L. Falasca, L.P. Pucillo, T. Alonzi, G. Chimini&M. Piacentini, ATP-binding cassette transporter 1 and transglutaminase 2 act on the same genetic pathway in the apoptotic cell clearance. *Cell Death Differ*, 2006. **13**(11): p. 1998-2001.
589. Jehle, A.W., S.J. Gardai, S. Li, P. Linsel-Nitschke, K. Morimoto, W.J. Janssen, R.W. Vandivier, N. Wang, S. Greenberg, B.M. Dale, C. Qin, P.M. Henson&A.R. Tall, ATP-binding cassette transporter A7 enhances phagocytosis of apoptotic cells and associated ERK signaling in macrophages. *The Journal of Cell Biology*, 2006. **174**(4): p. 547-556.
590. Cairns, A.P., A.D. Crockard&A.L. Bell, Complement receptor expression of relevance to apoptotic cell clearance in SLE. *Rheumatology (Oxford)*, 2003. **42**(3): p. 487-8.
591. Kim, J.&S. Amar, Periodontal disease and systemic conditions: a bidirectional relationship. *Odontology / the Society of the Nippon Dental University*, 2006. **94**(1): p. 10-21.
592. Genco, R.J.&S.G. Grossi, Is estrogen deficiency a risk factor for periodontal disease? *Compend Contin Educ Dent Suppl*, 1998(22): p. S23-9.
593. Wactawski-Wende, J., S.G. Grossi, M. Trevisan, R.J. Genco, M. Tezal, R.G. Dunford, A.W. Ho, E. Hausmann&M.M. Hreshchyshyn, The role of osteopenia in oral bone loss and periodontal disease. *J Periodontol*, 1996. **67**(10 Suppl): p. 1076-84.
594. Westfelt, E., H. Rylander, G. Blohme, P. Jonasson&J. Lindhe, The effect of periodontal therapy in diabetics. Results after 5 years. *J Clin Periodontol*, 1996. **23**(2): p. 92-100.
595. Kantarci, A., P. Augustin, E. Firatli, M.C. Sheff, H. Hasturk, D.T. Graves&P.C. Trackman, Apoptosis in Gingival Overgrowth Tissues. *Journal of dental research*, 2007. **86**(9): p. 888-892.
596. Murray, P.A.&M.R. Patters, Gingival crevice neutrophil function in periodontal lesions. *J Periodontal Res*, 1980. **15**(5): p. 463-9.
597. Cardoso, C.R., G.P. Garlet, G.E. Crippa, A.L. Rosa, W.M. Junior, M.A. Rossi&J.S. Silva, Evidence of the presence of T helper type 17 cells in chronic lesions of human periodontal disease. *Oral Microbiol Immunol*, 2009. **24**(1): p. 1-6.
598. Gemmell, E., K. Yamazaki&G.J. Seymour, Destructive periodontitis lesions are determined by the nature of the lymphocytic response. *Crit Rev Oral Biol Med*, 2002. **13**(1): p. 17-34.

References

599. Turner, J., Y. Cho, N.N. Dinh, A.J. Waring&R.I. Lehrer, Activities of LL-37, a cathelin-associated antimicrobial peptide of human neutrophils. *Antimicrob Agents Chemother*, 1998. **42**(9): p. 2206-14.
600. Gaut, J.P., G.C. Yeh, H.D. Tran, J. Byun, J.P. Henderson, G.M. Richter, M.-L. Brennan, A.J. Lusis, A. Belaaouaj, R.S. Hotchkiss&J.W. Heinecke, Neutrophils Employ the Myeloperoxidase System to Generate Antimicrobial Brominating and Chlorinating Oxidants during Sepsis. *Proceedings of the National Academy of Sciences of the United States of America*, 2001. **98**(21): p. 11961-11966.
601. Murray, D.A.&J.M.A. Wilton, Lipopolysaccharide from the Periodontal Pathogen *Porphyromonas gingivalis* Prevents Apoptosis of HL60-Derived Neutrophils In Vitro. *Infection and Immunity*, 2003. **71**(12): p. 7232-7235.
602. Preshaw, P.M., R.E. Schifferle&J.D. Walters, *Porphyromonas gingivalis* lipopolysaccharide delays human polymorphonuclear leukocyte apoptosis in vitro. *J Periodontal Res*, 1999. **34**(4): p. 197-202.
603. Pugin, J., V.V. Kravchenko, J.D. Lee, L. Kline, R.J. Ulevitch&P.S. Tobias, Cell Activation Mediated by Glycosylphosphatidylinositol-Anchored or Transmembrane Forms of CD14. *Infection and Immunity*, 1998. **66**(3): p. 1174-1180.
604. Landmann, R., S. Link, S. Sansano, Z. Rajacic&W. Zimmerli, Soluble CD14 Activates Monocytic Cells Independently of Lipopolysaccharide. *Infection and Immunity*, 1998. **66**(5): p. 2264-2271.
605. Yang, Z., M.A. Breider, R.C. Carroll, M.S. Miller&P.N. Bochsler, Soluble CD14 and lipopolysaccharide-binding protein from bovine serum enable bacterial lipopolysaccharide-mediated cytotoxicity and activation of bovine vascular endothelial cells in vitro. *J Leukoc Biol*, 1996. **59**(2): p. 241-7.
606. Vasselon, T., R. Pironkova&P.A. Detmers, Sensitive responses of leukocytes to lipopolysaccharide require a protein distinct from CD14 at the cell surface. *J Immunol*, 1997. **159**(9): p. 4498-505.
607. Bikoue, A., F. George, P. Poncelet, M. Mutin, G. Janossy&J. Sampol, Quantitative analysis of leukocyte membrane antigen expression: normal adult values. *Cytometry*, 1996. **26**(2): p. 137-47.
608. Savill, J., I. Dransfield, C. Gregory&C. Haslett, A blast from the past: clearance of apoptotic cells regulates immune responses. *Nat Rev Immunol*, 2002. **2**(12): p. 965-75.
609. Poon, I.K.H., C.D. Lucas, A.G. Rossi&K.S. Ravichandran, Apoptotic cell clearance: basic biology and therapeutic potential. *Nat Rev Immunol*, 2014. **14**(3): p. 166-180.
610. Gokyu, M., H. Kobayashi, H. Nanbara, T. Sudo, Y. Ikeda, T. Suda&Y. Izumi, Thrombospondin-1 Production Is Enhanced by *Porphyromonas gingivalis* Lipopolysaccharide in THP-1 Cells. *PLoS ONE*, 2014. **9**(12): p. e115107.
611. Kukreja, A., S. Radfar, B.-H. Sun, K. Insogna&M.V. Dhodapkar, Dominant role of CD47–thrombospondin-1 interactions in myeloma-induced fusion of human dendritic cells: implications for bone disease. *Blood*, 2009. **114**(16): p. 3413-3421.
612. Buchmann, R., A. Hasilik, T.E. Van Dyke&D.E. Lange, Amplified crevicular leukocyte activity in aggressive periodontal disease. *J Dent Res*, 2002. **81**(10): p. 716-21.
613. Buchmann, R., A. Hasilik, M.E. Nunn, T.E. Van Dyke&D.E. Lange, PMN responses in chronic periodontal disease: evaluation by gingival crevicular fluid enzymes and elastase-alpha-1-proteinase inhibitor complex. *J Clin Periodontol*, 2002. **29**(6): p. 563-72.
614. de Torre-Minguela, C., M. Barberà-Cremades, A.I. Gómez, F. Martín-Sánchez&P. Pelegrín, Macrophage activation and polarization modify P2X7 receptor secretome influencing the inflammatory process. *Scientific Reports*, 2016. **6**: p. 22586.
615. Robbins, P.D.&A.E. Morelli, Regulation of Immune Responses by Extracellular Vesicles. *Nature reviews. Immunology*, 2014. **14**(3): p. 195-208.
616. Koizumi, S., Y. Shigemoto-Mogami, K. Nasu-Tada, Y. Shinozaki, K. Ohsawa, M. Tsuda, B.V. Joshi, K.A. Jacobson, S. Kohsaka&K. Inoue, UDP acting at P2Y6 receptors is a mediator of microglial phagocytosis. *Nature*, 2007. **446**(7139): p. 1091-5.
617. Grin'kina, N.M., E.E. Karnabi, D. Damania, S. Wadgaonkar, I.A. Muslimov&R. Wadgaonkar, Sphingosine Kinase 1 Deficiency Exacerbates LPS-Induced Neuroinflammation. *PLoS ONE*, 2012. **7**(5): p. e36475.
618. Allende, M.L., M. Bektas, B.G. Lee, E. Bonifacino, J. Kang, G. Tuymetova, W. Chen, J.D. Saba&R.L. Proia, Sphingosine-1-phosphate Lyase Deficiency Produces a Pro-inflammatory Response While Impairing Neutrophil Trafficking. *The Journal of Biological Chemistry*, 2011. **286**(9): p. 7348-7358.

References

619. Nagata, K., K. Ohashi, T. Nakano, H. Arita, C. Zong, H. Hanafusa & K. Mizuno, Identification of the product of growth arrest-specific gene 6 as a common ligand for Axl, Sky, and Mer receptor tyrosine kinases. *J Biol Chem*, 1996. **271**(47): p. 30022-7.
620. Arur, S., U.E. Uche, K. Rezaul, M. Fong, V. Scranton, A.E. Cowan, W. Mohler & D.K. Han, Annexin I is an endogenous ligand that mediates apoptotic cell engulfment. *Dev Cell*, 2003. **4**(4): p. 587-98.
621. Fadok, V.A., D.L. Bratton, D.M. Rose, A. Pearson, R.A. Ezekewitz & P.M. Henson, A receptor for phosphatidylserine-specific clearance of apoptotic cells. *Nature*, 2000. **405**(6782): p. 85-90.
622. Cinti, S., G. Mitchell, G. Barbatelli, I. Murano, E. Ceresi, E. Faloia, S. Wang, M. Fortier, A.S. Greenberg & M.S. Obin, Adipocyte death defines macrophage localization and function in adipose tissue of obese mice and humans. *J Lipid Res*, 2005. **46**(11): p. 2347-55.
623. Ziegler-Heitbrock, H.W. & R.J. Ulevitch, CD14: cell surface receptor and differentiation marker. *Immunol Today*, 1993. **14**(3): p. 121-5.
624. Regueiro, V., M.A. Campos, P. Morey, J. Sauleda, A.G. Agusti, J. Garmendia & J.A. Bengoechea, Lipopolysaccharide-binding protein and CD14 are increased in the bronchoalveolar lavage fluid of smokers. *Eur Respir J*, 2009. **33**(2): p. 273-81.
625. Flora, P.K. & C.D. Gregory, Recognition of apoptotic cells by human macrophages: inhibition by a monocyte/macrophage-specific monoclonal antibody. *Eur J Immunol*, 1994. **24**(11): p. 2625-32.
626. Wilensky, A., R. Tzach-Nahman, J. Potempa, L. Shapira & G. Nussbaum, Porphyromonas gingivalis gingipains selectively reduce CD14 expression, leading to macrophage hyporesponsiveness to bacterial infection. *J Innate Immun*, 2015. **7**(2): p. 127-35.
627. Sugawara, S., E. Nemoto, H. Tada, K. Miyake, T. Imamura & H. Takada, Proteolysis of human monocyte CD14 by cysteine proteinases (gingipains) from Porphyromonas gingivalis leading to lipopolysaccharide hyporesponsiveness. *J Immunol*, 2000. **165**(1): p. 411-8.
628. Tada, H., S. Sugawara, E. Nemoto, N. Takahashi, T. Imamura, J. Potempa, J. Travis, H. Shimauchi & H. Takada, Proteolysis of CD14 on human gingival fibroblasts by arginine-specific cysteine proteinases from Porphyromonas gingivalis leading to down-regulation of lipopolysaccharide-induced interleukin-8 production. *Infect Immun*, 2002. **70**(6): p. 3304-7.
629. Roth, G.A., H.J. Ankersmit, V.B. Brown, P.N. Papananou, A.M. Schmidt & E. Lalla, Porphyromonas gingivalis infection and cell death in human aortic endothelial cells. *FEMS Microbiol Lett*, 2007. **272**(1): p. 106-13.
630. Geatch, D.R., J.I. Harris, P.A. Heasman & J.J. Taylor, In vitro studies of lymphocyte apoptosis induced by the periodontal pathogen Porphyromonas gingivalis. *J Periodontal Res*, 1999. **34**(2): p. 70-8.
631. Hayashi, J., T. Masaka & I. Ishikawa, Increased Levels of Soluble CD14 in Sera of Periodontitis Patients. *Infection and Immunity*, 1999. **67**(1): p. 417-420.
632. Takashiba, S., M. Takigawa, K. Takahashi, F. Myokai, F. Nishimura, T. Chihara, H. Kurihara, Y. Nomura & Y. Murayama, Interleukin-8 is a major neutrophil chemotactic factor derived from cultured human gingival fibroblasts stimulated with interleukin-1 beta or tumor necrosis factor alpha. *Infection and Immunity*, 1992. **60**(12): p. 5253-5258.
633. Al-Karawi, S.E.H. & M.S. Al-Rubaie, Estimation of Soluble CD14 Level in Saliva of Patients with Chronic Periodontitis & Its Correlation with Periodontal Health Status & Disease Severity. *Journal of Dental and Medical Sciences*, 2014. **13**(4): p. 24-30.
634. Guentsch, A., M. Kramesberger, A. Sroka, W. Pfister, J. Potempa & S. Eick, Comparison of gingival crevicular fluid sampling methods in patients with severe chronic periodontitis. *J Periodontol*, 2011. **82**(7): p. 1051-60.
635. Jagels, M.A., J. Travis, J. Potempa, R. Pike & T.E. Hugli, Proteolytic inactivation of the leukocyte C5a receptor by proteinases derived from Porphyromonas gingivalis. *Infection and Immunity*, 1996. **64**(6): p. 1984-1991.
636. Furuta, N., H. Takeuchi & A. Amano, Entry of Porphyromonas gingivalis outer membrane vesicles into epithelial cells causes cellular functional impairment. *Infect Immun*, 2009. **77**(11): p. 4761-70.
637. Grenier, D. & D. Mayrand, Functional characterization of extracellular vesicles produced by Bacteroides gingivalis. *Infect Immun*, 1987. **55**(1): p. 111-7.
638. Duncan, L., M. Yoshioka, F. Chandad & D. Grenier, Loss of lipopolysaccharide receptor CD14 from the surface of human macrophage-like cells mediated by Porphyromonas gingivalis outer membrane vesicles. *Microb Pathog*, 2004. **36**(6): p. 319-25.

References

639. Hoffmann, O., K. Klaushofer, K. Koller, M. Peterlik, T. Mavreas & P. Stern, Indomethacin inhibits thrombin-, but not thyroxin- stimulated resorption of fetal rat limb bones. *Prostaglandins*, 1986. **31**(4): p. 601-608.
640. Uehara, A., T. Imamura, J. Potempa, J. Travis & H. Takada, Gingipains from *Porphyromonas gingivalis* synergistically induce the production of proinflammatory cytokines through protease-activated receptors with Toll-like receptor and NOD1/2 ligands in human monocytic cells. *Cell Microbiol*, 2008. **10**(5): p. 1181-9.
641. Ottonello, L., M. Cutolo, G. Frumento, N. Arduino, M. Bertolotto, M. Mancini, E. Sottofattori & F. Dallegri, Synovial fluid from patients with rheumatoid arthritis inhibits neutrophil apoptosis: role of adenosine and proinflammatory cytokines. *Rheumatology (Oxford)*, 2002. **41**(11): p. 1249-60.
642. Cross, A., T. Barnes, R.C. Bucknall, S.W. Edwards & R.J. Moots, Neutrophil apoptosis in rheumatoid arthritis is regulated by local oxygen tensions within joints. *J Leukoc Biol*, 2006. **80**(3): p. 521-8.
643. Frantz, S. & M. Nahrendorf, Cardiac macrophages and their role in ischaemic heart disease. *Cardiovascular Research*, 2014. **102**(2): p. 240-248.
644. DeLeon-Pennell, K.Y., Y. Tian, B. Zhang, C.A. Cates, R.P. Iyer, P. Cannon, P. Shah, P. Aiyetan, G.V. Halade, Y. Ma, E. Flynn, Z. Zhang, Y.F. Jin, H. Zhang & M.L. Lindsey, CD36 Is a Matrix Metalloproteinase-9 Substrate That Stimulates Neutrophil Apoptosis and Removal During Cardiac Remodeling. *Circ Cardiovasc Genet*, 2016. **9**(1): p. 14-25.
645. Courtney, P., A. Crockard, K. Williamson, A. Irvine, R. Kennedy & A. Bell, Increased apoptotic peripheral blood neutrophils in systemic lupus erythematosus: relations with disease activity, antibodies to double stranded DNA, and neutropenia. *Annals of the Rheumatic Diseases*, 1999. **58**(5): p. 309-314.
646. Uddin, M., G. Nong, J. Ward, G. Seumois, L.R. Prince, S.J. Wilson, V. Cornelius, G. Dent & R. Djukanovic, Prosurvival activity for airway neutrophils in severe asthma. *Thorax*, 2010. **65**(8): p. 684-9.
647. Haziot, A., B.Z. Tsuberi & S.M. Goyert, Neutrophil CD14: biochemical properties and role in the secretion of tumor necrosis factor-alpha in response to lipopolysaccharide. *J Immunol*, 1993. **150**(12): p. 5556-65.
648. Svendsen, E.R., K.B. Yeatts, D. Peden, S. Orton, N.E. Alexis, J. Creason, R. Williams & L. Neas, Circulating neutrophil CD14 expression and the inverse association of ambient particulate matter on lung function in asthmatic children. *Ann Allergy Asthma Immunol*, 2007. **99**(3): p. 244-53.
649. Rodeberg, D.A., R.E. Morris & G.F. Babcock, Azurophilic granules of human neutrophils contain CD14. *Infection and Immunity*, 1997. **65**(11): p. 4747-4753.
650. Chow, J.C., D.W. Young, D.T. Golenbock, W.J. Christ & F. Gusovsky, Toll-like receptor-4 mediates lipopolysaccharide-induced signal transduction. *J Biol Chem*, 1999. **274**(16): p. 10689-92.
651. Triantafilou, M. & K. Triantafilou, Lipopolysaccharide recognition: CD14, TLRs and the LPS-activation cluster. *Trends Immunol*, 2002. **23**(6): p. 301-4.
652. da Silva Correia, J., K. Soldau, U. Christen, P.S. Tobias & R.J. Ulevitch, Lipopolysaccharide is in close proximity to each of the proteins in its membrane receptor complex. transfer from CD14 to TLR4 and MD-2. *J Biol Chem*, 2001. **276**(24): p. 21129-35.
653. Kishimoto, M., A. Yoshimura, M. Naito, K. Okamoto, K. Yamamoto, D.T. Golenbock, Y. Hara & K. Nakayama, Gingipains inactivate a cell surface ligand on *Porphyromonas gingivalis* that induces TLR2- and TLR4-independent signaling. *Microbiol Immunol*, 2006. **50**(4): p. 315-25.
654. Lambert, C., F.W. Preijers, G.Y. Demirel & U. Sack, Monocytes and macrophages in flow: An ESCCA initiative on advanced analyses of monocyte lineage using flow cytometry. *Cytometry B Clin Cytom*, 2015.
655. Cappelletti, M., P. Presicce, F. Calcaterra, D. Mavilio & S. Della Bella, Bright expression of CD91 identifies highly activated human dendritic cells that can be expanded by defensins. *Immunology*, 2015. **144**(4): p. 661-667.
656. Maniecki, M.B., H.J. Moller, S.K. Moestrup & B.K. Moller, CD163 positive subsets of blood dendritic cells: the scavenging macrophage receptors CD163 and CD91 are coexpressed on human dendritic cells and monocytes. *Immunobiology*, 2006. **211**(6-8): p. 407-17.
657. Shaw, S., G.G. Luce, W.R. Gilks, K. Anderson, K. Ault, B.S. Bochner, L. Boumsell, S.M. Denning, E.G. Engleman, T. Fleisher, A.S. Freedman, D.A. Fox, J. Gailit, J.C. Gutierrez-Ramos, P.E. Hurtubise, P. Lansdorp, M.T. Lotze, S. Mawhorter, G. Marti, Y. Matsuo, J. Minowada, A. Michelson, L. Picker, J. Ritz, E. Roos, C.E. Van Der Schoot, T.A. Springer,

- T.F. Tedder, M.J. Telen, J.S. Thompson & P. Valent, Leucocyte differentiation antigen database. 1995.
658. Ghiran, I., L.B. Klickstein & A. Nicholson-Weller, Calreticulin is at the surface of circulating neutrophils and uses CD59 as an adaptor molecule. *J Biol Chem*, 2003. **278**(23): p. 21024-31.
659. Yu, M., M. Jiang, Y. Chen, S. Zhang, W. Zhang, X. Yang, X. Li, Y. Li, S. Duan, J. Han & Y. Duan, Inhibition of Macrophage CD36 Expression and Cellular Oxidized Low Density Lipoprotein (oxLDL) Accumulation by Tamoxifen: A PEROXISOME PROLIFERATOR-ACTIVATED RECEPTOR (PPAR) gamma-DEPENDENT MECHANISM. *J Biol Chem*, 2016. **291**(33): p. 16977-89.
660. Moheimani, F., J.T.M. Tan, B.E. Brown, A.K. Heather, D.M. van Reyk & M.J. Davies, Effect of Exposure of Human Monocyte-Derived Macrophages to High, versus Normal, Glucose on Subsequent Lipid Accumulation from Glycated and Acetylated Low-Density Lipoproteins. *Experimental Diabetes Research*, 2011. **2011**: p. 10.
661. Hart, S.P., C. Jackson, L.M. Kremmel, M.S. McNeill, H. Jersmann, K.M. Alexander, J.A. Ross & I. Dransfield, Specific Binding of an Antigen-Antibody Complex to Apoptotic Human Neutrophils. *The American Journal of Pathology*, 2003. **162**(3): p. 1011-1018.
662. Roberts, H.M., M.R. Ling, R. Insall, G. Kalna, J. Spengler, M.M. Grant & I.L.C. Chapple, Impaired neutrophil directional chemotactic accuracy in chronic periodontitis patients. *Journal of Clinical Periodontology*, 2015. **42**(1): p. 1-11.
663. Van Dyke, T.E., H.U. Horoszewicz, L.J. Cianciola & R.J. Genco, Neutrophil chemotaxis dysfunction in human periodontitis. *Infect Immun*, 1980. **27**(1): p. 124-32.
664. Clark, R.A., R.C. Page & G. Wilde, Defective neutrophil chemotaxis in juvenile periodontitis. *Infect Immun*, 1977. **18**(3): p. 694-700.
665. Lavine, W.S., E.G. Maderazo, J. Stolman, P.A. Ward, R.B. Cogen, I. Greenblatt & P.B. Robertson, Impaired neutrophil chemotaxis in patients with juvenile and rapidly progressing periodontitis. *Journal of Periodontal Research*, 1979. **14**(1): p. 10-19.
666. Van Dyke, T.E., M. Schweinebraten, L.J. Cianciola, S. Offenbacher & R.J. Genco, Neutrophil chemotaxis in families with localized juvenile periodontitis. *Journal of Periodontal Research*, 1985. **20**(5): p. 503-514.
667. Van Dyke, T.E., M.J. Levine, L.A. Tabak & R.J. Genco, Reduced chemotactic peptide binding in juvenile periodontitis: a model for neutrophil function. *Biochem Biophys Res Commun*, 1981. **100**(3): p. 1278-84.
668. MacFarlane, G.D., M.C. Herzberg, L.F. Wolff & N.A. Hardie, Refractory periodontitis associated with abnormal polymorphonuclear leukocyte phagocytosis and cigarette smoking. *J Periodontol*, 1992. **63**(11): p. 908-13.
669. Genco, R.J., T.E. Van Dyke, B. Park, M. Ciminelli & H. Horoszewicz, Neutrophil chemotaxis impairment in juvenile periodontitis: evaluation of specificity, adherence, deformability, and serum factors. *J Reticuloendothel Soc*, 1980. **28**(Suppl): p. 81s-91s.
670. Van Dyke, T.E., M.J. Levine, L.A. Tabak & R.J. Genco, Juvenile periodontitis as a model for neutrophil function: reduced binding of the complement chemotactic fragment, C5a. *J Dent Res*, 1983. **62**(8): p. 870-2.
671. Luu, N.T., G.E. Rainger, C.D. Buckley & G.B. Nash, CD31 regulates direction and rate of neutrophil migration over and under endothelial cells. *J Vasc Res*, 2003. **40**(5): p. 467-79.
672. Fine, R., J.O. Shaw & W.R. Rogers, Effects of C5a on baboon alveolar macrophage migration. *Am Rev Respir Dis*, 1981. **123**(1): p. 110-14.
673. Green, T.D., J. Park, Q. Yin, S. Fang, A.L. Crews, S.L. Jones & K.B. Adler, Directed migration of mouse macrophages in vitro involves myristoylated alanine-rich C-kinase substrate (MARCKS) protein. *Journal of Leukocyte Biology*, 2012. **92**(3): p. 633-639.
674. Mukaida, N., Pathophysiological roles of interleukin-8/CXCL8 in pulmonary diseases. *Am J Physiol Lung Cell Mol Physiol*, 2003. **284**(4): p. L566-77.
675. Matter, M.L. & E. Ruoslahti, A signaling pathway from the alpha5beta1 and alpha(v)beta3 integrins that elevates bcl-2 transcription. *J Biol Chem*, 2001. **276**(30): p. 27757-63.
676. Huttenlocher, A. & A.R. Horwitz, Integrins in cell migration. *Cold Spring Harb Perspect Biol*, 2011. **3**(9): p. a005074.
677. Webb, D.J., J.T. Parsons & A.F. Horwitz, Adhesion assembly, disassembly and turnover in migrating cells -- over and over and over again. *Nat Cell Biol*, 2002. **4**(4): p. E97-100.
678. Stafford, P., J. Higham, A. Pinnock, C. Murdoch, C.W.I. Douglas, G.P. Stafford & D.W. Lambert, Gingipain-dependent degradation of mTOR pathway proteins by the periodontal pathogen *Porphyromonas gingivalis* during invasion. *Molecular oral microbiology*, 2013. **28**(5): p. 366-378.

References

679. Kinane, J.A., M.R. Benakanakere, J. Zhao, K.B. Hosur&D.F. Kinane, *Porphyromonas gingivalis* influences actin degradation within epithelial cells during invasion and apoptosis. *Cell Microbiol*, 2012. **14**(7): p. 1085-96.
680. Park, H., A. Dovas, S. Hanna, C. Lastrucci, C. Cougoule, R. Guet, I. Maridonneau-Parini&D. Cox, Tyrosine phosphorylation of Wiskott-Aldrich syndrome protein (WASP) by Hck regulates macrophage function. *J Biol Chem*, 2014. **289**(11): p. 7897-906.
681. Isaac, B.M., D. Ishihara, L.M. Nusblat, J.-C. Gevrey, A. Dovas, J. Condeelis&D. Cox, N-WASP has the Ability to Compensate for the Loss of WASP in Macrophage Podosome Formation and Chemotaxis. *Experimental cell research*, 2010. **316**(20): p. 3406-3416.
682. Li, Z., M. Hannigan, Z. Mo, B. Liu, W. Lu, Y. Wu, A.V. Smrcka, G. Wu, L. Li, M. Liu, C.K. Huang&D. Wu, Directional sensing requires G beta gamma-mediated PAK1 and PIX alpha-dependent activation of Cdc42. *Cell*, 2003. **114**(2): p. 215-27.
683. Nakayama, M., T. Inoue, M. Naito, K. Nakayama&N. Ohara, Attenuation of the Phosphatidylinositol 3-Kinase/Akt Signaling Pathway by *Porphyromonas gingivalis* Gingipains RgpA, RgpB, and Kgp. *The Journal of Biological Chemistry*, 2015. **290**(8): p. 5190-5202.
684. Monypenny, J., H.-C. Chou, I. Bañón-Rodríguez, A.J. Thrasher, I.M. Antón, G.E. Jones&Y. Calle, Role of WASP in cell polarity and podosome dynamics of myeloid cells. *European Journal of Cell Biology*, 2011. **90**(2-3): p. 198-204.
685. Rey Nores, J.E., A. Bensussan, N. Vita, F. Stelter, M.A. Arias, M. Jones, S. Lefort, L.K. Borysiewicz, P. Ferrara&M.O. Labeta, Soluble CD14 acts as a negative regulator of human T cell activation and function. *Eur J Immunol*, 1999. **29**(1): p. 265-76.
686. Sugiyama, T.&S.D. Wright, Soluble CD14 Mediates Efflux of Phospholipids from Cells. *The Journal of Immunology*, 2001. **166**(2): p. 826-831.
687. Pradhan, D., S. Krahlting, P. Williamson&R.A. Schlegel, Multiple systems for recognition of apoptotic lymphocytes by macrophages. *Molecular Biology of the Cell*, 1997. **8**(5): p. 767-778.
688. Roumenina, L.T., D. Sene, M. Radanova, J. Blouin, L. Halbwachs-Mecarelli, M.A. Dragon-Durey, W.H. Fridman&V. Fremeaux-Bacchi, Functional complement C1q abnormality leads to impaired immune complexes and apoptotic cell clearance. *J Immunol*, 2011. **187**(8): p. 4369-73.
689. Fraser, D.A., A.K. Laust, E.L. Nelson&A.J. Tenner, C1q differentially modulates phagocytosis and cytokine responses during ingestion of apoptotic cells by human monocytes, macrophages, and dendritic cells. *J Immunol*, 2009. **183**(10): p. 6175-85.
690. Burns, E., G. Bachrach, L. Shapira&G. Nussbaum, Cutting Edge: TLR2 is required for the innate response to *Porphyromonas gingivalis*: activation leads to bacterial persistence and TLR2 deficiency attenuates induced alveolar bone resorption. *J Immunol*, 2006. **177**(12): p. 8296-300.
691. Maekawa, T., J.L. Krauss, T. Abe, R. Jotwani, M. Triantafilou, K. Triantafilou, A. Hashim, S. Hoch, M.A. Curtis, G. Nussbaum, J.D. Lambris&G. Hajishengallis, *Porphyromonas gingivalis* manipulates complement and TLR signaling to uncouple bacterial clearance from inflammation and promote dysbiosis. *Cell Host Microbe*, 2014. **15**(6): p. 768-78.
692. Miyasaki, K.T., The neutrophil: mechanisms of controlling periodontal bacteria. *J Periodontol*, 1991. **62**(12): p. 761-74.
693. Mantovani, A., M.A. Cassatella, C. Costantini&S. Jaillon, Neutrophils in the activation and regulation of innate and adaptive immunity. *Nat Rev Immunol*, 2011. **11**(8): p. 519-31.
694. Arango Duque, G.&A. Descoteaux, Macrophage Cytokines: Involvement in Immunity and Infectious Diseases. *Frontiers in Immunology*, 2014. **5**: p. 491.
695. Cvetanovic, M.&D.S. Ucker, Innate immune discrimination of apoptotic cells: repression of proinflammatory macrophage transcription is coupled directly to specific recognition. *J Immunol*, 2004. **172**(2): p. 880-9.
696. Rose, D.M., V.A. Fadok, D.W. Riches, K.L. Clay&P.M. Henson, Autocrine/paracrine involvement of platelet-activating factor and transforming growth factor-beta in the induction of phosphatidylserine recognition by murine macrophages. *J Immunol*, 1995. **155**(12): p. 5819-25.
697. Fadok, V.A., D.J. Lasko, P.W. Noble, L. Weinstein, D.W. Riches&P.M. Henson, Particle digestibility is required for induction of the phosphatidylserine recognition mechanism used by murine macrophages to phagocytose apoptotic cells. *J Immunol*, 1993. **151**(8): p. 4274-85.
698. Gerbod-Giannone, M.-C., Y. Li, A. Holleboom, S. Han, L.-C. Hsu, I. Tabas&A.R. Tall, TNF α induces ABCA1 through NF- κ B in macrophages and in phagocytes ingesting apoptotic

- cells. Proceedings of the National Academy of Sciences of the United States of America, 2006. **103**(9): p. 3112-3117.
699. Kurtis, B., G. Tuter, M. Serdar, P. Akdemir, C. Uygur, E. Firatli&B. Bal, Gingival crevicular fluid levels of monocyte chemoattractant protein-1 and tumor necrosis factor-alpha in patients with chronic and aggressive periodontitis. *J Periodontol*, 2005. **76**(11): p. 1849-55.
700. Andrukhov, O., S. Ertlschweiger, A. Moritz, H.P. Bantleon&X. Rausch-Fan, Different effects of *P. gingivalis* LPS and *E. coli* LPS on the expression of interleukin-6 in human gingival fibroblasts. *Acta Odontol Scand*, 2014. **72**(5): p. 337-45.
701. Lehnardt, S., C. Lachance, S. Patrizi, S. Lefebvre, P.L. Follett, F.E. Jensen, P.A. Rosenberg, J.J. Volpe&T. Vartanian, The toll-like receptor TLR4 is necessary for lipopolysaccharide-induced oligodendrocyte injury in the CNS. *J Neurosci*, 2002. **22**(7): p. 2478-86.
702. Park, B.S., D.H. Song, H.M. Kim, B.S. Choi, H. Lee&J.O. Lee, The structural basis of lipopolysaccharide recognition by the TLR4-MD-2 complex. *Nature*, 2009. **458**(7242): p. 1191-5.
703. Ogawa, T., Y. Asai, Y. Makimura&R. Tamai, Chemical structure and immunobiological activity of *Porphyromonas gingivalis* lipid A. *Front Biosci*, 2007. **12**: p. 3795-812.
704. Herath, T.D.K., R.P. Darveau, C.J. Seneviratne, C.-Y. Wang, Y. Wang&L. Jin, Tetra- and Penta-Acylated Lipid A Structures of *Porphyromonas gingivalis* LPS Differentially Activate TLR4-Mediated NF- κ B Signal Transduction Cascade and Immuno-Inflammatory Response in Human Gingival Fibroblasts. *PLoS ONE*, 2013. **8**(3): p. e58496.
705. Reife, R.A., S.R. Coats, M. Al-Qutub, D.M. Dixon, P.A. Braham, R.J. Billharz, W.N. Howald&R.P. Darveau, *Porphyromonas gingivalis* lipopolysaccharide lipid A heterogeneity: differential activities of tetra- and penta-acylated lipid A structures on E-selectin expression and TLR4 recognition. *Cell Microbiol*, 2006. **8**(5): p. 857-68.
706. Thomas, L., The Role of the Innate Immune System in the Clearance of Apoptotic Cells. 2011, Aston University.
707. Azuma, Y., K. Kaji, R. Katogi, S. Takeshita&A. Kudo, Tumor necrosis factor-alpha induces differentiation of and bone resorption by osteoclasts. *J Biol Chem*, 2000. **275**(7): p. 4858-64.
708. Graves, D.T., M. Oskoui, S. Volejnikova, G. Naguib, S. Cai, T. Desta, A. Kakouras&Y. Jiang, Tumor necrosis factor modulates fibroblast apoptosis, PMN recruitment, and osteoclast formation in response to *P. gingivalis* infection. *J Dent Res*, 2001. **80**(10): p. 1875-9.
709. McDonald, P.P., V.A. Fadok, D. Bratton&P.M. Henson, Transcriptional and translational regulation of inflammatory mediator production by endogenous TGF-beta in macrophages that have ingested apoptotic cells. *J Immunol*, 1999. **163**(11): p. 6164-72.
710. Groux, H., A. O'Garra, M. Bigler, M. Rouleau, S. Antonenko, J.E. de Vries&M.G. Roncarolo, A CD4+ T-cell subset inhibits antigen-specific T-cell responses and prevents colitis. *Nature*, 1997. **389**(6652): p. 737-42.
711. Gao, Y., J.M. Herndon, H. Zhang, T.S. Griffith&T.A. Ferguson, Antiinflammatory effects of CD95 ligand (FasL)-induced apoptosis. *J Exp Med*, 1998. **188**(5): p. 887-96.
712. Chen, W., M.E. Frank, W. Jin&S.M. Wahl, TGF-beta released by apoptotic T cells contributes to an immunosuppressive milieu. *Immunity*, 2001. **14**(6): p. 715-25.
713. Byrne, A.&D.J. Reen, Lipopolysaccharide induces rapid production of IL-10 by monocytes in the presence of apoptotic neutrophils. *J Immunol*, 2002. **168**(4): p. 1968-77.
714. Ogden, C.A., J.D. Pound, B.K. Bath, S. Owens, I. Johannessen, K. Wood&C.D. Gregory, Enhanced apoptotic cell clearance capacity and B cell survival factor production by IL-10-activated macrophages: implications for Burkitt's lymphoma. *J Immunol*, 2005. **174**(5): p. 3015-23.
715. Chung, E.Y., J. Liu, Y. Homma, Y. Zhang, A. Brendolan, M. Saggese, J. Han, R. Silverstein, L. Sella&X. Ma, Interleukin-10 Expression in Macrophages during Phagocytosis of Apoptotic Cells Is Mediated by the TALE homeoproteins Pbx-1 and Prep-1. *Immunity*, 2007. **27**(6): p. 952-964.
716. Berg, D.J., R. Kuhn, K. Rajewsky, W. Muller, S. Menon, N. Davidson, G. Grunig&D. Rennick, Interleukin-10 is a central regulator of the response to LPS in murine models of endotoxic shock and the Shwartzman reaction but not endotoxin tolerance. *J Clin Invest*, 1995. **96**(5): p. 2339-47.
717. Sindrilaru, A., T. Peters, S. Wieschalka, C. Baican, A. Baican, H. Peter, A. Hainzl, S. Schatz, Y. Qi, A. Schlecht, J.M. Weiss, M. Wlaschek, C. Sunderkötter&K. Scharffetter-Kochanek, An unrestrained proinflammatory M1 macrophage population induced by iron

- impairs wound healing in humans and mice. *The Journal of Clinical Investigation*, 2011. **121**(3): p. 985-997.
718. Xu, X., A. Grijalva, A. Skowronski, M. van Eijk, M.J. Serlie&A.W. Ferrante, Obesity Activates a Program of Lysosomal-Dependent Lipid Metabolism in Adipose Tissue Macrophages Independently of Classic Activation. *Cell metabolism*, 2013. **18**(6): p. 816-830.
719. Kratz, M., B.R. Coats, K.B. Hisert, D. Hagman, V. Mutskov, E. Peris, K.Q. Schoenfelt, J.N. Kuzma, I. Larson, P.S. Billing, R.W. Landerholm, M. Crouthamel, D. Gozal, S. Hwang, P.K. Singh&L. Becker, Metabolic dysfunction drives a mechanistically distinct proinflammatory phenotype in adipose tissue macrophages. *Cell Metab*, 2014. **20**(4): p. 614-25.
720. Fujii, K., I. Manabe&R. Nagai, Renal collecting duct epithelial cells regulate inflammation in tubulointerstitial damage in mice. *J Clin Invest*, 2011. **121**(9): p. 3425-41.
721. Laria, A., A. Lurati, M. Marrazza, D. Mazzocchi, K.A. Re&M. Scarpellini, The macrophages in rheumatic diseases. *Journal of Inflammation Research*, 2016. **9**: p. 1-11.
722. Roszer, T., Understanding the Mysterious M2 Macrophage through Activation Markers and Effector Mechanisms. *Mediators Inflamm*, 2015. **2015**: p. 816460.
723. Fuentes, L., T. Roszer&M. Ricote, Inflammatory mediators and insulin resistance in obesity: role of nuclear receptor signaling in macrophages. *Mediators Inflamm*, 2010. **2010**: p. 219583.
724. Yu, T., L. Zhao, X. Huang, C. Ma, Y. Wang, J. Zhang&D. Xuan, Enhanced Activity of the Macrophage M1/M2 Phenotypes and Phenotypic Switch to M1 in Periodontal Infection. *J Periodontol*, 2016. **87**(9): p. 1092-102.
725. Lam, R.S., N.M. O'Brien-Simpson, J.C. Lenzo, J.A. Holden, G.C. Brammar, K.A. Walsh, J.E. McNaughtan, D.K. Rowler, N. Van Rooijen&E.C. Reynolds, Macrophage depletion abates *Porphyromonas gingivalis*-induced alveolar bone resorption in mice. *J Immunol*, 2014. **193**(5): p. 2349-62.
726. Yang, R.B., M.R. Mark, A. Gray, A. Huang, M.H. Xie, M. Zhang, A. Goddard, W.I. Wood, A.L. Gurney&P.J. Godowski, Toll-like receptor-2 mediates lipopolysaccharide-induced cellular signalling. *Nature*, 1998. **395**(6699): p. 284-8.
727. Liu, R., T. Desta, M. Raptis, R.P. Darveau&D.T. Graves, *Porphyromonas gingivalis* and *E. coli* Lipopolysaccharide Exhibit Different Systemic but Similar Local Induction of Inflammatory Markers. *Journal of periodontology*, 2008. **79**(7): p. 1241-1247.
728. Hajishengallis, G., M. Martin, R.E. Schifferle&R.J. Genco, Counteracting interactions between lipopolysaccharide molecules with differential activation of toll-like receptors. *Infect Immun*, 2002. **70**(12): p. 6658-64.
729. Yoshimura, A., T. Kaneko, Y. Kato, D.T. Golenbock&Y. Hara, Lipopolysaccharides from periodontopathic bacteria *Porphyromonas gingivalis* and *Campylobacter jejuni* are antagonists for human toll-like receptor 4. *Infect Immun*, 2002. **70**(1): p. 218-25.
730. Takayama, K., N. Qureshi, P. Mascagni, M.A. Nashed, L. Anderson&C.R. Raetz, Fatty acyl derivatives of glucosamine 1-phosphate in *Escherichia coli* and their relation to lipid A. Complete structure of A diacyl GlcN-1-P found in a phosphatidylglycerol-deficient mutant. *J Biol Chem*, 1983. **258**(12): p. 7379-85.
731. Brandenburg, K., H. Mayer, M.H. Koch, J. Weckesser, E.T. Rietschel&U. Seydel, Influence of the supramolecular structure of free lipid A on its biological activity. *Eur J Biochem*, 1993. **218**(2): p. 555-63.
732. Frečer, V., B. Ho&J.L. Ding, Molecular dynamics study on lipid A from *Escherichia coli*: insights into its mechanism of biological action. *Biochim Biophys Acta*, 2000. **1466**(1-2): p. 87-104.
733. Ogawa, T., Chemical structure of lipid A from *Porphyromonas (Bacteroides) gingivalis* lipopolysaccharide. *FEBS Lett*, 1993. **332**(1-2): p. 197-201.
734. Nichols, F.C., B. Bajrami, R.B. Clark, W. Housley&X. Yao, Free Lipid A Isolated from *Porphyromonas gingivalis* Lipopolysaccharide Is Contaminated with Phosphorylated Dihydroceramide Lipids: Recovery in Diseased Dental Samples. *Infection and Immunity*, 2012. **80**(2): p. 860-874.
735. Ogawa, T., Immunobiological properties of chemically defined lipid A from lipopolysaccharide of *Porphyromonas (Bacteroides) gingivalis*. *Eur J Biochem*, 1994. **219**(3): p. 737-42.
736. Cunningham, M.D., R.A. Shapiro, C. Seachord, K. Ratcliffe, L. Cassiano&R.P. Darveau, CD14 employs hydrophilic regions to "capture" lipopolysaccharides. *J Immunol*, 2000. **164**(6): p. 3255-63.

References

737. Juan, T.S., E. Hailman, M.J. Kelley, S.D. Wright&H.S. Lichenstein, Identification of a domain in soluble CD14 essential for lipopolysaccharide (LPS) signaling but not LPS binding. *J Biol Chem*, 1995. **270**(29): p. 17237-42.
738. McGinley, M.D., L.O. Narhi, M.J. Kelley, E. Davy, J. Robinson, M.F. Rohde, S.D. Wright&H.S. Lichenstein, CD14: physical properties and identification of an exposed site that is protected by lipopolysaccharide. *J Biol Chem*, 1995. **270**(10): p. 5213-8.
739. Juan, T.S., E. Hailman, M.J. Kelley, L.A. Busse, E. Davy, C.J. Empig, L.O. Narhi, S.D. Wright&H.S. Lichenstein, Identification of a lipopolysaccharide binding domain in CD14 between amino acids 57 and 64. *J Biol Chem*, 1995. **270**(10): p. 5219-24.
740. Stelter, F., M. Bernheiden, R. Menzel, R.S. Jack, S. Witt, X. Fan, M. Pfister&C. Schutt, Mutation of amino acids 39-44 of human CD14 abrogates binding of lipopolysaccharide and *Escherichia coli*. *Eur J Biochem*, 1997. **243**(1-2): p. 100-9.
741. Cunningham, M.D., J. Bajorath, J.E. Somerville&R.P. Darveau, *Escherichia coli* and *Porphyromonas gingivalis* lipopolysaccharide interactions with CD14: implications for myeloid and nonmyeloid cell activation. *Clin Infect Dis*, 1999. **28**(3): p. 497-504.
742. Haziot, A., S. Chen, E. Ferrero, M.G. Low, R. Silber&S.M. Goyert, The monocyte differentiation antigen, CD14, is anchored to the cell membrane by a phosphatidylinositol linkage. *J Immunol*, 1988. **141**(2): p. 547-52.
743. Rock, F.L., G. Hardiman, J.C. Timans, R.A. Kastelein&J.F. Bazan, A family of human receptors structurally related to *Drosophila* Toll. *Proc Natl Acad Sci U S A*, 1998. **95**(2): p. 588-93.
744. Viriyakosol, S.&T.N. Kirkland, A region of human CD14 required for lipopolysaccharide binding. *J Biol Chem*, 1995. **270**(1): p. 361-8.
745. Morandini, A.C., C.R. Sipert, E.S. Ramos-Junior, D.T. Brozoski&C.F. Santos, Periodontal ligament and gingival fibroblasts participate in the production of TGF-beta, interleukin (IL)-8 and IL-10. *Braz Oral Res*, 2011. **25**(2): p. 157-62.
746. Korn, T., E. Bettelli, M. Oukka&V.K. Kuchroo, IL-17 and Th17 Cells. *Annu Rev Immunol*, 2009. **27**: p. 485-517.
747. Zhang, B., A.A. Elmabsout, H. Khalaf, V.T. Basic, K. Jayaprakash, R. Kruse, T. Bengtsson&A. Sirsjö, The periodontal pathogen *Porphyromonas gingivalis* changes the gene expression in vascular smooth muscle cells involving the TGFbeta/Notch signalling pathway and increased cell proliferation. *BMC Genomics*, 2013. **14**: p. 770-770.
748. Yamazaki, K., K. Tabeta, T. Nakajima, Y. Ohsawa, K. Ueki, H. Itoh&H. Yoshie, Interleukin-10 gene promoter polymorphism in Japanese patients with adult and early-onset periodontitis. *Journal of clinical periodontology*, 2001. **28**(9): p. 828-832.
749. Fenol, A., R.K. Sasidharan&S. Krishnan, Levels of Interleukin -10 in Gingival Crevicular Fluid and its Role in the Initiation and Progression of Gingivitis to Periodontitis. *Journal of Oral Hygiene & Health*, 2014.
750. Sasaki, H., Y. Okamatsu, T. Kawai, R. Kent, M. Taubman&P. Stashenko, The interleukin-10 knockout mouse is highly susceptible to *Porphyromonas gingivalis*-induced alveolar bone loss. *J Periodontal Res*, 2004. **39**(6): p. 432-41.
751. Claudino, M., T.P. Garlet, C.R. Cardoso, G.F. de Assis, R. Taga, F.Q. Cunha, J.S. Silva&G.P. Garlet, Down-regulation of expression of osteoblast and osteocyte markers in periodontal tissues associated with the spontaneous alveolar bone loss of interleukin-10 knockout mice. *Eur J Oral Sci*, 2010. **118**(1): p. 19-28.
752. De Rossi, A., L.B. Rocha&M.A. Rossi, Interferon-gamma, interleukin-10, Intercellular adhesion molecule-1, and chemokine receptor 5, but not interleukin-4, attenuate the development of periapical lesions. *J Endod*, 2008. **34**(1): p. 31-8.
753. Zhang, X.&Y.T. Teng, Interleukin-10 inhibits gram-negative-microbe-specific human receptor activator of NF-kappaB ligand-positive CD4+-Th1-cell-associated alveolar bone loss in vivo. *Infect Immun*, 2006. **74**(8): p. 4927-31.
754. Zhang, Q., B. Chen, F. Yan, J. Guo, X. Zhu, S. Ma&W. Yang, Interleukin-10 Inhibits Bone Resorption: A Potential Therapeutic Strategy in Periodontitis and Other Bone Loss Diseases. *BioMed Research International*, 2014. **2014**: p. 284836.
755. Stuart, L.M., M. Lucas, C. Simpson, J. Lamb, J. Savill&A. Lacy-Hulbert, Inhibitory effects of apoptotic cell ingestion upon endotoxin-driven myeloid dendritic cell maturation. *J Immunol*, 2002. **168**(4): p. 1627-35.
756. Figueredo, C.M., M.S. Ribeiro, R.G. Fischer&A. Gustafsson, Increased interleukin-1beta concentration in gingival crevicular fluid as a characteristic of periodontitis. *J Periodontol*, 1999. **70**(12): p. 1457-63.

References

757. Stathopoulou, P.G., M.R. Benakanakere, J.C. Galicia&D.F. Kinane, The host cytokine response to *Porphyromonas gingivalis* is modified by gingipains. *Oral Microbiol Immunol*, 2009. **24**(1): p. 11-7.
758. Makino, M., Y. Maeda, M. Kai, T. Tamura&T. Mukai, GM-CSF-mediated T-cell activation by macrophages infected with recombinant BCG that secretes major membrane protein-II of *Mycobacterium leprae*. *FEMS Immunol Med Microbiol*, 2009. **55**(1): p. 39-46.
759. Kyriakis, J.M.&J. Avruch, Mammalian mitogen-activated protein kinase signal transduction pathways activated by stress and inflammation. *Physiol Rev*, 2001. **81**(2): p. 807-69.
760. Hiramine, H., K. Watanabe, N. Hamada&T. Umemoto, *Porphyromonas gingivalis* 67-kDa fimbriae induced cytokine production and osteoclast differentiation utilizing TLR2. *FEMS Microbiol Lett*, 2003. **229**(1): p. 49-55.
761. Scott, R.S., E.J. McMahon, S.M. Pop, E.A. Reap, R. Caricchio, P.L. Cohen, H.S. Earp&G.K. Matsushima, Phagocytosis and clearance of apoptotic cells is mediated by MER. *Nature*, 2001. **411**(6834): p. 207-11.
762. Asif, K.&S.V. Kothiwale, Phagocytic activity of peripheral blood and crevicular phagocytes in health and periodontal disease. *Journal of Indian Society of Periodontology*, 2010. **14**(1): p. 8-11.
763. Leers, M.P., V. Bjorklund, B. Bjorklund, H. Jornvall&M. Nap, An immunohistochemical study of the clearance of apoptotic cellular fragments. *Cell Mol Life Sci*, 2002. **59**(8): p. 1358-65.
764. Li, M., D.F. Carpio, Y. Zheng, P. Bruzzo, V. Singh, F. Ouaz, R.M. Medzhitov&A.A. Beg, An essential role of the NF-kappa B/Toll-like receptor pathway in induction of inflammatory and tissue-repair gene expression by necrotic cells. *J Immunol*, 2001. **166**(12): p. 7128-35.
765. Fadok, V.A., D.L. Bratton, L. Guthrie&P.M. Henson, Differential effects of apoptotic versus lysed cells on macrophage production of cytokines: role of proteases. *J Immunol*, 2001. **166**(11): p. 6847-54.
766. Stern, M., J. Savill&C. Haslett, Human monocyte-derived macrophage phagocytosis of senescent eosinophils undergoing apoptosis. Mediation by alpha v beta 3/CD36/thrombospondin recognition mechanism and lack of phlogistic response. *Am J Pathol*, 1996. **149**(3): p. 911-21.
767. Henson, P.M.&R.M. Tuder, Apoptosis in the lung: induction, clearance and detection. *Am J Physiol Lung Cell Mol Physiol*, 2008. **294**(4): p. L601-11.
768. Koziel, J., P. Mydel&J. Potempa, The link between periodontal disease and rheumatoid arthritis: an updated review. *Curr Rheumatol Rep*, 2014. **16**(3): p. 408.
769. Lund, H., P. Boysen, C.P. Åkesson, A.M. Lewandowska-Sabat&A.K. Storset, Transient Migration of Large Numbers of CD14(++) CD16(+) Monocytes to the Draining Lymph Node after Onset of Inflammation. *Frontiers in Immunology*, 2016. **7**: p. 322.
770. Wakelin, M.W., M.J. Sanz, A. Dewar, S.M. Albelda, S.W. Larkin, N. Boughton-Smith, T.J. Williams&S. Nourshargh, An anti-platelet-endothelial cell adhesion molecule-1 antibody inhibits leukocyte extravasation from mesenteric microvessels in vivo by blocking the passage through the basement membrane. *J Exp Med*, 1996. **184**(1): p. 229-39.
771. Wu, Y., P. Stabach, M. Michaud&J.A. Madri, Neutrophils lacking platelet-endothelial cell adhesion molecule-1 exhibit loss of directionality and motility in CXCR2-mediated chemotaxis. *J Immunol*, 2005. **175**(6): p. 3484-91.
772. Grunwald, U., X. Fan, R.S. Jack, G. Workalemahu, A. Kallies, F. Stelter&C. Schutt, Monocytes can phagocytose Gram-negative bacteria by a CD14-dependent mechanism. *J Immunol*, 1996. **157**(9): p. 4119-25.
773. Schiff, D.E., L. Kline, K. Soldau, J.D. Lee, J. Pugin, P.S. Tobias&R.J. Ulevitch, Phagocytosis of gram-negative bacteria by a unique CD14-dependent mechanism. *J Leukoc Biol*, 1997. **62**(6): p. 786-94.
774. Burns, E., T. Eliyahu, S. Uematsu, S. Akira&G. Nussbaum, TLR2-dependent inflammatory response to *Porphyromonas gingivalis* is MyD88 independent, whereas MyD88 is required to clear infection. *J Immunol*, 2010. **184**(3): p. 1455-62.
775. Eskin, M.A., G. Hajishengallis&D.F. Kinane, Differential Activation of Human Gingival Epithelial Cells and Monocytes by *Porphyromonas gingivalis* Fimbriae. *Infection and Immunity*, 2007. **75**(2): p. 892-898.
776. Polak, D., R. Naddaf, L. Shapira, E.I. Weiss&Y. Hour-Haddad, Protective potential of non-dialyzable material fraction of cranberry juice on the virulence of *P. gingivalis* and *F. nucleatum* mixed infection. *J Periodontol*, 2013. **84**(7): p. 1019-25.
777. Gibson, F.C., 3rd&C.A. Genco, Prevention of *Porphyromonas gingivalis*-induced oral bone loss following immunization with gingipain R1. *Infect Immun*, 2001. **69**(12): p. 7959-63.

References

778. Yonezawa, H., T. Kato, H.K. Kuramitsu, K. Okuda&K. Ishihara, Immunization by Arg-gingipain A DNA vaccine protects mice against an invasive Porphyromonas gingivalis infection through regulation of interferon-gamma production. *Oral Microbiol Immunol*, 2005. **20**(5): p. 259-66.
779. Miyachi, K., K. Ishihara, R. Kimizuka&K. Okuda, Arg-gingipain A DNA vaccine prevents alveolar bone loss in mice. *J Dent Res*, 2007. **86**(5): p. 446-50.